

# **Phospho-regulation of Fkh2 in *Candida albicans***

PhD research thesis

University of Sheffield

Department of Molecular Biology and Biotechnology

**Jamie Alan Greig**

Submitted: May 2014

# Thesis Summary

The opportunistic human fungal pathogen, *Candida albicans*, undergoes morphological and transcriptional adaptation in the switch from commensalism to pathogenicity. Previous research on this switch has focused on genes involved in the morphological switch from yeast to hyphal growth. However, very few genes have been found that directly control hyphal morphogenesis, suggesting primary control at the post-translational level. The Cyclin Dependent Kinases (CDK), Cdk1, has been previously implicated in this process; therefore it was sought to identify phospho-regulatory targets of Cdk1 involved in *C. albicans* hyphal morphogenesis.

Fkh2 was a likely CDK target that shows differential phosphorylation between yeast and hyphal growth; being phosphorylated in conjunction with cell cycle progression during yeast growth, but not in hyphae, where phosphorylation occurs for a short period on hyphal induction. Further investigations have found that Fkh2 is phosphorylated at C-terminal CDK consensus sites on hyphal induction, but is not a regulatory target of Cdk1, or any other CDK related protein present in *C. albicans*.

Although the kinase responsible remains elusive, the physiological consequences of the phosphorylation have been found to be quite profound, with phosphorylation of Fkh2 being a requirement for the maintenance of invasive filamentous growth. Loss of Fkh2 phosphorylation specifically prevents the expression of genes required for: filamentous growth, pathogenesis, host interaction and biofilm formation, which are required for the transition from commensalism to pathogenesis. Thus phosphorylation of Fkh2 on hyphal induction provides a cell cycle-independent function that contributes to pathogenesis.

# Acknowledgements

Firstly I would like to thank my mother, father and Andrew for their continued support and encouragement for whichever direction I choose to go.

I would like to thank my supervisors: Prof. Pete Sudbery and Prof. Yue Wang for the help they have provided, and for giving me the opportunity to live and work in Singapore for two years.

I would like to thank members of the Sudbury lab: Dr. David Caballero-Lima – for his help with many experimental techniques, Dr. Lina Alaalm - for ensuring I remained caffeinated, Simon Watton – for the banter, and to other members of the Sudbery lab past and present.

I would also like to thank all the members of the WY lab; especially Dr. Guisheng Zeng for teaching me the dark art of cloning, and Xu Xiaoli and Yanming Wang for helping me find stuff and trying to teach me Chinese.

I would like to thank Dr. Vivien Koh from the Biopolis microarray facility and Dr. Sheena Wee from the IMCB proteomics facility for their help.

To Rav and Guy for being great housemates and letting me scrounge food off them; and to Shashenk, Lala, Nora and all others that passed through 46b in my time there.

A special thank you to JY for all the help, encouragement, teh ping and xiao long baos that got me to this point.

Finally I'd also like to thank Dr. Dinesh Nair, without whom this thesis might not have been possible.

# Terms and Abbreviations

ALS	Agglutinin Like Sequence
APC	Anaphase Promoting Complex
ATP	Adenosine triphosphate
BLAST	Basic Local Alignment Search Tool
BSA	Bovine Serum Albumin
CAK	CDK activating kinase
cAMP	Cyclic adenosine monophosphate
CDK	Cyclin Dependent Kinase
cDNA	Complementary DNA
CFG	Centre for Functional Genomics
CGD	<i>Candida</i> Genome Database
CKI	Cyclin Dependent kinase inhibitor
CoIP	Co-Immunoprecipitation
DAPI	4',6-diamidino-2-phenylindole
DEPC	Diethylpyrocarbonate
DMSO	Dimethyl sulfoxide
DTT	Dithiothreitol
ECL	Enhanced Chemiluminescence
EDTA	Ethylenediaminetetraacetic Acid
EGTA	ethylene glycol tetraacetic acid
ESCRT	Endosomal Sorting Complexes Required for Transport
FA	Formaldehyde Agarose
FHA	Fork-head associated
FITC	Fluorescein isothiocyanate
FOX	Fork-head Box
GAP	GTPase activating protein
GEF	Guanine nucleotide exchange factor
GFP	Green Fluorescent Protein
GMM	Glucose Minimal media
GO	Gene Ontology
GPCR	G-Protein Coupled Receptor
GPI	Glycosylphosphatidylinositol
GST	Glutathione-S-transferase
GTP	Guanosine-5'-triphosphate
HA	Haemagglutinin
HDAC	Histone Deacetylase Complex
HIV	Human Immunodeficiency Virus
HSF	Heat Shock Factor
IP	Immunoprecipitate
IPTG	Isopropyl $\beta$ -D-1-thiogalactopyranoside
LB	Luria Bertani

LiAc	Lithium Acetate
mA	milli-Amps
MALDI-qTOF	Matrix-Assisted Laser Desorption/Ionization, quantitative Time Of Flight
MAPK	Mitogen Activated Protein Kinase
MBF	MluI Binding Factor
mRNA	messenger RNA
ORF	Open Reading Frame
PAGE	Polyacrylamide Gel Electrophoresis
PBS	Phosphate-Buffered-Saline
PCR	Polymerase Chain Reaction
PKA	Protein Kinase A
PVDF	Polyvinylidene Fluoride
qPCR	quantitative PCR
RNA	Ribonucleic acid
RT	Reverse Transcription
SAPs	Secreted Aspartyl Protease
SBF	DNA binding factor composed of Swi4 and Swi6
SCF	Skip-Cullin-Factor
SDS	Sodium dodecyl sulfate
SDW	Sterile Distilled Water
SUMO	Small Ubiquitin Like Modifier
SYBR Green	N',N'-dimethyl-N-[4-[(E)-(3-methyl-1,3-benzothiazol-2-ylidene)methyl]-1-phenylquinolin-1-ium-2-yl]-N-propylpropane-1,3-diamine
TAE	Tris-Acetate-EDTA
TBS	Tris-Buffered-Saline
TE	Tris-EDTA
TEMED	Tetramethylethylenediamine
TOR	Target of Rapamycin
w/v	weight / volume
YEPD	Yeast Extract Peptone Dextrose
YEPG	Yeast Extract Peptone Galactose
YFP	Yellow Fluorescent Protein
λppase	Lambda phosphatase

# Table of Contents

1. General Introduction.....	1
1.1. <i>Candida albicans</i> .....	1
1.2. <i>C. albicans</i> biology.....	2
1.3. <i>C. albicans</i> morphological forms and pathogenesis.....	3
1.4. Regulation of morphogenesis in <i>C. albicans</i> .....	6
1.4.1. cAMP-PKA pathway.....	7
1.4.2. Cph1-MAPK pathway.....	9
1.4.3. pH regulation of morphogenesis.....	9
1.4.4. Negative regulators of morphogenesis.....	10
1.4.5. Temperature-dependent regulation of morphogenesis.....	11
1.4.6. Cell-cycle arrest-dependent morphogenesis.....	11
1.4.7. Hyphal-specific genes.....	12
1.5. Regulation of polarised growth.....	13
1.5.1. Budding yeast model.....	13
1.5.2. Polarised growth of <i>C. albicans</i> hyphae.....	16
1.6. Regulation of cell separation.....	18
1.7. Role of post-translational modification in morphogenesis.....	20
1.8. Methods for studying kinases and their targets.....	23
1.9. Aims of thesis study.....	25
2. Materials and Methods.....	26
2.1. <i>C. albicans</i> growth media.....	26
2.2. <i>E. coli</i> culture media.....	27
2.3. <i>C. albicans</i> culture conditions.....	27
2.4. Microscopy.....	28
2.5. Molecular biology: DNA techniques.....	29
2.6. Molecular biology: RNA techniques.....	35
2.7. Molecular biology: protein biochemistry techniques.....	39
2.8. <i>C. albicans</i> strains used in this study.....	46
2.9. <i>E. coli</i> strains used in this study.....	48

2.10. Vectors used in this study.....	49
2.11. Primers used in this study.....	52
2.12. Antibodies used in this study.....	59
<b>3. Cyclin-Dependent Kinase targets.....</b>	<b>61</b>
3.1. Introduction.....	61
3.1.1. Cdk1.....	61
3.1.2. The role of Cdk1 in morphogenesis.....	63
3.1.3. The role of Cdk1 in <i>C. albicans</i> morphogenesis.....	65
3.2. Results.....	67
3.2.1. Orf19.3469.....	68
3.2.1.1. Introduction.....	68
3.2.1.2. C-terminal tagging of Orf19.3469 with GFP.....	69
3.2.1.3. Orf19.3469 phosphorylation during yeast and hyphal growth.....	71
3.2.2. Orf19.1948.....	72
3.2.2.1. Introduction.....	72
3.2.2.2. Orf19.1948 phosphorylation during yeast and hyphal growth.....	73
3.2.2.3. Localisation of Orf19.1948.....	74
3.2.3. Sfl1.....	75
3.2.3.1. Introduction.....	75
3.2.3.2. Sfl1 phosphorylation during yeast and hyphal growth.....	76
3.2.3.3. Sfl1 localisation.....	77
3.2.4. Fkh2.....	78
3.2.4.1. Introduction.....	78
3.2.4.2. Fkh2 phosphorylation during yeast and hyphal growth.....	80
3.2.4.3. Fkh2 localisation.....	81
3.3. Discussion.....	81
3.3.1. Orf19.3469.....	82
3.3.2. Orf19.1948.....	82
3.3.3. Sfl1.....	83
3.3.4. Fkh2.....	83
3.3.5. Conclusions.....	84

4. Fkh2 Phospho-regulation.....	85
4.1. Introduction.....	85
4.1.1. Fork-head transcription factors.....	85
4.1.2. Fork-head transcription factors in morphogenesis and cell cycle progression.....	86
4.1.3. <i>Candida albicans</i> Fkh2.....	89
4.2. Results.....	91
4.2.1. Fkh2 undergoes cell cycle-dependent phosphorylation in yeast.....	91
4.2.2. Fkh2 is phosphorylated independently of the cell cycle on hyphal induction.....	92
4.2.3. Determining the residues phosphorylated on Fkh2 after hyphal induction.....	93
4.2.4. Mutagenesis studies of Fkh2 phosphorylation.....	96
4.2.4.1. Construction of a <i>fkh2Δ/Δ</i> strain.....	96
4.2.4.2. Cloning of <i>FKH2</i> .....	99
4.2.4.3. Mutation of sites from phospho-peptide mapping.....	100
4.2.4.4. Mutation of CDK consensus sites.....	101
4.2.4.5. Mutation of CDK consensus and minimal sites.....	102
4.2.4.6. Fkh2 C-terminal truncation ( <i>fkh2 1-426</i> ).....	103
4.2.5. Determining if Cdk1 is responsible for Fkh2 phosphorylation.....	104
4.2.5.1. Cdk1 can phosphorylate Fkh2 <i>in vitro</i> .....	104
4.2.5.2. Inhibition of analogue-sensitive Cdk1 does not affect Fkh2 phosphorylation.....	106
4.2.5.3. Fkh2 phosphorylation in Cdk1 cyclin knockout strains.....	107
4.2.5.4. Investigating if Fkh2 and Cdk1 physically interact.....	109
4.2.6. Other kinases that may phosphorylate Fkh2.....	110
4.2.6.1. Deletion of <i>CRK1</i> does not affect Fkh2 phosphorylation.....	110
4.2.6.2. Deletion of <i>HOG1</i> does not affect Fkh2 phosphorylation.....	111
4.2.6.3. Inhibiting cAMP-dependent protein kinases does not affect Fkh2 phosphorylation.....	111
4.2.6.4. Deletion of <i>SSN3</i> does not affect Fkh2 phosphorylation.....	111

4.2.6.5. Repression of the CDK <i>PHO85</i> does not affect Fkh2 phosphorylation.....	112
4.3. Discussion.....	113
4.3.1. Fkh2 is differentially phosphorylated between yeast and hyphal growth.....	113
4.3.2. Fkh2 is phosphorylated at CDK consensus sites on hyphal induction.....	115
4.3.3. Difficulties determining the kinase responsible for Fkh2 phosphorylation.....	116
5. Fkh2 Mutants.....	118
5.1. Morphological consequences of Fkh2 phosphorylation.....	118
5.1.1. Blocking Fkh2 phosphorylation affects yeast cell shape.....	118
5.1.2. Blocking Fkh2 phosphorylation results in altered hyphal morphology and prevents maintenance of invasive filamentous growth.....	119
5.1.3. The phosphorylation status of Fkh2 does not affect its localisation.....	121
5.1.4. Phenotypes of other Fkh2 phosphorylation mutants.....	122
5.1.4.1. Mutation of CDK consensus and minimal sites.....	123
5.1.4.2. Mutation of sites detected by phospho-peptide mapping.....	124
5.1.4.3. Mutation of Fkh2 C-terminal CDK consensus and minimal sites.....	125
5.1.4.4. Truncation of Fkh2's C-terminus (1-426).....	125
5.2. Fkh2-dependent regulation of transcriptional programs.....	125
5.2.1. Overview: regulation of <i>C. albicans</i> virulence factor expression during filamentous invasive growth through phosphorylation of Fkh2.....	128
5.2.2. Confirming Fkh2's phosphorylation-dependent regulation of genes for filamentous invasive growth.....	135
5.2.3. Detailed analysis of microarray results: <i>FKH2</i> deletion alters gene expression during yeast growth.....	138

5.2.3.1. Genes down-regulated during yeast growth upon <i>FKH2</i> deletion.....	138
5.2.3.2. Genes up-regulated during yeast growth upon <i>FKH2</i> deletion.....	140
5.2.4. Blocking Fkh2 phosphorylation affects gene expression during yeast growth.....	140
5.2.4.1. Genes down-regulated during yeast growth on blocking Fkh2 phosphorylation.....	142
5.2.4.2. Genes up-regulated during yeast growth on blocking Fkh2 phosphorylation.....	142
5.2.5. <i>FKH2</i> deletion alters hyphal transcription programs.....	144
5.2.5.1. Genes down-regulated during hyphal growth upon <i>FKH2</i> deletion.....	145
5.2.5.2. Genes up-regulated during hyphal growth upon <i>FKH2</i> deletion.....	145
5.2.6. Further transcriptional investigation of blocking Fkh2 phosphorylation during hyphal growth.....	146
5.2.6.1. Genes down-regulated during hyphal growth on blocking Fkh2 phosphorylation.....	147
5.2.6.2. Genes up-regulated during hyphal growth on blocking Fkh2 phosphorylation.....	148
5.3. Searching for interacting partners of Fkh2.....	149
5.3.1. Mass-Spectromic identification of Fkh2 interacting partners.....	149
5.3.2. Pob3 physically interacts with Fkh2.....	150
5.3.3. Fkh2's interaction with Pob3 is dependent on Fkh2's phosphorylation status.....	151
5.4. <i>FKH2</i> over-expression.....	152
5.4.1. Over-expression strategy.....	152
5.4.2. Comparison of Fkh2 expression levels upon over-expression.....	153
5.4.3. <i>FKH2</i> over-expression causes filamentation under yeast growth conditions.....	154
5.4.4. <i>FKH2</i> over-expression causes a cell cycle arrest phenotype.....	155
5.4.5. Microarray analysis of <i>FKH2</i> over-expression.....	157

5.4.5.1. Genes down-regulated upon <i>FKH2</i> over-expression.....	158
5.4.5.2. Genes up-regulated upon <i>FKH2</i> over-expression.....	158
5.5. Discussion.....	159
5.5.1. Fkh2 phosphorylation affects yeast and hyphal morphologies.....	159
5.5.2. Fkh2 and transcriptional programs.....	160
5.5.2.1. Fkh2 phosphorylation is required to regulate genes for filamentous invasive growth and pathogenesis.....	161
5.5.2.2. Other roles of Fkh2 in the regulation of transcriptional programs.....	163
5.5.3. Novel interacting partners of Fkh2.....	164
5.5.4. <i>FKH2</i> over-expression causes cell cycle arrest filamentation.....	165
5.5.5. Conclusion.....	166
 6. General Discussion.....	 167
 Figure List.....	 171
Table list.....	174
References.....	175

# 1

## General Introduction

---

### 1.1. *Candida albicans*

*C. albicans* taxonomy:

**Kingdom:** *Mycota*

**Phylum:** *Ascomycota*

**Class:** *Hemiascomycetes*

**Order:** *Saccharomycetales*

**Family:** *Candidaceae*

**Genus:** *Candida*

**Species:** *Candida albicans*

*C. albicans* is an opportunistic fungal pathogen commensal to the gastrointestinal and genitourinary tract of humans. It is only in immune-compromised individuals that pathogenesis occurs; ranging from superficial mucosal infections in generally healthy people (Candidiasis), to systemic infections in severely immune-deficient patients, resulting from tissue invasion and dissemination in the blood (Candidemia). Candidemia can affect patients taking immunosuppressive drugs for transplant therapy, sufferers of Human Immunodeficiency Virus (HIV), neutropenia, and individuals undergoing chemotherapy or at extremes of age. The use of assisted ventilation or an indwelling catheter has been shown to provide a route of entry for infection. Removal of the competing microbial flora has been shown to promote fungal colonisation (Pfaller & Diekema 2010). It is the fourth most common cause of nosocomial infections in the United States, with mortality rates from Candidemia up to 50%. This was previously estimated to cost of more than \$1 billion annually (Miller et al. 2001). In the United Kingdom *Candida* species are the eighth most common cause of nosocomial infections; with Candidemia costing the health service £16.2 million and resulting in 683 deaths annually (Hassan et al. 2009).

## 1.2. *C. albicans* biology

*C. albicans* is generally found as an obligate diploid, only able to undergo mating in the elongated opaque state, which is homozygous at the mating type locus (Morschhäuser 2010). This occurs through a parasexual cycle involving formation of a tetraploid intermediate followed by concerted chromosome loss in order to regenerate the diploid state (Fig. 1.1.) (Noble & Johnson 2007). However, recent evidence has shown that mating-competent haploid *C. albicans* isolates can be generated in the laboratory on exposure to anti-fungal drugs (Hickman et al. 2013). It was previously thought impossible to form haploids as each haploid genome contains many recessive lethal mutations that can only be maintained in the diploid state; but in forming a haploid, selection against these deleterious mutations must be possible.

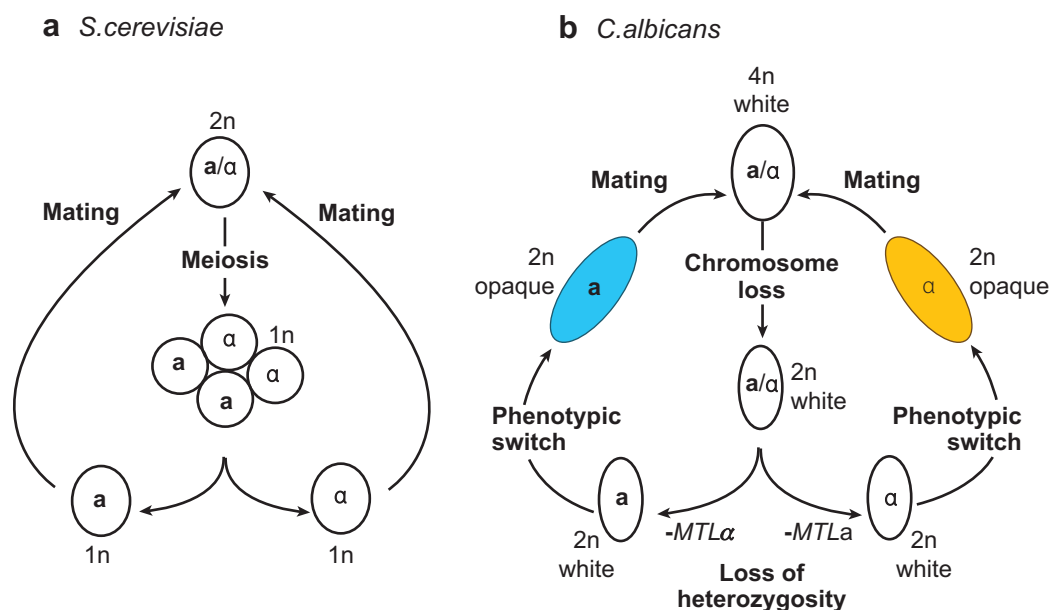


**Fig. 1.1. Comparison of mating programs between *S. cerevisiae* and *C. albicans*.** Adapted from Noble and Johnson 2007. **A)** In *S. cerevisiae* two haploid cells of opposite mating types come together to form a diploid, which then undergoes meiosis to generate haploid progeny. **B)** In *C. albicans* diploid cells have to undergo loss of heterozygosity at the mating type locus to become mating competent. Opaque cells of a and α mating types come together to make a tetraploid intermediate, which undergoes concerted chromosome loss to regenerate diploid cells that are heterozygous at the mating type locus.

The fact that *C. albicans* is a non-mating competent diploid, increases the difficulty in carrying out standard genetic analysis. Further, *Candida* species also have a modified genetic code, where the CTG codon in DNA encodes serine rather

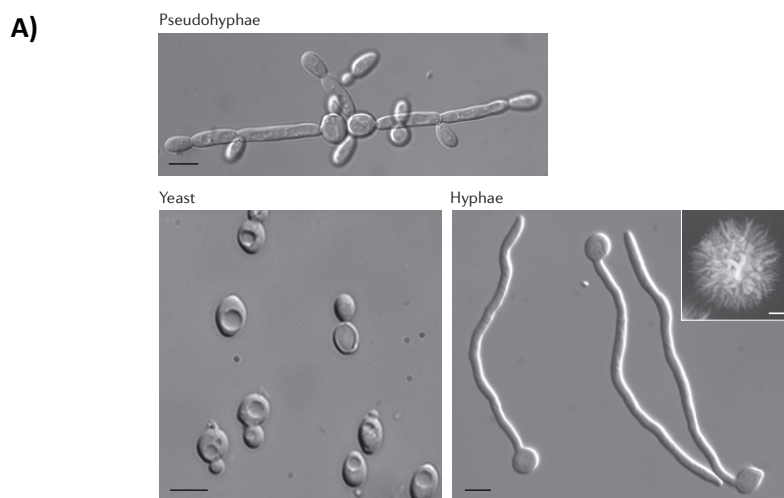
than leucine (Santos & Tuite 1995). This means that reporter genes such as GFP have had to be modified in order for correct expression in *Candida* (Cormack et al. 1997). The altered codon usage may affect the function of highly conserved proteins, with the polar, hydrophilic serine allowing more hydrogen bonding capacity compared with the non-polar aliphatic leucine, which will have its functional group buried within the protein structure. The appearance of serine residues in proteins may have also brought about new phosphorylation sites, allowing proteins to undergo differential regulation.

The study of *C. albicans* has been aided by the development of modified molecular biology tools. The CAI4 (Fonzi & Irwin 1993) and then BWP17 (Wilson et al. 1999) strains generated with the Ura-Blaster method (Alani et al. 1987), have provided strains with auxotrophic markers, allowing transformation of foreign genetic material, through prototrophic selection. PCR-mediated gene tagging or deletion has further allowed quick and efficient generation of *C. albicans* mutants in the above-mentioned strains. The CIP10 plasmid allows insertion of modified genetic material or reporters into a gene's native locus, or ectopically at the RP10 locus (Murad et al. 2000). For genes that are essential, regulatable promoters, such as the *MET3* (Care et al. 1999) or tetracycline-regulated promoters (Nakayama et al. 2000), allow knock-down or shut off of gene expression when desired. These regulatable promoters also allow the effect of over-expression of a gene of interest to be studied. In addition to regulatable promoters, a variety of different epitope tags to study protein function have also been optimised (Berman & Sudbery 2002).

### **1.3. *C. albicans* morphological forms and pathogenesis**

*C. albicans* has an adaptive morphology, undergoing reversible morphogenetic switching in response to external environmental cues and internal stresses. *C. albicans* can grow in a budding yeast form, and two distinct filamentous forms of pseudohyphae and true hyphae depending on the environmental conditions (Fig. 1.2.) (Sudbery et al. 2004). It is also able to switch between white and mating-competent opaque cells, and form chlamydospores – large rounded cells with thick cell walls, whose function is as yet unknown (Nobile et al. 2003). The ability to switch between growth modes is thought to be essential for

pathogenesis, allowing *C. albicans* to survive in varying niches through the different stages of infection. The filamentous forms are believed to be important during tissue invasion; while the yeast form is thought to facilitate dissemination in the blood stream, allowing the colonisation of major organs (Gow et al. 2002). White opaque switching to allow a parasexual cycle to occur is thought to be important for adaption in the host during infection, allowing *C. albicans* to combat the host defences (Morschhäuser 2010).



**B)**

Yeast	Pseudohyphae	Hyphae
<ul style="list-style-type: none"> <li>• Temperature below 30°C</li> <li>• pH 4.0</li> <li>• Cell density &lt;math&gt;&lt;10^7&lt;/math&gt; cells ml<sup>-1</sup></li> </ul>	<ul style="list-style-type: none"> <li>• Temperature ~ 35°C</li> <li>• pH 6.0</li> <li>• Nitrogen limited growth</li> <li>• High Phosphate</li> </ul>	<ul style="list-style-type: none"> <li>• Temperature 37°C</li> <li>• pH 7.0</li> <li>• N-acetylglucosamine</li> <li>• Serum</li> </ul>

**Fig. 1.2. *C. albicans* morphological forms.** Adapted from Sudbery et al. 2004 and Sudbery 2011. **A)** Yeast, hyphal and pseudohyphal morphologies. **B)** Environmental cues that bring about phenotypic switching. Scale bar - 1µm.

The best-studied morphological transition in *C. albicans* is that from budding yeast to filamentous growth. The yeast, pseudohyphal and true hyphal forms have characteristic features that are indicative of growth mode. Yeast and pseudohyphal cells grow by budding, with constrictions at the neck boundary between mother and daughter cells; whereas hyphal cells form a highly polarised, rapidly extending, tubular structure from the mother that has parallel-sided walls. In

addition to the morphological differences, there are also differences in septin organisation and nuclear kinetics between the morphologies (Sudbery et al. 2004) (Fig. 1.3.).

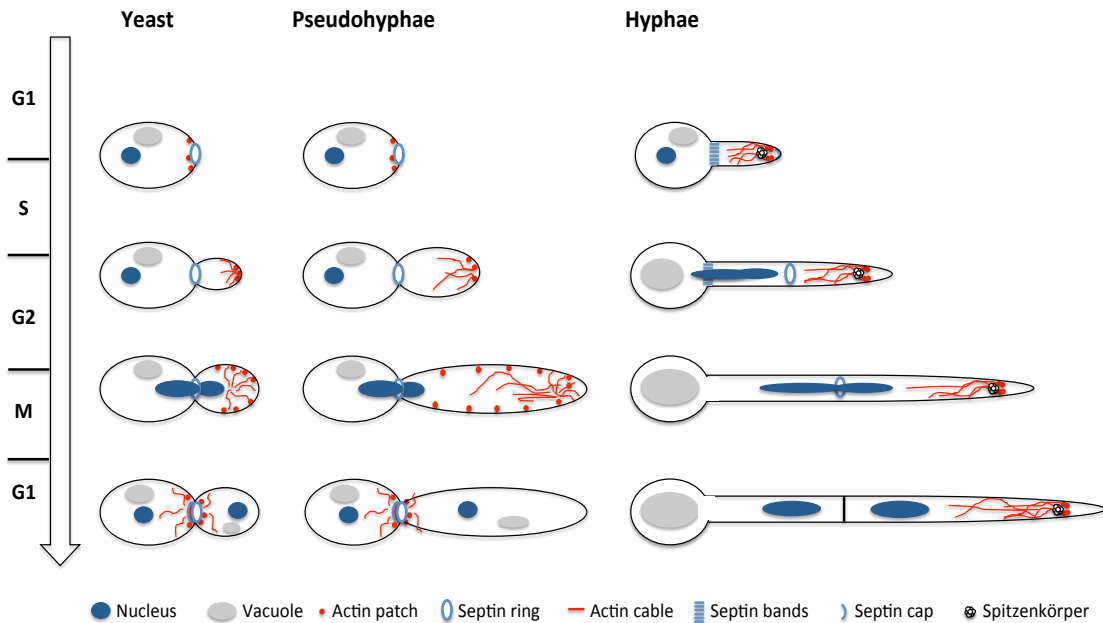


**Fig. 1.3. Differences in growth and cell cycle organisation between the three main morphological forms of *C. albicans*.** Adapted from Sudbery et al. 2004. Diagram shows growth stages in each of the morphological forms throughout the cell cycle. Also included are the septin, actin and nuclear structures and organisation in yeast, pseudohyphae and hyphae.

As well as morphology switching, *C. albicans* possesses other mechanisms for survival and pathogenesis in its mammalian host. Adhesion to host cells is a key step in pathogenesis, occurring prior to invasion. This is mediated by adhesins such as the agglutinin-like sequence (ALS) proteins, which are glycosylphosphatidylinositol-linked cell surface glycoproteins (Martin et al. 2011). Of these, the hyphal-specific Als3 and Hwp1 have been shown to be particularly important for host adhesion (Zhao et al. 2004; Staab et al. 1999). Once attached to host cells *C. albicans* can either penetrate the host cells by switching to the hyphal form, or by being passively taken up by endocytosis (Phan et al. 2007).

Another group of hyphal-specific genes that are involved in morphogenesis-independent pathogenesis are the Secreted Aspartyl Proteases (SAPs). These facilitate damage to the host tissues as well as nutrient acquisition, with SAPs 4-6 being required for *C. albicans* virulence (Sanglard et al. 1997). Along with the SAPs

*C. albicans* also secretes phospholipases that are thought to be involved in damaging host membranes (Ibrahim et al. 1995).

In order to avoid being killed by the hosts immune cells *C. albicans* has evolved a broad stress response network, regulated upstream by the Hog1 kinase. Temperature and oxidative stresses are combated by a series of heat shock proteins such as Hsp70/90. These prevent protein unfolding and the formation of toxic aggregates (Leach & Cowen 2013). Reactive oxygen or nitrogen species are produced in macrophages and neutrophils to kill phagocytised pathogens. Detoxification of the reactive oxygen species is accomplished by *C. albicans* through the catalase Cta1 (Wysong et al. 1998) and the superoxide dismutases Sod1 and Sod5 (Martchenko et al. 2004); whereas, detoxification of reactive nitrogen species is carried out by the flavohaemoglobin Yhb1 (Ullmann et al. 2004). Osmotic stress is opposed by glycerol production to offset water loss. This is achieved through the glycerol-3-phosphatase Gpp1 and glycerol-dehydrogenase Gpd2 (Wächtler et al. 2011).

*C. albicans* has to have an adaptive metabolism to allow survival in varying host niches, such as those where minimal glucose is available. It is also able to sequester essential minerals such as iron (Almeida et al. 2009) and zinc (Citiulo et al. 2012) from the host, a process that has been shown to be important for virulence.

On biological and non-biological surfaces *C. albicans* can form biofilms, which provide increased resistance to anti-fungal drug treatment (Fanning & Mitchell 2012). Biofilms are formed by the adherence of yeast cells to a surface before proliferation and hyphal production, forming a matrix where other extracellular material is deposited. Later yeast cells disperse from biofilms to invade other areas. Current research on this area has been focusing on the transcriptional pathways involved (Nobile et al. 2012).

#### **1.4. Regulation of morphogenesis in *C. albicans***

Morphogenesis from yeast to filamentous growth requires both positive and negative regulators. Studies on this have focused on how environmental signals are transduced to control the gene transcription program for the specific

morphology. The two best characterised morphogenesis signalling pathways are the pheromone response Mitogen Activated Protein Kinase (MAPK) Pathway, targeting the Cph1 transcription factor; and the cyclic Adenosine Monophosphate Protein Kinase A (cAMP-PKA) Pathway, targeting the Efg1 transcription factor. Both of which are downstream of the Ras1 GTPase. There are also other pathways that complement those mentioned above as summarised in Fig. 1.4.

#### **1.4.1. cAMP-PKA pathway**

The cAMP-PKA pathway is the primary pathway controlling hyphal morphogenesis in response to serum (Harcus et al. 2004). Activation of the pathway can occur through multiple routes, centering on the adenylyl cyclase Cyr1/Cdc35. The transmembrane ammonium permease Mep2 activates the cAMP-PKA pathway under low ammonium concentrations through its downstream effector Ras1 (Biswas & Morschhäuser 2005), a GTPase that interacts with Cyr1 to increase cAMP production (Fang & Wang 2006). The G-protein coupled receptor (GPCR) Gpr1 along with its associated G $\alpha$  subunit Gpa2 activate Cyr1 in a glucose and amino acid-dependent manner (Miwa et al. 2004; Maidan et al. 2005). Cyr1 itself can also act as a receptor, being stimulated by intracellular carbon dioxide (CO<sub>2</sub>) levels (Klengel et al. 2005), as well as a breakdown product of bacterial peptidoglycan present in serum, which binds to the leucine-rich region of Cyr1 (Xu et al. 2008). Cyr1 is the cells only source of cAMP and therefore deletion prevents hyphal morphogenesis from occurring (Rocha et al. 2001). Cyr1 acts in a tripartite complex with the cyclase-associated protein Srv2/Cap1 and monomeric actin. The complex is necessary for the serum response and provides a link between the serum response and actin cytoskeletal rearrangements that are a requirement of hyphal morphogenesis (Zou et al. 2010). Negative regulation of cAMP levels occurs via the phosphodiesterases Pde1 and Pde2, which convert cyclic-AMP to AMP (Hoyer et al. 1994; Bahn et al. 2003).

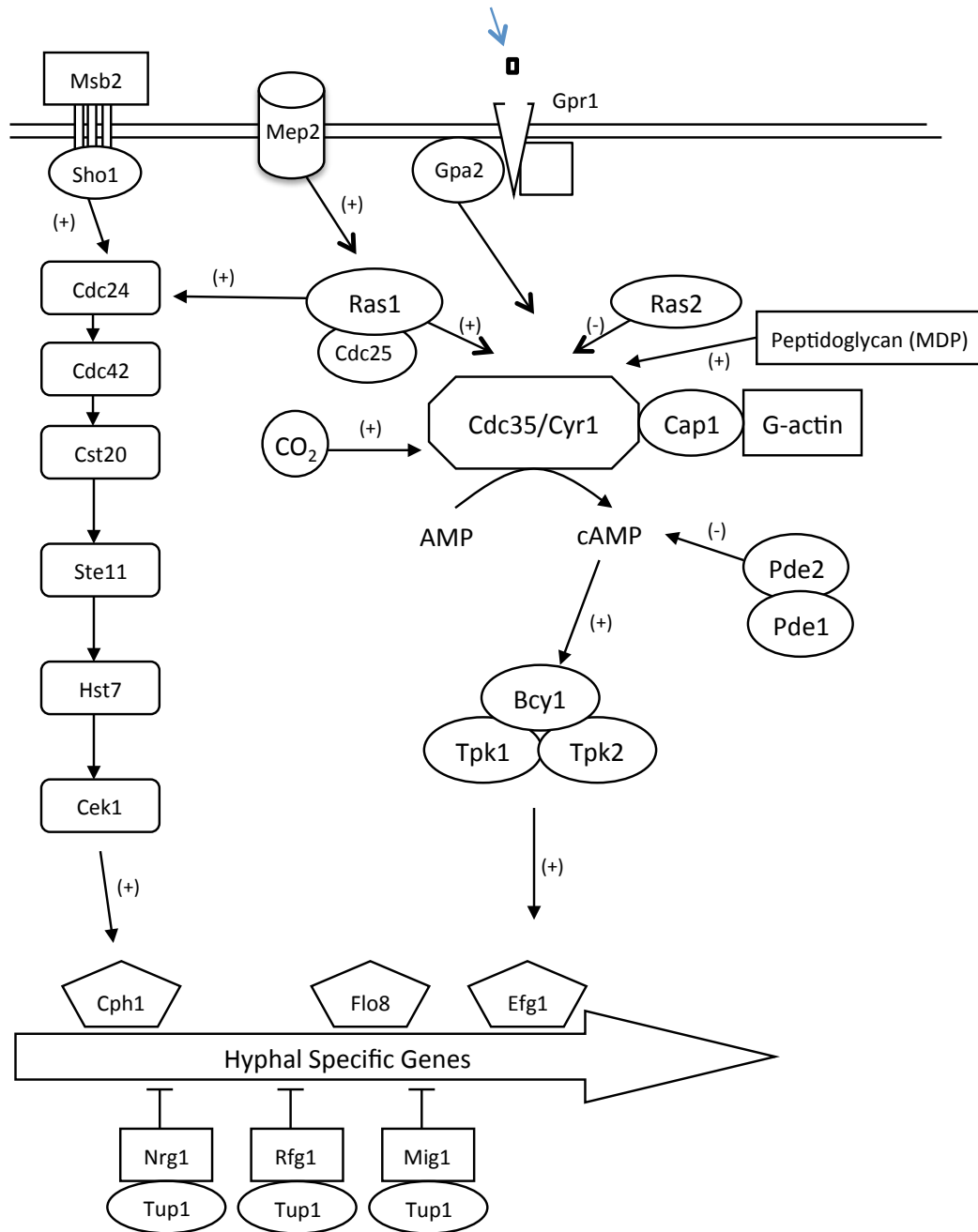


**Fig.1.4. The MAPK and cAMP-PKA morphogenesis pathways in *C. albicans*.** Multiple signals converge on the Cyr1 adenylyl cyclase to increase cellular cAMP levels and thus activate the cAMP-PKA pathway, causing phosphorylation of the Efg1 transcription factor to allow transcription of hyphal-specific genes. Nutrient and polarisation signals activate the pheromone response MAPK pathway, which results in the transcription of hyphal-specific genes via the Cph1 transcription factor.

The cAMP spike generated through Cyr1 causes activation of protein kinase A, which is made up of two catalytic subunits, Tpk1 and Tpk2, along with the regulatory subunit Bcy1. Tpk1 and Tpk2 are positive regulators of hyphal growth, being required for filamentation on solid and liquid media respectively (Bockmühl

et al. 2001). The best characterised target of the PKA in hyphal morphogenesis is the transcription factor Efg1, which PKA phosphorylates at T206 to promote the expression of hyphal specific genes (Bockmühl & Ernst 2001). Other transcription factors thought to be downstream targets of PKA signalling are the positive filamentation regulators Flo8 (Cao et al. 2006) and Mss11 (Su et al. 2009), along with the antagonistic Sfl1 (Li et al. 2007).

#### **1.4.2. Cph1-MAPK pathway**

The MAPK morphogenesis pathway was identified through homology with the pheromone response pathway in *S. cerevisiae* (Whiteway et al. 1992; Leberer et al. 1996). It is not as important for filamentous growth as the cAMP-PKA pathway, with deletion of any of the kinases in the cascade only affecting morphogenesis on poor carbon sources (Leberer et al. 1996; Liu et al. 1994). Activation of this pathway can occur via Msb2-Sho1 under cell wall stress (Román et al. 2005; Román, Cottier, et al. 2009), or, as with the cAMP-PKA pathway, through the Mep2-Ras1 module (Biswas & Morschhäuser 2005). Ras1 activates the GTPase Cdc42 through its GEF Cdc24, leading to the activation of the p21-activated kinase (PAK kinase) Cst20. The signal is then passed down the MAPK cascade through Ste11 and Hst7 to the MAPKs Cek1 and Cek2. Cek1 then directly activates the Cph1 transcription factor to aid in the expression of hyphal-specific genes (Sudbery 2011). Negative regulation of this pathway may occur through the quorum sensing molecule farnesol, which has been shown to repress the expression of *HST7* and *CPH1* transcripts (Sato et al. 2004).

#### **1.4.3. pH regulation of morphogenesis**

pH regulation of morphogenesis centres on the Rim101 transcription factor. In both alkaline and acidic environments, Rim101 undergoes proteolytic cleavage of its C-terminal domain, mediated by the protease Rim13 (Li et al. 2004) in conjunction with the endosomal sorting complex required for transport (ESCRT) component Snf7, and the scaffold protein Rim20 (Xu & Mitchell 2001; Wolf & Davis 2010). It is however only in alkali environments that this cleavage event

accomplishes activation of Rim101 (Li et al. 2004). The environmental pH-sensing and subsequent signal transduction is thought to be carried out through the membrane spanning proteins Rim21 and Dfg16 (Barwell et al. 2005), and requires the phosphorylation of the  $\beta$ -arrestin-like protein Rim8 to signal between Rim21 and Rim101 (Gomez-Raja & Davis 2012). Rim101 is required for the proper transcription of the pH-responsive genes *PHR1* and *PHR2*, both of which encode cell surface glycosylphosphatidylinositol (GPI)-anchored glycosidases (Fonzi 1999). *PHR1* is expressed under alkaline conditions, and is required for the maintenance of hyphal growth and host invasion (Calderon et al. 2010); whereas *PHR2* is expressed under acidic growth conditions and is required for mucosal infections (De Bernardis et al. 1998). The opposing expression patterns of these two genes may help contribute to adaptation within different host niches.

#### **1.4.4. Negative regulators of morphogenesis**

During yeast form growth, the transcriptional programs required for hyphal morphogenesis need to remain dormant. This is achieved through the general transcriptional repressor Tup1 in conjunction with Nrg1 or Rfg1, which target Tup1 to the promoters of hyphal-specific genes. Deletion of *TUP1* causes cells to grow constitutively as pseudohyphae (Braun & Johnson 1997), and allows the expression of hyphal-associated transcripts (Braun et al. 2000). Tup1 is thought to be regulated by the quorum sensing molecule farnesol (Kebaara et al. 2008), causing repression of hyphal-specific genes in dense cell populations. *NRG1* is required for yeast form growth, with deletion promoting filamentous growth. It encodes a zinc finger transcription factor which binds upstream of a subset of hyphal growth expression specific genes, such as *ALS3*, *HYR1*, *HWP1* and *ECE1* (Murad et al. 2001; Braun et al. 2001). Recently it was shown that the cAMP-PKA pathway, along with reduced Target of Rapamycin (TOR) signalling, is required for removal of Nrg1 from these promoters, which results in a change in the local chromatin structure (Lu et al. 2011). Rfg1 contributes in a similar manner to Nrg1, and again deletion of *RFG1* results in constitutive filamentous growth (Kadosh & Johnson 2001). Rfg1 may also however play a positive role in the regulation of

pseudohyphal growth, as over-expression can also cause filamentation to occur (Cleary et al. 2010).

#### **1.4.5. Temperature-dependent regulation of morphogenesis**

Temperature-dependent regulation of morphogenesis is believed to centre on the heat-shock chaperone Hsp90. Depletion of Hsp90, or its pharmacological inhibition with geldanamycin results in filamentation in *C. albicans* (Shapiro et al. 2009), suggesting a role for Hsp90 in the repression of filamentous growth. Hsp90 is thought to negatively regulate the cAMP-PKA pathway through its co-chaperone Sgt1, which can directly bind the adenylyl cyclase Cyr1 (Shapiro et al. 2009; Shapiro, Zaas, et al. 2012). Hsp90 has also been shown to regulate morphogenesis through Cyclin Dependent Kinase (CDK) signalling. Filaments formed when Hsp90 function is compromised are delayed in mitosis, resembling those formed upon cell cycle arrest. This is thought to be due to Cdc28/Cdk1 being a client of Hsp90, requiring it for stability (Senn et al. 2012). Hsp90 has also been shown to regulate morphogenetic signalling from the CDK Pho85 and its cyclin Pcl1, to the transcriptional regulator Hms1 that is required for the expression of some filamentation specific transcripts (Shapiro, Sellam, et al. 2012). Hsp90 genetic screens have also shown the possibility of other roles in adaptation to different growth conditions (Diezmann et al. 2012). There are also other heat shock proteins, such as Hsf1 (Nicholls et al. 2011) that are thought to contribute to morphogenesis.

#### **1.4.6. Cell-cycle arrest-dependent morphogenesis.**

Events that perturb cell cycle progression in *C. albicans* are associated with a terminal morphogenetic switch to filamentous growth. These include treatment with drugs such as hydroxyurea (Fig. 1.5A.) (Bachewich et al. 2005) and nocodazole (Bai et al. 2002), which arrest cells in S-phase or mitosis respectively; and mutants of genes that are involved in cell cycle regulation, a list of which can be found in Fig. 1.5B (Berman 2006). The associated filamentation appears dependent on the cell cycle stage that the cells are arrested in; with G1 arrest by

*CLN3* depletion resulting in cell enlargement followed by the formation of what appear to be true hyphal filaments (Chapa et al. 2005); whereas arrest post initiation of S-phase results in bud elongation to form a filament that still has a constriction at the mother daughter boundary (Fig. 1.5A.) (Bachewich et al. 2005). Such post S-phase inhibition activates the spindle checkpoints, which are required for the associated filamentous growth phenotype. Nocodazole arrest filamentation requires the Mad2 spindle assembly checkpoint (Bai et al. 2002); whereas, *CDC5* repression (Fig. 1.5A.) requires the Bub2 mitotic checkpoint for filamentous growth (Bachewich et al. 2005). It still remains unknown whether these pathways function during normal hyphal growth in *C. albicans*.

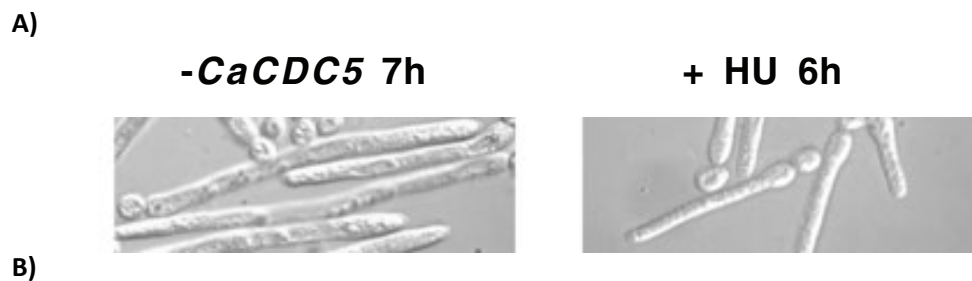


Table 1		
List of cell cycle conditions and mutants that cause changes in morphogenesis.		
Gene or condition	Cell cycle arrest <sup>a</sup> /delay stage	Altered morphology
Cln3-depletion	G <sub>1</sub> <sup>a</sup>	Large round, then hyphal
<i>cdc4Δ/Δ</i>	G <sub>1</sub>	Constitutive hyphal
Hydroxyurea treatment	S <sup>a</sup>	Polarized growth
<i>rad52Δ/Δ</i>	S/G <sub>2</sub>	Polarized growth
<i>grr1Δ/Δ</i>	G <sub>2</sub> /M?	Constitutive pseudohyphal
<i>fkh2Δ/Δ</i>	G <sub>2</sub> /M	Constitutive pseudohyphal
<i>clb4Δ/Δ</i>	G <sub>2</sub> /M, spindle assembly	Constitutive pseudohyphal
Cdc5p-depletion	M <sup>a</sup>	Polarized growth
Nocodazole treatment	M <sup>a</sup>	Polarized growth
Cib2p-depletion	Anaphase <sup>a</sup>	Highly polarized tubes
<i>SOL1</i> overexpression	Late mitosis	Highly polarized growth
<i>cdc14Δ/Δ</i>	Mitotic exit	Cell separation defects, hyphal growth defective

**Fig. 1.5. Cell cycle arrest filamentation in *C. albicans*.** Adapted from Berman 2006 and Bachewich et al 2005. A) Filaments formed on depletion of *CDC5* or addition of hydroxyurea. B) Table of cell cycle alterations and how they affect polarised growth in *C. albicans*.

#### 1.4.7. Hyphal-specific genes

The aforementioned signal transduction pathways for morphogenesis allow transcriptional changes to occur, dependent on the external environmental conditions that *C. albicans* encounters. For hyphal morphogenesis, one outcome of

the signal transduction pathways is to activate the expression of hyphal form specific genes. Gene expression studies in *C. albicans* have found a number of genes that are up-regulated during hyphal growth (Kadosh & Johnson 2005); and a common minimal set of genes that are required for hyphal growth under all conditions tested (Carlisle & Kadosh 2013). These include: genes for cell surface proteins that likely promote interactions with host cells (*HWP1*, *HYR1*, *ALS3/10* and *PHR1*), genes required for host invasion (*ECE1* and *SAP5*), and for proteins that are possibly mechanistically involved in hyphal germ tube growth (*CDC10*, *RDI1* and *KIP4*). Up-regulation of the transcription factor *UME6* on hyphal induction further activates the transcription of hyphal specific genes, forming a layer of positive feedback (Carlisle et al. 2009). *UME6* regulates the expression of the hyphal specific cyclin *HGC1*, which needs to be present in order to maintain hyphal growth (Carlisle & Kadosh 2010). *HGC1* is an example of a gene that is not significantly up-regulated on hyphal induction, but is essential for prolonged filamentous growth (Zheng et al. 2004). Many other such genes have been, and continue to be discovered through deletion studies (Uhl et al. 2003; Noble et al. 2010).

## **1.5. Regulation of Polarised Growth**

### **1.5.1. Budding yeast model**

Bud morphogenesis in *S. cerevisiae* is an extensively studied process, which highlights the conserved machinery used to bring about morphogenetic transitions (Howell & Lew 2012). Bud formation and growth is also closely linked with cell cycle progression. Initiation of this process involves bud site selection; a process that, in budding yeast, is dependent of the genetic content and mating type of the cell (Hicks et al. 1977). The primary machinery involved in this process is the Rsr1 GTPase module. Rsr1 is a Ras-like GTPase, whose over-expression can rescue cell with polarisation defects (Bender & Pringle 1989). Regulation of Rsr1 is carried out through the GTPase activating protein Bud2, and Guanine nucleotide Exchange Factor (GEF) Bud5 (Fig. 1.6.) (Bender 1993). Deletion of any of these components results in random bud site selection (Ruggieri et al. 1992; Park et al. 1993). Rsr1

localises to future sites of polarised growth and is required for the recruitment of the GEF of Cdc42, Cdc24, and possibly its subsequent activation (Park et al. 2002; Shimada et al. 2004). This leads on to polarisation of the actin cytoskeleton via the aforementioned GTPase Cdc42. Even in the absence of the above-mentioned Rsr1 module, Cdc42 can still polarise cells, albeit in a random fashion. Interestingly in the absence of Rsr1 only one bud still forms; this is thought to be due to multiple oscillatory clusters of Cdc42 forming which compete for resources until the largest cluster wins, thus bringing about cell polarisation at its location (Howell et al. 2009; Howell et al. 2012).

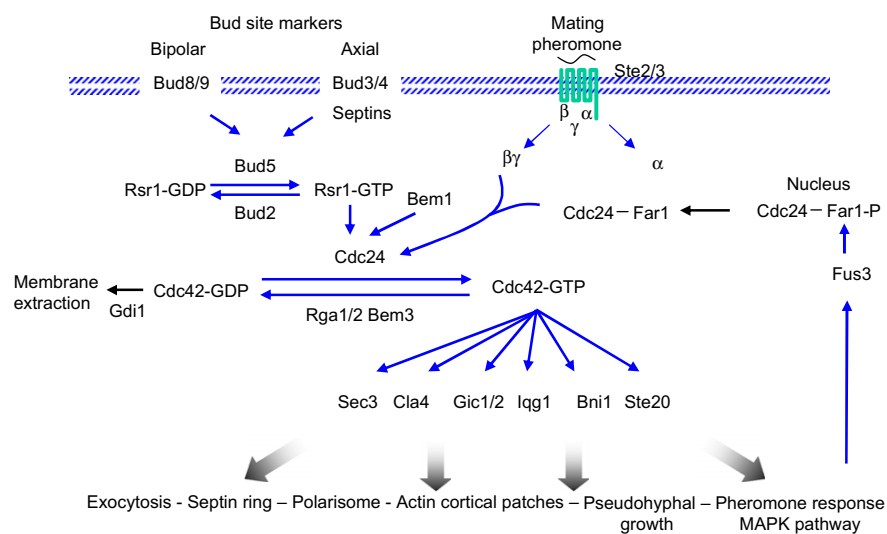


**Fig. 1.6. Roles of Cdc42 in *S. cerevisiae* morphogenesis.** Taken with permission from Sudbery 2008. Bud site selection is followed by Cdc42 activation to establish polarised growth via multiple signals.

As mentioned above, after bud site establishment the Cdc42 GTPase module becomes polarised to the incipient bud site, where it attached to the membrane through geranylgeranylation at its C-terminus (Ziman et al. 1993). Cdc42 is positively regulated by the essential GEF Cdc24 (Zheng et al. 1994), and negatively regulated by the GTPase activating proteins (GAPs) Bem3, Rga2 and its paralog Rga1 (Fig. 1.6.) (Smith et al. 2002). The guanine nucleotide dissociation inhibitor Rdi1 regulates Cdc42 by inhibiting GTP hydrolysis and extracting Cdc42 from the plasma membrane for recycling (Richman et al. 2004). Active Cdc42 at sites of polarised growth recruits a complex of Cdc24-Bem1-and the effector kinase Cla4, allowing activation of more Cdc42 molecules, thus forming a positive feedback loop (Kozubowski et al. 2008). Positive feedback is also thought to be obtained

through active Cdc42 orienting actin cables to the site of polarised growth, allowing more Cdc42 to be delivered (Wedlich-Soldner et al. 2003).

Active Cdc42-GTP is responsible for controlling many processes involved in polarised growth; such as: actin cable assembly, actin patch polarisation, exocyst complex formation and septin ring assembly (Fig. 1.6.). Active Cdc42 is required for localisation of the formin Bni1 (Evangelista et al. 1997), which is part of the polarisome complex of: Spa2, Bud6, Pea1 and Bni1. This complex nucleates the formation of actin cables away from the cell periphery, allowing secretory vesicles to be transported from the Golgi to the site of polarised growth (Sagot et al. 2002).

Cdc42 and Cdc24 are required for correct localisation of actin patches to sites of polarised growth (Adams et al. 1990); possibly through the effector kinase Cla4 or through Cdc42 GAP interaction with the endocytic machinery (Bi & Park 2012).

Cdc42 is known to interact with the exocyst landmark proteins Sec3 and Exo70 (Zhang et al. 2001; Wu et al. 2010), possibly allowing correct localisation of these components before delivery of the rest of the complex (Sec5, Sec6, Sec8, Sec10, Sec15, Exo84) on secretory vesicles. This complex then acts to promote fusion of secretory vesicles with the plasma membrane (He & Guo 2009).

The septins are a group of GTP binding proteins (Cdc10, Cdc11, Cdc3, Cdc12 and Shs1/Sep7) that form into higher ordered structures, acting as scaffolds and diffusion barriers (Oh & Bi 2011). Cdc42 in conjunction with Gic1/2 is required for the recruitment of septin complexes to the site of polarised growth (Cid et al. 2001; Iwase et al. 2006). Here the septin complexes attach to the plasma membrane, before undergoing a conformational change to ring structures that is dependent on the GTPase activity of Cdc42 (Zhang et al. 1999; Gladfelter et al. 2002). Cla4 has also been shown to be important for this process, further linking the role of Cdc42. The actin cytoskeleton is then thought to amend the septin ring into its final structure (Kadota et al. 2004).

Once the core machinery is in place transport of secretory vesicles to the polarisation site causes growth and expansion of the yeast bud to occur. Vesicles bleb off from the Golgi and associate with the type V myosin, Myo2, to be transported along actin cables to the polarisation site (Fig. 1.7.) (Pruyne et al. 2004). The process is regulated by the vesicle associated Rab GTPase Sec4 and its

GEF Sec2 (Salminen & Novick 1987; Walch-Solimena et al. 1997). Vesicles dock with the exocyst complex before fusion with plasma membrane, delivering membrane and materials required for new cell wall generation (Fig. 1.7.) (He & Guo 2009).

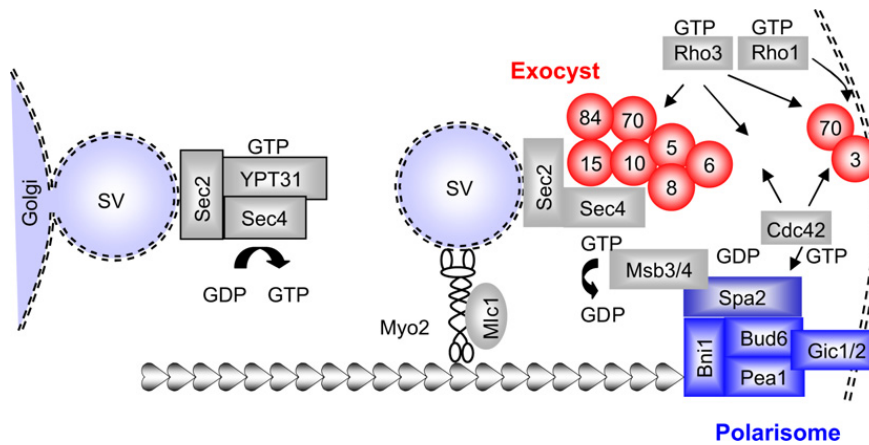


**Fig. 1.7. Polarised secretion in *S. cerevisiae*.** Taken with permission from Sudbery 2008. Vesicles from the Golgi associate with the Sec4 GTPase complex, facilitating association with the Myo2 motor, which carries the vesicle to sites of polarised growth via polarisome nucleated actin cables. Vesicles dock with the exocyst landmark proteins on the cell membrane allowing vesicle fusion and cell surface expansion.

Polarisation of the yeast bud tip occurs through G1 and G2 phases of the cell cycle; but this then switches to isotropic growth at G2/M, with Cdc42 localising around the cell periphery of the daughter bud (Park & Bi 2007). During mitosis polarity components then localise to the mother-daughter bud neck, regulating contraction of the actomyosin ring at cytokinesis (Bi & Park 2012).

### 1.5.2. Polarised growth of *C. albicans* hyphae

Using the *S. cerevisiae* model, it has been possible to postulate how hyperpolarised growth can occur to generate the hyphal filaments observed in *C. albicans*. Cdc42 and Cdc24 are again key regulators of this process, localising to a crescent at the hyphal tips; but are required at a higher concentrations than during yeast form growth (Bassilana et al. 2003). Evidence for a higher Cdc42 concentration comes from gene knockouts of the GAPs for Cdc42, Rga2 and Bem3, which results in hyperpolarisation of cell growth with characteristics of true

hyphal growth (Court & Sudbery 2007). Rga2 was found to be absent from hyphal tips, suggesting a mechanism by which removing a Cdc42 GAP could increase the local concentration of active Cdc42-GTP at the hyphal tip. The absence of Rga2 from the hyphal tips was later found to be phosphorylation dependent (Zheng et al. 2007). Localisation of Cdc42 is partially dependent on the *C. albicans* bud site selection homologues Rsr1 and Bud2. Absence of these proteins produces wider hyphae, suggesting that Rsr1 and Bud2 may be required for highly focused localisation of the Cdc42 module (Hausauer et al. 2005).

Other polarity components regulated by Cdc42 localise to a crescent at the hyphal tips. From here actin cables stretch 5-10µm back down the hypha to the Golgi apparatus (Fig. 1.8.), which is present in the germ tube (Sudbery 2011). The vesicle transport machinery (Myo2, Mlc1, Sec4/2) localise to a spot, just behind and distinct from the crescent of the exocyst and polarisome components (Jones & Sudbery 2010). This is an area rich in secretory vesicles that resembles the Spitzenkörper (apical body) present in other filamentous fungi (Crampin et al. 2005). Vesicles are thought to be delivered via actin cables to the Spitzenkörper (Fig. 1.8.), where they then diffuse away to dock with the exocyst on the plasma membrane. The position of a Spitzenkörper ensures that the focus of vesicle delivery is highly polarised, producing the observed hyphal morphology (Bartnicki-Garcia et al. 1989).

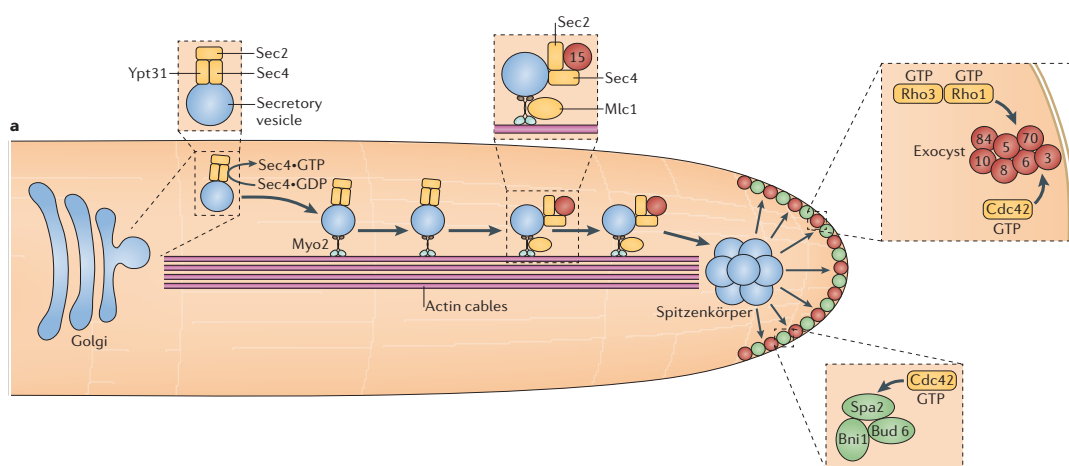


**Fig. 1.8. Polarised growth in *C. albicans* hyphae.** Secretory vesicles bleb off the Golgi apparatus and travel along actin cables, nucleated by the polarisome, to the Spitzenkörper. From here vesicles diffuse away to dock with the exocyst complex on the plasma membrane.

During hyphal growth septin complexes form different structures to those observed during yeast growth. Upon germ tube formation the septin Cdc11 localises to bands at the base of the germ tube, and a crescent at the tip of the germ tube (Sudbery 2001). This persists until the septin ring is formed inside the germ tube, not at the mother daughter boundary as in yeast. Possibly due to this, the nucleus migrates into the germ tube before division occurs.

Actin cables and patches are again key cytoskeletal components of polarised growth. Perturbing actin cable-mediated transport causes hyphal tips to swell (Hazan & Liu 2002), and deletion of components of the exocytic machinery prevents hyphal morphogenesis (Martin et al. 2007). Microtubules are also present along the length of the hyphal tube (Barton & Gull 1988), providing structures for nuclear migration and division (Finley & Berman 2005).

An important difference between hyphal morphogenesis and the production of a yeast bud is in the timing of events. Unlike during bud morphogenesis, hyphal elongation occurs independently of the cell cycle (Hazan et al. 2002). However there are clear morphological differences in hyphae formed at different stages of the yeast cell cycle; as hyphae formed after the cell has committed to making a bud still retain a constriction at the mother daughter boundary.

## **1.6. Regulation of cell separation**

A key event that has to occur during hyphal morphogenesis is the prevention of cell separation. This allows the generation of a long, multi-sectional hypha that can continue to extend from the apical compartment.

As previously mentioned, during bud formation and growth the septin subunits assemble into a ring. When yeast cells divide at the end of mitosis, the septin ring splits and contraction of the actomyosin ring occurs between the two septin rings, dividing the cytoplasm between the mother and daughter cell (cytokinesis) (Bi & Park 2012). A primary septum forms as the actomyosin ring contracts, where chitin is deposited to seal off the new daughter cell from the mother (Lesage & Bussey 2006). The actomyosin ring is then disassembled and the primary septum is reinforced with new cell wall material, forming a secondary

septum. Cell separation enzymes are then secreted to degrade the primary septum, allowing the mother and daughter cells to separate (Weiss 2012). Mitotic exit is regulated by the Cdc14 phosphatase, which is released from the nucleolus in early anaphase (Yoshida et al. 2002). Cdc14 activity is also required for cell separation, through the transcription factor Ace2, which controls transcription of genes required for septum degradation (Fig. 1.9A.) (Weiss 2012). During most of the cell cycle Ace2 remains inactivated by CDK dependent phosphorylation and kinase-independent functions of Pho85, retaining it in the cytoplasm (Mazanka & Weiss 2010). At the end of mitosis Ace2 is phosphorylated by the kinase Cbk1 to allow it to enter the nucleus and activate the transcription of septum degrading enzymes (Fig. 1.9A.). During early G1 phase Ace2 is then exported from the nucleus due to loss of Cbk1 phosphorylation.

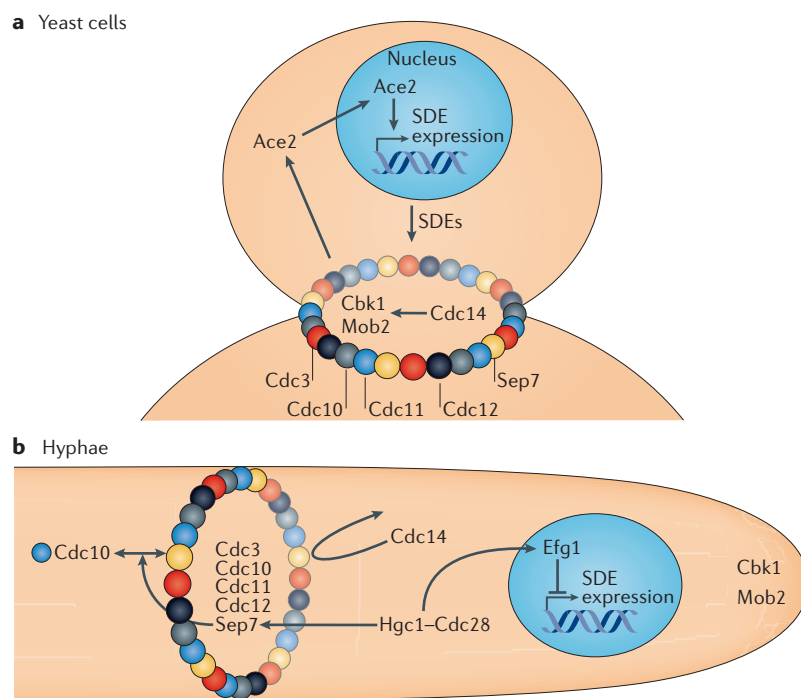


**Fig. 1.9. Regulation of cell separation in yeast and hyphal cells. A)** At the end of mitosis in yeast growth Cdc14 activates Cbk1 which then phosphorylates Ace2 to allow entry into the daughter cell nucleus where Ace2 activates the expression of cell separation enzymes, **B)** In hyphal growth Cdc14 is excluded from the septum to prevent Cbk1 activation and Ace2 nuclear entry. Cdk1-Hgc1 phosphorylates Efg1 to further prevent the expression of cell separation enzymes.

In *C. albicans* hyphae karyokinesis and cytokinesis occur in the hyphal tube, which again are followed by the formation of a septum as a barrier between the apical and sub-apical cell (Sudbery 2001). However in *C. albicans* the primary

septum is not degraded, thus allowing the compartments to remain attached. This process is regulated in part by the transcription factor Efg1, which is phosphorylated to prevent the expression of septum degrading enzymes during hyphal growth (Fig. 1.9B.) (Wang et al. 2009). There is also the possibility that Ace2 itself is directly regulated to prevent expression of these enzymes. The phosphatase Cdc14 is absent from the septum in *C. albicans* hyphae, but not during yeast growth (Fig. 1.9B.). This is likely to prevent the activation of Cbk1 and thus prevent Ace2 from localising to the apical cell nucleus. Cdc14 exclusion from the septum is thought to be partially dependent of the Cdk1 cyclin and Hgc1 (Clemente-Blanco et al. 2006), and the septin subunit Sep7 (González-Novo et al. 2008).

### **1.7. Role of post-translational modification in morphogenesis**

Although many proteins required for morphogenesis have been identified, how these proteins are regulated in the morphogenetic yeast to hyphae transition remains relatively unknown. This has made post-translational control of morphogenesis become an area of significant interest. Many proteins undergo reversible and irreversible modifications to regulate their function. Such modifications include: phosphorylation, ubiquitination, methylation, acetylation, sumoylation, neddylation and glycosylation.

Phosphorylation is an extensively studied reversible protein modification, required for the control of a diverse range of cellular processes. It involves kinase-mediated addition of the  $\gamma$ -phosphate from ATP to a serine, threonine or tyrosine residue in the target protein, creating a negatively charged patch on the protein. Phosphorylation can occur on one, or multiple sites in the case of proteins that are hyper-phosphorylated (Cohen 2000). Reversion of this event (de-phosphorylation) is through hydrolysis of the phosphate linkage, a process mediated by phosphatases. Phosphorylation can modify a proteins activity in several ways, such as: activating, deactivating or targeting a protein for degradation; it can change the subcellular localisation of a protein, or the interactions of the protein, be that with other proteins or molecules such as DNA/RNA and lipid structures (Cohen 2000). Phosphorylation can be used to transduce external signals from receptors to

intracellular effectors, as is found in the aforementioned cAMP-PKA and MAPK pathways. Another role of phosphorylation is during the shift to hyphal-promoting temperatures, where the heat shock protein Hsf1 is phosphorylated to aid in adaptation (Nicholls et al. 2011). CDKs have also been shown to be required for control of hyphal growth (Wang 2009). This will be covered in much greater detail in Chapter 3. The nuclear Dbf2-related kinase Cbk1 appears to exert a strong effect upon hyphal growth, as *cbk1Δ/Δ* mutants are completely unable to form hyphae (McNemar & Fonzi 2002). However the mechanisms by which Cbk1 influences hyphal growth remain relatively unknown. Current investigation of Cbk1's role in hyphal morphogenesis is focussed on how it regulates the hyphal repressor Nrg1 (Alaalm et al. unpublished)

Ubiquitination is a reversible addition of a ubiquitin moiety via isopeptide bond between the carboxyl terminus of ubiquitin and the amino group of a substrate lysine or cysteine. This occurs in a three step process involving activation (E1 enzyme), followed by transfer of activated ubiquitin to a ubiquitin-conjugating enzyme (E2 enzyme), and then finally ligation of the ubiquitin to the target via a ubiquitin ligase (E3 enzyme) (Fig. 1.10.) (Komander 2009). Multiple ubiquitin moieties can be added to form chains on a single target residue (E4 ubiquitin ligase). Removal of ubiquitin is controlled by ubiquitin-deconjugating enzymes. One of the first identified key roles of ubiquitin is the polyubiquitination of mitotic cyclins to target them to the proteasome for destruction at the end of the cell cycle (Seufert et al. 1995). However ubiquitination can also alter protein function along with targeting to specific cellular compartments (Komander 2009). *C. albicans* genome encodes two ubiquitin genes; the ubiquitin hybrid *UBI3* involved in ribosome biogenesis (Roig et al. 2000), and the polyubiquitin gene *UBI4* that when deleted causes cell cycle arrest filamentation (Leach et al. 2011), suggesting a possible role for ubiquitination in morphogenesis. Most ubiquitination targets in *Candida* so far have been found to be involved in metabolism (Fig. 1.10.) (Leach et al. 2011); however it is likely that roles in morphogenesis exist, as such in other related organisms.

Sumoylation is the addition of a small ubiquitin-like modifier (SUMO) to a target protein in a manner similar to that of ubiquitination (Fig. 1.10.) (Gill 2004). Deletion of the single SUMO gene *SMT3* in *C. albicans* results in morphological

abnormalities that, like deletion of the polyubiquitin gene *UBI4*, appear to be due to cell cycle delay (Leach et al. 2011). Proteomic analysis of sumoylation in *C. albicans* revealed that components of the cytoskeleton Tub1 and Mlc1, along with secretory pathway proteins Sec24 and Sec7, are *in vivo* sumoylation targets (Fig. 1.10.) (Leach et al. 2011). Sumoylation may also regulate septin ring dynamics as is found in the related *S. cerevisiae* (Johnson & Blobel 1999). Together this suggests a possible role for sumoylation in the initiation and maintenance of hyphal morphogenesis in *C. albicans*.

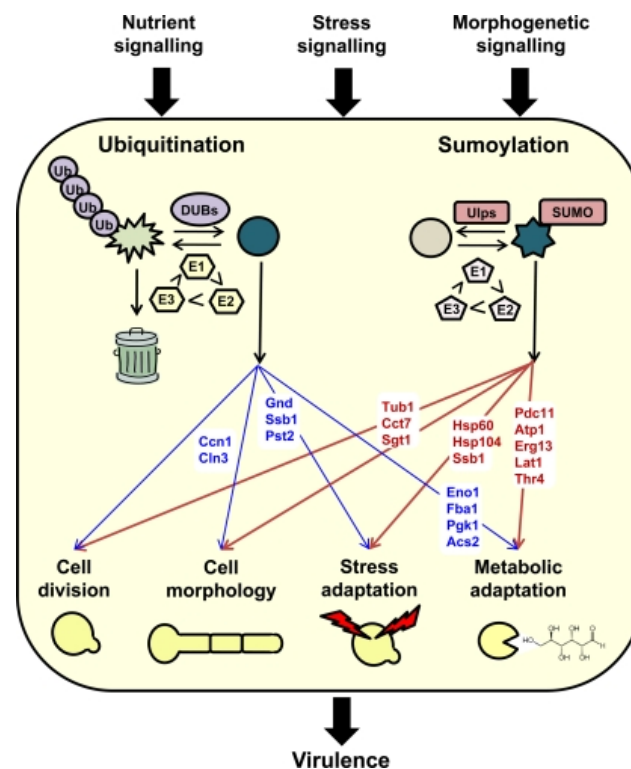


**Fig. 1.10. Roles of ubiquitination and sumoylation in *C. albicans*.** Taken with permission from Leach and Brown 2012. Diagram shows schematics of ubiquitin or SUMO addition, followed by ubiquitination and sumoylation targets in *C. albicans* and their functions.

Glycosylation, although not required specifically for morphogenesis, is important for the modification of cell wall proteins involved in *C. albicans* host invasion. Glycosylation is the addition of an oligosaccharide moiety to a protein, which generally occurs along the secretory pathway (Spiro 2002). Oligosaccharides can be added to an amino group of either asparagine (N-linked) or to the carboxyl group of serine, threonine or tyrosine residues (O-linked). Other

carbohydrate attachments such as the GPI anchors occur through glypiation between the C-terminus of the protein and cell membrane phospholipids (Spiro 2002). This is important for the aforementioned pH regulatory proteins Phr1 and Phr2. A similar mechanism is used to attach proteins to the mannan present in the fungal cell wall (Leach & Brown 2012).

### **1.8. Methods for studying kinases and their targets**

Kinases carry out phosphorylation events, adding the  $\gamma$ -phosphate group from ATP to the target protein in order to modify its function. In yeast the primary phosphorylation events occur on serine or threonine residues. Some tyrosine phosphorylation is present, however it is uncommon (Chi et al. 2007).

In order to determine whether a protein of interest is a phospho-protein there are multiple lines of investigation that can be taken. Firstly the primary sequence of the protein can be analysed for the presence of known kinase phosphorylation motifs (Songyang et al. 1996). This will also give suggestions of possible kinases that may phosphorylate the protein of interest. To determine whether the protein of interest is phosphorylated *in vivo* different biochemical methods can be used (Peck 2006). In order to study the protein there needs to be a means of isolating it from the rest of the proteins in the cell and to detect it after Western blotting. To do this the protein can either be epitope tagged, or a specific antibody raised against the protein. A caveat to looking at the phosphorylation of a specific protein is that phosphorylation is a dynamic process, and may only occur at certain times, or under certain conditions.

Addition of phosphate groups to proteins can alter their mobility on SDS-PAGE (Wegener & Jones 1984), which may be due to the negative charge from the phosphate preventing SDS from binding, and thus altering its electrophoretic mobility. An electrophoretic mobility shift due to phosphorylation should be sensitive to phosphatase treatment (Peck 2006). It may not always be possible to detect such shifts, and can only be reliably done with proteins that are hyper-phosphorylated.

In order to better separate out phosphorylated isoforms of proteins 2-Dimensional gel electrophoresis can be performed. This first separates proteins by

their isoelectric point, and then by their mass. This is a useful technique when multiple phosphorylated isoforms of a protein exist, or for carrying out global studies on changes in the phospho-proteome (Hardie 1999).

*In vivo* phosphorylation of a protein can also be detected using specific antibodies that recognise phosphorylated residues, such as phospho-serine or threonine (Tingley et al. 1997). In order to do this the protein of interest has to be immunoprecipitated (IP'd) to avoid background signal on the subsequent Western blot.

In order to determine the exact sites that are phosphorylated *in vivo*, mass-spectrometry based phospho-peptide mapping can be carried out (Mann et al. 2002). To do this a sufficient amount of the protein has to be purified from cells. The protein is then digested, ideally with multiple proteases, before running the sample on a Matrix Assisted Laser Desorption quantitative Time Of Flight (MALDI-qTOF) machine. This will generate an ion spectrum for the protein fragments, which can be compared to the expected spectra for the fragments. In doing this, the change in mass to charge ratio by the addition of a phosphate group can be detected.

Knowing the exact residues and motifs that are phosphorylated will provide suggestions to the kinase that is responsible; as previously mentioned the different classes of kinases have different target motifs. To test whether a kinase can directly phosphorylate a substrate, an *in vitro* kinase assay can be carried out (Peck 2006). This involves epitope tagging and purifying the suspected kinase; and either purifying the substrate, or using a recombinant substrate expressed in *E. coli*. The kinase and the substrate are then incubated at physiological temperatures with either radiolabelled  $\gamma$ -P<sup>32</sup> Adenosine triphosphate (ATP), or non-labelled ATP. Phosphorylation of the substrate is then detected by autoradiography or Western blot with a phospho-specific antibody (Ross et al. 2002).

To determine the physiological consequences of phosphorylation, the phospho-acceptor sites can be mutated; either preventing phosphorylation from occurring, or mimicking the phosphorylation charge to observe the effects of constitutive phosphorylation (Figurski 2013). Mutating the serine, threonine or tyrosine in the phosphorylation motif to alanine removes the hydroxyl group, thus preventing kinase mediated addition of the  $\gamma$ -phosphate from ATP. Mutation of

serine to aspartic acid or threonine to glutamic acid mimics the negative charge that would be present from the addition of a phosphate group. This was first shown for the Simian Virus 40 T-antigen (Schneider & Fanning 1988).

### **1.9. Aims of thesis study**

The cyclin dependent kinase (CDK) Cdk1 is known to have important roles in hyphal morphogenesis (Wang 2009), which will be discussed in detail in Chapter 3. Due to the importance of this kinase, the PhD project was designed to identify regulatory targets of Cdk1 during hyphal growth. Initially bioinformatics was used to identify potential CDK targets. The phosphorylation states of the candidates were determined during yeast and hyphal growth. Candidate proteins that showed a differential phosphorylation pattern between yeast and hyphal growth were then studied further.

The candidature of the PhD is split over two locations; with the initial investigation of potential CDK targets being carried out at the University of Sheffield. Further characterisation of differentially regulated potential CDK targets was then carried out at the Institute for Molecular and Cell Biology in Singapore.

# 2

## Materials and Methods

---

### 2.1. *C. albicans* Growth Media

#### **Yeast Extract Peptone Dextrose (YEPD)**

1% w/v Bacto™-Yeast Extract (BD Biosciences, USA), 2% w/v Bacto™-Peptone (BD Biosciences, USA), 2% w/v D-Glucose, 80mg. l<sup>-1</sup> Uridine.

#### **Yeast Extract Peptone Galactose (YPG) for expression from *GAL1* promoter**

1% w/v Bacto™-Yeast Extract, 2% w/v Bacto™-Peptone, 2% w/v Galactose, 80mg. l<sup>-1</sup> Uridine.

#### **Glucose Minimal Media (GMM)**

0.67% w/v Yeast Nitrogen Base (YNB) without Amino Acids (BD Biosciences, USA), 2% w/v D-glucose

#### **GMM Dropout Media for selection of prototrophic transformants**

0.67% w/v Yeast Nitrogen Base without Amino Acids, 1.5% w/v Bacto™-agar. Uridine, Arginine or Histidine were used at a final concentration of 80mg. l<sup>-1</sup> for auxotrophic strains.

#### **Media for repression of the *MET3* Promoter**

YEPD or GMM media supplemented with 10mM methionine and 2mM cysteine.

#### **Media for expression of FLP Recombinase from the *SAP2* promoter**

2.34% Yeast Carbon Base (BD Biosciences, USA), 0.04% Bovine Serum Albumin (BSA), 100µg. ml<sup>-1</sup> Uridine.

### **5-Fluoroorotic acid media (5-FOA) Agar**

0.67% Yeast Nitrogen Base without Amino Acids, 2% Glucose, 2% Bacto™-Agar. A 5-FOA solution was added to the autoclaved mix to a final concentration of 0.1%. Amino Acid supplements were added depending on the selection required.

## **2.2. *E. coli* culture media**

### **Luria-Bertani (LB)**

1% w/v Bacto™-tryptone (BD Biosciences, USA), 0.5% w/v Bacto™-Yeast Extract, 1% w/v NaCl, pH 7.0

### **2TY**

1.1% w/v Bacto™-tryptone, 1% w/v Bacto™-yeast extract, and 0.5% w/v NaCl.

## **2.3. *C. albicans* culture conditions**

### **Yeast Morphology**

An overnight stationary phase culture was diluted to an OD<sub>600</sub> of 0.8 into YEPD or GMM at pH 4.0 and a temperature of 30°C. The culture was then grown at 30°C for the required amount of time.

### **Hyphal Morphology**

An overnight stationary phase culture was diluted to an OD<sub>600</sub> of 0.8 into YEPD or GMM at pH 7.0 and a temperature of 37°C, along with the addition of 20% v/v of Fetal calf serum. Cells were then grown at 37°C for the required amount of time.

### **Elutriation**

An overnight stationary phase culture of *C. albicans* in YEPD was diluted 1/10,000 times into a litre of fresh YEPD media, and left to grow overnight at 30°C. The OD<sub>600</sub> of the culture was measured, as to ensure that the culture was still in log phase growth the next morning.

The elutriating rotor (Beckman JE 5.0) was set up, and SDW was passed through at a flow rate of 200mls/min; the rotor was turned to help facilitate the removal of air bubbles from the chamber. The centrifuge was set to 1000rpm and then left to spin for a few minutes, until all air bubbles were out of the chamber and tubing. The speed was increased to 4200rpm; and once settled, the flow rate set at 60mls/min. The YEPD culture was gently sonicated and then added to the sample chamber via the input tube, ensuring that the pressure in the pipes did not go above 10psi. After all the cells had entered the chamber, the input was switched back to SDW and left to flow through for 5 minutes. The centrifuge speed can then be decreased to 4100rpm to allow cells to begin migration through the chamber. Once the output fractions show small un-budded cells, these can be collected. The centrifuge speed was decreased 100rpm at a time to a minimum of 3800rpm, while constantly checking the fractions under the microscope to ensure small un-budded cells were present. These cells were combined and then used directly in yeast and hyphal time-course experiments.

#### **Inactivation of the Cdc28 analogue sensitive allele with 1NM-PP1**

A 15mM stock of 1NM-PP1 (Calbiochem) was made up in Dimethylsulfoxide (DMSO) and added to the pre-warmed culture media to a final concentration of 30 $\mu$ M.

#### **Repression of genes under the control of the tetracycline promoter**

Doxycycline-HCl was added to YEPD media to a final concentration of 20 $\mu$ g/ml. For efficient shutdown, overnight cultures were grown with doxycycline before re-inoculation into fresh media containing doxycycline.

## **2.4. Microscopy**

### **Microscope apparatus**

Microscopy was carried out using a Leica DMR microscope fitted with a Hamamatsu digital camera and interfaced with metamorph software (Molecular Devices); or with an Olympus Delta Vision Fluorescence Microscope (Applied

precision). All images were taken at x100 magnification unless otherwise stated. For fluorescence imaging the FITC channel (ex 494nm, em 518nm) was used for GFP signals, and the DAPI channel (ex 358nm em 461nm) was used for 4', 6-Diamidino-2-Phenylindole, Dihydrochloride (DAPI) signals to visualize nuclear DNA. For M-cherry epitope detection, an excitation of 587nm and an absorbance of 610nm was used.

### **Formaldehyde fixation of cells for microscopy**

Formaldehyde was added to a final concentration of 1.05%; the sample was mixed by inversion and was left to incubate at room temperature for 10minutes. Cells were pelleted by centrifugation at 3000rpm for 45seconds, and then re-suspended in 1xPBS. Fixed cells can then be stored at 4°C.

### **Ethanol fixing of cells**

1ml of culture was pelleted by centrifugation at 3000rpm for 45s, and then re-suspended in 500µl of 70% ethanol. Cells were stored at 4°C until required. Before microscopy, cells were washed once with 1xPBS and then re-suspended in 1xPBS.

### **Pepsin treatment to separate clumped hyphae**

1ml of a fixed hyphal cells were pelleted by centrifugation at 3000rpm for 45s. Cells were then re-suspended in 500µl of pepsin solution (5mg/ml in 55mM HCl) and mixed by pipetting. The samples were then incubated for 30mins at 37°C on a shaking platform. Cells were pelleted again as above and then re-suspended in 500µl of 1xPBS.

## **2.5. Molecular biology: DNA techniques**

### **Buffers and solutions**

#### **50x Tris-Acetate EDTA (TAE) Buffer:**

24.2% w/v Tris-base, 5.71% v/v Acetic acid, 0.05M EDTA

### **10x Tris-EDTA (TE) Buffer:**

100mM Tris-HCl pH 7.5, 10mM EDTA

### **Polymerase Chain Reaction (PCR)**

PCR fragments were generated from *C. albicans* genomic DNA or from pre-existing vectors using the KOD Hot-start Polymerase (Merck-Novagen). 50µl reactions contained the following: 5µl 10x KOD buffer, 5µl dNTPs (2mM each), 2µl Magnesium sulphate (25mM), 0.5µl each primer from 100µM stock and 200ng genomic DNA or 1ng plasmid DNA. The reaction was then made up to 49µl before 1µl KOD polymerase was added. PCR reaction conditions were as follows:

<b><u>Step</u></b>	<b><u>Temperature</u></b>	<b><u>Time</u></b>	<b><u># Cycles</u></b>
Initial	94°C	2mins	<b>1</b>
Denaturation	94°C	15secs	
Annealing	Primer Dependent	30secs	<b>30</b>
Extension	72°C	20secs/Kb	

### **Purification of PCR products**

PCR products were purified either using the PCR Cleanup kit (QIAGEN) or by Ethanol-Sodium acetate precipitation. For precipitation; 1/10<sup>th</sup> volume of 3M sodium acetate pH5.3 was added to the sample, followed by 2 times the new volume of 100% ethanol. Samples were then left at -20°C for a minimum of 1hr to allow the DNA to precipitate.

### **DNA agarose gel electrophoresis**

PCR products, along with cut and uncut plasmid vectors, were run on a 1% agarose TAE gel in order to separate DNA fragments by size. 1% w/v agarose was dissolved in 1xTAE buffer through gentle heating. When cooled sufficiently, 0.05% v/v of ethidium bromide was added to the gel before it was poured into Bio-Rad wide or mini sub cell apparatus, and the well comb added. Once set, gels were placed in the corresponding tanks and submerged with 1xTAE buffer. Samples were combined with 6xDNA loading dye to facilitate loading into the gel wells.

DNA ladders, hyperladder-1 (Bioline) or NEB 1Kb DNA Ladder, were used as size standards. Gels were run at constant volts between 100-140V. Visualisation of ethidium bromide intercalated DNA was carried out using a trans-illuminator with attached camera.

### **Restriction Endonuclease- based cloning**

Purified PCR products (32µl) or plasmids containing inserts were digested in a total volume of 40µl, and the final vector (23µl) was digested in a total volume of 30µl. Digestions were carried out overnight at 37°C using equal units of the required enzymes and appropriate buffers (New England Biolabs). Both digests were run on a DNA mini-gel, with the appropriate fragments being cut out and purified using a QIAquick Gel Extraction Kit (QIAGEN). The eluted fragments were combined in a final volume of 13µl to be used in ligation with 1.5µl 10x T4 DNA ligation buffer and 1µl T4 DNA ligase (Fermentas). Ligations were carried out at room temperature for a minimum of 45mins or overnight at 4°C. 1µl of the ligation reaction was then transformed in XL1-Blue electrocompetent *E. coli* cells (Aligent Technologies) by electroporation at 1.80V. Cells were plated out on LB-ampicillin plates and left to incubate at 37°C overnight. Colonies were selected for mini-prep the following day and then checked by digestion, followed by sequencing.

### **Site-Directed Mutagenesis**

Mutagenesis was carried out using either the Site-Directed Mutagenesis kit (#200519) or Multi Site-Directed Mutagenesis kit (#200514) from Aligent Biotechnologies, or by manual PCR mutagenesis. For the kits, mutagenesis was carried out as stated in the manufacturers instructions.

### **Skip-PCR**

Skip-PCR was used to remove the intron from the C-terminal fragments that were expressed as a GST fusion protein for the kinase assay. Primers were designed to amplify the stretches of sequence adjacent to the sequence to be removed. The 3' primer of the upstream fragment contained 10bp of reverse sequence from the beginning of the downstream fragment; whereas the 5' primer of the downstream fragment contained 10bp of forward sequence from the end of the upstream

fragment. Both fragments were then used as templates in another PCR reaction with the 5' primer from the upstream fragment and the 3' primer from the downstream fragment. This amplifies across the new template allowing generation of a fragment with the desired piece of sequence removed.

### ***E. coli* Heat-shock transformation**

Chemically competent DH5 $\alpha$  cells were thawed on ice and then left to incubate with 1-2 $\mu$ l of plasmid or ligation for 15mins. Cells were then heat-shocked by placing in a 42°C waterbath for 45sec. Cells could be plated straight out, or undergo a recovery step through addition of 300 $\mu$ l 2TY media and 1hour incubation at 37°C. After recovery different aliquots were plated out on 2TY+Ampicillin agar in order to get single colonies from over-night incubation at 37°C.

### ***E. coli* Electroporation transformation**

Electrocompetent XL1-Blue *E. coli* cells (Aligent Technologies) were thawed on ice. 1 $\mu$ l of ligation or mutagenesis, or 0.5 $\mu$ l of pure plasmid was added to a 20 $\mu$ l aliquot of the cells. The cells were then transferred to an electrocuvette (Bio-Rad) and pulsed once at 180V. The cells were then plated out on LB plates with 0.1mg/ml ampicillin and incubated as above.

### **Preparation of plasmid DNA from *E. coli***

*E. coli* were cultured in 5-10mls of LB-Ampicillin media over-night or in 2TY media with 0.1mg/ml ampicillin for 4-5hours. Cells were then lysed, and plasmid DNA purified using the QIAGEN plasmid mini kit (#12125). Final elution was carried out in 50-100 $\mu$ l SDW.

### ***C. albicans* genomic DNA isolation**

Purification of genomic DNA was carried out either with the Yeast Genomic DNA purification kit (Epicenter), or using the following protocol:

1.5ml of an overnight culture was pelleted in a screw cap tube by a short spin at maximum speed, and then re-suspended in 250 $\mu$ l extraction buffer (0.01M Tris-HCl pH 8, 1% w/v SDS 0.1M NaCl and 1mM EDTA). Equal volume of acid washed

glass beads (0.4mm) were added to the cells. Samples were then vortexed at maximum speed for 1min, before addition of 150µl of 1xTE buffer and 300µl of Phenol: Chloroform: Isoamyl alcohol (PCI) (25:24:1). After vortexing for a further 3mins, the samples were centrifuged at 13,000rpm for 5mins. The aqueous layer was then removed to a fresh tube, and an equal volume of PCI added followed by vortexing for 1min to mix. Samples were centrifuged as above, with the aqueous layer of the supernatant again removed to a fresh tube. To this, 1/10<sup>th</sup> volume of 3M sodium acetate pH 5.2 was added, followed by 2x the new volume of 100% ethanol. Samples were placed at -20°C for a minimum of 1hour to allow the DNA to precipitate. The genomic DNA was pelleted by centrifugation at 13,000rpm for 30mins at 4°C, and then washed twice with 70% ethanol. The pellet was then dried in a sterile hood to remove remaining ethanol, before being re-suspended in 50µl of SDW. RNase treatment was carried out by the addition of 1µl of 10mg/ml RNase A, and the samples were incubated at 37°C for 30mins. After this, DNA was precipitated as above, and re-suspended in a final volume of 30µl.

**PCR to generate a transformation cassette.** For initial C-terminal GFP-epitope tagging of proteins, transformation cassettes were used. For this the primers contained 5' and 3' homology to the region for targeted recombination in the *C. albicans* genome, as well as plasmid specific sequences to allow amplification of a plasmid of GFP plus a terminator region and a selectable marker. To generate enough DNA cassettes for transformation, ten 50µl reactions were carried out. Each of these contained: 25µl Biomix-red (Bioline), 1µl plasmid DNA (diluted 1/20 from mini-prep stock), 2µl each primer from a 5µM stock and 20µl SDW. Reactions were carried out as follows:

<u>Step</u>	<u>Temperature</u>	<u>Time</u>	<u># Cycles</u>
Initial Denaturation	94°C	2mins	<b>1</b>
Denaturation	94°C	30secs	
Annealing	Primer Dependent	30secs	<b>35</b>
Extension	68°C	1min/Kb	
Final Extension	68°C	10mins	<b>1</b>

PCR reactions were then combined and the DNA precipitated using sodium acetate and ethanol.

### ***C. albicans* Transformation**

**Electroporation.** Competent cells were prepared by taking a 10ml overnight culture in YEPD, pelleted and washed twice with equal volumes of SDW. Cells were then re-suspended in 4ml 1x Lithium Acetate-TE (0.1M LiAc pH 7.2, 1xTE pH 8.0) and incubated under gentle agitation at 30°C for 45mins. 100µl 1M DTT was then added to the cells and left to incubate for a further 15min. Cells were washed twice with 10ml cold SDW and once with 2ml cold 1M sorbitol. Cells were finally re-suspended in 2ml of 1M sorbitol and kept at 4°C until required (for up to 2 days). 40µl of the competent cells were added to 10µl of purified digested plasmid DNA, gently mixed and added to the cold electroporation cuvette. The cells were pulsed once at 1.65V and then plated out on GMM agar with the appropriate selective supplements, then left to incubate at 30°C for 2 days.

**Fast Yeast-Transformation.** Rapid heat-shock transformation of *C. albicans* was carried out using the Fast Yeast Transformation kit from G-biosciences.

**Overnight Heat-shock transformation.** A *C. albicans* overnight culture was re-inoculated into 50ml fresh YEPD to an OD<sub>600</sub> of 0.2 (~300µl), and then incubated with agitation at 30°C until the culture reached an OD<sub>600</sub> of 0.6 (~4hours). Cells were spun down at 3000rpm for 5min at room temperature. These were then washed with 1ml of SDW and transferred to an eppendorf tube, where the cells were pelleted by a short spin. The cells were washed in 1ml of transformation buffer (1xTE pH 8.0, 0.1M Lithium Acetate pH 7.2 (LiAc)), pelleted, and then re-suspended in 200µl transformation buffer. 100µl of this solution was placed in transformation and control tubes; to which the following was added: 36µl 1M LiAc, 30µl 10xTE and 10µl denatured salmon sperm DNA. To the transformation tube, 100µl purified PCR product or 30µl digested plasmid was added, and to the control tube 100µl SDW was added. 300µl 60% PEG 4000 was then placed in each tube,

and the contents mixed by gentle pipetting. The tubes were then placed in a 30°C water-bath overnight.

The next day 40µl DMSO was added to each tube, and placed at 42°C for 15min. After this, cells were pelleted by a 30sec spin at up to 8000rpm and then washed once with 1ml SDW. Cells were then re-suspended in 200µl SDW, and 2x110µl aliquots of the transformation were plated out on two GMM plates with appropriate selective markers. The whole of the control tube was plated out on a single plate. The plates were left at 30°C for 2days to allow colonies to grow.

***C. albicans* colony PCR.** A 10µl pipette tip was used to take a small amount of the colony, which was then re-suspended in 8.5µl SDW in a 200µl PCR tube. The solution was then boiled at 100°C for 6mins, and then placed at -80°C for a minimum of 1hour. The solution was defrosted and used in a 25µl PCR reaction containing 12.5µl Biomix-red (Bioline) and 2µl of each checking primer from a 5µM stock. Primers were designed to amplify a checking region of less than 1kb. PCR conditions were as for transformation cassette generation, except that 40 cycles were carried out and the extension step was for a maximum of 1min.

## **2.6. Molecular biology: RNA techniques**

### **Buffers and Solutions:**

**DEPC treatment of solutions:** Diethylpyrocarbonate (DEPC) was added to solutions to a final concentration of 0.1% v/v. The containing bottles were then left at 37°C overnight to allow RNase inactivation to occur, before autoclaving to break down the toxic DEPC.

**10x Formaldehyde-Agarose (FA) running buffer:** 200mM 3-[N-morpholinopropanesulfonic acid (MOPS), 50mM sodium acetate, 10mM EDTA. The solution was brought to pH 7.0 with NaOH. When diluting to 1x FA Buffer, 0.02% v/v of 37% formaldehyde was added.

**5x RNA loading dye:** 80µl of 0.5M EDTA pH 8.0, 2ml 100% glycerol, 4ml 10x FA buffer, 720µl 37% formaldehyde, 3.084ml formamide and 16µl saturated aqueous bromophenol blue solution. The loading dye was made up to 10mls with DEPC treated SDW.

### **Isolation of total cell RNA from *C.albicans***

A 25ml culture was grown for 3hours from a starting OD<sub>600</sub> of 0.2. Cells were then harvested by centrifugation and washed once with DEPC-treated SDW before the pellets were frozen at -80°C. For the Microarray experiments, RNA was extracted using the RNeasy kit from QIAGEN following the manufacturers instructions for yeast cells. For Microarray analysis, RNA was eluted in 88µl RNase free water before DNase treatment in a total volume of 100µl with 2µl of RNase free DNase 1 (Roche) at 37°C for 15min. Total RNA was then re-purified using the RNeasy column with cleanup protocol.

### **RNA Formaldehyde-Agarose (FA) gel electrophoresis**

1.2g agarose was melted in 80mls of RNase free (DEPC-treated) water, before addition of 10mls of 10x FA running buffer. The gel was then cooled to 65°C before 5µl of ethidium bromide and 1.8ml of 37% formaldehyde was added before the gel was poured in a fume hood. The set gel was left to equilibrate in 1x FA-formaldehyde running buffer before samples were loaded. RNA samples were heated to 65°C in RNA loading dye and then cooled for 5mins on ice before running on the gel. The gel was run at 90V for 60min, and the RNA samples visualised on a transilluminator.

### **Microarray experiments**

*C. albicans* whole genome arrays were manufactured by Microarrays Inc. These contain the full ORF sequences from assembly 19 of *C. albicans* genome.

Microarray hybridization experiments were carried out with the help of Vivien Koh of the microarray facility at Biopolis, Singapore. 10µg total RNA from samples was given to the microarray facility, where all subsequent steps were carried out. Spreadsheets generated from these experiments were then analysed by Dr. Ian Sudbery using the Limma method to generate a list of genes with a two-fold or

greater significant ( $p=0.05$ ) change in gene expression. Array data was then organized and analysed using Microsoft Excel.

### **Reverse Transcription (RT)**

Prior to qPCR reactions 0.5 $\mu$ g of total RNA was taken for cDNA synthesis. 0.5 $\mu$ g of RNA was treated with DNase 1 (Roche) in a 10 $\mu$ l reaction volume for 30mins at 37°C. To this reaction 1.25 $\mu$ l oligo dT (100mM stock) was added along with 1 $\mu$ l (10mM) dNTPs and 0.75 $\mu$ l DEPC SDW. The reaction was then incubated at 75°C for 10mins to inactivate the DNase and denature the oligo dT primer. After this 4 $\mu$ l Superscript III 5x buffer was added along with 1 $\mu$ l (100mM) DTT, 1 $\mu$ l RNase inhibitors and 1 $\mu$ l of the superscript III enzyme (Invitrogen). For each sample a negative RT reaction was carried out where everything was added except the RNase inhibitors and the reverse transcriptase enzyme. Reactions were placed in a PCR machine at 25°C for 5mins, followed by 1hour at 50°C and then finally 15mins at 70°C. 30 $\mu$ l of SDW was then added to the reaction before 40 $\mu$ l was removed and combined with an equal volume of SDW. This was done in order to dilute the sample for subsequent qPCR reactions.

### **qPCR reaction**

Primer pair stocks were made up to 5 $\mu$ M for use in reactions. For each pair triplicate reactions were set up for both the positive and negative RT reactions. Each reaction contained the following: 1 $\mu$ l (5 $\mu$ M) primer pair stock, 3 $\mu$ l SDW, 5 $\mu$ l 2xSensiMix (Bioline) and 1 $\mu$ l of the cDNA or negative RT reaction mix. A triplicate with no template control was also carried out for the primer pair, where the reaction contained everything except the 1 $\mu$ l of RT reaction mix, which was substituted with water. This controls for any signal that the primers may generate in the absence of the template. Reactions were carried out as follows:

<b><u>Step</u></b>	<b><u>Temperature</u></b>	<b><u>Time</u></b>	<b><u>No. cycles</u></b>
Initial Denaturation	95°C	10mins	1
Denaturation	95°C	30secs	
Annealing	58°C	30secs	40
Extension	72°C	30secs	

The 2xSensiMix contains the DNA intercalating dye SYBR green that preferentially binds to newly synthesised double stranded DNA. SYBR green is a fluorophore, absorbing blue light (497nm) and emitting green light (520nm). Thus the emission fluorescence can indicate the amount of double stranded DNA present, allowing DNA amplification during PCR to be followed in real-time. To measure the amount of DNA present after each PCR cycle, the Rotor-Gene 6000 system from QIAGEN was used. This provides a curved plot of the emission level over time, from which the 'takeoff' value can be obtained. Samples with a higher template content to begin with will therefore 'take-off' earlier than those with less template, thus allowing the transcript levels to be compared across samples.

### **Normalisation of qPCR data**

To normalise the expression levels for the genes of interest, a 'housekeeping' control gene was used, whose expression should be independent of the strain background the RNA was isolated from. Primers to the *ADE2* gene were used as the housekeeping control to normalise the expression levels of the experimental samples, controlling for possible differences in the amount of mRNA in the starting sample. This was done by subtracting the takeoff value for value for the gene of interest from that of *ADE2*, giving the value for  $\Delta CT(ADE2-GENE)$ . This value was then used as the exponent to the experimentally derived amplification value, providing an approximate value for the amount of template cDNA present. This method makes the assumption that the amplification value for the control gene is the same as that of the gene to be experimentally tested.

The  $\Delta\Delta CT$  method was also used to compare the expression of genes in mutant strains with that of wild-type strains. This was done by subtracting the  $\Delta CT$  values from above, i.e.  $\Delta\Delta CT = \Delta CT(\text{Mutant}) - \Delta CT(\text{Wild-type})$ , giving the expression of a particular gene in the mutant strain as a percentage of that in the wild-type strain.

## **2.7. Molecular biology: protein biochemistry techniques**

### **Buffers and Solutions**

**RIPA Lysis Buffer:** 50mM Tris-HCl pH7.2, 0.1% v/v Triton X-100, 0.1% w/v sodium deoxycholate, 150mM NaCl

**SG Lysis Buffer:** 50mM Tris-HCl [pH7.4], 150mM KCl, 1% NP-40

For lysis buffers, PhosSTOP Phosphatase Inhibitor Cocktail Tablets (Roche #04906837001) and cOmplete ULTRA Tablets, mini, EDTA-free (Roche #05892791001) were added as required

**6x Protein Loading Buffer:** 30% v/v glycerol, 10% w/v SDS, 9.3% w/v DTT, 0.012% w/v bromophenol blue, 50mM Tris-HCl pH 6.8

**2x Lamelli Loading dye:** 125mM Tris-HCl [pH 6.8], 10%v/v glycerol, 5%v/v  $\beta$ -mercaptoethanol, 2%w/v SDS 0.015%v/v bromophenol blue

**SDS-PAGE (Running) Buffer:** 125mM Tris-base, 460mM glycine, 0.5% w/v SDS

**Tris-Glycine (Transfer) Buffer:** 125mM Tris-base, 460mM glycine, 20% v/v methanol

**Tris Buffered Saline (TBS) Buffer:** 0.242% w/v Tris-Base with 0.8%w/v NaCl. The pH is then adjusted to 7.6 using HCl.

**Phosphate Buffered Saline (PBS) (10x):** 16g.l<sup>-1</sup> NaCl, 400mg.l<sup>-1</sup> KCl, 2.88g.l<sup>-1</sup> Na<sub>2</sub>HPO<sub>4</sub>, 480 mg.l<sup>-1</sup> KH<sub>2</sub>PO<sub>4</sub> adjusted to pH 7.4.

When TBS or PBS was used for blocking and washing solutions in western blotting, 0.1% v/v Tween-20 was added.

### **Enhanced chemiluminescence (ECL)**

**ECL 1:** 100mM Tris-HCl pH 8.5, 2.5mM Luminol (in DMSO) and 0.4mM p-Coumaric acid.

**ECL 2:** 100mM Tris-HCl pH 8.5, 0.0006% v/v hydrogen peroxide

Solutions were mixed in a 1:1 ratio and then incubated on the protein bound membrane.

### **Extraction of total cell protein from *C. albicans***

A 24 or 48hour culture was inoculated into fresh media to an OD<sub>600</sub> of 0.8, and grown under yeast or hyphal inducing conditions. Cells were harvested by centrifugation at 3500rpm for 1min, and then washed with 1ml of chilled SDW allowing transfer to a screw-cap microfuge tube. The cells were then pelleted by short spin and snap frozen in liquid nitrogen or dry ice. The frozen pellets were weighed, with 2-3x the volume of RIPA including appropriate inhibitors added, along with 1x volume of acid washed glass beads (0.4mm). Homogenization was carried out using the TOMY Microsmash system (TOMY, Japan), with 3-4x 1min beating at 5000rpm followed by a short spin at 4°C. Alternatively; a Fast-prep machine from MP Biomedical was used at 4.5 m/s for two bursts of 30s; or 3x30s bursts in a mini bead-beater (Bio-spec products). Glass beads and cell debris were removed by centrifugation at 15,000rpm for 10mins. The protein lysate can be removed for downstream applications or added to loading dye and boiled to run on a gel or store at -80°C.

### **Bradford Protein Assay**

Protein standards were made at 0.2, 0.40, 0.6, 0.8 and 0.9mg/ml using Bovine Serum Albumin (BSA) in RIPA buffer with the necessary inhibitors. The Bio-Rad protein assay reagent was diluted 1:5 to give a working solution. 20µl of each standard were added to 1ml of the reagent and the absorbance measured at A<sub>595</sub>, using 20µl of RIPA buffer in 1ml of reagent as a blank. The readings were used to plot a standard curve, from which the equation of the line was taken to calculate other protein concentrations from a given A<sub>595</sub> reading. Samples were diluted 1:20

before addition of reagent to ensure that a reading of less than  $OD_{596}=1$  was present.

### **Lambda phosphatase treatment of proteins**

Dephosphorylation of proteins was carried out using Lambda Phosphatase (NEB # P0753). 400 units of lambda phosphatase were used for 40 $\mu$ l 10mg/ml lysate in a total reaction volume of 50 $\mu$ l, including 1mM  $MnCl_2$  and 1x PMP buffer. The reaction was carried out at 30 °C for 1 hour on a shaking platform set at 200rpm.

### **Immunoprecipitation (IP) of Epitope tagged proteins**

**For Co-Immunoprecipitation and Western blot analysis:** 1-2mg of total cell extract was used at a final concentration of 2mg/ml. To this 20 $\mu$ g of agarose conjugated antibody or 50 $\mu$ l of magnetic bead conjugated antibody (Miltenyi Biotec) was added. Incubation was carried out at 4°C under gentle rotation for between 30mins – 2hours. For the magnetic beads, purification of the target protein was carried out using the magnetic column, following the manufacturers instructions. For agarose IPs, the beads were gently pelleted by short spin of <5000rpm at 4°C. The beads were then washed 3-4 times with 10x bead volumes of RIPA lysis buffer. An equal volume of 2x Lamelli loading dye was then added to the beads, which were subsequently boiled for 5-10mins to remove the bound protein. Samples could then be used directly in SDS-PAGE, or stored at -80°C for future use.

### **Large scale IP to purify protein of interest for phospho-peptide mapping.**

~1g total cell lysate was obtained from ~40g (dry weight) of cells. The lysate was centrifuged for a further 15mins at 15,000rpm to ensure that all cellular debris was cleared. 60 $\mu$ l Ez-view anti-HA agarose (Sigma-Aldrich) was added to the lysate in a falcon tube and left to mix by rotation overnight at 4°C. Pelleting and washing of the beads was carried out as above, ensuring at each step that as much of the agarose mix was obtained as possible. Beads were boiled for 10mins in 30 $\mu$ l 2x Lamelli buffer and stored at -80°C. Beads were then boiled for a second time before loading onto a SDS-PAGE gel.

## **Separation of proteins by SDS-PAGE**

Proteins were separated according to their molecular weight using the Bio-Rad® Protean II/III discontinuous electrophoresis system. Gels were run at a constant current of 25 milliamps (mA) and electric potential was limited to 125V maximally.

### **SDS-PAGE resolving gel**

375mM Tris-HCl pH 8.8, 0.1% w/v SDS, 0.1% ammonium persulfate. 50% Acrylamide:Bis-acrylamide (37.5:1) was added to final concentrations of either 6, 7, 8, 10 or 12%. Gel solutions were made up to 10ml with SDW and then 0.0006 % v/v Tetramethylethylenediamine (TEMED) was added to start the polymerization process. Gels were cast using 1 or 1.5mm casting plates from Bio-Rad.

### **SDS-PAGE stacking gel**

50mM Tris-HCl pH 6.8, 0.1% w/v SDS, 0.1% ammonium persulfate, 5% 37.5:1 Acrylamide:Bis-acrylamide. Gel solutions were made up to 5mls with SDW and then 0.001% v/v TEMED was added. 10 or 15 well stacking combs were then placed in the gel, which was left to set.

### **Staining of SDS-PAGE Gels**

SDS-PAGE gels were washed in SDW and then stained with InstantBlue™ Coomassie stain (Expedeon Protein Solutions) under agitation for one hour. To remove background stain, the gel was then washed in SDW.

### **Isolating bands from gels and dehydration for shipment**

Bands were cut from a Coomassie-stained gel in a sterile environment using a razor blade. Gel pieces were transferred to micro-centrifuge tubes and washed twice with 300µl of SDW. After removal of the water, 300µl of methanol was added, the tubes were vortexed and left to incubate for 10mins. The methanol was discarded, and the tubes then dried in a vacuum centrifuge.

### **Mass spectrometry for identification of gel bands**

Dehydrated bands from SDS-PAGE gels were sent to the Center for Functional Genomics (CFG) at the University of Albany for identification (<http://www.albany.edu/genomics/proteomics.html>).

### **Phospho-peptide Mapping**

Phospho-peptide mapping was carried out by the Proteomics facility at the IMCB in Singapore. IP samples were prepared as previously described to a final volume of 50µl in protein loading dye. Samples were run on NuPAGE precast gels from Invitrogen before Colloidal Blue staining. Bands for Fkh2 were removed and digested with trypsin before running on the LTQ Velos ETD machine (Thermo scientific).

### **Western blotting (transfer) to Nitrocellulose or PVDF membranes**

SDS-PAGE gels were equilibrated in transfer buffer along with foam pads, filter paper and Nitrocellulose membrane all cut to the required size. For PVDF, the membrane was first soaked in methanol for 1min and then equilibrated in transfer buffer for a minimum of 5min. Transfer apparatus was set up as required for the Bio-Rad Protean II system; an ice block was added and then the tank topped up with chilled transfer buffer. For one gel, transfer was carried out at 220mA for 2hours; and for 2 gels, 300mA for 3hours. All transfers were carried out at 4°C to avoid over-heating.

### **Antibody blotting of membranes**

Membranes were placed in 50ml tubes and blocked in 10% milk powder in either TBS-T (Nitrocellulose) or PBS-T (PVDF) for an hour at room temperature, or overnight at 4°C. The membranes were blotted with antibodies in 5% BSA made up in either TBS-T or PBS-T for the required membrane. Antibody concentrations used are listed in section 2.12. The membranes were incubated with primary antibodies for a minimum of 1hour to overnight at 4°C, with the membrane being washed 3 times for 5mins in the correct buffer, before addition of the secondary

antibody. The membrane was blotted with secondary antibodies for 1-3hours, again at 4°C; and then washed 4 times as before.

Alternatively; blocking and antibody blotting was carried out using a SNAP i.d. system (Millipore). A 1% BSA in TBS-T buffer was used for blocking and antibody incubation following the manufacturers instructions. For ECL detection of the antibody bound proteins, the above-mentioned ECL reagents were mixed in equal quantities and incubated on the membrane for 3min. Membranes were then either exposed to X-ray films that were then developed, or developed using a Genegnome (Syngene) Chemiluminescence Imager.

### **Antibody stripping from membranes**

PVDF membranes were re-hydrated and washed with TBS-T twice before 1hour incubation with 10mls stripping buffer (2% SDS, 62.5mM Tris-HCl pH 6.8, 0.8%  $\beta$ -mercaptoethanol) in a rolling falcon at room temperature. The blot was then washed sufficiently under the deionized water tap, before 5x10min washes with TBS-T. The membrane could then be re-blocked for subsequent antibody probing.

### **Glutathione S-Transferase (GST) fusion protein purification**

BL21 *E. coli* strain were transformed with the pGEX-4T1 N-terminal GST expression vector (GE Healthcare) containing the desired protein fragment. The *E. coli* were cultured overnight in LB plus 0.1mg/ml ampicillin at 37°C and then diluted 1:100 into fresh media. Cells were grown to an OD<sub>600</sub> of 0.7 before the addition of isopropylthio- $\beta$ -galactoside (IPTG) to a final concentration of 1mM. The cultures were then grown for a further 4hours before harvesting by centrifugation at 4,500rpm for 10mins. Cell pellets were washed twice in 1xPBS and then snap frozen in liquid nitrogen. Pellets were re-suspended in 1xPBS with protease inhibitors before 4 rounds of sonication for 30secs at maximum strength, with 1 min on ice in between. Triton X-100 was then added to the solution to a final concentration of 1%, which was left to incubate for 30mins at 4°C. After this, the lysate was cleared by centrifugation at 15,000rpm for 30mins at 4°C. During this time 1 $\mu$ l of Glutathione sepharose 4B beads(GE Healthcare) per ml of culture was taken and washed 3 times with cold PBS. The glutathione sepharose beads were added to the cleared lysate and then left to incubate for 2hours-overnight at 4°C.

The mixture was then run through a Bio-Rad disposable column, with the glutathione sepharose beads settling at the bottom. The beads were then washed three times with 2mls of cold PBS. Elution of the GST fusion protein was carried out three times, incubating the beads with 500 $\mu$ l of Elution buffer (20mM Tris-HCl pH 8.0, 100mM NaCl, 10% glycerol and 20mM glutathione) at 4°C for 15mins. Protein concentrations were quantified either using a Bradford assay (Bio-Rad), or using a Nano-drop Spectrophotometer (Thermo-scientific) to measure the absorbance of aromatic residues at 280nm. Samples of the GST fusions were stored at -80°C until required.

### **Kinase Assay**

**2x Kinase assay buffer:** 100mM Tris-HCl pH7.5, 2mM EGTA, 0.02% v/v Tween-20, 2mM DTT, 2mM  $\beta$ -glycerophosphate, 20mM magnesium chloride.

Cells expressing an epitope tagged version of the required kinase were grown in the conditions where phosphorylation of the target protein is normally observed. The cells were then harvested and lysed in RIPA buffer, and 2mg of total lysate was used to IP the kinase using an antibody to the epitope tag. The IP was washed 3 times with RIPA buffer (containing 150mM NaCl), before being re-suspended in 25 $\mu$ l of 2x kinase assay buffer. GST kinase substrates were diluted to 1mg/ml and 24 $\mu$ l was taken and added to the kinase reactions. For positive reactions 1 $\mu$ l of ATP was added from a 250mM stock to give a final concentration of 5mM. For negative reactions, 1 $\mu$ l of GST elution buffer was added. Reactions were incubated at 30°C for 1hour with gentle agitation. The beads were then pelleted and the reaction mixture removed and boiled in 10 $\mu$ l 6x protein loading dye. The beads were then re-suspended in 25 $\mu$ l RIPA buffer with 5 $\mu$ l protein loading dye and boiled separately. 15 $\mu$ l of the samples were run on a 10% SDS-PAGE gel and Western Blot was performed with an anti-phosphoserine CDK antibody (Cell-signalling technologies). Membranes were then stripped and re-probed with an anti-GST antibody (Santa-Cruz).

## 2.8. *C. albicans* strains used in this study

Strain	Genotype	Source / Reference
BWP17	<i>ura3::λimm434/ura3::λimm434 his1::hisG/his1::hisG arg4::hisG/arg4::hisG</i>	Wilson <i>et al.</i> , 1999
<i>FKH2-YFP</i>	BWP17 <i>FKH2/FKH2-YFP:URA3</i>	This Study
<i>19.1948-GFP</i>	BWP17 <i>19.1948/19.1948-GFP:URA3</i>	This Study
<i>19.3469-GFP</i>	BWP17 <i>19.3469/19.3469-GFP:URA3</i>	This Study
<i>SFL1-YFP</i>	BWP17 <i>SFL1/SFL1-YFP:URA3</i>	This Study
<i>FKH2-GFP in cdc28-1as</i>	BWP17 <i>cdc28::HIS1/cdc28<sup>F80G</sup>:ARG4, FKH2/FKH2/FKH2-GFP:URA3</i>	Made from Sinha <i>et al.</i> 2007
<i>FKH2-GFP in ccn1Δ/Δ</i>	BWP17 <i>HIS1::ccn1/ccn1::ARG4, FKH2/FKH2/FKH2-GFP:URA3</i>	This Study
<i>FKH2-GFP in hgc1Δ/Δ</i>	BWP17 <i>HIS1::hgc1/hgc1::ARG4, FKH2/FKH2/FKH2-GFP:URA3</i>	This Study
<i>FKH2-GFP in Cln3-sd</i>	BWP17 <i>Fr<sub>t</sub>::cln3/ARG4:P<sub>MET3</sub>-6Myc-CLN3, FKH2/FKH2/FKH2-GFP:URA3</i>	Made from Zeng <i>et al.</i> 2012
<i>FKH2-GFP in Clb2-sd</i>	BWP17 <i>clb2::HIS1/P<sub>MET3</sub>-CLB2:URA3::clb2, FKH2/FKH2/FKH2-GFP:ARG4</i>	Made from Bensen <i>et al.</i> 2005
<i>FKH2-GFP in Clb4-sd</i>	BWP17 <i>clb4::ARG4/P<sub>MET3</sub>-CLB4:URA3::clb4, FKH2/FKH2/FKH2-GFP:HIS1</i>	Made from Bensen <i>et al.</i> 2005
<i>fkh2/FKH2</i>	BWP17 <i>FKH2/fkh2::ARG4</i>	This Study

<i>fkh2Δ/Δ (URA<sup>+</sup>)</i>	BWP17 <i>URAF::fkh2/fkh2::ARG4</i>	This Study
<i>fkh2Δ/Δ (URA<sup>-</sup>)</i>	BWP17 <i>frt::fkh2/fkh2::ARG4</i>	This Study
<i>fkh2/FKH2-YFP</i>	BWP17 <i>ARG4::fkh2/FKH2-YFP:URA3</i>	This Study
<i>FKH2-YFP, CDC12-MCherry</i>	BWP17 <i>FKH2/FKH2-YFP:URA3, CDC12/CDC12-MCherry:ARG4</i>	This Study
<i>FKH2-6xMyc</i>	BWP17 <i>FKH2/FKH2/FKH2-6xmyc:URA3</i>	This Study
<i>FKH2-HA</i>	BWP17 <i>FKH2/FKH2-HA:URA3</i>	This Study
<i>fkh2(6A)-GFP</i>	BWP17 <i>frt::fkh2/fkh2::ARG4/fkh2(T7A, S503A, S573A, T583A, S643A, S674A)-GFP:URA3</i>	This Study
<i>fkh2(6E)-GFP</i>	BWP17 <i>frt::fkh2/fkh2::ARG4/fkh2(T7E, S503D, S573D, T583E, S643D, S674D)-GFP:URA3</i>	This Study
<i>fkh2(15A)-GFP</i>	BWP17 <i>frt::fkh2/fkh2::ARG4/fkh2(T7A, S503A, S573A, T583A, S643A, S674A, S14A, T100A, S150A, S226A, T448A, T514A, S627A, T638A, S656A)-GFP:URA3</i>	This Study
<i>fkh2(15E)-GFP</i>	BWP17 <i>frt::fkh2/fkh2::ARG4/fkh2(T7E, S503D, S573D, T583E, S643D, S674D, S14D, T100E, S150D, S226D, T448E, T514E, S627D, T638E, S656D)-GFP:URA3</i>	This Study
<i>fkh2(11A)-GFP</i>	BWP17 <i>frt::fkh2/fkh2::ARG4/fkh2(S503A, S573A, T583A, S643A, S674A, S226A, T448A, T514A, S627A, T638A, S656A)-GFP:URA3</i>	This Study
<i>POB3-HA, fkh2Δ/FKH2-YFP</i>	BWP17 <i>ARG4::fkh2/FKH2-YFP:URA3, POB3/POB3-HA:HIS1</i>	This Study

<i>POB3-HA, fkh2Δ/fkh2(6A<sub>CDK</sub>)-YFP</i>	BWP17 <i>frt::fkh2/fkh2::ARG4/fkh2(T7A, S503A, S573A, T583A, S643A, S674A)-GFP:URA3, POB3/POB3-HA:HIS1</i>	This Study
<i>POB3-HA, fkh2Δ/fkh2(6E<sub>CDK</sub>)-YFP</i>	BWP17 <i>frt::fkh2/fkh2::ARG4/fkh2(T7A, S503A, S573A, T583A, S643A, S674A)-GFP:URA3, POB3/POB3-HA:HIS1</i>	This Study
<i>GIN4-6xMyc</i>	BWP17 <i>GIN4/GIN4-6xMYC</i>	Li et al. 2012

## **2.9. *E. coli* strains used in this study**

<b>Strain</b>	<b>Genotype</b>	<b>Source</b>
DH5α	<i>F<sup>-</sup>, supE44, ΔlacU169 (80lacZΔM15), hsdR17, recA1, endA1, gyrA96, thi-1, relA1</i>	Delta Biotechnology
XL1-Blue	<i>recA1 endA1 gyrA96 thi-1 hsdR17 supE44 relA1 lac [F' proAB lacIqZΔM15 Tn10 (Tetr)]</i> .	Aligent Technologies
BL-21	<i>E. coli</i> B <i>F<sup>-</sup>, ompT, hsdS (rB -, mB -), gal, dcm</i>	G.E. Life Sciences

## 2.10. Vectors used in this study

Vector	Description	Source
pCIP10U $P_{FKH2}$ -FKH2-GFP	FKH2-6xMyc in CIP10U vector with <i>XhoI</i> -6xMyc-UTR- <i>PstI</i> cut out and replaced with <i>XhoI</i> -GFP-UTR- <i>PstI</i> fragment	This Study
pCIP10U $P_{FKH2}$ -FKH2-GFP H3ins	pCIP10U $P_{FKH2}$ -FKH2-GFP vector with <i>HindIII</i> restriction site in <i>FKH2</i> promoter	This Study
pCIP10U $P_{FKH2}$ -FKH2(6A <sub>MS</sub> )-GFP	pCIP10U $P_{FKH2}$ -FKH2-GFP H3ins vector with <i>fkh2</i> mutations: S226A, S503A, T583A, S643A, S656A, S674A.	This Study
pCIP10U $P_{FKH2}$ -FKH2(6A <sub>CDK</sub> )-GFP	pCIP10U $P_{FKH2}$ -FKH2-GFP H3ins vector with <i>fkh2</i> mutations: T7A, S503A, S573A, T583A, S643A, S674A.	This Study
pCIP10U $P_{FKH2}$ -FKH2(6E <sub>CDK</sub> )-GFP	pCIP10U $P_{FKH2}$ -FKH2-GFP H3ins vector with <i>fkh2</i> mutations: T7E, S503D, S573D, T583E, S643D, S674D.	This Study
pCIP10U $P_{FKH2}$ -FKH2(15A)-GFP	pCIP10U $P_{FKH2}$ -FKH2(6A <sub>CDK</sub> )-GFP with further <i>fkh2</i> mutations: S14A, T100A, S150A, S226A, T448A, T514A, S627A, T638A, S656A.	This Study
pCIP10U $P_{FKH2}$ -FKH2(15E)-GFP	pCIP10U $P_{FKH2}$ -FKH2(6E)-GFP with further <i>fkh2</i> mutations: S14D, T100E, S150D, S226D, T448E, T514E, S627D, T638E, S656D.	This Study
pCIP10U $P_{FKH2}$ -FKH2(1-426)-GFP	<i>AscI</i> - $P_{FKH2}$ ( <i>HindIII</i> ins)-FKH2(1-1278bp)- <i>XhoI</i> fragment PCR amplified from pCIP10U $P_{FKH2}$ -FKH2-GFP H3ins and cloned into pCIP10U with GFP 3' of <i>XhoI</i> cloning site.	This Study
pCIP10A $P_{FKH2}$ -FKH2-GFP	<i>NotI</i> -URA3- <i>MluI</i> fragment from pCIP10U $P_{FKH2}$ -FKH2-GFP	This Study

pCIP10U <i>P<sub>FKH2</sub>(BamHI)FKH2-6xMyc</i>	pCIP10U <i>P<sub>FKH2</sub>-FKH2-6xMyc</i> with <i>BamHI</i> restriction site introduced between the promoter and beginning of <i>FKH2</i> gene	This Study
pCIP10U <i>P<sub>GAL1</sub>FKH2-6xMyc</i>	<i>pCIP10U P<sub>FKH2</sub>(BamHI)FKH2-6xMyc</i> with <i>FKH2</i> promoter swapped with <i>AscI-P<sub>GAL1</sub>-BamHI</i> PCR fragment.	This Study
pCIP10U <i>P<sub>GAL1</sub>-FKH2-3xHA</i>	pCIP10U <i>P<sub>GAL1</sub>FKH2-6xMyc</i> with <i>XhoI-6xMyc-UTR-PstI</i> fragment replaced with <i>XhoI-3xHA-UTR-PstI</i> fragment	This Study
pCIP10U <i>P<sub>GAL1</sub>-FKH2-GFP</i>	pCIP10U <i>P<sub>GAL1</sub>-FKH2-3xHA</i> with <i>XhoI-3xHA-UTR-PstI</i> replaced with <i>XhoI-GFP-UTR-PstI</i> fragment	This Study
pBKs <i>FKH2</i> URAF Del	<i>KpnI-FKH2(5')-XhoI</i> and <i>NotI-FKH2(3')-SacII</i> fragments cloned upstream and downstream respectively of <i>C. albicans</i> URA Flipper selectable marker	This Study
pBKs <i>FKH2 ARG4</i> Del	pBKs <i>FKH2</i> URAF Del with <i>XhoI-URAF-NotI</i> replaced with <i>XhoI-P<sub>ARG4</sub>ARG4-NotI</i>	This Study
<i>FKH2-3xHA</i> in pCIP10U	<i>kpnI-FKH2(CT)-XhoI</i> fragment of <i>FKH2</i> cloned into pCIP10U with 3xHA 3' of <i>XhoI</i> cloning site	This Study
PGEX-4T1	N-terminal fusion GST expression vector with multiple cloning site 3' of GST	G.E. Life Sciences
GST- <i>FKH2(CT)</i>	<i>BamHI-FKH2(CT)-XhoI</i> fragment generated by skip PCR from pCIP10U <i>P<sub>FKH2</sub>-FKH2-GFP</i> to remove intron, cloned into pGEX-4T1	This Study
GST- <i>fkh2(CT)6A<sub>CDK</sub></i>	<i>BamHI-FKH2(CT)6A<sub>CDK</sub>-XhoI</i> fragment generated by skip PCR from pCIP10U <i>P<sub>FKH2</sub>-fkh2(6A<sub>CDK</sub>)-GFP</i> to remove intron, cloned into pGEX-4T1	This Study
pCIP10A <i>POB3-HA</i>	<i>KpnI-POB3(CT)-XhoI</i> fragment cloned upstream of HA epitope sequence in pCIP10A vector	This Study

pCIP10A <i>SRP1</i> -HA	<i>KpnI-SRP1(CT)-XhoI</i> fragment cloned upstream of HA epitope sequence in pCIP10A vector	This Study
pCIP10H <i>POB3</i> -HA	<i>POB3</i> -HA in pCIP10A vector with the <i>Candida</i> selectable <i>ARG4</i> marker swapped to <i>HIS1</i>	This Study
pCIP10A <i>CDC12</i> -MCherry	<i>kpnI-CDC12(CT)-XhoI</i> fragment sub-cloned into pCIP10A M-cherry vector	This Study

## 2.11. Primers used in this study

Primer	Description	Sequence (5' to 3')
19.1948 Rev Check	3' Primer to check ORF19.1948 N-terminal GFP tag	CCTCCATCTCCCCTGATGACG
19.1948-S1 Fwd	5' Primer for GFP tagging ORF19.1948 at the N-terminus	CCGAATAAACTCACTAAACTGACAGTGACAGTTT TAACTATACAAAGTTAAGGTTGCAAAAATTAAC CCGAAGCTTCGTACGCTGCAGGTC
19.1948-S2-GFP Rev	3' Primer for GFP tagging ORF19.1948 at the N-terminus	GGTTAGATCTCGGATCTTTTTTATCGGTGTATTC ATAGACACCATTGGATAATTTGTGATGACTCCA TAGCACCTGCGCCAGCCCCTGCGC
FKH2-Fwd Check	5' Primer to check FKH2 C-terminal YFP tag	GGGCGACCACAAGGCCAGCTAGG
FKH2-URA Rev	3' Primer for YFP tagging FKH2 at the C-terminus	CCTCTTATGTATGTAATTATTACGTATATACGTG TTATGTATCGTTCCTAAATCTACCTTTGTCAATG GTCTAGAAGGACCACCTTTGATTG
FKH2-YFP Fwd	5' Primer for YFP tagging Fkh2 at the C-terminus	CGAGAGAGGGAAAATGATGAAACCAATTCGCCA TTTAAAAAAAACAACGGACTGAAATGATTGAT CTGGGTGGTGGTTCTAAAGGTGAAGAATTATT
FP3-GFP	5' Primer to check N-terminal GFP tagging	CTCCAATTGGCGATGGCCC
19.3469-S1 Fwd	5' Primer for GFP tagging Orf19.3469 at the N-terminus	GTTAGTAGTTAGTAGTAGTAGTGAGAGAGAGAG TGTGTGTGTGACACAAAATACAACGACGCG ATC GAAGCTTCGTACGCTGCAGGTC
19.3469-S2-GFP Rev	3' Primer for GFP tagging Orf19.3469 at the N-terminus	TTCAAGTTCCTTTTTTAAGTGGAGTCTTTGCC TTTGGTTGTCCATTATCAATTATCGTTGCTGACA TAGCACCTGCGCCAGCCCCTGCGC

19.3469 Rev Check	3' Primer to check Orf19.3469 N-terminal GFP tag	GGACTATCTAGCATATCATCAGC
<i>SFL1</i> -YFP Fwd	5' Primer for YFP tagging <i>SFL1</i> at the C-terminus	AATGATAATAAAAACGATAACGGTAATAGTGAT GACAATGGGAACGATCATAAAAAGAGAAAATTA GAAGGTGGTGGTTCTAAAGGTGAAGAATTATT
<i>SFL1</i> -URA Rev	3' Primer for YFP tagging <i>SFL1</i> at the C-terminus	GGCTTATTGATGAACGAACAATCAATCAGAGTT CGGTGCGCTTATTTACAATTTCTCGTGAGTAGAC AGTCTAGAAGGACCACCTTTGATTG
<i>SFL1</i> Fwd Check	5' Primer to check <i>SFL1</i> C-terminal YFP tag	GTCACCTGAGTAATAAATCGC
<i>FKH2-KpnI</i> AF	5'Primer to amplify 5' region upstream of <i>FKH2</i>	GGTACCCTTTATCAACCAATAACACAC
<i>FKH2-XhoI</i> BR	3' Primer to amplify 5' region upstream of <i>FKH2</i>	CTCGAGGTAAATCCTAGCAAAAAAATG
<i>FKH2-NotI</i> CF	5'Primer to amplify 3' region downstream of <i>FKH2</i>	GCGGCCGCCACTTCACTCACACAGATATA
<i>FKH2-SacII</i> DR	3' Primer to amplify 3' region downstream of <i>FKH2</i>	CCGCGGGGAATTTGATATATCATTGAA
T3	5' Sequencing primer upstream of cloning sites in pCIP10 and pBKs	GCAATTAACCCTCACTAAAGG
T7	3' Sequencing primer downstream of cloning sites in pCIP10 and pBKs	TAATACGACTCACTATAGGG
<i>FKH2</i> Del Chk Fwd	5' Primer for checking <i>FKH2</i> deletions	GAACAAAAAATTAAGACAGAAC

URAF Del Rev Chk	3' primer for checking URA flipper deletions	CGGAAATCTATTGTTGTTGTCAC
ARG4 Del Rev Chk	3' primer for checking ARG4 cassette deletions	GAAATGACTGAATTATGTCCGGTC
FKH2+5' <i>AscI</i> Fwd	5' Primer to amplify FKH2 and 600bp of its promoter	GGCGCGCCAGCACTTTTGATCATTACAG
FKH2 <i>XhoI</i> Rev	3' Primer to amplify FKH2	CTCGAGCAGATCAATCATTTTCAGTCCG
FKH2 Fwd Seq 1	FKH2 sequencing primer, binds in promoter	CAA CCA ATA ACA CAC TTT TGA TTC
FKH2 Fwd Seq 2	FKH2 sequencing primer	CAG GAT ATG ATA AAT GCA GTG G
FKH2 Fwd Seq 3	FKH2 sequencing primer	GAA CAA ACG AAT TTC AAG TGG
FKH2 Fwd Seq 4	FKH2 sequencing primer	CTC AGC AAC AAA AAC AAC AAC
FKH2 (Pro) <i>HindIII</i> insertion	Mutagenic primer for <i>HindIII</i> mutation in FKH2 Promoter	AATTGGAAGCAAAAAGTAAGAA AAGCTT TCTTTATCCTGTTTTTTTTTA
FKH2 T7A	Mutagenic primer to mutate T7 to A in Fkh2	ATG TCA GCA CAA TTT ATC GCA CCG AAA AAG CGT CCC
FKH2 T7E	Mutagenic primer to mutate T7 to E in Fkh2	CGA TTA TTT ACA AAT GTC AGC ACA ATT TAT CGA GCC GAA AAA GCG TCC CCA CTC AC
FKH2 S14A	Mutagenic primer to mutate T14 to A in Fkh2	CCGAAAAAGCGTCCCCACGCACCACTAGATAGTA ATGAATTACTTC

<i>FKH2</i> S14D	Mutagenic primer to mutate T14 to D in Fkh2	CCGAAAAAGCGTCCCCACGATCCACTAGATAGTA ATGAATTACTTC
<i>FKH2</i> T100A	Mutagenic primer to mutate T100 to A in Fkh2	CCAGTAATACTAATATAACTGCACCTTTAATAGA TATTGACTTGGG
<i>FKH2</i> T100E	Mutagenic primer to mutate T100 to E in Fkh2	CCAGTAATACTAATATAACTGAACCTTTAATAG ATATTGACTTGGG
<i>FKH2</i> S150A	Mutagenic primer to mutate S150 to A in Fkh2	GTCAAAAAGTTAATGTTGATGCACCAAATGTTA ATGCATTACATTC
<i>FKH2</i> S150D	Mutagenic primer to mutate S150 to D in Fkh2	GTCAAAAAGTTAATGTTGATGATCCAAATGTTA ATGCATTACATTC
<i>FKH2</i> S226A	Mutagenic primer to mutate S226 to A in Fkh2	GATAAAGCTCATCTAACTCATGCCCTTCATCTA TTTCAGCAAACCTCG
<i>FKH2</i> S226D	Mutagenic primer to mutate S226 to D in Fkh2	GATAAAGCTCATCTAACTCATGACCCTTCATCTA TTTCAGCAAACCTCG
<i>FKH2</i> T448A	Mutagenic primer to mutate T448 to A in Fkh2	CAAATAGCGATCGTCGTTATGCACCATACCAACA ACTGCAAAACCC
<i>FKH2</i> T448E	Mutagenic primer to mutate T448 to E in Fkh2	CAAATAGCGATCGTCGTTATGAACCATACCAACA ACTGCAAAACCC
<i>FKH2</i> S503A	Mutagenic primer to mutate S503 to A in Fkh2	CAT TAA AAC CGA GCC CAG TGC TCC AAA AAG AAA TCCA TCT
<i>FKH2</i> S503D	Mutagenic primer to mutate S503 to D in Fkh2	CTG AGT AAC ATT AAA ACC GAG CCC AGT GAT CCA AAA AGA AAT CCA TCT A
<i>FKH2</i> T514A	Mutagenic primer to mutate T514 to A in Fkh2	ATCCATCTATTTCTAACAACGCACCAAAGATGGC TAAAGGCACAGG

<i>FKH2</i> T514E	Mutagenic primer to mutate T514 to E in Fkh2	ATCCATCTATTTCTAACAACGAACCAAAGATGGC TAAAGGCACAGG
<i>FKH2</i> S572A	Mutagenic primer to mutate S572 to A in Fkh2	GAG ACA TTG GAT TAA ACT TTG CCG CTC CCA AAA AGA TAA CTG CTT TAG
<i>FKH2</i> S572D	Mutagenic primer to mutate S572 to D in Fkh2	GGA GAC ATT GGA TTA AAC TTT GCC GAT CCC AAA AAG ATA ACT GCT TTA GA
<i>FKH2</i> T583A	Mutagenic primer to mutate T583 to A in Fkh2	AGA TAA CTG CTT TAG AAG CCT ATG CGC CGG AAA GAG
<i>FKH2</i> T583E	Mutagenic primer to mutate T583 to E in Fkh2	CCA AAA AGA TAA CTG CTT TAG AAG CCT ATG AGC CGG AAA GAG GTT C
<i>FKH2</i> S627A and T638A	Mutagenic primer to mutate S627 and T638 to A in Fkh2	CCAAATACAAATCAATCGGCACCGGCATTTTGGA ATTTTGTTC AATTTAGTGCACCTAATGGACAA
<i>FKH2</i> S627D and T638E	Mutagenic primer to mutate S627 and T638 to D and E respectively in Fkh2	CCAAATACAAATCAATCGGATCCGGCATTTTGGA ATTTTGTTC AATTTAGTGAACCTAATGGACAA
<i>FKH2</i> S643A	Mutagenic primer to mutate S643 to A in Fkh2	TTT GTT CAA TTT AGT ACA CCT AAT GGA CAA GCA CCA GTA AGA AAA AG
<i>FKH2</i> S643D	Mutagenic primer to mutate S643 to D in Fkh2	TTT GTT CAA TTT AGT ACA CCT AAT GGA CAA GAT CCA GTA AGA AAA AGT AGT GAA GAA GTA
<i>FKH2</i> S656A	Mutagenic primer to mutate S656 to A in Fkh2	GTGAAGAAGTAGGGAATAATGCTCCTACATTGA ATAGAAAAATAAA
<i>FKH2</i> S656D	Mutagenic primer to mutate S656 to D in Fkh2	GTGAAGAAGTAGGGAATAATGATCCTACATTGA ATAGAAAAATAAA
<i>FKH2</i> S674A	Mutagenic primer to mutate S674 to A in Fkh2	AGC GAG AGA GGG AAA ATG ATG AAA CCA ATG CGC CAT TTA AAA AAA

<i>FKH2</i> S674D	Mutagenic primer to mutate S674 to D in Fkh2	AAA AAT AAA GCG AGA GAG GGA AAA TGA TGA AAC CAA TGA TCC ATT TAA AAA AAA ACA ACG GAC
<i>FKH2</i> (1-426) <i>XhoI</i> Rev	Reverse primer to truncate Fkh2 to residue 426	CCG CTCGAG GGTTTGCATGGGATTAGAAGG
<i>P<sub>FKH2</sub></i> <i>BamHI</i> insertion	Mutagenic primer to introduce BamHI restriction site upstream of FKH2 in vector for promoter swap	TTTTAGTCATTTTTTTGCTA GGAT CC ACGATTATTTACAAATGTCA
<i>AscI-P<sub>GAL1</sub></i> Fwd	5' Primer to amplify the <i>GAL1</i> promoter	TTGGCGCGCCGTTTAAGTTTTTATTATTATGAGT TG
<i>BamHI-P<sub>GAL1</sub></i> Rev	3' Primer to amplify the <i>GAL1</i> promoter	CGCGGATCCGGTATAACTCTTTCTTATAAAAATC G
<i>POB3</i> (CT)- <i>KpnI</i> Fwd	5' primer to amplify Pob3(CT)	CGG GGTACC GCAGTAGTCAACGAAACTAGTGC
<i>POB3</i> (CT)- <i>XhoI</i> Rev	3' primer to amplify Pob3(CT)	CCG CTCGAG ATTCTTGGCCTTTTTCTTAGG
<i>SRP1</i> (CT)- <i>KpnI</i> Fwd	5' primer to amplify Srp1(CT)	CGG GGTACC GTGACTCTTCTGACAATCGAGAC
<i>SRP1</i> (CT)- <i>XhoI</i> Rev	3' primer to amplify Srp1(CT)	CCG CTCGAG AACTGAAAGTTCTGTTGTTGTTG
<i>FKH2</i> (CT)A Fwd- <i>BamHI</i>	5' primer for FKH2(CT) skip PCR upstream fragment	CGC GGATCC CCTTCTAATCCCATGCAAACC
<i>FKH2</i> (CT)B Rev	3' primer for FKH2(CT) skip PCR upstream fragment with overlap	TCTGTTGATACTGTGCCTTTAGCCATCTTTG

<i>FKH2(CT)</i> C Fwd	5' primer for <i>FKH2(CT)</i> skip PCR downstream fragment	AAAGGCACAGTATCAACAGAAAGCCATTTCGAG
<i>ADE2</i> q-F1	5' Primer for amplification of <i>ADE2</i> in qPCR reactions	AAGGAATCTCCATTGGTGGG
<i>ADE2</i> q-R1	3' Primer for amplification of <i>ADE2</i> in qPCR reactions	GGCCGCCACCATACCTGGCA
<i>HGC1</i> q-F1	5' Primer for amplification of <i>HGC1</i> in qPCR reactions	AATATGCAACCACCACCACC
<i>HGC1</i> q-R1	3' Primer for the amplification of <i>HGC1</i> in qPCR reactions	GAAACAGCACGAGAACCAGC
<i>KIP4</i> q-F1	5' Primer for amplification of <i>KIP4</i> in qPCR reactions	TACTGGGTTTGGAGGTGGAC
<i>KIP4</i> q-R1	3' Primer for amplification of <i>KIP4</i> in qPCR reactions	TTGCTGTTGTTGATGCTGCT
<i>SAP4</i> q-F1	5' Primer for amplification of <i>SAP4</i> in qPCR reactions	TGGTGGTATTGACAAGGCCA
<i>SAP4</i> q-R1	3' Primer for amplification of <i>SAP4</i> in qPCR reactions	ACACCAGCGTTGACATTGAC
<i>CHT2</i> q-F1	5' Primer for amplification of <i>CHT2</i> in qPCR reactions	ACAAATGTGTTGCCACTCCA
<i>CHT2</i> qR1	3' Primer for amplification of <i>CHT2</i> in qPCR reactions	GGCTTTTGGTTTTTGGAGCAG
<i>ECE1</i> q-F1	5' Primer for amplification of <i>ECE1</i> in qPCR reactions	TCTCAAGCTGCCATCATCC

<i>ECE1</i> q-R1	3' Primer for amplification of <i>ECE1</i> in qPCR reactions	TTGTGGAATGTTGCCAAGAA
------------------	--	----------------------

## **2.12. Antibodies used in this study**

<b>Antibody</b>	<b>Description</b>	<b>Dilution</b>	<b>Source</b>
Mouse, anti-GFP, monoclonal	1° antibody for detection/immunoprecipitation of GFP tagged proteins	1:3000	Roche
Mouse, anti-Myc, monoclonal	1° antibody for detection/immunoprecipitation of Myc tagged proteins	1:1000	Bioserv or Roche
Mouse, anti-HA monoclonal	1° antibody for detection/immunoprecipitation of HA tagged proteins	1:1000	Bioserv or Santa Cruz
Rabbit, anti-GST monoclonal	1° antibody for detection/immunoprecipitation of GST tagged proteins	1:5000	Santa Cruz Biotech
Mouse, anti-PSTAIRES monoclonal	1° antibody for the detection of Cyclin Dependent Kinases through their conserved PSTAIRES motif	1:10,000	Sigma
Rabbit, anti-Cdc11 polyclonal	1° antibody for the detection of Cdc11 (raised against <i>S. cerevisiae</i> Cdc11)	1:5000	Santa Cruz Biotech
Rabbit, anti-Phosphoserine CDK polyclonal	1° antibody for the detection of phosphorylated serines in CDK consensus motifs	1:2000	Cell-signaling
Rabbit anti-Phosphoserine CDK/MAPK polyclonal	1° antibody for the detection of phosphorylated serines in CDK/MAPK (SP) target motifs	1:2000	Cell Signaling

Goat, anti-mouse- HRP Polyclonal	2° antibody to mouse primary antibodies conjugated to horse radish peroxidase	1:1000- 1:10,000	Dako
Goat, anti-Rabbit- HRP Polyclonal	2° antibody to rabbit primary antibodies conjugated to horse radish peroxidase	1:5000- 1:10,000	Dako

# 3

## Cyclin-Dependent Kinase Targets

---

Initial screen of potential CDK targets in *C. albicans*

### 3.1. Introduction

Cyclin-dependent kinases (CDKs) are heterodimeric protein kinases that require the binding of a cyclin subunit for their activity and specificity. Originally discovered through genetic studies in yeast (Nurse & Thuriaux 1980; Hartwell et al. 1974) and biochemical studies in sea urchins (Evans et al. 1983), the cyclin-CDK module has been found to be ubiquitous in eukaryotes, with many organisms possessing multiple CDKs involved in diverse cellular processes (Enserink & Kolodner 2010). CDKs phosphorylate serine or threonine residues N-terminal to a proline residue (S/T-P minimal motif), with a preference for the basic residues arginine or lysine C-terminal to the phosphorylation site (S/T-P-x-K/R consensus motif) (Nigg 1993). However recent *in vitro* evidence suggests that CDKs may also be able to phosphorylate other sites (Egelhofer et al. 2008). Generally, CDK target proteins contain clusters of minimal and consensus motifs located in regions of intrinsic disorder, often referred to as low complexity regions. From this point on CDK function and regulation will be given in the context of the extensively studied *S. cerevisiae* Cdk1.

#### 3.1.1. Cdk1

Genetic screens in *S. cerevisiae* and *S. pombe* first identified the mitotic CDK; an essential gene whose temperature-sensitive conditional mutants could not progress through mitotic cell division (Hartwell et al. 1974; Nurse & Thuriaux 1980). Originally known as *Cdc2<sup>+</sup>* in *S. pombe* and *CDC28* in *S. cerevisiae*, the mitotic CDK in all eukaryotes is now referred to as *CDK1*. Cdk1 has been extensively studied in yeast and higher eukaryote models. It is the primary CDK controlling progress through all stages of cell division in yeast, and has been shown sufficient to drive the mammalian cell cycle on its own (Santamaría et al. 2007). Cyclins were

initially discovered through radiolabelling, as proteins that showed expression and degradation in synchrony with embryonic division in sea urchins (Evans et al. 1983). It has since been discovered that generally each CDK associates with multiple cyclin subunits to provide functional diversity; and in the case of Cdk1, the cyclin association and subsequent degradation acts to control passage through different stages of the cell cycle. *S. cerevisiae* has nine cyclins that periodically interact with Cdk1. Three of these are G1 cyclins (Cln1-3), which control progression through G1 and entry into S-phase of the cell cycle. Cln3 regulates the SBF (Swi4 cell-cycle box binding factor) and MBF (Mlu1 cell-cycle box binding factor) transcription factors controlling the transcriptional programs for START (entry into S-phase) (Dirick et al. 1995). Cln1 and Cln2 are expressed at START, being required for spindle pole body duplication (Haase et al. 2001) and initiation of polarised bud growth (Cvrcková & Nasmyth 1993). Of the six B-type cyclins, Clb5 and Clb6 are the first to be expressed, being active in G1 to aid the initiation of S-phase (Schwob et al. 1994), after which Clb6 is degraded (Jackson et al. 2006). Clb5 then goes on to regulate DNA replication during S-phase. (Donaldson et al. 1998). Clb3 and Clb4 are expressed in S-phase to further coordinate DNA replication, and to assemble the spindle for the subsequent mitosis (Richardson et al. 1992). Clb1 and Clb2 are the last to be expressed, being induced during the G2/M transition to control the polarised to isotropic growth switch and events up until the end of mitosis where they are then degraded (Lew & Reed 1993).

In addition to activation through cyclin binding, CDKs are also regulated by cyclin-dependent kinase inhibitors (CKIs), and by cyclin-dependent kinase activating kinases (CAKs). *S. cerevisiae* has two CKIs, Far1 and Sic1. Far1 is generally involved in Cdk1 inhibition mediated by pheromone signalling as part of the mating response (Chang & Herskowitz 1990); whereas Sic1 is expressed in late M/G1 phases (Knapp et al. 1996) and prevents S-phase entry through inhibition of Cdk1-Clb complexes (Schwob et al. 1994). This inhibition is relieved when Cdk1-Cln complexes increase above a threshold level, phosphorylating Sic1 for Skp-Cullin-Fbox (SCF)-mediated degradation (Schneider et al. 1996). The CAK, Cak1, activates Cdk1 through phosphorylation of T169 on the T-loop, causing readjustment to increase cyclin binding affinity (Kaldis et al. 1996). Cdk1 also undergoes inhibitory phosphorylation at Y19 through the action of the

morphogenesis checkpoint kinase Swe1, preventing mitosis occurring before the cell is ready (Booher et al. 1993). This phosphorylation is reversed by the phosphatase Mih1 (Russell et al. 1989). Acetylation has also been shown to be required for correct Cdk1 function (Choudhary et al. 2009).

### **3.1.2. The role of Cdk1 in morphogenesis**

As mentioned previously, Cdk1 controls timely progression through the mitotic cell cycle, linking morphogenesis to the onset of DNA replication, and then nuclear division with cytokinesis and cell separation. Regulation of Cdk1 activity ensures that each of these processes occurs at specific cell cycle stages, and that the cycle proceeds uni-directionally.

Cdk1-Cln complexes bring about the initiation of polarised growth at the start of the cell cycle. Cdk1-Cln2 phosphorylates the CDK inhibitor Far1 causing it to be degraded (Henchoz et al. 1997), and thus the release of Cdc24, which Far1 had been sequestering in the nucleus (Shimada et al. 2000). Cdc24, the GEF of Cdc42, then localises to the bud site causing activation of Cdc42 to allow polarisation of the actin cytoskeleton to commence (Park & Bi 2007). Cdk1-Cln phosphorylation of the Cdc24 associated proteins, Boi1 and Boi2, has been shown to be necessary for their correct bud neck localisation (McCusker et al. 2007).

Cdk1, in conjunction with the CDK Pho85, has been shown to provide inhibitory phosphorylation of the Cdc42 GAP Rga2 during G1 phase, preventing aberrant Cdc42 activation and untimely bud formation (Fig. 3.1.1) (Sopko et al. 2007). A similar mechanism has also been observed for other GAPs, Bem2 and Bem3, which are also involved in morphogenesis (Fig. 3.1.1.) (Knaus et al. 2007).

After initiation of morphogenesis Cdk1 regulates cell growth up until the point of division. In order for cell growth to occur, more membrane lipids are required along with remodelling of the cell wall. Cdk1 directly phosphorylates the triglycerol lipase Tgl4 to stimulate the breakdown of triglycerols into fatty acids and diacylglycerol precursors for membrane lipids (Kurat et al. 2009). Tus1, a GEF for the GTPase Rho1 involved in the cell wall integrity pathway, is also a target of Cdk1 for activation at the G1/S transition (Fig. 3.1.1) (Kono et al. 2008); thus linking Cdk1 to the maintenance of the cell wall. Cdk1 also retains the chitin

synthase Chs2 in the endoplasmic reticulum via phosphorylation that is reversed at upon mitotic cyclin destruction at the end of mitosis (Teh et al. 2009), allowing transport to the Golgi, and on to the bud neck for cell separation to occur.

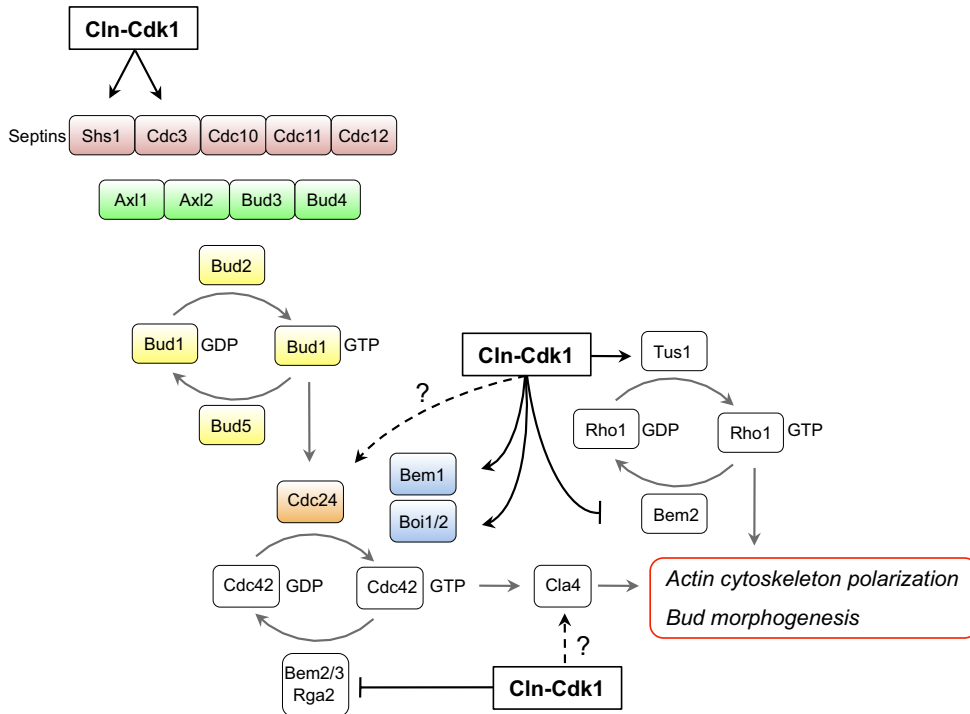


**Fig. 3.1.1. Roles of Cdk1 during bud morphogenesis in *S. cerevisiae*.** Modified from Enserink and Kolodner 2010.

Cdk1 has recently been shown to regulate the exocyst complex, involved in the fusion of secretory vesicles with the plasma membrane at sites of polarised growth. This occurs through inhibitory phosphorylation of the Exo84 subunit. Cdk1-Clb2 phosphorylates Exo84 during mitosis to destabilise the exocyst and thus stop cell surface expansion while division is occurring (Luo et al. 2013).

Cdk1 is required for the polarised to isotropic bud growth switch; yet the precise role of Cdk1 in this process remains elusive. Cdk1-Clb2 can negatively regulate the transcription of the Cln cyclins required for polarised bud growth (Amon et al. 1993); but it is also possible that Cdk1 can regulate the phospholipid flippases (Ubersax et al. 2003), which are known to be important for the isotropic switch (Saito et al. 2007).

Cdk1 can also control morphogenesis through regulation of septin subunits. Cdk1-Cln has been shown to phosphorylate the septins Cdc3 and Shs1.

Phosphorylation of Shs1 is required for the recruitment of the septin associated kinase Gin4 (Egelhofer et al. 2008), whereas phosphorylation of Cdc3 is required for disassembly of the old septin during the G1 phase of the cell cycle (Tang & Reed 2002). Cdk1 dependent control of the septins has been shown to be very important in *C. albicans* and will be covered below.

### 3.1.3. The role of Cdk1 in *C. albicans* morphogenesis

*C. albicans* Cdk1 has conserved roles in regulating morphogenesis and cell cycle progression as in related yeast species. However it also has been shown to be a key regulator of the specialised yeast-to-hyphal transition observed in *C. albicans*. Inhibition of an analogue sensitive version of *Ca*Cdk1 (F85G) with the 1NM-PP1 ATP analogue causes defects in hyphal development. Hyphal-like germ tubes are formed, but these cannot be maintained – leading to the formation of short, kinked projections that cannot polarise further (Fig. 3.1.2) (Bishop et al. 2010).

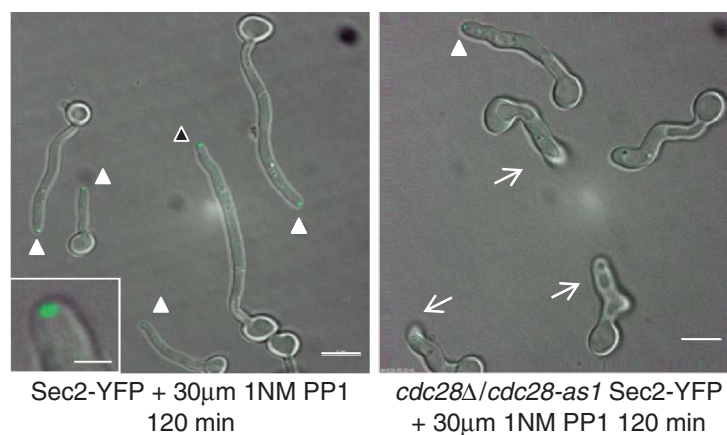


**Fig. 3.1.2. Inhibition of Cdk1 during hyphal growth in *C. albicans*.** Taken from Bishop et al. 2010. *Cdc28*(WT) or *Cdc28as* cells were incubated with 30µM 1NM-PP1 for 2hrs.

The *C. albicans* genome encodes only two G1 cyclins (*CCN1* and *CLN3*), and two G2 cyclins (*CLB2* and *CLB4*), along with a novel hyphal-specific cyclin *HGC1* (Zheng et al. 2004). *CLN3* is an essential gene, required for both yeast and hyphal morphogenesis (Chapa et al. 2005). Depletion of *CLN3* using a regulatable promoter results in large unbudded cells that eventually form hyphal-like filaments as a terminal phenotype. Shut-down of *CLN3* expression on hyphal

induction produces kinked hyphae with swollen tips, demonstrating that it may have a role in hyphal as well as yeast morphogenesis. *CCN1* is not essential for viability; however it is required for maintaining hyphal growth (Loeb, Sepulveda-Becerra, et al. 1999), appearing earlier in hyphae and persisting for longer (Bensen et al. 2005). The essential G2 cyclin *Clb2* is required for mitotic exit, and along with the non-essential *Clb4*, negatively regulates pseudohyphal growth. In true hyphae cells G2 cyclin accumulation is delayed, with premature activation resulting in the production of shorter and wider germ tubes (Bensen et al. 2005). *Clb4* has been shown to be the S-phase cyclin, carrying functional homology to *S. cerevisiae* *Clb5/6* (Ofir & Kornitzer 2010). The hyphal specific cyclin *Hgc1* is non-essential, but is required for true hyphal formation and for virulence in murine infection models (Zheng et al. 2004). Currently it has not been shown if *HGC1* undergoes cell cycle specific expression, which would be a likely reason for the observation that hyphal formation is not dependent on the cell cycle stage. Regulation of *HGC1* expression occurs via the cAMP-PKA pathway and the transcriptional repressors *Nrg1* and *Tup1* (García-Sánchez et al. 2005). Since the discovery of *Hgc1*, there has been much interest in the roles of *Cdk1-Hgc1* and other cyclins in hyphal morphogenesis. A number of studies have highlighted the specific roles of *Cdk1* in this process (Fig. 3.1.3.).

*Cdk1-Hgc1* has been shown to phosphorylate *Rga2*, the GAP for *Cdc42*, during hyphal growth (Zheng et al. 2007). This phosphorylation excludes *Rga2* from hyphal tips, allowing a higher concentration of active *Cdc42* at sites of polarised growth, promoting germ tube formation and extension. The septin subunit *Cdc11* is phosphorylated during hyphal growth; first by *Cdk1-Ccn1*, and then this phosphorylation is maintained by *Cdk1-Hgc1* (Sinha et al. 2007). The septin ring is also thought to be regulated by *Hgc1* through the *Sep7* subunit to control septin dynamics (González-Novo et al. 2008). Vesicle transport in hyphae is regulated through *Hgc1* dependent phosphorylation of *Sec2*, the Guanine nucleotide exchange factor (GEF) for the *Sec4* GTPase (Bishop et al. 2010). Phosphorylation of *Efg1* by *Cdk1-Hgc1* during hyphal growth has been shown to repress *Ace2* target genes, thus preventing cell separation from occurring (Wang et al. 2009). Further to this, *HGC1* is required to block the localisation of *Cdc14* to

the hyphal septum, likely to prevent cell separation during hyphal growth (Clemente-Blanco et al. 2006).

Due to the importance of Cdk1 mediated control on hyphal growth, we sought to elucidate Cdk1 target proteins that are differentially regulated between the yeast and hyphal growth modes.

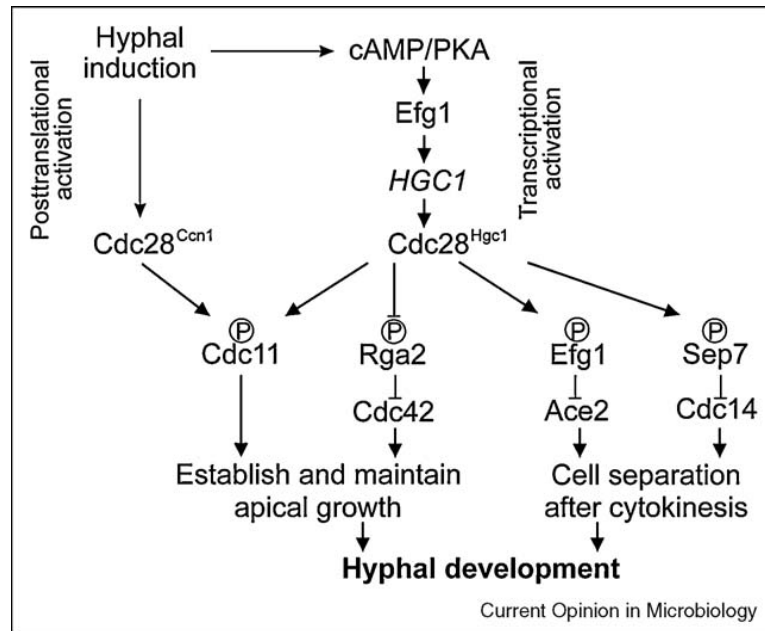


Fig. 3.1.3. Roles of Cdk1-Hgc1/Ccn1 in *C. albicans* hyphal growth. Modified from Wang, 2009.

### 3.2. Results

Initially, bioinformatic analysis was carried out in order to select potential CDK targets. Proteins containing the perfect CDK consensus site (S/TPxK/R) were searched for using the pattern-matching program on the *Candida* Genome Database (CGD) (<http://www.candidagenome.org/cgi-bin/PATMATCH/nph-patmatch>). From this a list was produced of 1482 proteins, ranked in order of the highest number of consensus sites per protein (See supplementary CD). This gave many proteins that are known Cdk1 targets in the related *S. cerevisiae*, demonstrating that this is a reliable method for identifying potential targets. From this list, four proteins were chosen for further study and validation. Proteins were chosen based on the criteria of a known or expected role in filamentous growth and a high number of consensus CDK sites. The proteins selected were two transcription factors known to have a role in *C. albicans* morphogenesis; Sfl1 and

Fkh2; along with two un-annotated open reading frames, Orf19.3469 and Orf19.1948, which contain nine and six CDK consensus sites respectively. To study these proteins further, the domain architecture around the potential phosphorylation sites was worked out using the SMART programme at EMBL (<http://smart.embl-heidelberg.de>). To study the proteins *in vivo* C-terminal GFP/YFP fusions were made, allowing detection of phosphorylation statuses through band retardation on 1D SDS-PAGE combined with Western blotting and antibody detection. The use of a fluorophore tag also allows visualisation of the proteins subcellular localisation where possible.

### **3.2.1. Orf19.3469**

#### **3.2.1.1. Introduction**

Orf19.3469 is currently uncharacterised in *C. albicans*; however it shows weak homology to *S. cerevisiae* Stb1 (e-value  $1.6 \times 10^{-4}$ ), a Swi6 binding protein which has a role in regulating MBF but not SBF dependent transcription at START in the cell cycle (Costanzo et al. 2003). ScStb1 has previously been shown to be an *in vitro* regulatory target for Cdk1-Cln phosphorylation (Ho et al. 1999). Microarray experiments in *C. albicans* have recently shown that the *ORF19.3469* mRNA transcript is up-regulated during biofilm development (Nobile et al. 2012), suggesting it may be important for morphogenesis and pathogenesis. The transcript has also been shown to be up-regulated on deletion of the adenylate cyclase *CYR1*, a key up-stream component of the cAMP-PKA pathway involved in hyphal morphogenesis (Harcus et al. 2004). Orf19.3469 contains nine consensus CDK sites, two of which are conserved with ScStb1, along with seventeen minimal sites, many of which are clustered around low complexity – disordered regions, which as previously mentioned is indicative of a true CDK target. (Fig. 3.2.1.)

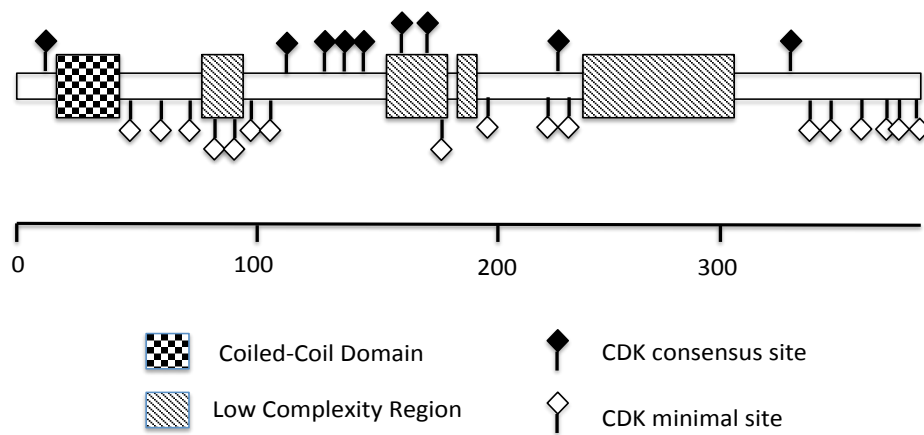


**Fig. 3.2.1. Domain structure of Orf19.3469, including potential CDK phosphorylation sites.** Scale bar represents amino acids in the primary sequence.

### 3.2.1.2. C-terminal tagging of Orf19.3469 with GFP

A PCR cassette was generated from the pFA-GFP-URA3 plasmid using a 5'-3' primer with 69bp of homology to the 3' region of *ORF19.3469*, excluding the stop codon, along with the plasmid specific S1 sequence. The 3'-5' primer contained the plasmid specific S2 sequence followed by 69bp of reverse complemented homology to a region a few hundred base-pairs (bp) downstream of the gene (Fig. 3.2.2. 3.2.3A). The cassette was transformed using the overnight transformation protocol; the transformant colonies were first checked by PCR (Fig. 3.2.3B) and then Western blot (Fig. 3.2.3C). This method was used to tag and check all of the other target proteins.

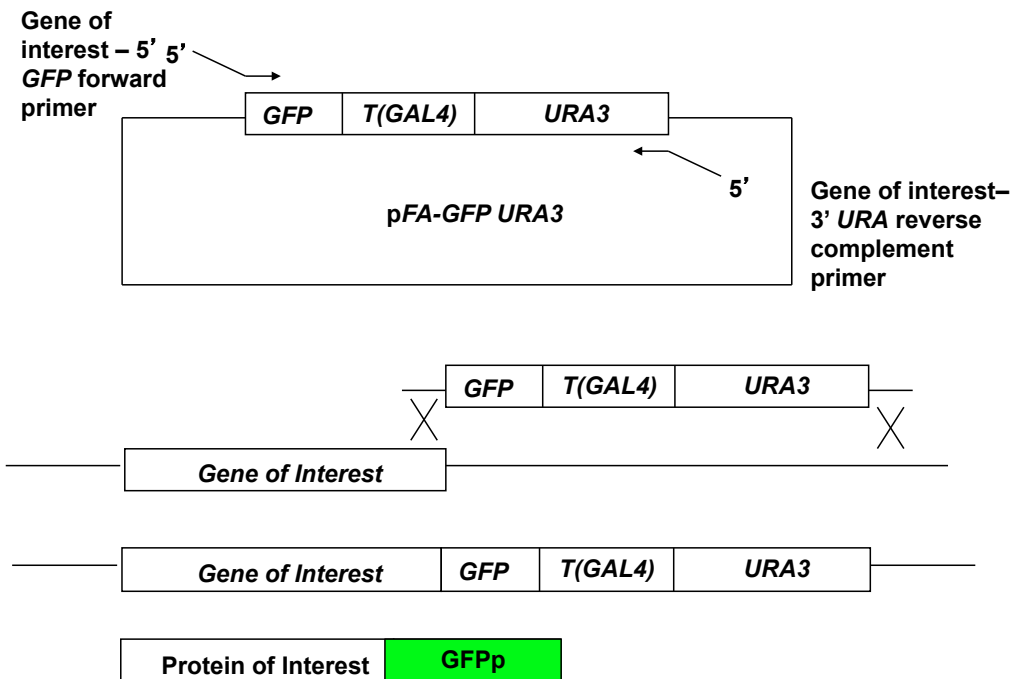
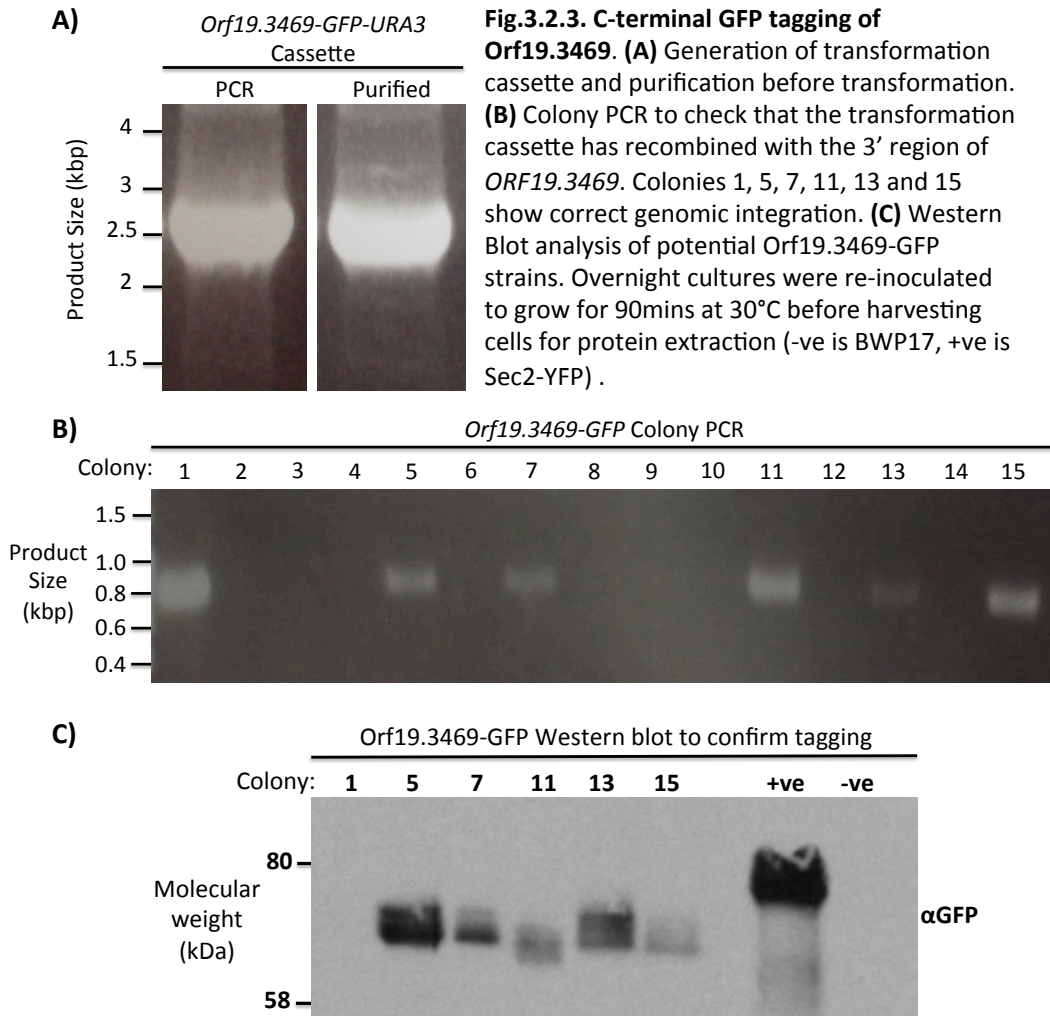


**Fig. 3.2.2. Schematic of C-terminal PCR cassette epitope tagging.** The forward amplification primer is identical to the last 69bp of the gene of interest not including the stop codon, followed by the 5' (S1) sequence for amplification of GFP from the plasmid. The reverse primer contains 69bp of identity to a region downstream of the gene, oriented for the 3'-5' strand, followed by a plasmid specific sequence to allow amplification from the selectable marker back towards the GFP tag (S2). Once generated by PCR, the cassette is transformed into *C. albicans*, with recombination occurring between the identical sequences present in the PCR cassette and at the gene of interest's locus. Correct genomic integration yields a gene fusion product where the gene-GFP sequence is transcribed as one mRNA, terminating at the *GAL4* terminator integrated from the cassette. This mRNA will then be translated into the desired C-terminal GFP fusion protein.



### 3.2.1.3. Orf19.3469 phosphorylation during yeast and Hyphal growth

During yeast and hyphal growth Orf19.3469 appears to exhibit similar patterns of phosphorylation, with a more retarded form of the protein appearing at around 60mins after re-inoculation, and being maintained up to the observed 180mins (Fig. 3.2.4A.). However it has been difficult to observe Orf19.3469 on a Western blot, especially in hyphae, where levels of expression appear lower than in yeast growth. Phosphatase treatment of Orf19.3469 at 120mins in both yeast and hyphal growth confirms that it is indeed phosphorylated at these times (Fig. 3.2.4B.). The presence of a more intense band on the Western blot after phosphatase ( $\lambda$ ppase) treatment suggests that there are multiple phosphorylated forms, that when spread out over a greater area make it difficult to observe the protein on a Western blot.

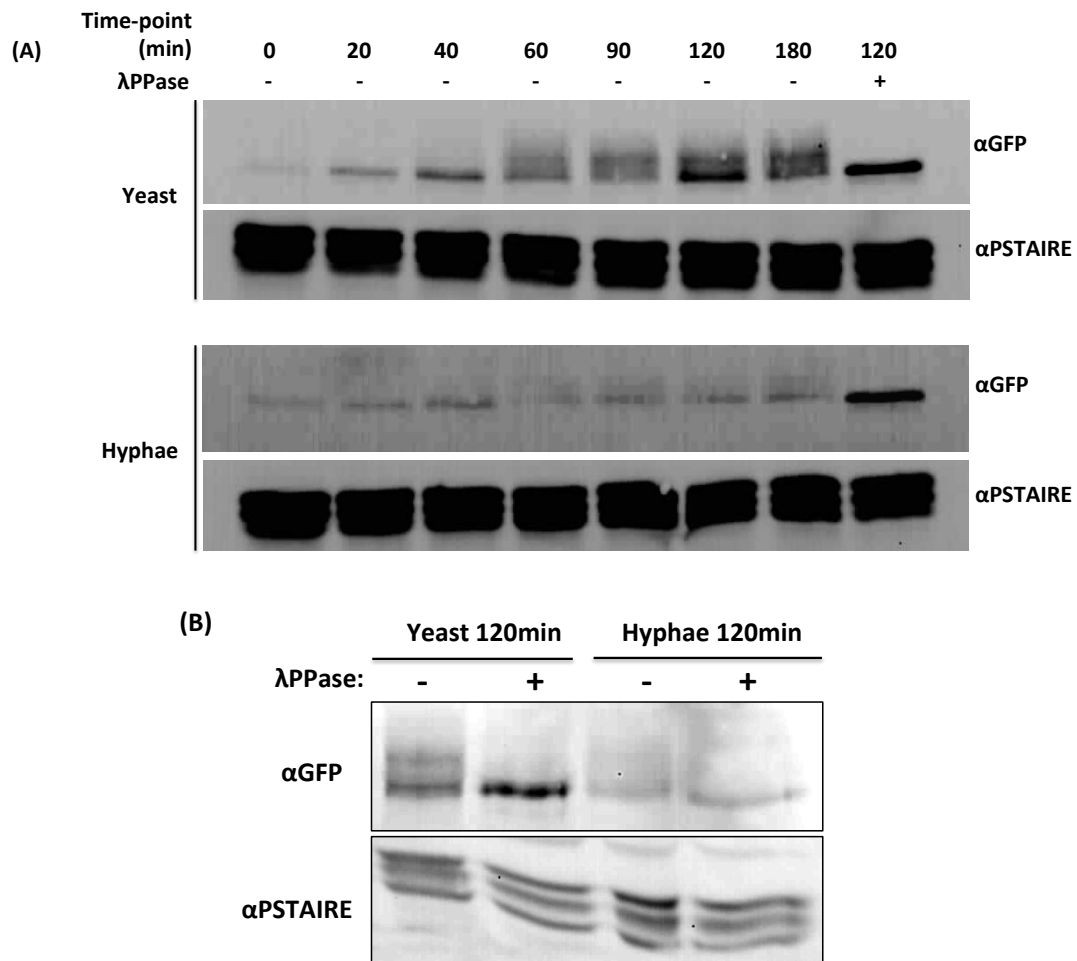


**Fig. 3.2.4. Orf19.3469 phosphorylation during yeast and hyphal growth.** (A) Yeast and hyphal phosphorylation time-courses. Samples were harvested for protein extraction at the shown time-points and 50 $\mu$ g total cell lysate was run on a 10% SDS-PAGE gel. Western blots were probed with an  $\alpha$ GFP antibody to detect Orf19.3469-GFP and  $\alpha$ PSTAIRES to detect CDK levels, confirming equal loading. (B) Comparison of yeast and hyphal phosphorylation, confirmed by lambda phosphatase ( $\lambda$ ppase) treatment.

### 3.2.2. Orf19.1948

#### 3.2.2.1. Introduction

The uncharacterised Orf19.1948 has no known homologues in related yeast species; however it does show weak homology to factors involved in polarised growth such as the Nim1-related kinase Hsl1, but contains no detectable kinase domain. Orf19.1948 has six consensus CDK sites, four of which are clustered close together in the proteins primary sequence, surrounding a low-complexity region. As previously mentioned, this is suggestive of a true kinase target. There are also

seven minimal CDK sites in the protein, mainly located around the N-terminus (Fig. 3.2.5.).

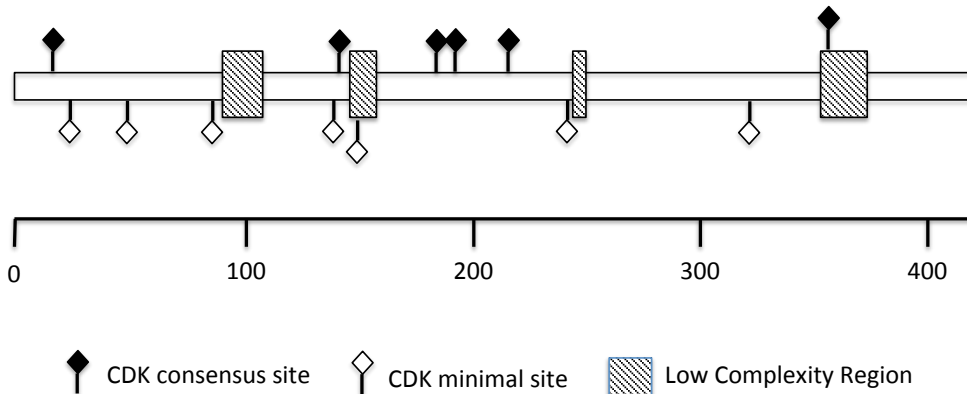


**Fig. 3.2.5. Domain structure of Orf19.1948, including potential CDK phosphorylation sites.** Scale bar represents amino acids in the primary sequence.

### 3.2.2.2. Orf19.1948 phosphorylation during yeast and hyphal growth

Orf19.1948 shows similar patterns on a 1D SDS-PAGE Western blot during both yeast and hyphal growth; however it appears to be show reduced expression in hyphal cells. Orf19.1948 is expressed between 60-90mins into yeast growth after re-inoculation, and appears present as two isoforms of slightly different molecular weights. In hyphal growth, as well as the expression level of Orf19.1948 being lower it is also expressed later, appearing between 90-120mins after re-inoculation into hyphal-inducing conditions (Fig. 3.2.6A.). Again Orf19.1948 appears present as two bands on the 1D SDS-PAGE Western blot. To see if the more retarded isoform is due to phosphorylation, phosphatase treatment ( $\lambda$ ppase) was carried out. Duplicate samples were taken at 120min into yeast and hyphal growth; one of the samples underwent phosphatase treatment while the other was left untreated. Comparison of the samples on a 1D SDS-PAGE Western blot showed that Orf19.1948 does indeed undergo phosphorylation at this time-point (Fig 3.2.6B.).

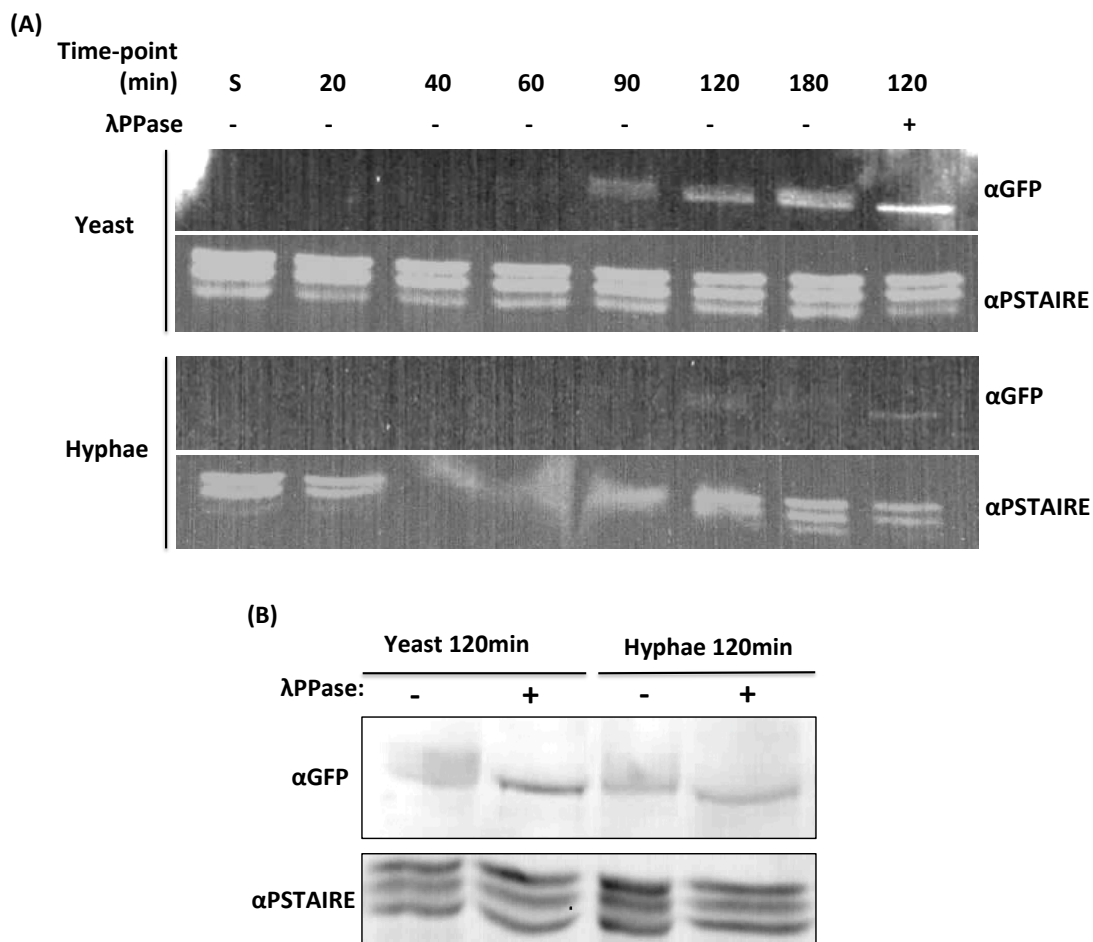


**Fig. 3.2.6. Phosphorylation of Orf19.1948 during yeast and hyphal growth. (A)** Yeast and hyphal phosphorylation time-courses. Cells were harvested for protein extraction at the shown time-points. 50 $\mu$ g of protein from each time-point was run on a 10% SDS-PAGE gel. Western blotting was carried out with an  $\alpha$ GFP antibody to detect Orf19.1948-GFP and  $\alpha$ PSTAIRES to detect CDKs as a loading control. **(B)** Comparison of yeast and hyphal phosphorylation and confirmation by lambda phosphatase ( $\lambda$ PPase) treatment.

### 3.2.2.3. Localisation of Orf19.1948

During yeast growth Orf19.1948 localises to a distinct area of the cell. The GFP signal does not co-localise with DAPI, showing that Orf19.1948 does not localise to the nucleus. During hyphal growth, the Orf19.1948-GFP signal can be seen throughout the hypha and mother cell (Fig 3.2.7.); however, due to the difficulty of detecting Orf19.1948-GFP by western blot, this abundantly observed fluorescence might be non-specific. To observe if this is the case, an untagged BWP17 strain could be used as a control; with the excitation channel for GFP being used and seeing if similar fluorescence is observed.

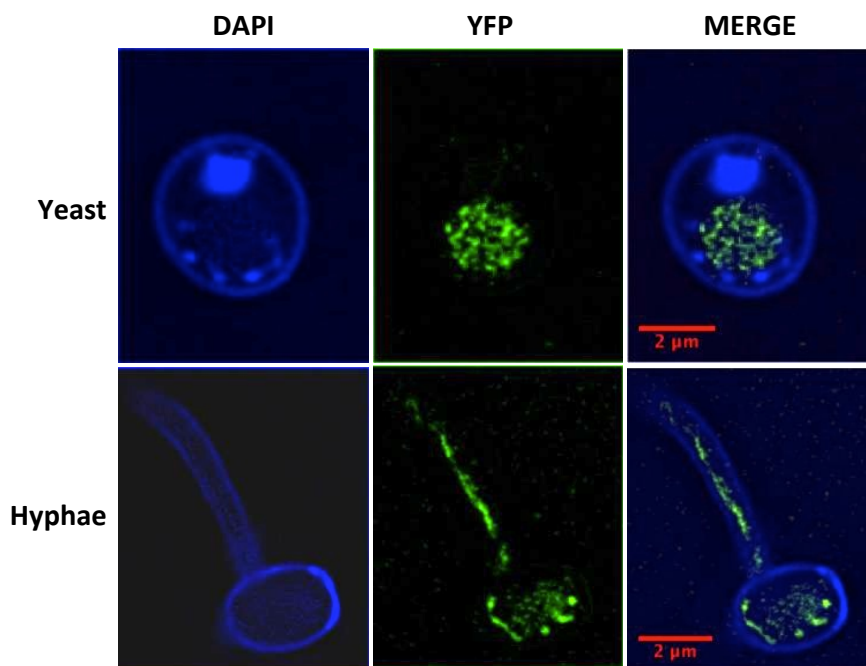


**Fig .3.2.7. Orf19.1948-GFP localisation during yeast and hyphal growth.** Images were taken from log-phase yeast cells, and hyphal cells grown for 120mins. Scale bar is equal to 2 $\mu$ m.

### 3.2.3 Sfl1

#### 3.2.3.1 Introduction

Sfl1 is a heat-shock domain-containing transcription factor, which has been shown to negatively regulate hyphal growth (Bauer & Wendland 2007), with deletion of *SFL1* resulting in a constitutively filamentous phenotype (Fig. 3.2.8.). It acts as part of the Ssn6-Tup1 complex to decrease expression of certain hyphal specific genes such as *HWP1*, and is believed to work antagonistically with the positive hyphal regulator Flo8 (Li et al. 2007). Further to its role as a negative regulator, *CaSfl1* has also been shown to up-regulate the expression of the heat shock proteins Hsp30 and Hsp90 (Zhang et al. 2008). Recently the roles of Sfl1 as an activator and a repressor have been confirmed (Znaidi et al. 2013). Sfl1 can up-regulate the expression of genes required for growth in the yeast morphology, as well as negatively regulating genes, such as *UME6*, required for hyphal growth. *CaSfl1* contains two perfect and fourteen minimal CDK sites (Fig. 3.2.9.).

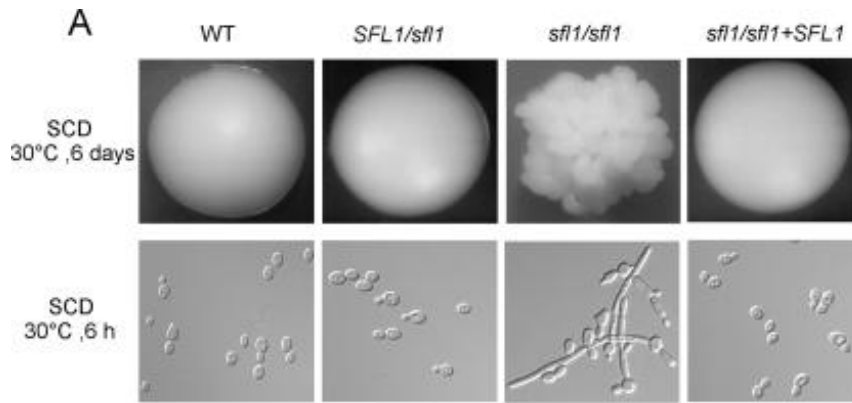


**Fig.3.2.8. *sfl1Δ/Δ* constitutive filamentation phenotype.** Taken from, with permission, from Li. et al 2007

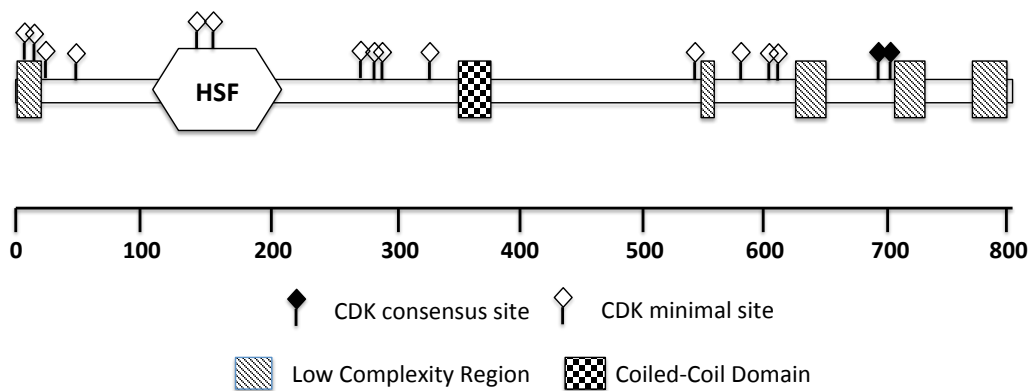


**Fig. 3.2.9. Domain structure of *C. albicans* Sfl1, including potential CDK phosphorylation sites.** Sfl1 contains an N-terminal Heat Shock Factor (HSF) DNA binding domain. Scale bar represents amino acids in the primary sequence.

### 3.2.3.2. Sfl1 phosphorylation during yeast and hyphal growth

Sfl1-YFP shows a similar pattern of 1D-PAGE mobility during both yeast and hyphal growth. After around 120mins post induction, a second, more retarded form of Sfl1-YFP appears on a 1D SDS-PAGE Western blot during both yeast and hyphal growth (Fig. 3.2.10A.). Phosphatase ( $\lambda$ ppase) treatment of a 120mins sample from both yeast and hyphae caused this more retarded form to disappear, demonstrating that it is indeed phosphorylation that is occurring (Fig. 3.2.10B.). Sfl1 appears as two isoforms of slightly different molecular weights on a 1D SDS-PAGE Western blot. This could be due to different isoforms of Sfl1 being present, or a breakdown product of the full-length Sfl1.

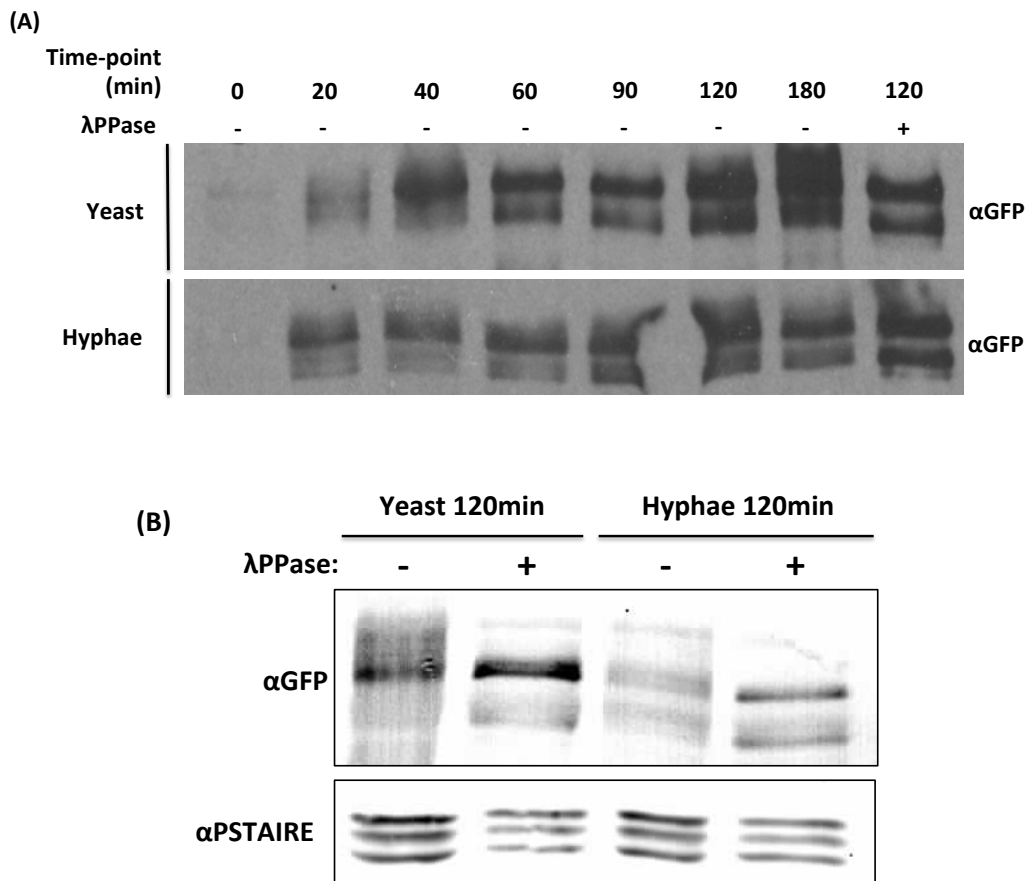


**Fig. 3.2.10. Sfl1 Phosphorylation during yeast and hyphal growth. (A)** Yeast and hyphal time-course experiments. Protein extracts were taken from cells at the specified time-points and 50 $\mu$ g was run on a 7% SDS-PAGE gel. **(B)** Comparison of Sfl1 phosphorylation between yeast and hyphal growth, including phosphatase ( $\lambda$ ppase) treatment to confirm phosphorylation.

### 3.2.3.2 Sfl1 Localisation

Sfl1-YFP co-localises with DAPI during yeast growth, confirming the previously observed nuclear localisation (Li et al. 2007). The DAPI signal could not easily be observed during hyphal growth; however the YFP signal showed a similar pattern to the yeast localisation, suggesting that Sfl1 was remaining in the nucleus (Fig. 3.2.11.).

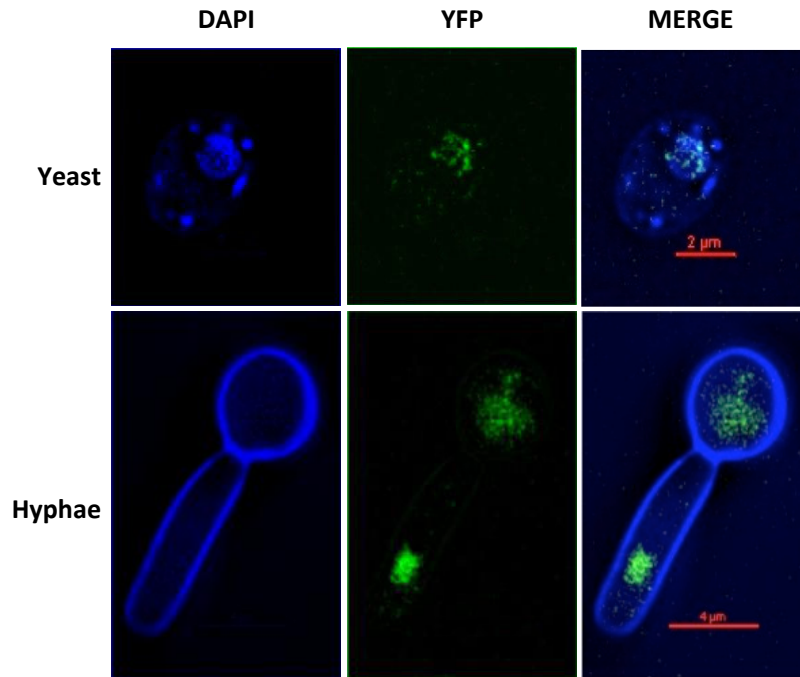


**Fig. 3.2.11. Sfl1-YFP localisation during yeast and hyphal growth.** Images were taken from log phase yeast cells, and hyphal cells grown for 120mins. Scale bar is equal to 2µm.

### 3.2.4. Fkh2

#### 3.2.4.1. Introduction

Fkh2 is a fork-head transcription factor homologous to *S. cerevisiae* Fkh1 and Fkh2. *CaFkh2* shares the highest homology with *ScFkh2*, a known regulatory target of *ScCdk1-Clb5* in the control of G2 cell cycle progression (Pic-Taylor et al. 2004). In *C. albicans*, *FKH2* is required for both yeast and true hyphal morphogenesis (Fig. 3.2.12.), and has been shown to negatively regulate the S-phase cyclin *CLB4* (Bensen et al. 2002), suggesting a conserved role in the control of cell cycle progression. mRNA transcript levels of *FKH2* are increased in infection models with reconstituted human oral epithelium (Zakikhany et al. 2007), suggesting that Fkh2 may have a function in pathogenesis.

Fkh2 contains six perfect CDK sites located around regions of intrinsic disorder, along with nine minimal CDK sites (Fig. 3.2.13.).

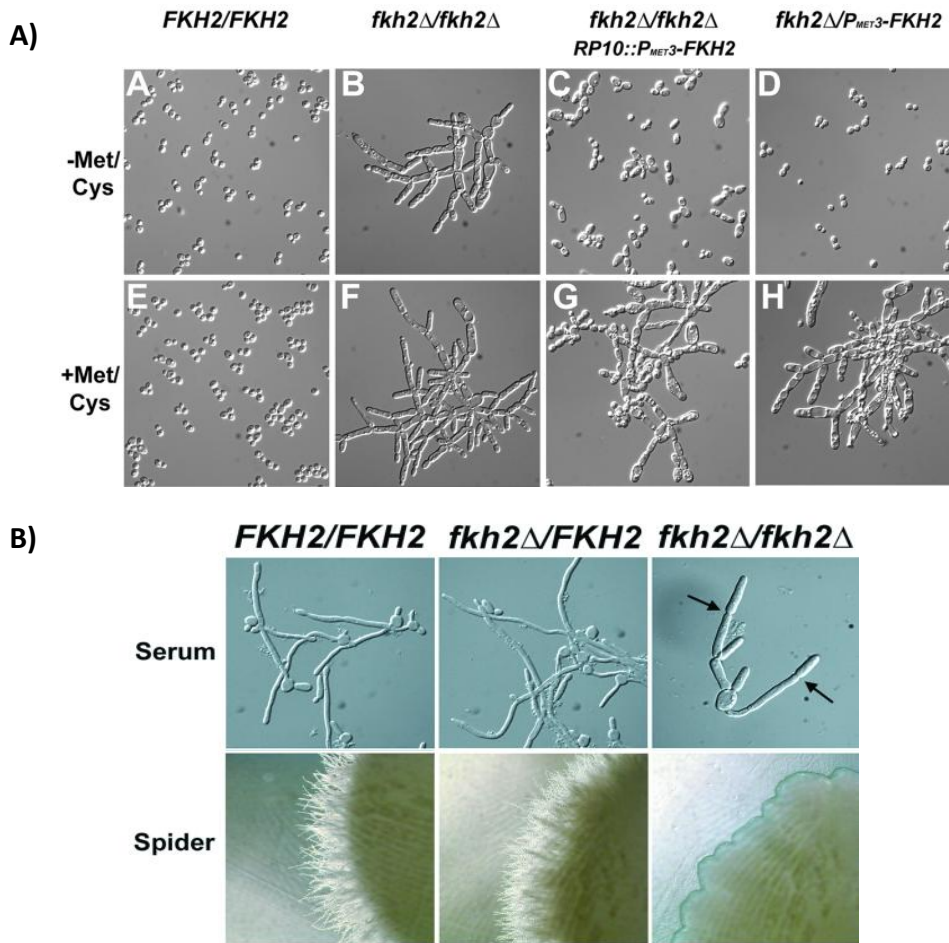


**Fig. 3.2.12. *fkh2Δ/Δ* yeast and hyphal phenotypes.** Taken, with permission, from Bensen. et al 2002. **(A)** *fkh2Δ/Δ* is constitutively pseudohyphal when grown under yeast inducing conditions. **(B)** *fkh2Δ/Δ* cannot form true hyphae under standard induction conditions.

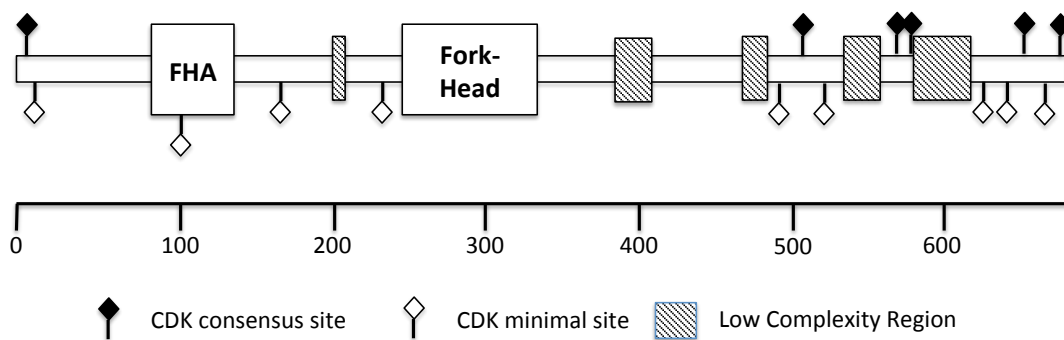


**Fig. 3.2.13. Domain structure of *C. albicans* Fkh2 including potential CDK phosphorylation sites.** Fkh2 contains an N-terminal Fork-head DNA binding domain, along with a Fork Head Associated (FHA) domain. Scale bar represents amino acids in the primary sequence.

### 3.2.4.2. Fkh2 phosphorylation during yeast and hyphal growth

Fkh2 exhibits a different pattern of phosphorylation between yeast and hyphal growth modes. During yeast growth Fkh2-YFP initially shows a second more retarded band on a 1D SDS-PAGE Western blot around 60mins, which appears to remain at least up to the observed 180mins. However during hyphal growth, Fkh2-YFP shows an upper band 20mins after induction. This more retarded band is maintained until around 60-80mins-post induction; and is then lost, appearing not to return again up to the observed 180mins (Fig. 3.2.14A). To confirm that the second band observed at these time-points is due to phosphorylation of Fkh2, 40min hyphae and 60min yeast time-point samples were taken and lysates were phosphatase ( $\lambda$ ppase) treated before comparing them with non-phosphatase treated samples on a 1D SDS-PAGE Western blot (Fig. 3.2.14B.). This showed that the band shift was due to phosphorylation occurring, implying that the timing of Fkh2 phosphorylation may be different between growth modes.

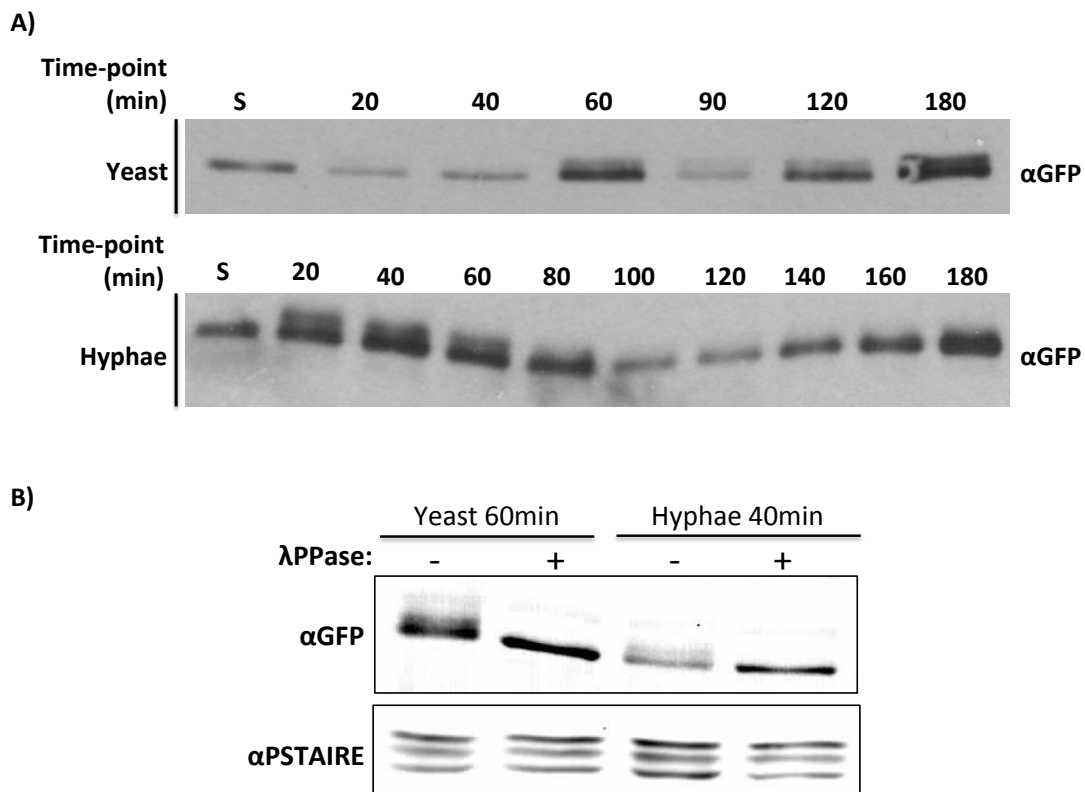


**Fig. 3.2.14. Fkh2 phosphorylation during yeast and hyphal growth. (A)** Yeast and hyphal time-course experiments. Protein extracts were taken from cells at the specified time-points and 50 $\mu$ g was run on a 7% SDS-PAGE gel. **(B)** Confirmation of phosphorylation at the specified time-points by lambda phosphatase ( $\lambda$ ppase) treatment.

### 3.4.2.3. Fkh2 Localisation

Fkh2-GFP co-localises with DAPI during yeast growth, confirming the previous observation that it is a nuclear protein (Bensen et al. 2002). During hyphal growth the Fkh2-GFP signal appears in a distinct structure that is likely the nucleus (Fig. 3.2.15.).

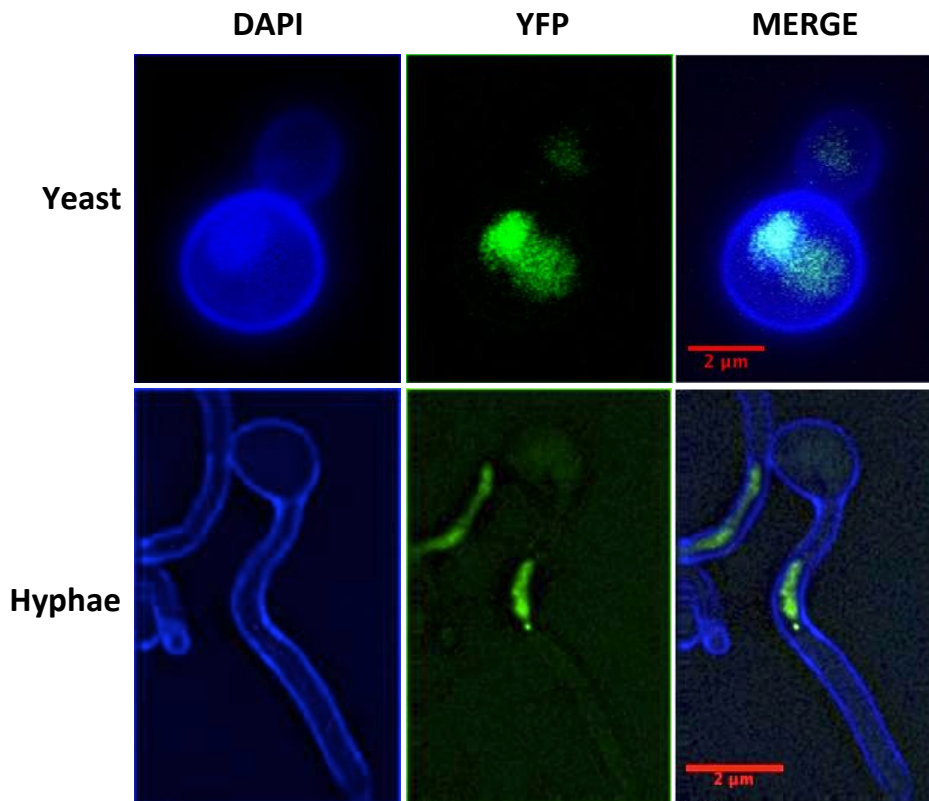


**Fig. 3.2.15. Fkh2-GFP localisation during yeast and hyphal growth.** Images were taken from log phase yeast cells, and hyphal cells grown for 120mins. Scale bar is 2μm.

## 3.3 Discussion

Four potential CDK targets, identified by bioinformatics, were C-terminally tagged with GFP/YFP. This allowed the phosphorylation states to be observed during yeast and hyphal growth through band retardation of phosphorylated isoforms on 1D SDS-PAGE Western blot, and, where possible, to observe the localisation of the protein. In order to determine whether these proteins are indeed true CDK targets, further experiments would need to be carried out as detailed in chapter one.

### 3.3.1. Orf19.3469

Orf19.3469 is phosphorylated after 60mins during yeast growth (Fig. 3.2.4.), with the phosphorylation being maintained up to the observed three hours. The phosphorylation also appears to coincide with an increase in the level of Orf19.3469. These results suggest that Orf19.3469 may have a role in the later stages of yeast growth, after the initiation of the cell cycle. In hyphae a similar pattern of phosphorylation was observed; however it was difficult to ascertain, as levels of Orf19.3469 were much lower during hyphal compared to yeast growth (Fig. 3.2.4.). This may mean that less Orf19.3469 is required during hyphal growth. In *S. cerevisiae* the un-phosphorylated form of Stb1 is thought to bind Swi6 during the G1 phase of the cell cycle (Ho et al. 1999; Costanzo et al. 2003), possibly negatively regulating MBF and SBF transcription through the Sin3 Histone deacetylase complex (HDAC) (de Bruin et al. 2008). These data correlate with the observed phosphorylation of Orf19.3469 during yeast growth, as after 60mins into yeast growth it would be expected that most cells would have passed START in the cell cycle. Therefore it can be speculated that Orf19.3469 is indeed the homologue of *ScStb1*, and that the observed phosphorylation is required to relieve repression of transcriptional programs to enter the cell cycle. To further investigate this in *C. albicans*, time-course experiments could be repeated with synchronised cells to determine whether the phosphorylation is cell cycle dependent. Also, interactions with Swi6 and Sin3 homologues in *C. albicans* could be followed during such time-courses, and phosphorylation blocked/phosphomimetic mutants of Orf19.3469 could be used to see if they affect such interactions and the timing of START.

### 3.3.2. Orf19.1948

Orf19.1948 is only detected after 90mins into both yeast and hyphal growth, which is concurrent with the presence of a more retarded phospho-isoform of the protein on 1D SDS-PAGE (Fig. 3.2.6.). This suggests a later role for Orf19.1948 in the yeast and hyphal growth programs or cell cycles. This could be further investigated by synchronising the cells before carrying out time-course experiments, in order to see if there are fluctuations in Orf19.1948 expression and

phosphorylation in conjunction with cell cycle progression. Orf19.1948 shows much lower expression levels during hyphal growth (Fig. 3.2.6.), suggesting a likely yeast growth-specific role.

### **3.3.3. Sfl1**

Sfl1 is appears as two isoforms when run on a 1D SDS-PAGE (Fig. 3.2.10.). Assuming that there are not due to breakdown occurring, this suggests the presence of different forms of Sfl1 that may differ in function. *SFL1* does not contain any introns, and therefore the different isoforms cannot be due to alternative splicing occurring. Sfl1 is not expressed in stationary phase cells (Fig. 3.2.10A.), suggesting a role only during the resumption of growth, from when the level of Sfl1 remains constant. Phosphorylation of Sfl1 occurs during the later stages of yeast and hyphal growth (Fig. 3.2.10.), suggesting there may be a function independent of its known role in the repression of hyphal growth. This function could be investigated by using mass spectrometry to determine the sites in Sfl1 that are phosphorylated at 120mins into yeast and hyphal growth. These sites could then be mutated to non-phosphorylatable alanine or phosphomimetic glutamic/aspartic acid residues, and the phenotypic consequences observed. We have also confirmed the observations of Li et al 2007, showing that Sfl1 is a nuclear protein (Fig. 3.2.11.).

### **3.3.4. Fkh2**

Fkh2 is the only protein in this study to show a clear difference in phosphorylation between yeast and hyphal growth (Fig. 3.2.14). During yeast growth Fkh2 shows a similar phosphorylation pattern to that observed in *S. cerevisiae*, where phosphorylation occurs after START in order to control progression through the G2/M phase boundary (Pic-Taylor et al. 2004). This will be confirmed by using synchronous cells obtained through centrifugal elutriation. During hyphal growth Fkh2 shows a highly unexpected pattern of phosphorylation that is considerably different from that observed during yeast growth. Fkh2 is phosphorylated 20min after hyphal induction, and only remains so for the first

60min. This suggests a function that is independent of that observed during yeast growth in related organisms. Due to the timing of the phosphorylation, it is likely that it is required for the initiation of hyphal growth, or in preparation for later events that occur during hyphal growth. The fact that Fkh2 is localised to the nucleus in both yeast and hyphae, suggests the function in hyphal growth is likely to depend on Fkh2's activity as a transcriptional regulator. To investigate this further, the phosphorylation sites on Fkh2 can be determined and phosphomimetic and phosphorylation-blocked mutants can be made as mentioned above. Such mutants can then be used to observe the phenotypic effects of the phosphorylation, and to test whether they affect Fkh2-dependent transcriptional programs.

### **3.3.5. Conclusions**

Due to the clear differences in phosphorylation of Fkh2 between yeast and hyphal growth, further work will be carried out to elucidate the function of the early phosphorylation of Fkh2. We will attempt to determine whether, as expected, Cdk1 is responsible for the observed phosphorylation, and the physiological consequences that this phosphorylation has.

# 4

## **Fkh2 Phosho-regulation**

---

### **4.1 Introduction**

#### **4.1.1. Fork-head transcription factors**

Fork-head (Fkh) transcription factors are a family of proteins containing the Fork-head box, winged helix, DNA-binding domain. Fork-head transcription factors were initially discovered through forward genetic studies in *Drosophila melanogaster* (Weigel et al. 1989). Mutants were isolated in which two-spiked head structures were formed in the embryo, and were found to be defective in anterior and posterior gut formation. The Fork-head (Fkh) gene responsible for this phenotype was then cloned through chromosome walking. Further investigation of the Fkh protein revealed nuclear localisation, suggesting a role in transcription of other genes. However the Fkh protein lacked discernable domains that, at the time, were expected in transcription factors. Later it was discovered that a 110 amino acid domain present in the Fkh protein was conserved with mammalian HNF-3 transcription factors, thus defining a novel transcription factor family (Weigel & Jäckle 1990). Structural studies of DNA bound HNF-3 showed that the fork head domain consists of three alpha helices in a helix-turn-helix motif, flanked by two large loops referred to as wings (Clark et al. 1993). Thus the domain was named the winged helix DNA binding domain.

Since the initial discovery of *D. melanogaster* Fork-head, many winged helix DNA-binding transcription factors have been discovered in organisms from yeast to humans. In multicellular organisms the abundance of Fork-head transcription factors and a high variation in function has led to new nomenclature rules being agreed upon. Such transcription factors in higher organisms are now referred to as Fork-head box (FOX) transcription factors, and are assigned a letter based on their class, and then a number within the particular class (Kaestner et al. 2000).

#### 4.1.2. Fork-head transcription factors in morphogenesis and cell cycle progression

The initial work on Fork-head transcription factors was carried out in multicellular eukaryote systems; however the roles of Fork-head transcription factors in cell cycle progression and morphogenesis have been best studied in yeast models. In *S. cerevisiae* there are four Fork-head transcription factors: Fkh1, Fkh2, Hcm1 and Fhl1. Of these, three are involved in cell cycle progression (Fkh1, Fkh2 and Hcm1) (Murakami et al. 2010), whereas Fhl1 is required for the transcription of ribosomal protein genes (Martin et al. 2004).

*HCM1* is expressed during G1/S phase and is required for the expression of Fkh1/2, along with other S-phase-specific genes necessary for budding and chromosome segregation (Pramila et al. 2006). Fkh1/2 are required for the correct timing of *CLB2* cluster gene expression and maintenance of a correct yeast morphology (Zhu et al. 2000; Pic et al. 2000) (Fig. 4.1.1.). Further elucidation of this regulatory mechanism revealed that Fkh1 and Fkh2 have opposing roles in *CLB2* cluster gene expression (Hollenhorst et al. 2000). Deletion of *FKH1* brings about earlier expression of *CLB2* cluster genes and increases the rate of progression through S and G2 phases of the cell cycle. This suggests a negative role in regulating *CLB2* cluster genes during G1/S, which is supported by the observation that Fkh1 along with the chromatin-remodeling enzyme Isw1 can repress expression during G2/M phases of the cell cycle (Sherriff et al. 2007). Deletion of *FKH2* results in slower progression through the cell cycle in ordinance with reduced *CLB2* cluster expression.

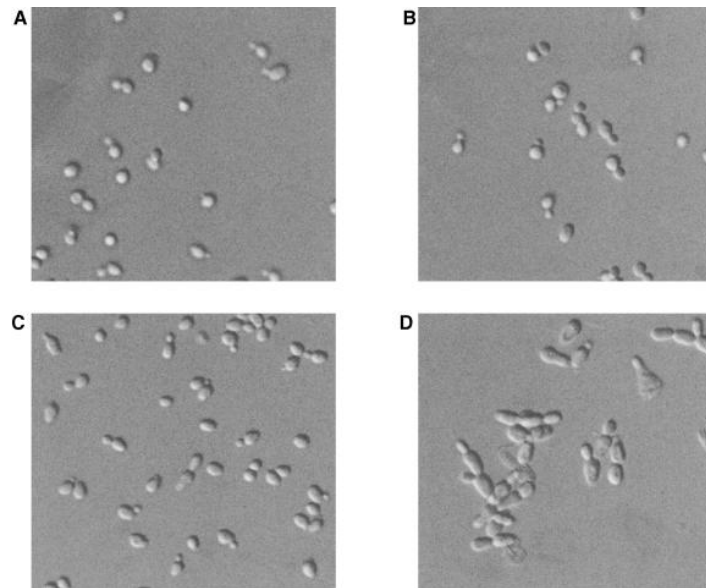


**Fig. 4.1.1. Fork-head transcription factor deletion phenotypes in *S. cerevisiae*.** Taken from Pic et al 2000. **A)** Wild type W303 cells **B)** *fkh1Δ* cells **C)** *fkh2Δ* cells **D)** *fkh1Δfkh2Δ* cells showing altered morphology and cell separation defects

Activation of the *CLB2* cluster requires a protein complex formed of Mcm1, Fkh2 and its co-activator Ndd1, which assembles in the upstream promoter sequences of *CLB2* cluster genes (Fig.4.1.2.) (Pic et al. 2000; Koranda et al. 2000). Fkh1 can bind to *CLB2* cluster promoters *in vitro*, but not *in vivo* as it cannot interact with Mcm1 to activate transcription (Hollenhorst et al. 2001). Mcm1 present in up-stream promoters recruits Fkh2 through DNA bending (Lim et al. 2003), with Fkh2 binding through a region N-terminal to its DNA binding domain (Boros et al. 2003). Fkh2 competes with the Yox1 repressor for binding to a hydrophobic pocket on Mcm1 (Darieva et al. 2010). Fkh2 is phosphorylated by Cdk1-Clb5 during S-phase to relieve repression at *CLB2* cluster promoters (Pic-Taylor et al. 2004), likely mediated by Fkh2 and Isw2 during the G1 phase of the cell cycle (Sherriff et al. 2007). Ndd1 is thought to undergo inhibitory phosphorylation by protein kinase C early during G1/S (Darieva et al. 2012), but is later phosphorylated at threonine 319 by Cdk1-Clb2 during the G2 cell cycle phase, triggering Ndd1 to bind the FHA domain of Fkh2 (Reynolds et al. 2003; Darieva et al. 2003) to activate transcription. Phosphorylation of Ndd1 by Cdc5 further activates *CLB2* cluster expression, of which *CDC5* is a member, therefore providing positive feedback (Darieva et al. 2006).

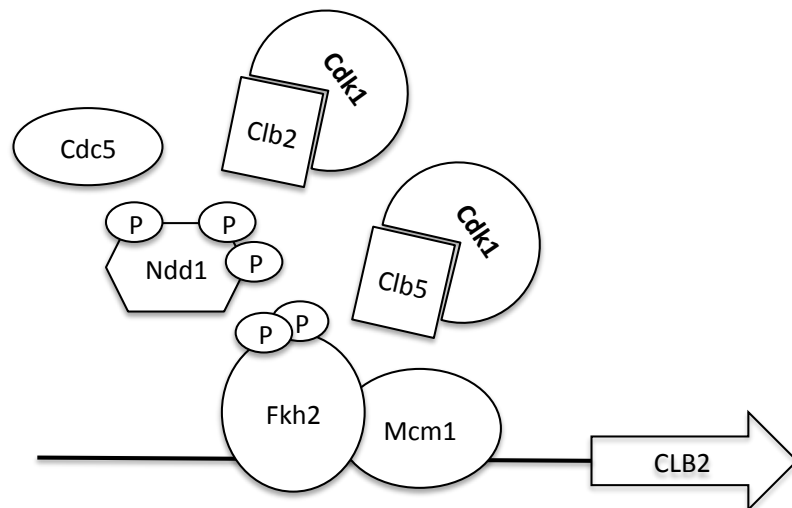


**Fig. 4.1.2. Schematic of Mcm1-Fkh2-Ndd1 complex formation at *CLB2* cluster promoters.**

Fkh2 associates with Mcm1 during S-phase and is later phosphorylated to by Cdk1-Clb5 to promote interaction with Ndd1. Ndd1 is also phosphorylated by Cdk1-Clb2 to promote the interaction, and is later phosphorylated by Cdc5 to fully activate transcription of the *CLB2* cluster.

Fkh1 and Fkh2 have also recently been shown to be involved in other important cellular processes. Fkh1 and Fkh2 associate with early replicating origins during S-phase, causing them to cluster into replication foci (Knott et al. 2012). It is likely that this role is more dependent on Fkh1, with Fkh2's primary role being in transcription. Both Fkh1 and Fkh2 have also been genetically shown to regulate *S. cerevisiae* chronological lifespan in combination with the anaphase promoting complex (APC), likely due to roles in stress response as well as the key roles in cell cycle regulation (Postnikoff et al. 2012).

In *S. pombe*, Fkh2 is also required for transcriptional dependent mitotic progression (Buck et al. 2004), being regulated by Cdk8, the CDK component of the mediator complex. Phosphorylation of Fkh2 prevents ubiquitination and subsequent degradation of Fkh2, allowing expression of cluster 1 genes for mitotic commitment (Szilagyi et al. 2012). Fkh2 is also regulated by the primary cell cycle CDK, Cdc2 (Cdk1), to repress *STE11* transcription and thus prevent mating during the mitotic cell cycle (Shimada et al. 2008).

The mammalian Fork-head transcription factor involved in cell cycle progression is FOXM1 (Trident), which is primarily expressed in proliferating cells (Korver et al. 1997). FOXM1 shares a conserved function with the yeast homologue in regulating transcription required for mitotic progression (Wang et al. 2005; Laoukili et al. 2005). However, FOXM1 is also thought to have a role in regulating

the G1/S transition in cell cycle through targeting the Jnk1 kinase required for the transition (Wang et al. 2008). FOXM1 is phosphorylated in its C-terminal domain by Cdk2-CyclinA during S/G2 phases, relieving inhibition by FOXM1's N-terminal domain (Laoukili et al. 2008). This also allows the Polo kinase Plk1 to bind and further phosphorylate the C-terminal domain, fully activating FOXM1's transcriptional ability (Fu et al. 2008). Again this provides a positive feedback circuit, as Plk1 is transcriptionally regulated by FOXM1.

#### **4.1.3. *Candida albicans* Fkh2**

*C. albicans* *FKH2* was discovered through homology searching with the related yeast *S. cerevisiae* (Bensen et al. 2002). It is the single homologue of *FKH1* and *FKH2* from *S. cerevisiae*, but shares highest homology in its Fork-head DNA binding domain with *ScFkh2* (Fig.4.1.3.). Due to this high similarity it is thought that *CaFKH2* shares the conserved role in cell cycle progression with *ScFKH1* and *ScFKH2*. This was shown by the fact that *CaFKH2* will rescue the morphological defect phenotype of the *S. cerevisiae* *fkh1Δ*, *fkh2Δ* mutant. The Fkh2 minimal DNA binding motif (AAACAAA) has also been shown associated with genes transcribed during S-phase of the cell cycle (Côte et al. 2009). A subset of such genes expressed from S to G2 phases may have an involvement in hyphal growth (Gordân et al. 2012). It has been shown that *CaFkh2* is a nuclear protein, and that deletion results in morphogenetic defects, such as constitutive pseudohyphal growth along with cell separation defects. Microarray analysis of 319 ORFs in a *fkh2Δ/Δ* mutant showed that some cell cycle and hyphal specific genes have their expression down-regulated in the absence of *FKH2* (Fig.4.1.4A-C). It was confirmed by northern analysis that Fkh2 regulates *HWP1*, *ECE1* and *CLB4* mRNA levels (Fig.4.1.4D.). *FKH2* has also been shown to be up-regulated in a reconstituted oral epithelium model of infection (Zakikhany et al. 2007), suggesting a possible role in virulence. Recently it has been shown that overexpression of *FKH2* leads to filamentous growth on both solid and liquid media (Chauvel et al. 2012); however how increased levels of Fkh2 causes filamentation has not been explored.

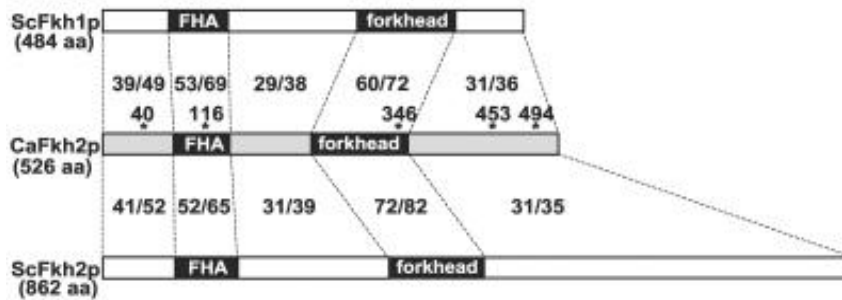


**Fig. 4.1.3. Schematic comparing *CaFkh2* homology with *ScFkh1* and *ScFkh2*.** Taken, with permission, from Bensen et al 2002. *CaFkh2* shares homology to *ScFkh1/2*, but is most similar to *ScFkh2* in the Fork-head DNA binding domain. Fractions represent the number of residues that are similar in each domain.

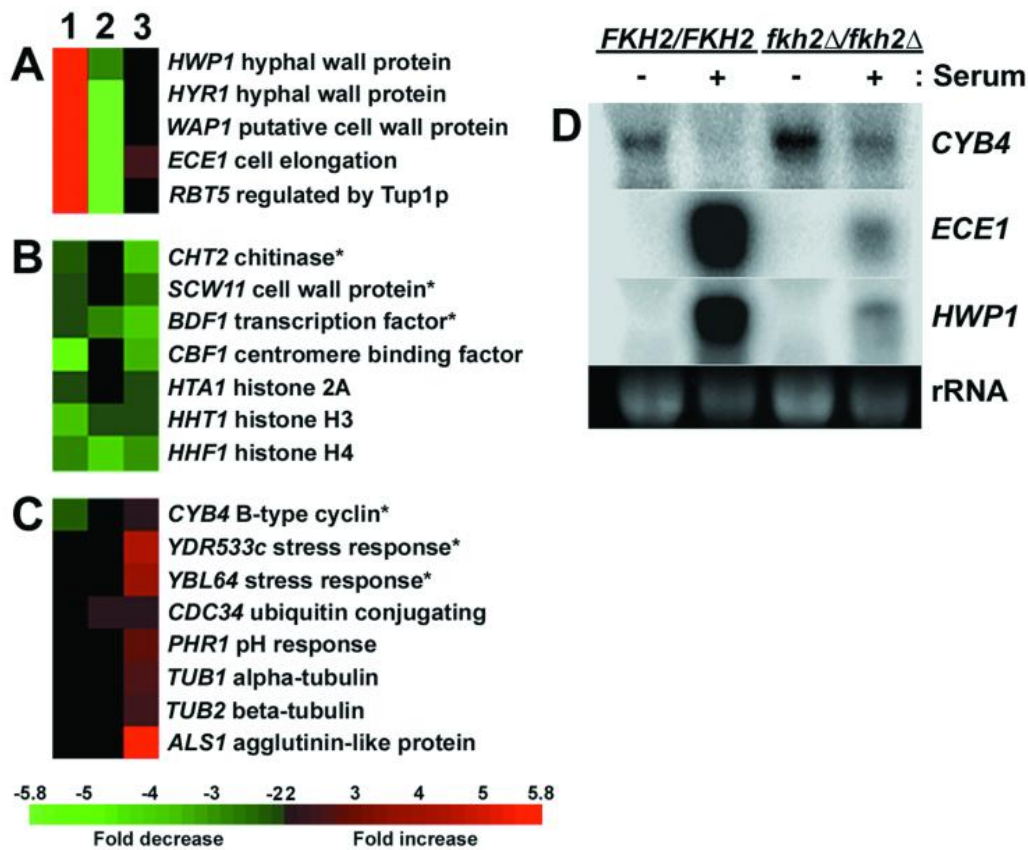


**Fig. 4.1.4. Transcriptional effects of knocking out *FKH2* in *C. albicans*.** Taken from Bensen et al. 2002. Transcriptional array of 319 *C. albicans* open reading frames. **1)** *FKH2/FKH2* 3hour hyphae vs. *FKH2/FKH2* 3hour yeast **2)** *fkh2Δ/Δ* 3hour hyphae vs. *FKH2/FKH2* 3hour hyphae **3)** *fkh2Δ/Δ* yeast vs. *FKH2/FKH2* yeast. **A)** Genes with increased expression during hyphal growth in *FKH2/FKH2* but not in *fkh2Δ/Δ*. **B)** Genes with expression down-regulated in *fkh2Δ/Δ* compared with *FKH2/FKH2* during yeast growth. **C)** Genes with expression up-regulated in *fkh2Δ/Δ* cells compared with *FKH2/FKH2* during yeast growth. **D)** Northern blot confirmation that *CLB4* mRNA levels increase during yeast growth on deletion of *FKH2*, and that *ECE1* and *HWP1* mRNA levels during hyphal growth decrease upon deletion of *FKH2*.

## 4.2 Results

### 4.2.1. Fkh2 undergoes cell cycle-dependent phosphorylation in yeast

In the previous chapter it was shown that Fkh2 is differentially phosphorylated during yeast and hyphal growth. However, asynchronous cells were used for this previous experiment, and therefore the observed differences in yeast and hyphal phosphorylation may have been due to cells in the population being at different stages of the cell cycle. Some of the cells in the asynchronous culture may have arrested in S/G2 and could have undergone rapid phosphorylation upon re-inoculation into fresh media. To overcome this problem, and to determine at which points during yeast and hyphal growth Fkh2 is phosphorylated, cells were synchronised by elutriation before being re-inoculated into yeast or hyphal growth conditions. Time-points were taken every 20mins after re-inoculation, with samples also being taken and fixed for microscopy, which were subsequently stained with DAPI to observe cell cycle progression. During synchronous yeast growth, phosphorylation of Fkh2 occurred in a cell cycle dependent manner coinciding with periods of small bud growth (Fig. 4.2.1.). Phosphorylation of Fkh2 peaked at the time of the polarised to isotropic growth switch at around 100min. The phosphorylation level then appeared to decrease until the new daughter cells began to form buds at the beginning of the next cell cycle. This result is similar to that observed for Fkh2 in *S. cerevisiae*, which shows that phosphorylation occurs on small bud formation after release from alpha factor (Pic et al. 2000).

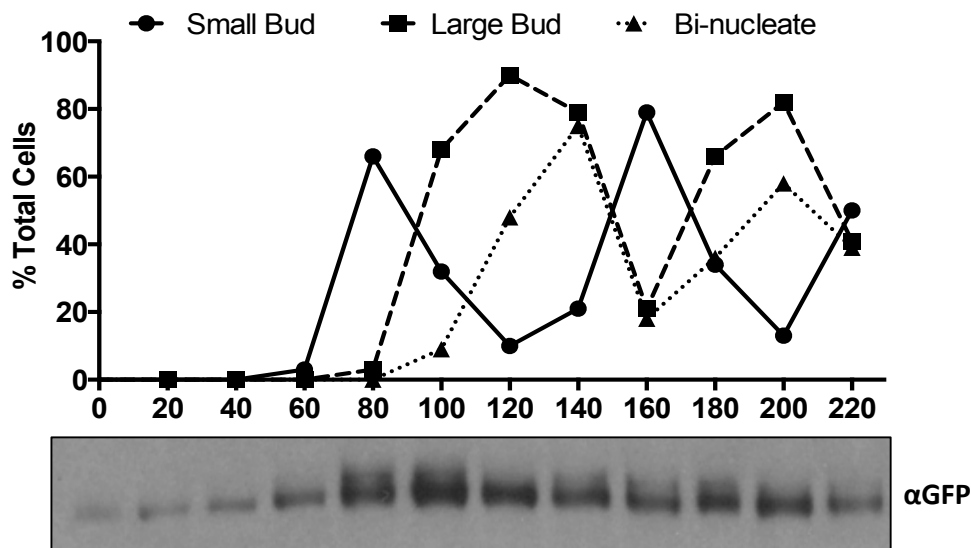


**Fig. 4.2.1. Fkh2 undergoes cell cycle-dependent phosphorylation during synchronous yeast growth.** *FKH2/FKH2-YFP* G1 cells were obtained by elutriation from a log phase yeast culture and then re-inoculated into yeast growth conditions. Samples were taken for Western blot and microscopy at the shown time-points. 50µg of protein extract was run on a 7% SDS-PAGE gel, and an αGFP antibody was used to detect Fkh2 after Western blotting. Small and large bud growth was used to follow yeast growth phases, and DAPI was used as a nuclear marker to observe when nuclear division was occurring. Values for each time-point are the average of 50 separate cells.

#### 4.2.2. Fkh2 is phosphorylated independently of the cell cycle on hyphal induction

During synchronous hyphal growth, Fkh2 is phosphorylated by 20mins post induction and remains so up until around 60min post induction. This observed phosphorylation does not appear to return later on in hyphal growth (Fig. 4.2.2.). The hyphal phosphorylation coincides with highly polarised growth while the germ tube is being formed, and then disappears once all cells in the population have produced a germ tube. In this strain the septin Cdc12 was C-terminally tagged with mCherry, allowing visualization of septin ring formation, which can be used as a marker of cell cycle progression past START (Cid et al. 2001; Bensen et al. 2005). From this it can be seen that formation of the hyphal septin ring only occurs after Fkh2 has been phosphorylated and subsequently dephosphorylated. This suggests that the hyphal phosphorylation of Fkh2 occurs before the beginning of the cell cycle, and is therefore independent of cell cycle progression.

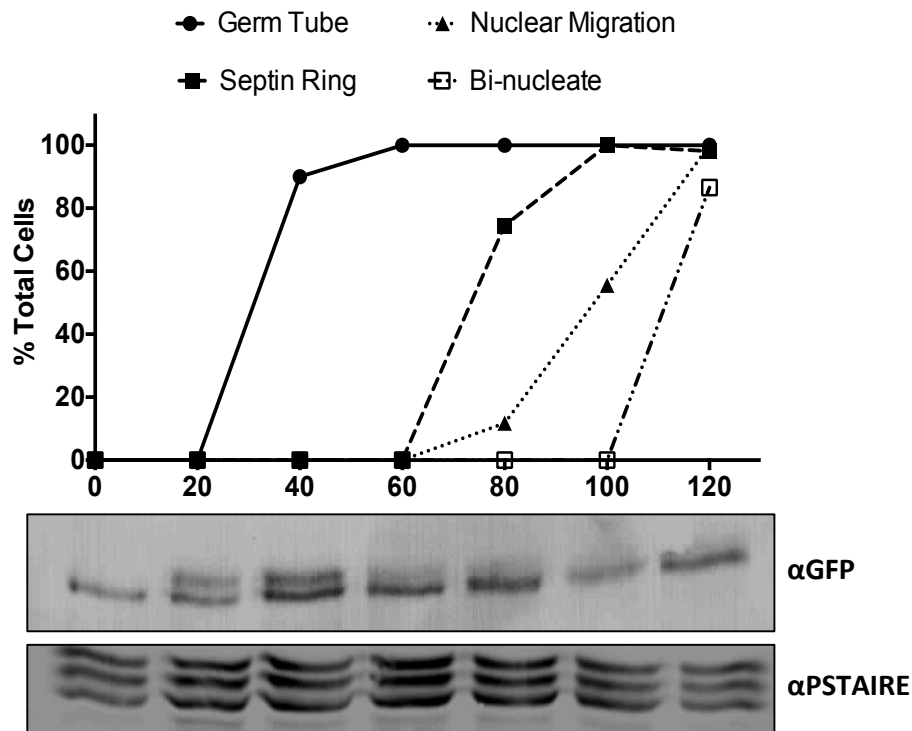


**Fig. 4.2.2. Fkh2 is phosphorylated early after hyphal induction, independent of cell cycle stage.** *FKH2/FKH2-YFP* G1 cells were obtained from a log phase culture through elutriation and then re-inoculated into hyphal inducing conditions. Samples were taken at the shown time-points for microscopy and protein extraction. 50µg of protein extract from each time-point was run on a 7% SDS-PAGE gel, and an αGFP antibody was used to detect Fkh2-GFP on the subsequent Western blot. Samples were re-run on a 10% SDS-PAGE gel for an αPSTAIR loading control Western blot. Hyphal growth was followed by microscopy using DAPI as a marker for the nucleus and Cdc12-mCherry to mark the septin ring. Each time-point contains average values for 50 cells.

#### 4.2.3. Determining the residues phosphorylated on Fkh2 after hyphal induction

To determine which sites on Fkh2 are phosphorylated early on in hyphal growth, phospho-peptide mapping was carried out. The C-terminal fragment of the *FKH2* gene was cloned into a vector with the Hemagglutinin epitope (HA) and a *URA3* selectable marker 3' of the cloning site. This vector was then digested with *NcoI* to cut it once and allow integration through recombination with a copy of *FKH2* in the genome. This strain was confirmed by previously mentioned techniques.

The *FKH2-HA* strain was used to immunoprecipitate (IP) Fkh2-HA from a 5L culture, grown for 40mins in hyphal inducing conditions. The purified Fkh2-HA

was eluted from the beads and run on a gel, before Coomassie staining and excision of the band that corresponded to Fkh2-HA (Fig. 4.2.3A). The band was digested and then run on the mass spectrometer. The results from the phosphopeptide mapping show that Fkh2 is phosphorylated at this time-point, and that some of the phosphorylation occurs at CDK consensus phosphorylation motifs (Fig. 4.2.3B-C).

To support the observation that Fkh2 is phosphorylated at CDK consensus and minimal sites on hyphal induction, the phosphorylation status of Fkh2 was investigated with an antibody ( $\alpha P_{SER}$ ) that recognises phosphorylated serines in CDK consensus and minimal sites (Fig. 4.2.4A.). Fkh2-YFP was IP'd from cultures 40min after hyphal induction. Samples underwent SDS-PAGE gel separation and the subsequent Western blot was probed with the above-mentioned phospho-specific antibody. Fkh2 is indeed phosphorylated at CDK sites containing serine upon hyphal induction, supporting the previous phospho-peptide mapping data (Fig. 4.2.3.). This experiment was also carried out for Fkh2 during yeast growth conditions (120mins) using cells expressing a 6xMyc C-terminally tagged Fkh2 (Fig. 4.2.4B.). For this experiment an antibody ( $\alpha P_{SER(CDK)}$ ) that detects phosphorylation only at serine residues in CDK consensus sites was used. This showed that Fkh2 is phosphorylated at serine residues in CDK sites during yeast growth. Gin4-6Myc has previously been shown to be phosphorylated at CDK sites during yeast growth using this antibody (Li et al. 2012), and was therefore used as a positive control (Fig. 4.2.4B). An IP from a log phase BWP17 culture was used as a negative control for non-specific binding of the phospho-antibody on the western blot (Fig. 4.2.4B).

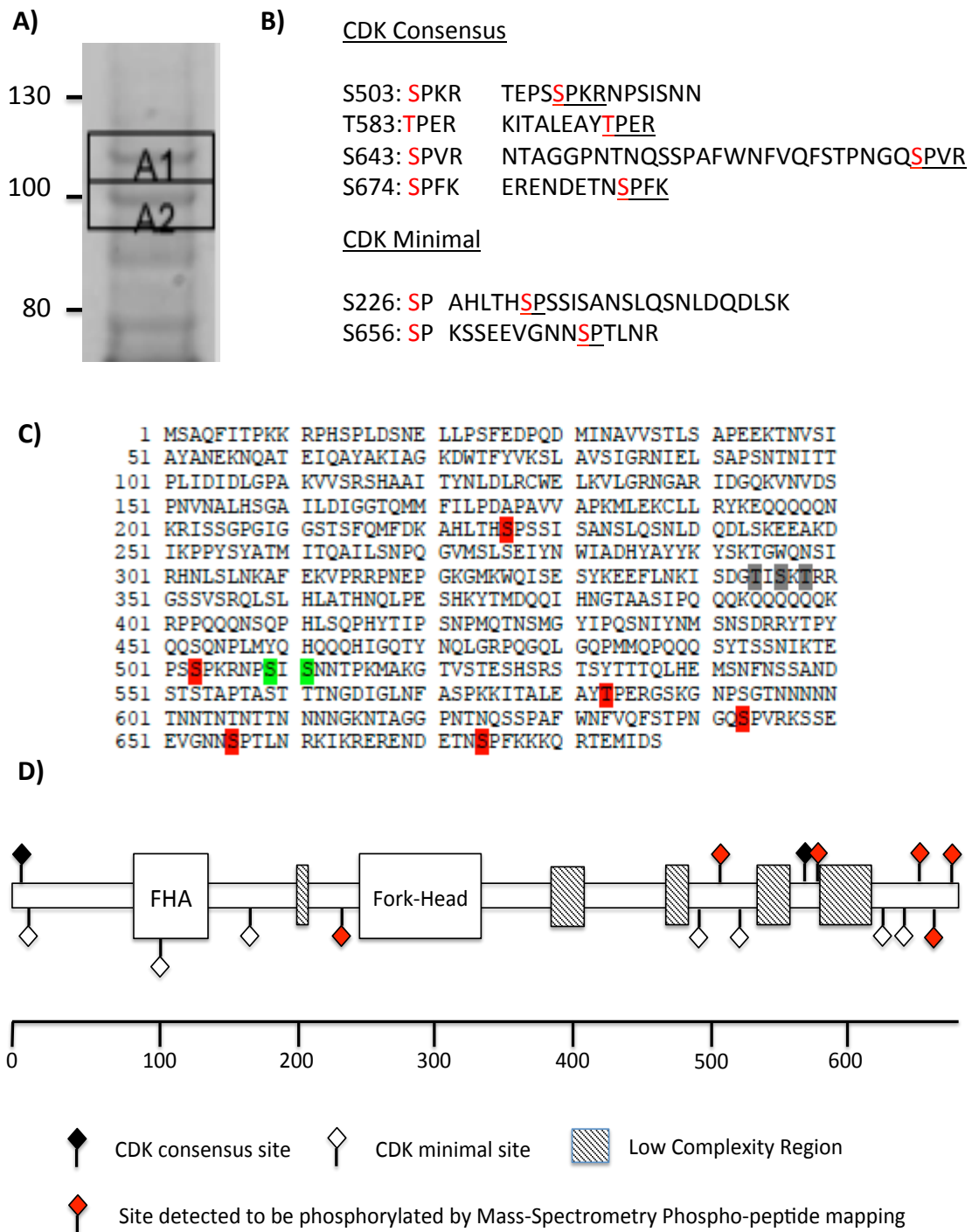


**Fig. 4.2.3. Investigating Fkh2 early hyphal phosphorylation by mass-spectrometry phospho-peptide mapping.** **A)** Coomassie stained gel of Fkh2-HA IP for phospho-peptide mapping – values represent kDa molecular weight markers. **B)** Table of residues phosphorylated and peptide hits. Phosphorylated residues in the peptide are coloured red. **C)** Results from phospho-peptide mapping. Red – significant hit, Grey – possible phosphorylation site, Green – either site is phosphorylated. **D)** Schematic of Fkh2 phosphorylation sites observed from biological replicates of Fkh2-3HA expressing cells grown for 40mins under hyphal induction

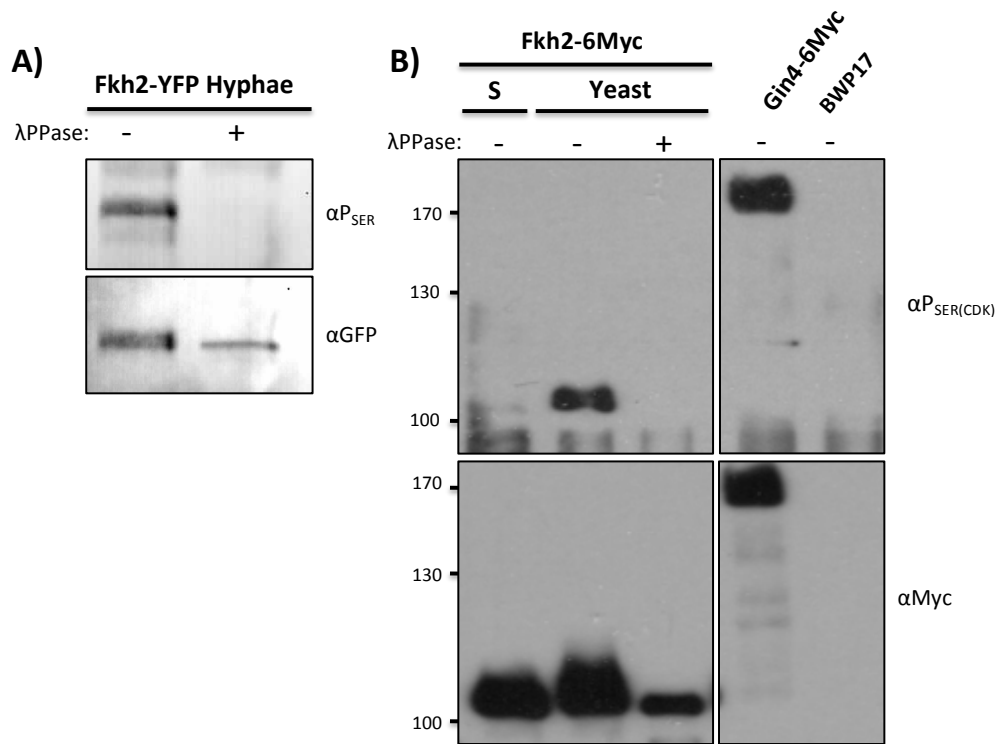


**Fig. 4.2.4. Investigating Fkh2 phosphorylation with phospho-specific antibodies. A)** Fkh2-YFP was IP'd from expressing cells 40mins after hyphal induction. After Western blotting the membrane was probed with an  $\alpha$ Phosphoserine CDK/MAPK (S/P site) antibody ( $\alpha$ P<sub>SER</sub>) (Cell Signaling). The membrane was then stripped and re-probed with an  $\alpha$ GFP antibody (Roche). **B)** Fkh2-6xMyc was IP'd from expressing cells at 120mins after re-inoculation into yeast growth conditions. After Western blotting the membrane was probed with an  $\alpha$ Phosphoserine CDK (SPxR/K site) antibody ( $\alpha$ P<sub>SER(CDK)</sub>) (Cell Signaling); then stripped and re-probed with an  $\alpha$ Myc antibody. Between carrying out these experiments the  $\alpha$ Phosphoserine CDK (SPxR/K site) antibody was discontinued by Cell Signaling.

#### 4.2.4. Mutagenesis studies of Fkh2 phosphorylation

In order to further understand the phospho-regulation of Fkh2, the phosphorylation sites were mutated. From this, the sites that are phosphorylated could be confirmed, along with the physiological consequences of these mutations, which will be covered later.

##### 4.2.4.1 Construction of a *fkh2Δ/Δ* strain

In order to determine the effect of reintroducing mutant copies of Fkh2 into the cell, a genetic background where there are no copies of *FKH2* present would be required. To do this a knockout vector was created where the upstream and downstream sequences of the *FKH2* were cloned into a vector containing a

selectable auxotrophic marker (Fig. 4.2.5A). A 500bp 5' upstream fragment of *FKH2* was amplified with a 5' *KpnI* and 3' *XhoI* restriction site (Fig. 4.2.5B). This was cloned into the pBluescript (pBks) vector upstream of the *ARG4* gene and its promoter from *C. albicans* (Fig. 4.2.5C). A 400bp downstream fragment of *FKH2* with 5' *NotI* and 3' *SacII* sites was then cloned in downstream of the *ARG4* gene (Fig. 4.2.5B-C). This vector was then sequenced to check that the *FKH2* up and down-stream sequences were correct, and did not contain mutations. To transform the *FKH2* 5'-*ARG4*-*FKH2* 3' fragment it was cut from the vector with *KpnI* and *SacII*. This then recombined with the homologous sequences in the genome, removing one allele of *FKH2* and replacing it with the *ARG4* selectable marker, allowing selection of *ARG4*<sup>+</sup> correct transformants. These transformant colonies were then checked by PCR to determine that the knockout cassette had inserted into the correct locus (Fig. 4.2.5D).

In order to knockout the second allele of *FKH2*, the selectable marker in the knockout vector was replaced with a different selectable marker. The *P<sub>ARG4</sub>-ARG4* marker was cut out of the vector with *XhoI* and *NotI*, and replaced with the URA-Flipper (URAF) marker that had been cut out of a pBks vector (Hickman et al. 2013) with the same restriction sites. Once generated, this vector was transformed into the *fkh2*/*FKH2* strain. Homozygous deletion colonies were selected for as being prototrophic for both arginine and uridine. These were then confirmed by PCR to determine correct genomic integration (Fig. 4.2.5D).

Using the URAF selectable marker allows excision of the *URA3* marker, so that it can be recycled to carry out other transformations into the strain. The URA-Flipper contains the *FLP* recombinase under the control of the *SAP2* promoter, which is induced under conditions where protein is the sole nitrogen source. A *fkh2Δ/Δ URA3*<sup>+</sup> colony was grown overnight in yeast carbon base-BSA to activate the *SAP2* promoter. The expressed FLP recombinase then excises the *URA3* cassette by recombining the two *FRT* sites either side of the cassette. *ura3*<sup>-</sup> colonies were then selected for by plating out the culture onto 5-FOA agar. Correct colonies were confirmed by PCR to show that the URAF marker was no longer present (Fig. 4.2.5E).

The *fkh2Δ/Δ* strain shows the same phenotype as previously noted by Bensen et al 2002, further confirming that both copies of *FKH2* have been knocked out (Fig. 4.2.5F).

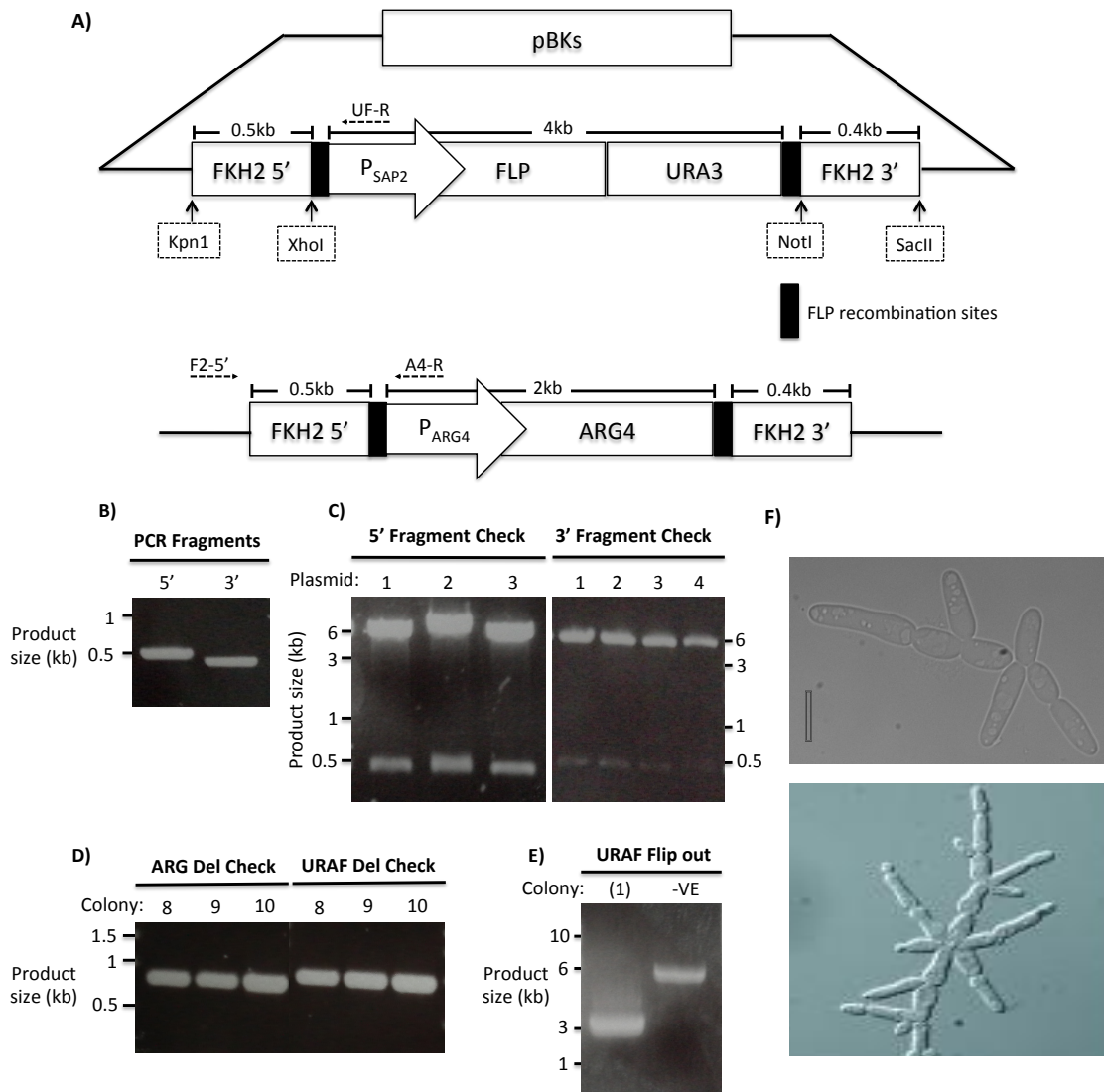


**Fig. 4.2.5. Construction of a *fkh2Δ/Δ* strain.** **A)** Diagram of pBluescript (pBKs) vector containing *FKH2* *ARG4* deletion cassette ( $P_{ARG4}$  is the *ARG4* promoter region), and the *URA3*-Flipper deletion cassette ( $P_{SAP2}$  is the *SAP2* promoter region). **B)** *KpnI*-*FKH2* 5'-*XhoI* and *NotI*-*FKH2* 3'-*SacII* PCR fragments. **C)** Confirmation of integration of each *FKH2* fragment into the pBKs vector by digesting with the same enzymes used to integrate. **D)** PCR to check integration of the deletion cassettes at the correct genomic locus in *C. albicans*, using *FKH2* Del Chk Fwd and either *URAF* or *ARG4* Del Rev Chk primers. **E)** PCR to check that the *URA3* gene has been excised from the *FKH2* genomic locus, using *FKH2-kpn1* AF and *FKH2-SacII* DR. The *URA*<sup>+</sup> *fkh2Δ/Δ* strain was used as the negative control. **F)** Top panel – phenotype of the *fkh2Δ/Δ* strain generated in the above process. Bottom panel – phenotype of the *fkh2Δ/Δ* strain generated by Bensen et al 2002.

#### 4.2.4.2. Cloning of *FKH2*

In order to introduce mutations at the phosphorylation sites in Fkh2, the *FKH2* gene along with its promoter were initially cloned into a vector with a C-terminal 6xMyc epitope tag (Fig. 4.2.6A). The *FKH2* gene and an upstream 600bp of sequence were amplified by PCR with a 5' *AscI* and 3' *XhoI* Restriction site (Fig. 4.2.6B). This fragment was then ligated into the pCIP10U vector that had been digested with the same enzymes. Recombinant plasmids recovered from *E. coli* were first checked by restriction digest for the fragment (Fig. 4.2.6C), and then sequenced to check that no mutations had been introduced. The 6xMyc epitope tag in the vector was then swapped for GFP through sub-cloning from another vector. GFP was to be used as the epitope tag for the mutants as this was the tag used for the initial experiments.

In order to allow re-integration of this plasmid back into the *FKH2* chromosomal locus, a *HindIII* restriction site was introduced into the *FKH2* promoter region in the vector, using site-directed mutagenesis. Correct introduction of the *HindIII* site was checked by restriction digest (Fig. 4.2.6D) followed by sequencing.

A)

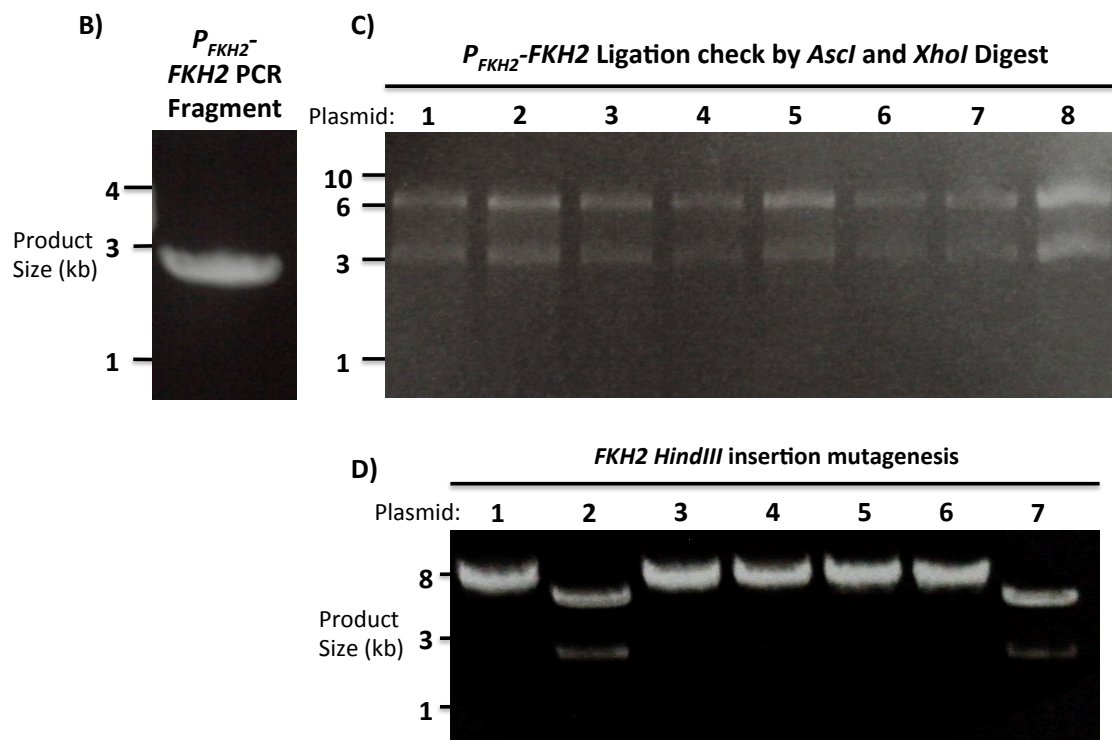
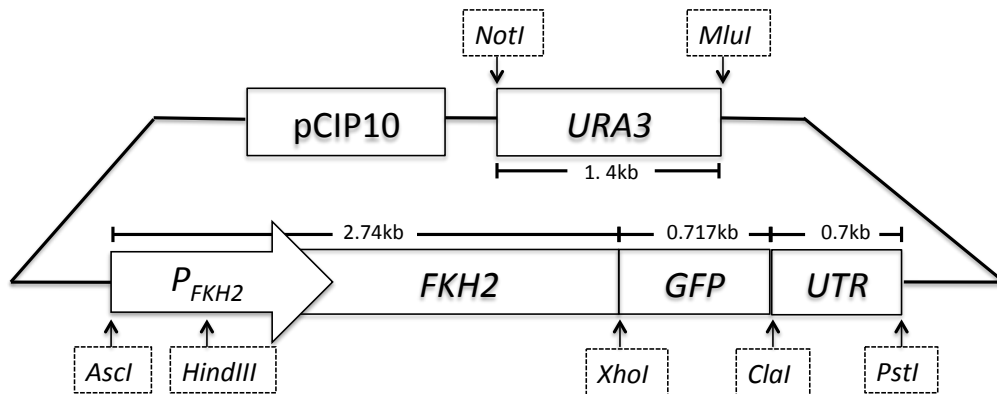


**Fig.4.2.6. Construction of a *FKH2*-GFP vector for phosphorylation site mutagenesis.** A) Diagram of the  $P_{FKH2}$ -FKH2-GFP pCIP10 URA3 vector, showing inserted *HindIII* restriction site B) PCR fragment amplified of *Ascl*- $P_{FKH2}$ -FKH2-*XhoI* fragment. C) *Ascl*/*XhoI* digests of plasmids from transformant colonies after ligation. D) *HindIII* digests to check mutagenesis to add a *HindIII* restriction site into the *FKH2* promoter, with correct plasmids being present as only a single band.

#### 4.2.4.3. Mutation of sites from Phospho-peptide mapping

In order to observe the effect of loss of phosphorylation at the six sites identified by mass-spectrometry, the serine/threonine at these sites were replaced with non-phosphorylatable alanine residues simultaneously. This was carried out as detailed in the materials and methods, using the mutagenic primers listed.

When comparing this mutant (Fkh2(6A<sub>MS</sub>)) with wild-type Fkh2 tagged with GFP, it can be observed that there is no difference in the phosphorylation level during yeast growth or on hyphal induction (Fig. 4.2.7A). The upper band corresponding to the phosphorylated isoform of Fkh2 is still present when analysed by SDS-PAGE followed by αGFP Western blotting.

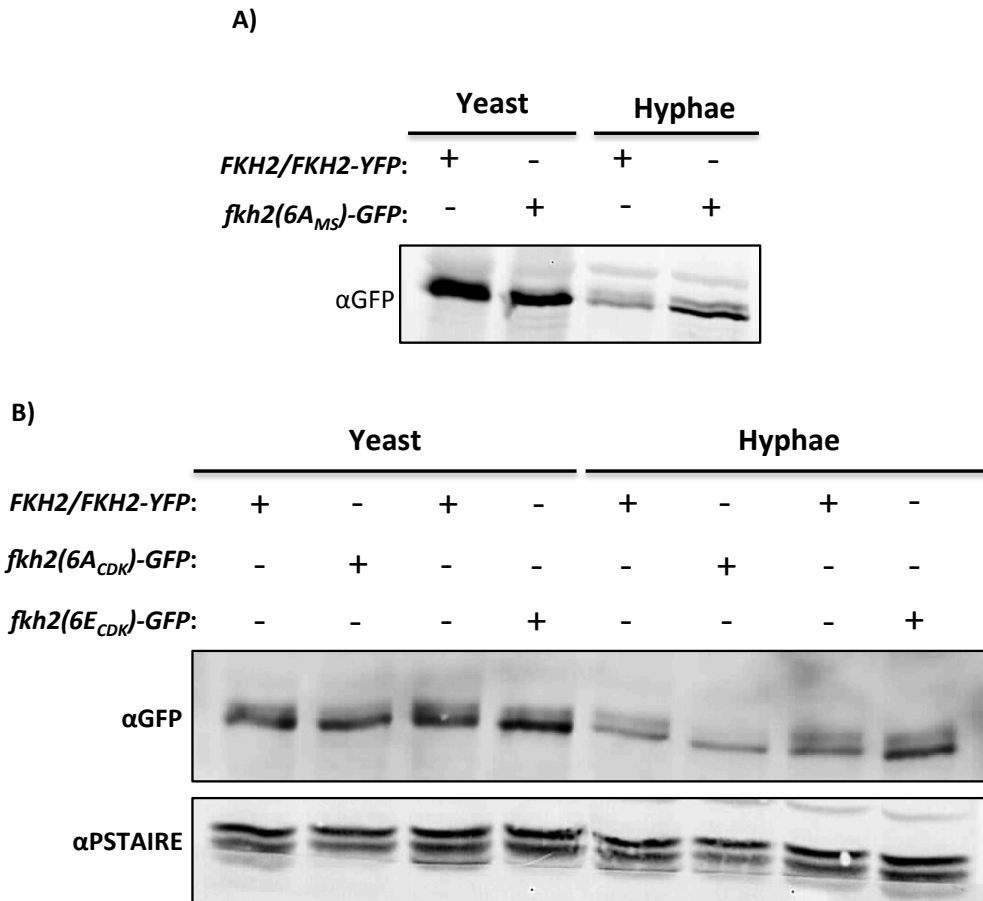


**Fig. 4.2.7. Mutational analysis of Fkh2 phosphorylation.** A) *fkh2*(6A<sub>MS</sub>)-GFP and *FKH2*/*FKH2*-YFP cells were grown for 120mins as yeast and 40mins as hyphae; 50µg protein extract from these cells was run on a 7% SDS-PAGE gel to separate phospho-isoforms and the subsequent Western blot was probed with αGFP B) *fkh2*(6A<sub>CDK</sub>)-GFP and *fkh2*(6E<sub>CDK</sub>)-GFP were grown as above with the *FKH2*/*FKH2*-YFP strain, and the protein extracted for αGFP Western blotting as before. Samples were re-run on a 10% SDS-PAGE gel that was then Western blotted and probed with αPSTAIR as a control for equal loading.

#### 4.2.4.4. Mutation of CDK consensus sites

Due to the fact that mutating the mapped phosphorylation sites did not cause a loss of Fkh2 phosphorylation, the CDK consensus sites in Fkh2 were mutated to non-phosphorylatable alanine (6A<sub>CDK</sub>) or to phosphomimetic glutamic for threonine residues, or aspartic acid for serine residues (6E<sub>CDK</sub>). Blocking

phosphorylation at the CDK sites prevents Fkh2 from being phosphorylated on hyphal induction (Fig. 4.2.7B), demonstrating that these are the sites that are phosphorylated on hyphal induction. However there still appears to be a partial band-shift during yeast growth, suggesting that there are other sites that are phosphorylated during yeast growth. The *fkh2(6E<sub>CDK</sub>)-GFP* strain mimicking phosphorylation still shows a band shift on hyphal induction and during yeast growth.

#### 4.2.4.5. Mutation of CDK consensus and minimal sites

In addition to mutating the CDK consensus sites, the nine minimal (S/TP) sites were also mutated to either block or mimic phosphorylation. This generated *fkh2(15A)-GFP* and *fkh2(15E)-GFP* plasmids that were integrated back into the *fkh2Δ/Δ* strain and checked as previously mentioned. Along with this the eleven CDK consensus and minimal sites C-terminal to the DNA binding domain were mutated to alanine, allowing confirmation that the phosphorylation of Fkh2 occurs in its C-terminal domain. The plasmid for this strain was generated by making use of two internal *KpnI* sites in the *FKH2* sequence. The *fkh2(15A)-GFP* and the *FKH2-GFP* plasmids were digested with *KpnI* and *XhoI* to release two C-terminal fragments from each vector. The two fragments containing the phosphorylation blocking mutations were cloned back into the wild-type vector, generating a construct in which all the C-terminal CDK sites of Fkh2 had alanine mutations. Correct orientation of integration of the DNA fragments containing mutations was confirmed by sequencing. This plasmid was again integrated back into the *fkh2Δ/Δ* strain at the *FKH2* promoter.

The *Fkh2(15A)-GFP* did not show phosphorylation upon hyphal induction or during yeast growth (Fig. 4.2.8.). This confirms the result observed with the *fkh2(6A)-GFP* strain during hyphal growth, and demonstrates that there are indeed other residues on Fkh2 that are phosphorylated during yeast growth. The *Fkh2(15E)-GFP* protein shows a band-shift during both yeast and hyphal growth, similar to that observed with the *Fkh2(6E<sub>CDK</sub>)-GFP* protein (Fig. 4.2.8.). The *fkh2(11A)-GFP* strain shows a loss of phosphorylation on hyphal induction and during yeast growth (Fig. 4.2.8.). This demonstrates that the CDK sites in the C-

terminus of Fkh2 are targeted for phosphorylation, and not the few sites located in the N-terminus.

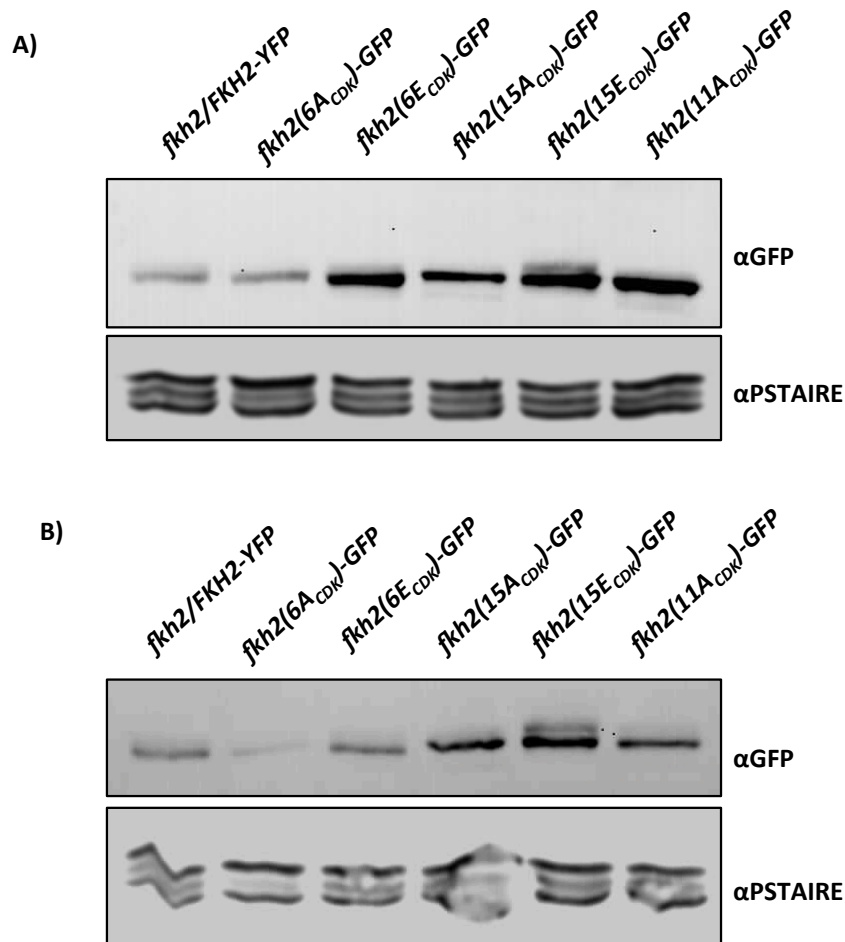


**Fig. 4.2.8. Comparison of Fkh2 Phospho-mutants.** A) Phosphorylation mutants isolated from cells after 120min yeast growth. B) Phosphorylation mutants isolated from cells 40min after hyphal induction. Gels were run and Western blotting carried out as previously described. Samples were re-run and blots probed with  $\alpha$ PSTAIR to confirm equal loading.

#### 4.2.4.6. Fkh2 C-terminal truncation (*fkh2* 1-426)

The majority of CDK consensus and minimal target sites are located within the region C-terminal to the DNA-binding domain. To confirm if this region is where Fkh2 is phosphorylated; the region was truncated, and the phosphorylation pattern of this mutant was observed. The truncation was carried out by amplifying Fkh2 from the *P<sub>FKH2</sub>-FKH2-GFP* plasmid, from the promoter with the integration site up until just after the Fork-head domain. This was cloned back into the plasmid with *AscI* and *XhoI* as previously described. Integration of the plasmid

back into the *fkh2Δ/Δ* strain showed nearly a full rescue of the phenotype (Fig. 5.1.7.).

The phosphorylation status of this strain was tested on hyphal induction and during yeast growth (Fig. 4.2.9.). Due to the difference in molecular weight of *fkh2(1-426)*, the phospho-shifts could not easily be compared with a wild-type Fkh2-YFP; therefore, identical samples were compared with and without phosphatase treatment. There was no phospho-shift observed on hyphal induction or during yeast growth.

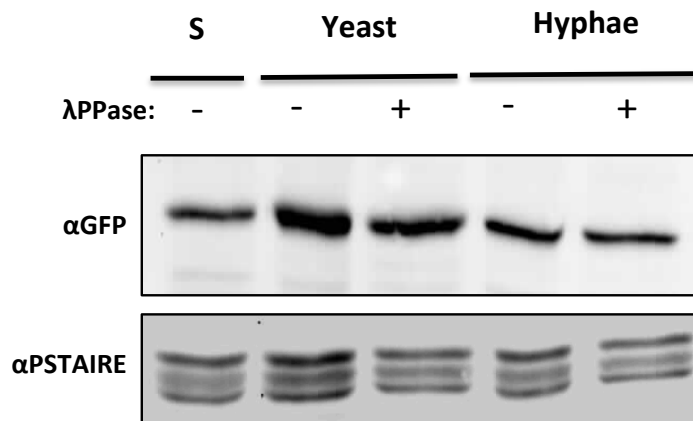


**Fig. 4.2.9. Truncation of Fkh2 affects its phosphorylation status.** *fkh2(1-426)-GFP* cells were grown under yeast or hyphal inducing conditions as previously described. 50μg samples were run on SDS-PAGE and Western blotted; the blot was probed with αGFP to detect if a band-shift was present. Phosphatase (λppase) treatment was used to confirm that no phospho-band shift was observed. A separate αPSTAIR was again used as a loading control.

#### 4.2.5. Determining if Cdk1 is responsible for Fkh2 phosphorylation

Due to phosphorylation of Fkh2 occurring in CDK consensus motifs, it was then sought to determine if, as expected, Cdk1 is responsible for the observed phosphorylation

##### 4.2.5.1 Cdk1 can phosphorylate Fkh2 *in vitro*

To determine whether Cdk1 can directly phosphorylate Fkh2, an *in vitro* kinase assay was carried out. Initially the DNA sequence of the C-terminal region of Fkh2 was amplified from the wild-type and *fkh2(6A<sub>CDK</sub>)-GFP* vectors and cloned

into the N-terminal GST expression vector pGEX-4T1. Due to the intron present in the 3' region of the *FKH2* gene, skip PCR was used to amplify only the coding sequence, as the intron cannot be spliced out in *E. coli* and would therefore prevent expression of the C-terminal fragment. The GST-Fkh2 C-terminal (CT) fragment plasmids were transformed into BL21, allowing expression and purification of the GST-Fkh2(CT) fragment (Fig.4.2.10.).

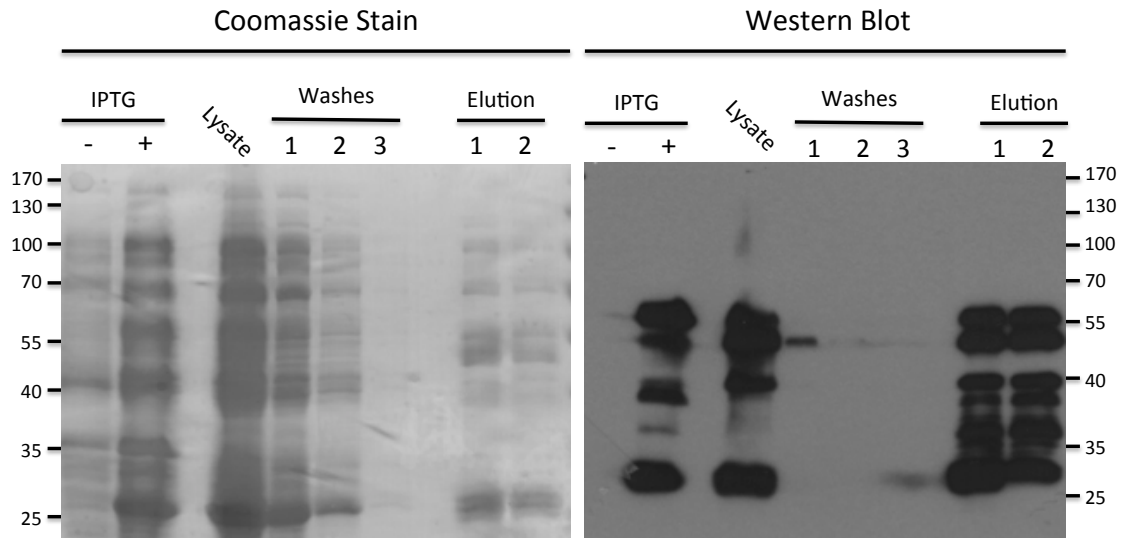


**Fig. 4.2.10. Purification of GST-Fkh2(CT) from *E. coli*.** 800ml BL21 *E. coli* containing the *GST-FKH2(CT)* plasmid were induced with 100 $\mu$ M IPTG overnight at 37°C to express the GST-Fkh2(CT) fusion protein. The fragment was then affinity purified with glutathione sepharose from which it was eluted with glutathione in 20mM Tris-HCl. Shown on the left is the Coomassie stained gel following the purification process including material removed on washing glutathione beads. On the right is an  $\alpha$ GST blot of identical samples. The GST-Fkh2(CT) fragment is present as two bands at ~50kDa.

The GST fragments were used in kinase reactions with Cdk1-HA purified from cells 40mins after hyphal induction (Fig. 4.2.11). Reactions were also carried out for both GST fragments where no kinase was added, to determine whether the fragments can auto-phosphorylate. Another reaction was carried out where no ATP was added, to determine whether the IP'd kinase was ATP bound. A negative kinase IP was carried out from a BWP17 cell lysate, to show that any phosphorylation observed was not due to a co-precipitating kinase that was bound to be beads used to purify the kinase. Samples were Western blotted and then the blots probed with an antibody ( $\alpha$ P<sub>SER(CDK)</sub>) that recognises phosphorylated serines

in CDK phosphorylation motifs. Only the positive kinase reaction for the wild-type GST-Fkh2 fragment was detected by the antibody. This shows that Cdk1 can directly phosphorylate Fkh2, and that the phosphorylation was not due a co-precipitating kinase or auto-phosphorylation occurring. The observation that the fragment (GST-Fkh2-A-(CT)) where phosphorylation was blocked at CDK sites was not phosphorylated, also shows that Cdk1 directly targets these sites for phosphorylation.

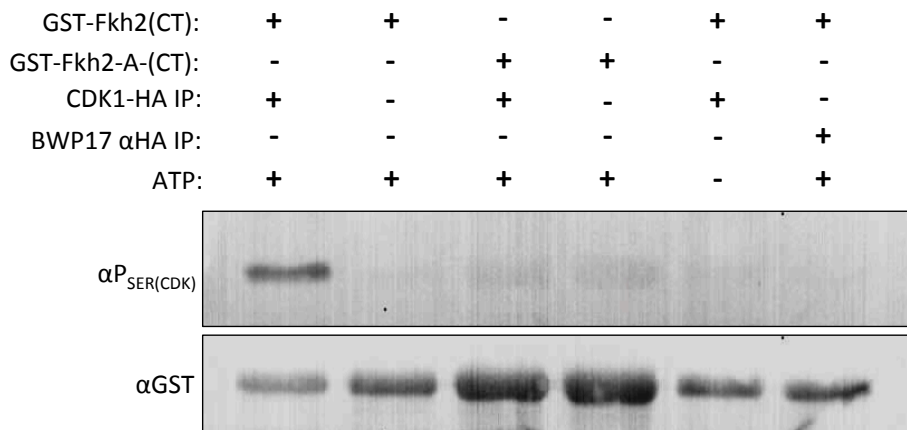


**Fig. 4.2.11. Cdk1 can phosphorylate the C-terminus of Fkh2 *in vitro*.** GST-Fkh2(CT) WT and 6A<sub>CDK</sub> purified from *E. coli* were used in the reactions. A BWP17 negative IP and a sample without ATP were used as negative controls. Samples were run on a 10% SDS-PAGE gel and the subsequent Western blot blotted first with  $\alpha$ Phosphoserine-CDK ( $\alpha$ P<sub>SER(CDK)</sub>) (Cell Signaling) and then stripped and re-probed with  $\alpha$ GST as a loading control.

#### 4.2.5.2. Inhibition of analogue-sensitive Cdk1 does not prevent Fkh2 phosphorylation

To determine whether the observed *in vitro* phosphorylation of Fkh2 occurs *in vivo*, an analogue-sensitive allele of Cdk1 was used. Fkh2 was C-terminally tagged with GFP in a 1NM-PP1 analogue-sensitive Cdk1 strain generated by Sinha and colleagues (Sinha et al. 2007). This strain was grown up overnight and then aliquots were taken and treated with the 1NM-PP1 analogue or DMSO for 30min. The inhibitor is dissolved in DMSO; therefore adding DMSO alone allows determination of whether the observed phenotype on addition of 1NM-PP1 is actually due to the effect of the DMSO that it is dissolved in. These cells were then re-inoculated into yeast or hyphal growth conditions and grown as previously. Samples were compared with those from BWP17 cells expressing Fkh2-GFP with two functional *CDK1* alleles present. On addition of DMSO or 1NM-PP1 there was

no loss of Fkh2-GFP band-shift on hyphal induction or during yeast growth (Fig. 4.2.12A). To show that the 1NM-PP1 analogue was working, an aliquot of the cells was kept growing under hyphal-inducing conditions, so that the phenotype could be observed. Indeed the correct phenotype was observed for inhibition of Cdk1 (Fig. 4.2.12B), suggesting that Cdk1 does not phosphorylate Fkh2 *in vivo*. This experiment was repeated more than 10 times, varying the conditions, but still showing the same result. Interestingly the  $\alpha$ PSTAIR loading control appears as two bands in the analogue-sensitive strain. This strain only has one allele of CDK1, suggesting that the other allele of CDK1 produces a protein product of a different size.

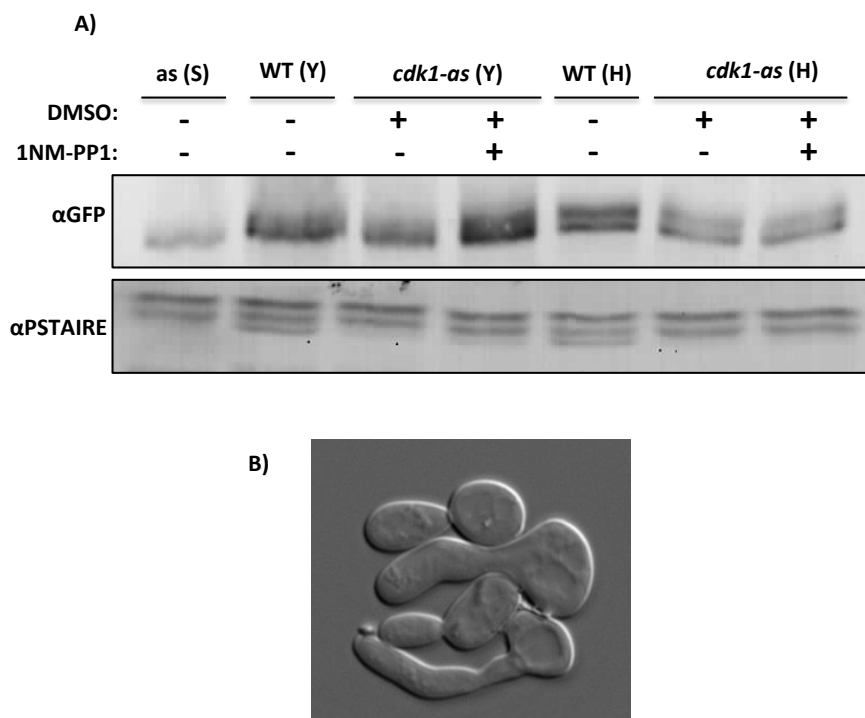


**Fig. 4.2.12. Inhibiting Cdk1 does not affect Fkh2 phosphorylation.** Aliquots of *cdk1-as/FKH2-GFP* cells were taken and treated for 30mins with either DMSO or 30 $\mu$ M of 1NM-PP1 ATP analogue (Merck) dissolved in DMSO. These aliquots were re-inoculated into yeast or hyphal growth conditions and grown for 120mins or 40mins respectively. Samples were compared with a *FKH2/FKH2-YFP* strain. A) 50 $\mu$ g of total cell lysate was run on a 7% SDS-PAGE gel, with the Western blot being probed with  $\alpha$ GFP to detect the Fkh2-GFP band-shift. A separate  $\alpha$ PSTAIR blot was used as a loading control. A sample from the 1NM-PP1 treated cells was kept for microscopy to confirm the kinase was inhibited

#### 4.2.5.3. Fkh2 phosphorylation in Cdk1 cyclin knockout strains

To further investigate whether Cdk1 is responsible for phosphorylating Fkh2, Fkh2 was C-terminally tagged with GFP in knockout or shutdown strains of the cyclin-interacting partners of Cdk1.

In the *ccn1Δ* strain, Fkh2-GFP still shows a band-shift on hyphal induction and during yeast growth (Fig. 4.2.13.). Knockout of *HGC1* or shutdown of *CLN3* with the *MET3* promoter does not affect Fkh2's phosphorylation status in yeast or hyphae (Fig. 4.2.13.); however, Fkh2 appears more stable in the *hgc1Δ/Δ* strain.. *MET3* promoter shutdown of the G2 cyclin *CLB4* appears not to affect the phosphorylation of Fkh2 (Fig. 4.2.13.). Shutting down *CLB2* expression affects either the stability or expression of Fkh2, as there is a marked reduction in Fkh2 levels. This supports the above observation that Cdk1 is not responsible for the phosphorylation of Fkh2 in *C. albicans*, although it may have a role in regulating Fkh2's abundance. Interestingly on depletion of *CLB2* the middle band is lost for the  $\alpha$ PSTAIR loading control (Fig. 4.2.13.), suggesting that differential regulation of CDKs occurs on depletion of *CLB2*.

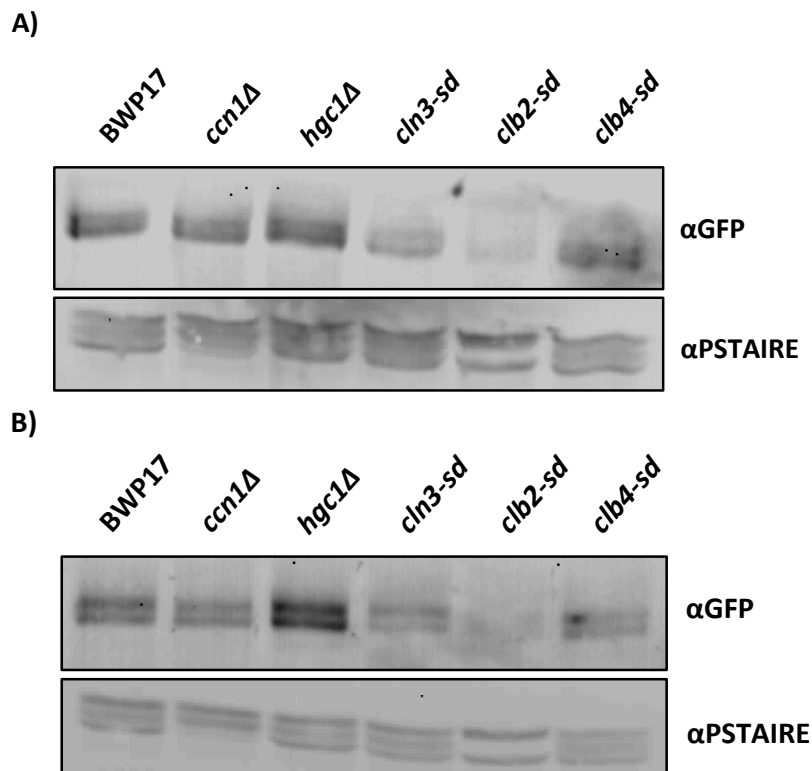


**Fig. 4.2.13. Investigating Fkh2 phosphorylation in Cdk1 cyclin knockouts/shutdown strains.** All strains were grown up overnight in YEPD to allow partial shutdown of the *MET3* promoter. For *P<sub>MET3</sub>* shutdown strains, cells were re-inoculated into YEPD supplemented with methionine and cysteine. The strains were grown as yeast for 120mins (A) or hyphae for 40mins (B). Samples were run and gels processed as previously described.

#### 4.2.5.4. Investigating if Fkh2 and Cdk1 physically interact

If Fkh2 is a regulatory target of Cdk1 it would be expected that they interact physically. However such kinase-substrate interactions are likely to be transient, lasting only long enough for the addition of a  $\gamma$ -phosphate from ATP, and therefore may be difficult to capture.

Fkh2-YFP expressing cells were harvested early after hyphal induction, and Fkh2 was immunoprecipitated using an  $\alpha$ GFP antibody. To detect whether Cdk1 co-precipitated, Fkh2-GFP samples were run on a gel, Western blotted, and then probed with an  $\alpha$ PSTAIRES antibody that recognises the conserved PSTAIRES motif found in CDKs (Fig. 4.2.14.). An IP from a BWP17 lysate was used as a negative control for non-specific CDK binding to the  $\alpha$ GFP beads used for IP. There does not appear to be a difference between the positive and negative IPs, suggesting that no interaction is present; however, due to the inefficiency of the IP, it cannot be certain that they do not interact. A non-specific band is observed below that of Fkh2-GFP (Fig. 4.2.14.). This is unlikely to be the  $\alpha$ GFP antibody heavy chain as the band is much higher than the expected 50kDa on a 10% gel, and therefore may be a co-precipitant.

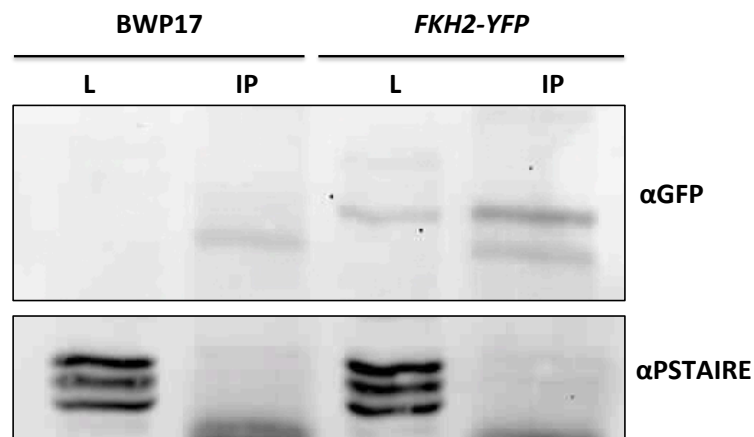


**Fig. 4.2.14. Examining if Fkh2 and Cdk1 physically interact.** Fkh2-YFP was IP'd from 2mg of *fkh2/FKH2-YFP* lysate 40mins after hyphal induction. IPs were washed twice with RIPA buffer and then run on a 10% gel. The subsequent Western blot was probed with an  $\alpha$ PSTAIRES antibody that recognises the PSTAIRES motif on cyclin dependent kinases. The blot was also probed with  $\alpha$ GFP to confirm the IP of Fkh2. 50 $\mu$ g total lysate from the strain was run to show the correct position of the PSTAIRES bands. A BWP17  $\alpha$ GFP IP and lysate was used as a negative control.

#### 4.2.6. Other kinases that may phosphorylate Fkh2

Due to the observation that loss of Cdk1 activity does not prevent Fkh2 phosphorylation, other kinases that could carry out the phosphorylation were sought. These were chosen on the basis that they would be able to at least phosphorylate CDK minimal motifs (S/TP).

##### 4.2.6.1 Deletion of *CRK1* does not affect Fkh2 phosphorylation

The Cdc2-related kinase Crk1 has previously been shown to be important for hyphal morphogenesis in *C. albicans* (Chen et al. 2000). Crk1 can phosphorylate CDK consensus motifs, and therefore was a likely candidate to carry out the early hyphal phosphorylation of Fkh2. A C-terminally GFP tagged Fkh2 in a *crk1Δ/Δ* strain still shows the same early hyphal phosphorylation pattern observed for Fkh2-GFP in the BWP17 wild-type strain (Fig. 4.2.15B), indicating that Crk1 is not responsible for phosphorylating Fkh2. Crk1 was also found not to be important for Fkh2 phosphorylation during yeast growth (Fig. 4.2.15A)

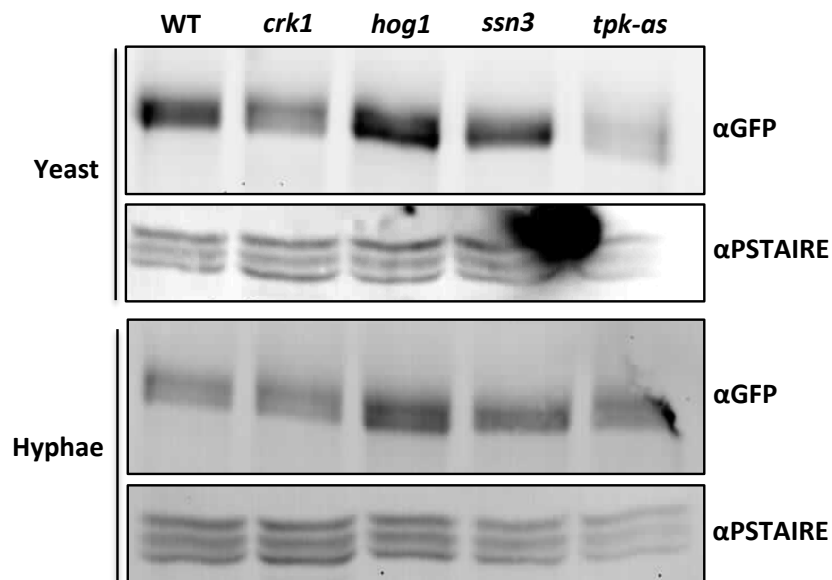


**Fig. 4.2.15. Investigating if other kinases phosphorylate Fkh2.** Kinase knockout strains *crk1Δ/Δ*, *hog1Δ/Δ* and *ssn3Δ/Δ* were used, along with an analogue sensitive Tpk1 strain in which *TPK2* had been knocked out. Fkh2 was tagged with GFP in each of these strains and the band shift of Fkh2-GFP was observed during yeast growth or 40mins after hyphal induction. These strains were compared against the *FKH2/FKH2-YFP* strain.

#### **4.2.6.2. Deletion of *HOG1* does not affect Fkh2 phosphorylation**

To determine whether stress-activated protein kinase Hog1 is responsible for the phosphorylation of Fkh2; Fkh2 was C-terminally tagged with GFP in a *hog1Δ/Δ* strain. The phosphorylation state of Fkh2-GFP in this strain was then compared with Fkh2-GFP in BWP17. Fkh2-GFP in *hog1Δ* still appears as two bands when analysed by 1D SDS-PAGE with an  $\alpha$ GFP Western blot (Fig. 4.2.15). This shows that in the absence of *HOG1*, Fkh2 can still be phosphorylated upon hyphal induction and during yeast growth, and thus Hog1 is not responsible for phosphorylation of Fkh2. Interestingly, there appears to be more Fkh2 present in the *hog1Δ/Δ* mutant, suggesting that Fkh2 may be more stable or higher expressed when *HOG1* is knocked out.

#### **4.2.6.3. Inhibiting cAMP-dependent protein kinases does not affect Fkh2 phosphorylation**

The cAMP-dependent protein kinases Tpk1 and Tpk2 are key components of the hyphal morphogenesis program (Bockmühl et al. 2001). It is thought that they are partially redundant, as deletion of either one separately does not affect viability, however, deletion of both is lethal. Due to this a strain has been constructed where *TPK2* has been knocked out, and *TPK1* mutated in order to make it sensitive to the 1NM-PP1 ATP analogue (Bockmühl et al. 2001). Fkh2 was GFP tagged C-terminally in this strain to allow the phosphorylation status to be detected through a band-shift on a 1D SDS-PAGE gel. No loss of Fkh2-GFP phosphorylation could be detected on addition of 1NM-PP1 during yeast growth or on hyphal induction (Fig. 4.2.15.).

#### **4.2.6.4. Deletion of *SSN3* does not affect Fkh2 phosphorylation**

Ssn3 is the homologue of Cdk8, which in *S. pombe* has been shown to be required for phosphorylation of Fkh2 (Szilagyi et al. 2012). *CaSsn3* has recently been shown to phosphorylate the transcription factor Sef1 as a requirement for virulence (Chen & Noble 2012). The *ssn3Δ/Δ* strain from this study was obtained

and then transformed to C-terminally tag Fkh2 with GFP. This strain was tested as previously to determine the phosphorylation status on hyphal induction and during yeast growth. No loss of Fkh2-GFP phosphorylation could be detected in this strain (Fig. 4.2.15.).

#### **4.2.6.5. Repression of the CDK *PHO85* does not affect Fkh2 phosphorylation**

Pho85 is a CDK that has been shown to work in partial redundancy with Cdk1 in *S. cerevisiae*, phosphorylating substrates such as Rga2 (Sopko et al. 2007). Recently it has been shown that Pho85 is required for temperature dependent filamentation in *C. albicans* (Shapiro et al. 2012). This evidence suggests that Pho85 could be responsible for phosphorylation of Fkh2 on hyphal induction. The *tetO-PHO85/pho85Δ* strain from the above study was acquired and Fkh2 was again tagged with GFP. The strains tetracycline-off promoter (Nakayama et al. 2000) was repressed/de-repressed with doxycycline overnight, before re-inoculation into fresh medium under the same repressing conditions. This was carried out for yeast and hyphal growth as above, as well as for the wild-type *FKH2/FKH2-YFP* control (Fig. 4.2.16.). Without repression *PHO85* was clearly over-expressed, as can be seen from the  $\alpha$ PSTAIRE loading control. Repression of *PHO85* depletes the protein level but does not remove it completely, suggesting that either the shutdown is not complete or that Pho85 is not readily turned over (Fig. 4.2.16.). Neither repression nor over-expression of *PHO85* affected the phosphorylation status of Fkh2, with more retarded forms being present in the yeast and hyphal samples that are also present in the *FKH2/FKH2-YFP* wild-type strain. When comparing the un-phosphorylated stationary phase sample with the yeast and hyphal samples, it is clear that phosphorylation is still occurring (Fig. 4.2.16.).

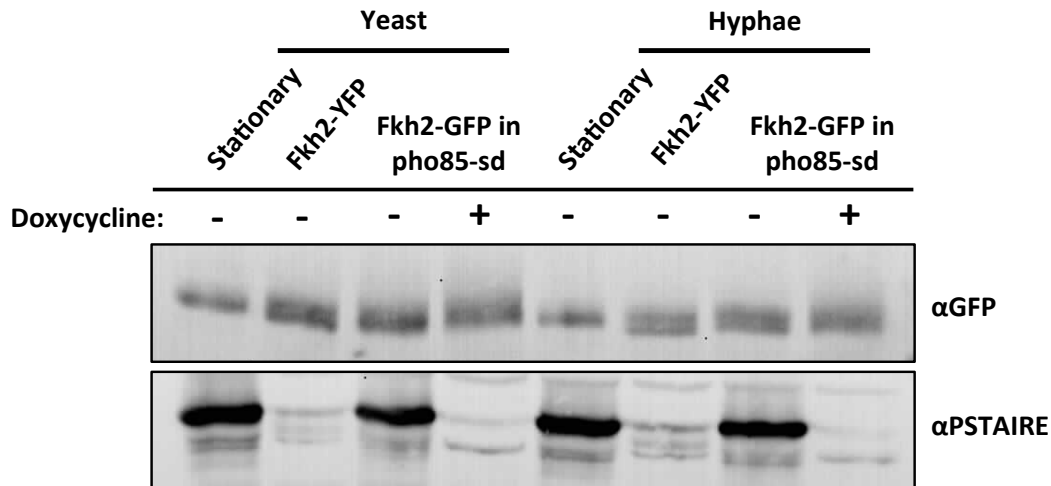


**Fig. 4.2.16. Fkh2 phosphorylation is not affected by repression/over-expression of *PHO85*.** Fkh2 was tagged with GFP in the *tetO-PHO85/pho85 $\Delta$*  strain obtained from Shapiro et al. 2012. This strain was grown overnight with or without 20 $\mu$ g/ml doxycycline as described in the above paper, before yeast or hyphal induction into fresh media with or without doxycycline. Samples were processed as previously mentioned. Stationary phase samples without doxycycline were also kept for protein extracts. A separate  $\alpha$ PSTAIRES blot was used as a loading control and to measure extent of *PHO85* shutdown.

## 4.3 Discussion

### 4.3.1. Fkh2 is differentially phosphorylated between yeast and hyphal growth

In the previous chapter it was shown that, when re-inoculated from asynchronous overnight cultures, Fkh2 shows a different pattern of phosphorylation between yeast and hyphal growth (Fig. 3.2.14.). Further investigation using synchronous cultures confirmed this difference, showing that it was not due to the possibility that cells were finishing the previous cell cycle on re-inoculation before committing to hyphal growth.

During yeast growth Fkh2-GFP shows a similar pattern of phosphorylation to that observed in *S. cerevisiae* (Pic-Taylor et al. 2004), occurring in coincidence with bud formation (Fig. 4.2.1.). However, timing of events in the two experiments cannot be accurately compared due to the different methods used for cell synchronisation. For the *S. cerevisiae* experiments alpha-factor was used to

synchronise the cells, which arrests large G1 cells just prior to START (Hartwell et al. 1974). Using elutriation is the only method for synchronisation in *C. albicans*, but this selects for small G1 cells that still have to grow before entry into START, allowing better observation of events that occur during G1. The timing of the phosphorylation in *C. albicans* yeasts suggests that Fkh2 is phosphorylated after the cell has passed START, as the cells already have small buds forming (Fig. 4.2.1.). In the synchronous yeast time-course in *C. albicans* Fkh2 also undergoes short periods of de-phosphorylation at 120 and 200mins (Fig. 4.2.1.), both of which occur when most cells are bi-nucleate having just undergone nuclear division. This suggests that Fkh2 is dephosphorylated at the end of mitosis, possibly by the Cdc14 phosphatase as part of resetting the cell to a G1 state (Rock & Amon 2009).

During hyphal growth Fkh2-GFP is phosphorylated from 20-60mins post induction, with the phosphorylation peaking at 40mins (Fig. 4.2.2.). By this time nearly 100% of the cells have formed a hyphal germ tube, suggesting that the phosphorylation may have a role in this process. With the peak in phosphorylation the level of Fkh2 is also greater, suggesting that Fkh2 phosphorylation may have a role in controlling its own expression. It is likely that the phosphorylation is occurring before the beginning of the cell cycle, as marked by the formation of a septin ring (Fig. 4.2.1.). In yeast cells START occurs just prior to bud emergence, so this can be used as a marker for the beginning of the cell cycle (Hartwell et al. 1974; Hazan et al. 2002). However this is not the case in hyphae, with germ tubes forming before the beginning of the cell cycle (Hazan et al. 2002). Therefore the formation of the septin ring was used as marker for the beginning of the cell cycle, as it has been shown to be during yeast growth (Cid et al. 2001; Finley & Berman 2005). After 60mins into hyphal growth Fkh2 is dephosphorylated and appears to remain so, at least up until the end of nuclear division, as was tested (Fig. 4.2.2.). Looking at the timing of this de-phosphorylation and comparing that with Cdc14 hyphal expression (Clemente-Blanco et al. 2006), it is unlikely that Cdc14 could be involved in this process.

If the phosphorylation of Fkh2 is unlinked from the cell cycle in hyphae, it suggests a role for Fkh2 that is independent of its expected role inferred from *S. cerevisiae* (Zhu et al. 2000). Due to the phosphorylation in both yeast and hyphae

occurring during polarised growth phases (Fig. 4.2.1-2.) it could be speculated that the physiological function of the phosphorylation is to regulate polarised growth. However this phosphorylation event occurring early on hyphal induction may be required later for cell cycle progression.

#### **4.3.2. Fkh2 is phosphorylated at CDK consensus sites on hyphal induction**

Phospho-peptide mapping of Fkh2 40mins after hyphal induction showed that phosphorylation is occurring at CDK sites (Fig. 4.2.3.). This follows the prediction from studies in other eukaryotes, that Fkh2 is targeted by CDK dependent phosphorylation (Pic-Taylor et al. 2004; Szilagy et al. 2012; Murakami et al. 2010). Mutation of the serine/threonine in sites detected by phospho-peptide mapping to alanine did not affect Fkh2 phosphorylation (Fig. 4.2.7A); however mutation of all the CDK consensus sites to the phosphorylation-blocked alanine did prevent Fkh2 phosphorylation on hyphal induction (Fig. 4.2.7B). This means that some of the CDK consensus phosphorylation sites weren't detected by the phospho-peptide mapping. A likely reason for this is due to the fact that the protein was only cleaved with trypsin prior to running in the mass-spectrometer. Trypsin preferentially cleaves proteins after arginine and lysine residues (Keil 1992), such as found in CDK consensus motifs (S/PxR/K). Therefore it is likely that tryptic cleavage occurred in phosphorylated CDK motifs, and therefore the phosphorylated serine or threonine wouldn't be present on one of the peptides.

Mutation of the six CDK consensus sites in Fkh2 to alanine appears to affect the protein level (Fig. 4.2.7B. 4.2.8B), as well as the phosphorylation shift. This could be due to the absence of phosphorylation making Fkh2 unstable, or preventing Fkh2 from positively reinforcing its own expression. The glutamic or aspartic acid substitutions at these sites give increased levels of Fkh2 compared with both the A mutant and the wild-type strain (Fig. 4.2.7-8.). Also the peak in Fkh2 phosphorylation occurs coincidental with peak protein level (Fig. 4.2.1-2.). These observations suggest that phosphorylation of Fkh2 may reinforce its own expression.

Mutation of the six consensus sites to phosphomimetic glutamic or aspartic acid still produced two bands for Fkh2 on a 1D SDS-PAGE gel (Fig. 4.2.7-8.). It

would be expected that this change in the molecular weight, and charge of the protein, would cause the whole protein to run at the same level as the upper band of the wild-type phosphorylated form. However as observed this is not the case, suggesting that the CDK phosphorylation may prime further phosphorylation or other post-translational modifications to occur.

Mutating the CDK minimal and consensus sites to A or E/D showed the same band-shift patterns observed for the consensus site mutants only (Fig. 4.2.8.). This was also the case for the *fkh2(11A)* mutant with all the minimal and consensus CDK sites C-terminal to the DNA binding domain mutated to A (Fig. 4.2.8.). Interestingly, the protein levels were greater for the 15A and 11A mutants compared with the 6A<sub>CDK</sub> mutant (Fig. 4.2.8.). Assuming that all these sites can be phosphorylated, this would suggest that a partial alteration of regulation is more severe than a complete loss of possible regulation. Another reason could be that these mutants have activated an alternative pathway that could regulate *FKH2* independently of Fkh2 itself.

The C-terminal truncation of Fkh2 (1-426) and mutation of the CDK sites in the C-terminus of the protein (11A) both cause loss of phosphorylation (Fig. 4.2.8-9.). This implies that it is the C-terminus of Fkh2 that is targeted for phosphorylation. This is as would be expected due to the clustering of CDK consensus and minimal sites within disordered C-terminus of Fkh2.

#### **4.3.3. Difficulties in determining the kinase responsible for Fkh2 phosphorylation**

It was expected that Fkh2 is a substrate of a CDK, and that it was Cdk1 that carried out the phosphorylation. This is due to the cluster of CDK consensus sites in the C-terminus of the protein located in an intrinsically disordered region, and the fact that homologues of Fkh2 in related organisms are CDK substrates.

*In vitro* experiments confirmed that Cdk1 could phosphorylate the C-terminus of Fkh2 (Fig. 4.2.11.). However this does not appear to occur *in vivo*, as inhibition of Cdk1 (Fig. 4.2.12.) or deletion/repression of the associated cyclins (Fig. 4.2.13.) has no effect on Fkh2 phosphorylation. This is also supported by the fact that an interaction between Fkh2 and CDKs could not be detected (Fig.

4.2.14.). The *in vitro* phosphorylation data cannot be taken as enough to confirm that Fkh2 is a Cdk1 target, as the conditions for the assay are very different from those found *in vivo*. The fact that the C-terminus of Fkh2 has the target phosphorylation motifs for CDKs, along with the high concentrations of kinase, substrate and ATP will favor phosphorylation occurring.

As Cdk1 could not be shown to be responsible for Fkh2 phosphorylation, a series of other kinases were tested. These were selected based on the likelihood that they would phosphorylate CDK consensus motifs. Neither Ssn3, Crk1, Tpk1/Tpk2 nor Hog1 could be seen to be responsible for the phosphorylation of Fkh2 (Fig. 4.2.15.). The only other CDK in *C. albicans* with a full PSTAIRE motif is Pho85. However testing this kinase has proved difficult, as the tetracycline promoter strain did not allow complete depletion of Pho85 on addition of doxycycline (Fig. 4.2.16.). On repression of Pho85 there was no change observed in the level of Fkh2 phosphorylation in yeast or hyphae; and conversely, over-expression of Pho85 by not repressing the tetracycline promoter did not cause any increase in Fkh2 phosphorylation, with Fkh2 remaining dephosphorylated in stationary phase (Fig. 4.2.16.). These results would suggest that Pho85 is not responsible for the phosphorylation of Fkh2. There is however a possibility that Pho85 and Cdk1 could be acting redundantly, but as yet it has not been possible to generate a strain in which both of these kinases are inhibited in order to test this.

The data above suggest that Fkh2's phospho-regulation is not conserved from that observed in related yeast species. There are many other kinases that could be tested, some of which knockout mutants are available for. However this has not currently been possible. A BLAST search of the CDK PSTAIRE motif (EGVPSTAIREISLLKE) against the *Candida* genome found Orf19.1619 to have 78.6% identity. This protein is a possible homologue of *S. cerevisiae* CTK1, which has been shown to be a kinase subunit of RNA polymerase II (Lee & Greenleaf 1991). Orf19.1619 would be a good starting point for further investigation into the kinase responsible for phosphorylation of Fkh2.

In the previous chapter the phospho-regulation of Fkh2 was investigated. Although the kinase that phosphorylates Fkh2 remains unidentified, the sites that are phosphorylated upon hyphal induction are now known. Using the mutants generated in the previous chapter the effect of Fkh2 phosphorylation can be dissected. These mutants allow the observation of the phenotypic consequences of Fkh2 not being phosphorylated (*6A<sub>CDK</sub>*), and mimicking constitutive phosphorylation (*6E<sub>CDK</sub>*). Due to differential phosphorylation of Fkh2 in hyphae compared to yeast, it is of interest to look at how this phosphorylation affects hyphal formation and maintenance. The phenotypic consequences of the phosphorylation can be compared with the phenotype of other Fkh2 mutants, such as that of the *fkh2Δ/Δ* strain (Bensen et al. 2002) and the *FKH2* overexpression strain (Chauvel et al. 2012). In addition, further investigation into the above mentioned mutants could be carried out.

## 5.1 Morphological consequences of Fkh2 phosphorylation

### 5.1.1. Blocking of Fkh2 phosphorylation affects yeast cell shape

In order to look at the effects of Fkh2 phosphorylation on yeast morphology, YEPD overnight cultures of the phospho-mutants were refreshed into minimal media pH 4.0 at 30°C to grow for 4 hours. Microscopic observation of the mutants showed that the *fkh2(6A<sub>CDK</sub>)* cells had an altered yeast morphology (Fig. 5.1.1A.). These cells are much larger than the *fkh2(6E<sub>CDK</sub>)* or *fkh2/FKH2* cells, which are of similar size. This was further confirmed by quantifying the volume of the cells (Fig. 5.1.1B.).

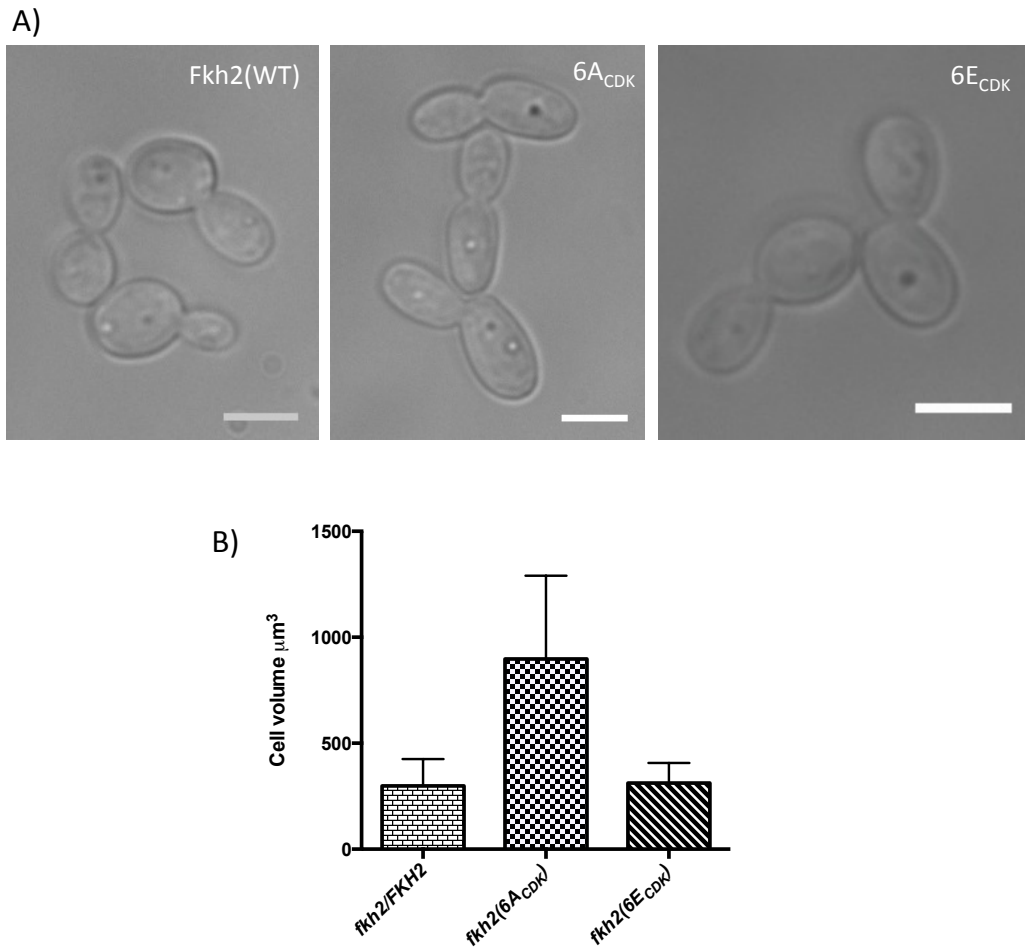


**Fig. 5.1.1. Phenotypes of Fkh2 phospho-mutants during yeast growth. A)** 100x DIC microscope images of the *fkh2/FKH2*, *fkh2(6A<sub>CDK</sub>)* and *fkh2(6E<sub>CDK</sub>)* strains. Scale bars represent 5μm. **B)** Quantitation of the cell volume for each of the mutants (n=50).

### 5.1.2. Blocking Fkh2 phosphorylation results in altered hyphal morphology and prevents maintenance of invasive filamentous growth.

Overnight cultures of the Fkh2 phospho-mutants and the wild type strain were refreshed into minimal media with 20% serum at 37°C pH 7, and then grown for 5 hours to allow observation of the long-term effects of Fkh2 phosphorylation on hyphal growth (Fig. 5.1.2.). All three strains formed clumps in liquid culture, suggesting that the mutants could form hyphae normally, or at least can express adhesins that are required for the clumping phenotype. To observe the individual hyphal cells, samples were fixed with formaldehyde and then pepsin treated to separate hyphal clumps. Observation of these cells shows that the *fkh2(6E<sub>CDK</sub>)*

strain has a similar morphology to the wild-type strain. The *fkh2(6A<sub>CDK</sub>)* strain can begin to form hyphae normally; however, constrictions form at the tips later in hyphal growth (Fig. 5.1.2A.). Quantitation shows that more than half of the *fkh2(6A<sub>CDK</sub>)* hyphae contain constrictions (Fig. 5.1.2C.) This suggests that the cells are failing to maintain polarisation, possibly starting to revert back to the yeast morphology. This is supported by the observed branching in the *fkh2(6A<sub>CDK</sub>)* strain (Fig. 5.1.2C.). The phosphorylation status of Fkh2 does not appear to affect the rate of hyphal growth, as after 5 hours the mutant and wild-type Fkh2 hyphae are of similar length (Fig. 5.1.2B.).

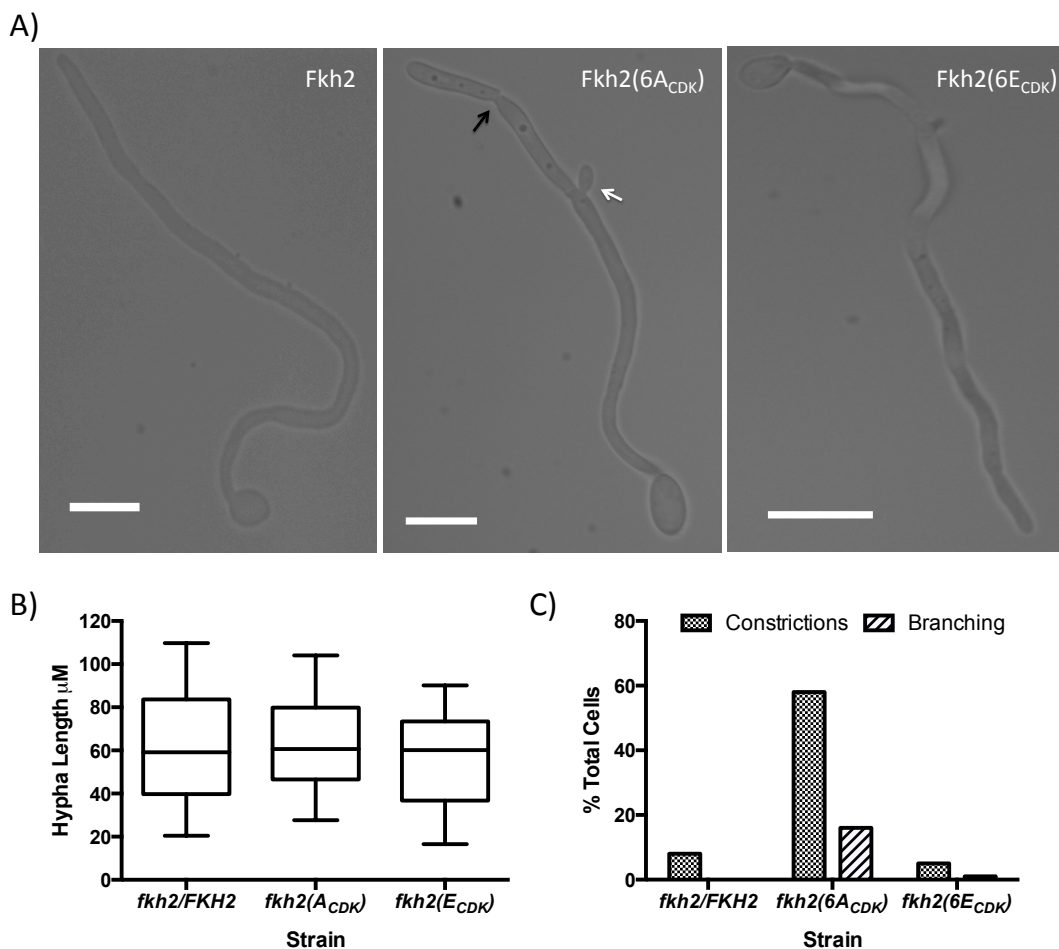


**Fig. 5.1.2. Phenotypes of Fkh2 phospho-mutants in liquid hyphal culture.** A) DIC images of wild-type *fkh2/FKH2* and *fkh2(6A<sub>CDK</sub>)/(6E<sub>CDK</sub>)* strains at x100 magnification. Solid white bar is equal to 10μm. White arrows indicate branching, and black arrows constrictions B) Measurements of hypha length in each of the 3 strains, taken from an average of 50 measurements. C) Quantitation of the number of hyphae with constrictions and branches forming (n=50).

Due to the suggested loss of polarisation in the *fkh2(6A<sub>CDK</sub>)* strain, the ability of the mutant strains to maintain long-term hyphal growth on solid media was monitored (Fig.5.1.3.). Cells were serially diluted onto YEPD agar plates with

20% serum to induce hyphal formation. BWP17, *FKH2/FKH2-YFP* and *fkh2/FKH2-YFP* strains were used as controls to ensure that any observed phenotypes were not due to haploinsufficiency or the GFP tag affecting Fkh2 function. The *FKH2/FKH2-YFP* and *fkh2/FKH2-YFP* strains showed the same filamentation ability as BWP17, and when the surface colony was washed away extensive invasion of the underlying agar could be seen. This implies that the *fkh2/FKH2* strain is haplosufficient, and that tagging Fkh2 with GFP does not impair its function. The *fkh2(6A<sub>CDK</sub>)* strain formed smooth surface colonies on the serum agar that could easily be washed away, showing limited invasion of the agar substratum. The *fkh2(6E<sub>CDK</sub>)* strain was still able to invade the underlying agar, suggesting that it, unlike the *fkh2(6A<sub>CDK</sub>)* strain, could maintain invasive filamentous growth.

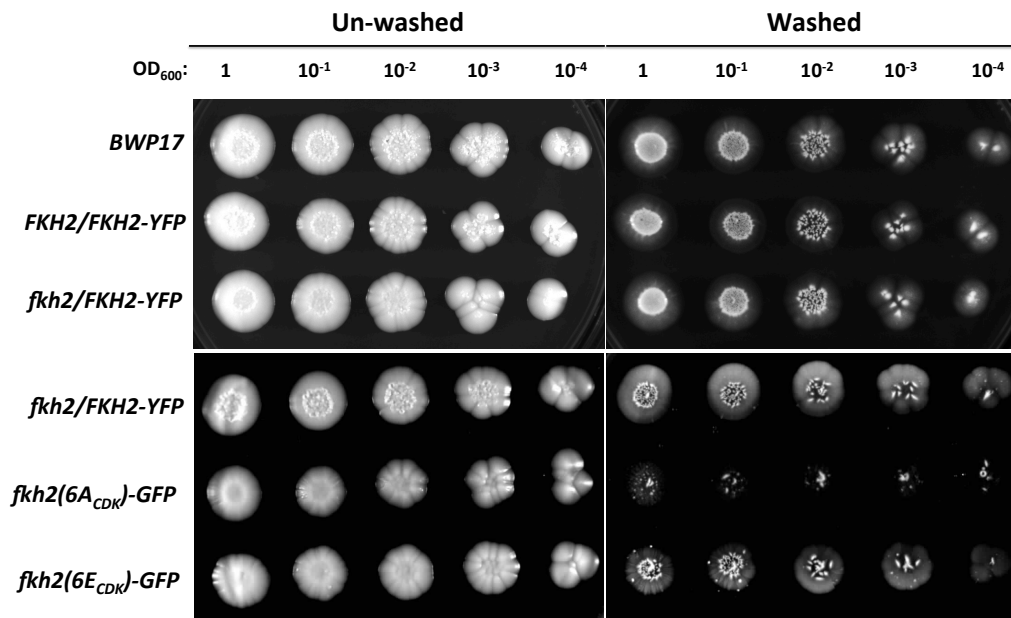


**Fig. 5.1.3. Invasive ability of Fkh2 phospho-mutants on solid media.** Overnight cultures were diluted to an OD<sub>600</sub> of 1.0 before 10 fold serial dilutions were spotted onto YEPD agar with 20% serum. Plates were incubated at 37°C for 5 days. Surface colonies were washed off using deionised water.

### 5.1.3. The phosphorylation status of Fkh2 does not affect its localisation

One way in which phosphorylation can affect protein function is to control subcellular localisation. It is known that Fkh2 normally localises to the distinct spot of the nucleus (Bensen et al. 2002); therefore the localisation of the phospho-

mutants was observed using their C-terminal GFP tag. Yeast cells were grown for microscopy as previously stated, with Fkh2 localisation subsequently observed by fluorescence microscopy (Fig. 5.1.4.). The GFP signal from the Fkh2 6A<sub>CDK</sub> and 6E<sub>CDK</sub> proteins is still primarily focused to a distinct area, similar to wild-type Fkh2 and consistent with a nuclear localisation. DAPI staining would have confirmed nuclear localisation; however, the vector-shield DNA stain used at the time fixed the cells causing a loss of the Fkh2-GFP signal, and therefore could not be used.

To observe the Fkh2 phosphorylation site mutant's localisation during hyphal growth, liquid hyphal cultures were induced as previously described. These cultures were grown for 5 hours so that the morphological abnormalities of the *fkh2(6A<sub>CDK</sub>)* mutant hyphae could be confirmed. As in yeast cells Fkh2 maintains its distinct localisation independent of its phosphorylation status, with both the phosphorylation blocked and phosphomimetic Fkh2-GFP proteins localising to distinct areas throughout the hyphal tube (Fig. 5.1.4.). This implies that the inability of *fkh2(6A<sub>CDK</sub>)* to maintain filamentous growth is not due to mis-localisation.

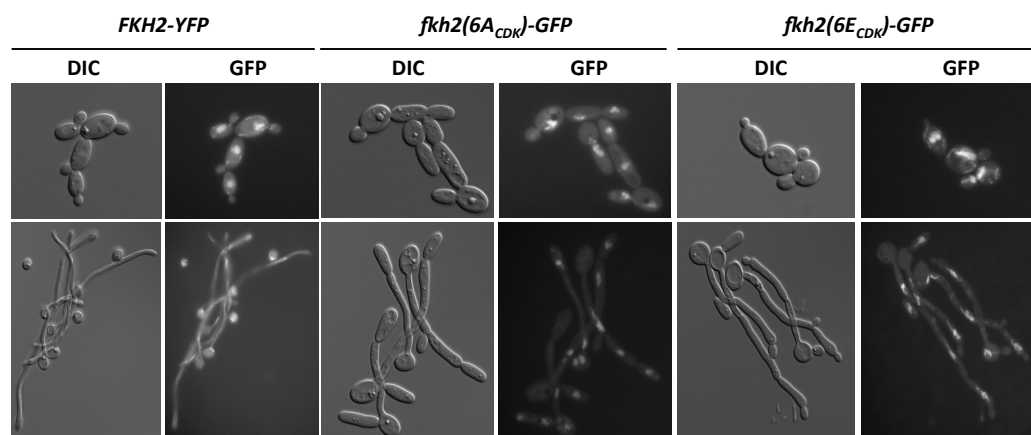


**Fig. 5.1.4. Localisation of Fkh2 CDK consensus site mutants during yeast and hyphal growth.** Cells were grown in yeast or hyphal growth conditions for the times shown. 20% serum was used for the hyphal induction after filtering with an Amicon 3K column. DIC and GFP images were taken at x100 magnification with a Leica DMR microscope.

#### 5.1.4. Phenotypes of other Fkh2 phosphorylation mutants.

In addition to the CDK consensus site mutants, other phospho-mutants were generated in order to confirm the phosphorylation sites on Fkh2. With these mutants it was of interest to see the phenotypic effects during yeast and hyphal

growth, and to compare these with the phenotypes of the other CDK consensus site mutants.

#### 5.1.4.1. Mutation of CDK consensus and minimal sites

Mutation of all the S/TP sites in Fkh2 to A or E/D gives similar phosphorylation patterns as for the respective CDK consensus site mutants (Fig. 4.2.8.). Observation of the *fkh2(15A)* phenotype in yeast and hyphae shows that yeast cells grow normally, whereas hyphal cells again form constrictions at the tip (Fig. 5.1.5.). This inability to maintain hyphal growth is confirmed by growth on solid media, where the *fkh2(15A)* mutant is unable to invade the agar substratum (Fig. 5.1.6.). The *fkh2(15E)* strain grows normally as yeast, but some hyphae show constrictions at the tip (Fig. 5.1.5.). When grown on solid YEPD media with serum this mutant is able to invade the underlying agar, suggesting that it can maintain filamentous invasive growth (Fig. 5.1.6.).

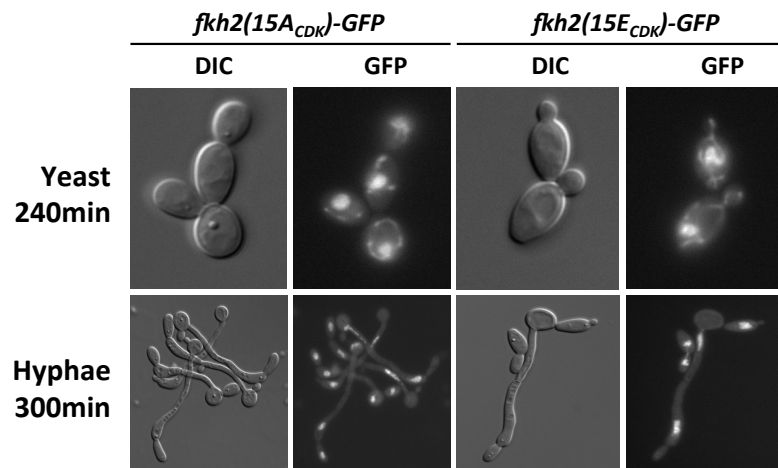


**Fig. 5.1.5. Phenotypes and localisation of Fkh2 CDK consensus and minimal site mutants during yeast and hyphal growth.** Cells were grown in yeast or hyphal growth conditions for the times shown. 20% serum was used for the hyphal induction after filtering with an Amicon 3K column to remove factors that promote hyphal clumping. DIC and GFP images were taken at x100 magnification.

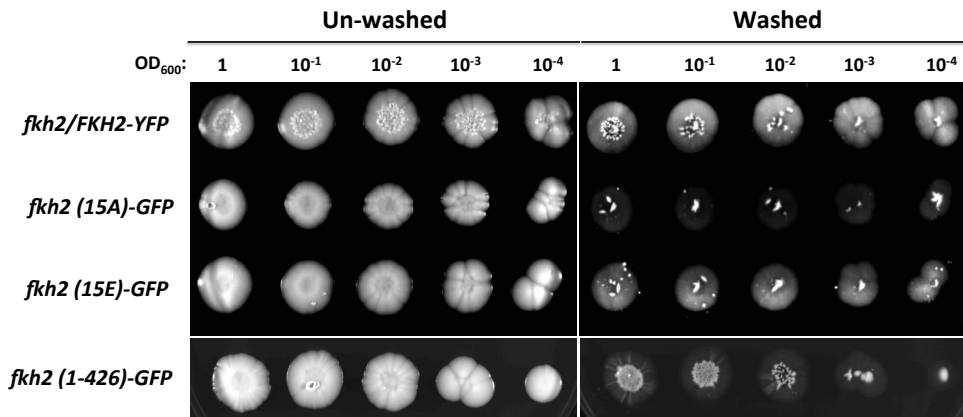


**Fig. 5.1.6. Invasive ability of other Fkh2 phosphorylation mutants on solid media.** Strains were serially diluted onto solid YEPD media with 20% serum, and then incubated for 5 days at 37°C. Surface colonies were photographed before being washed away to reveal the extent of agar invasion.

#### 5.1.4.2. Mutation of sites detected by phospho-peptide mapping

Although mutating the phosphorylation sites identified by phospho-peptide mapping does not affect observable Fkh2 phosphorylation, it is of interest to see if the mutations have any phenotypic effects on the cell. The *fkh2(6A<sub>MS</sub>)* cells grow normally as yeast, with Fkh2 remaining primarily localised to a distinct spot; however there is also some localisation to filament-like structures throughout the cell (Fig. 5.1.7.). During hyphal growth there are some hyphal tips that show constrictions, but this is not as prominent as in the *fkh2(6A<sub>CDK</sub>)* strain (Fig. 5.1.4.).

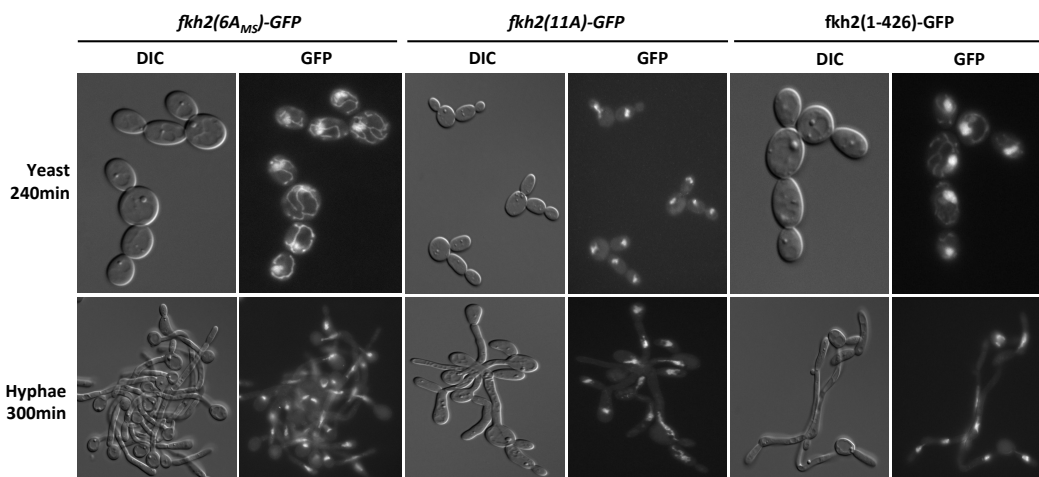


**Fig. 5.1.7. Phenotypes and localisation of other Fkh2 phosphorylation mutants during yeast and hyphal growth.** Cells were grown in yeast or hyphal inducing conditions for the times shown. 20% serum was used for the hyphal induction after filtering with an Amicon 3K column. DIC and GFP images were taken at x100 magnification with a Leica DMR microscope.

#### **5.1.4.3. Mutation of Fkh2 C-terminal CDK consensus and minimal sites**

The *fkh2(11A)* mutant is blocked for phosphorylation at all CDK sites C-terminal to the DNA binding domain. This mutant shows loss of the associated phospho-band-shifts, confirming that phosphorylation of Fkh2 occurs in its C-terminus (Fig. 4.2.8.). The *fkh2(11A)* strain grows normally as yeast, but has quite profound defects in hyphal maintenance, shown by swelling at the hyphal tips (Fig. 5.1.7.). *fkh2(11A)* maintained normal distinct localisation during yeast and hyphal growth, confirming that the absence of phosphorylation does not affect its localisation.

#### **5.1.4.4. Truncation of Fkh2's C-terminus (1-426)**

Truncation of the C-terminus of Fkh2 prevents phosphorylation of Fkh2 occurring during both yeast and hyphal growth. *fkh2(1-426)* yeast cells grow normally, but some hyphal cells again show constrictions near the tip (Fig. 5.1.7.). Truncation of Fkh2 causes minor filamentation defects on solid YEPD serum media, with only partial invasion of the agar substratum (Fig. 5.1.6.).

## **5.2 Fkh2-dependent regulation of transcriptional programs.**

Mutation of the phosphorylation sites in Fkh2 is shown above to affect the long-term maintenance of invasive filamentous growth. As previously mentioned, Fkh2 and its homologues are known transcriptional regulators; suggesting a hypothesis that the observed *fkh2(6A<sub>CDK</sub>)* phenotype is due to an altered hyphal transcriptional program. Previous microarray analysis with the *fkh2Δ/Δ* strain showed the hyphal expression-specific genes *ECE1* and *HYR1* are down-regulated in the absence of *FKH2* (Bensen et al. 2002). However this study used a limited array, only containing probes for 319 out of 6525 *C. albicans* ORFs, and therefore is likely to have under-represented the transcriptional role of Fkh2. To investigate the role of Fkh2 and its phospho-regulation in yeast and hyphal growth, complete arrays were carried out as listed below:

- A)** *fkh2* $\Delta/\Delta$  (Experimental) vs. BWP17 (Control): 3hours yeast growth in YEPD (Fig. 5.2.6.)
- B)** *fkh2(6A<sub>CDK</sub>)* (Experimental) vs. *FKH2/FKH2-YFP* (Control): 3hours yeast growth in YEPD (Fig.5.2.7)
- C)** *fkh2* $\Delta/\Delta$  (Experimental) vs. BWP17 (Control): 3hours hyphal growth in YEPD plus 20% serum (Fig. 5.2.2.)
- D)** *fkh2(6A<sub>CDK</sub>)* (Experimental) vs. *FKH2/FKH2-YFP* (Control): 3hours hyphal growth in YEPD plus 20% serum. (Fig. 5.2.3)
- E)** *P<sub>GAL1</sub>-FKH2-GFP* (Experimental) vs. *FKH2/FKH2-YFP* (control): 3hours yeast growth in YEPG. The results of this array will be presented in a separate section below (Fig. 5.4.5).

For the *fkh2(6A<sub>CDK</sub>)* array experiments the correct control strain to have used would be *fkh2/FKH2-YFP*, as this would negate any possible effects due to haploinsufficiency; however this strain was not available at the time the arrays were carried out, therefore the *FKH2/FKH2-YFP* strain was used. However as shown below, qPCR experiments using the *fkh2/FKH2-YFP* strain confirmed the main conclusions of the microarray (Fig. 5.2.5.).

Total RNA was isolated from each of the strains after the allotted time, with the quality being confirmed by formaldehyde agarose electrophoresis (Fig. 5.2.1.). These samples were then sent to the microarray facility at Biopolis shared facilities for further processing by Dr. Vivien Koh. Here samples were reverse transcribed and Cy3 (Control) or Cy5 (Experimental) dyes added, before hybridisation to the arrays and subsequent scanning. Each of the five arrays was carried out twice with the initial data being provided in excel spreadsheets. These data were then combined for each sample by Dr. Ian Sudbery, and filtered for genes with a greater than two-fold change in expression between the control and experimental

samples, resulting in a false discovery rate of less than 5%. The filtered data, of genes with significant expression changes, were then combined into one excel spreadsheet, allowing the comparison of each gene across all five arrays (See included CD). This spreadsheet has been sorted into five separate sheets; where each sheet shows up to the top 50 genes down or-up-regulated in each mutant strain compared with the control (Fig. 5.2-3, 5.2.6-7, 5.4.5.). Also included in the spreadsheet are the presence of Fkh2 consensus ((G/A)TAAA(C/T)AAA) or minimal (AAA(C/T)AAA) DNA binding sites (Gordân et al. 2012) in the 1kb upstream of the gene; found using the pattern matching program on the *Candida* genome Database <http://www.candidagenome.org/cgi-bin/PATMATCH/nph-patmatch>. As a standard up to 12.7% of genes in the *Candida* genome contain a Fkh2 consensus binding site in the 1kb of upstream sequence, and up to 61.6% of genes contain a minimal site. There is only a slight enrichment of consensus Fkh2 binding sites in the combined microarray data set (15.47% genes – 22% increase); however there is a greater enrichment of Fkh2 minimal binding sites (83.5% genes – 35% increase). Therefore this method can provide an indication of regulation by Fkh2, but will need to be confirmed by further *in vivo* experiments. Additional analysis of genes with a greater than two-fold change in expression between the control and experimental samples was carried out using the Gene Ontology (GO) process slim mapper <http://www.candidagenome.org/cgi-bin/GO/goTermMapper>, or, where possible, GO process term finder <http://www.candidagenome.org/cgi-bin/GO/goTermFinder> on the *Candida* genome database. Values from these tables are referenced in the results sections and full tables can be found in excel spreadsheets on the supplementary CD. The GO process slim mapper lists all of the process categories that any of the genes in the set fall into, and will list categories for all of the genes; whereas the GO process term finder identifies GO categories for which the given gene set shows significant enrichment. Sets of up or down-regulated genes from different arrays were compared using the list comparer from the Whitehead Institute at MIT <http://jura.wi.mit.edu/bioc/tools/compare.php>. These are presented in the Venn diagrams to allow visual comparison between samples (Fig. 5.2.4, 5.2.8-9).

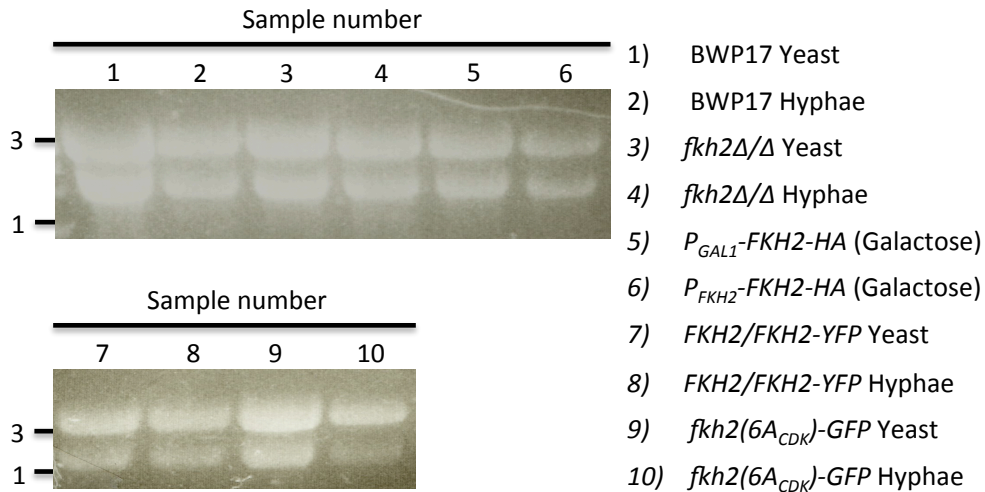


**Fig. 5.2.1. Determination of RNA quality from Fkh2 mutant strains before microarrays.** RNA samples were isolated from cultures grown for 3 hours in rich media for the listed conditions. 5  $\mu$ l of total RNA from each samples was run on a 1.2% formaldehyde-agarose gel, stained with ethidium bromide. Values along the left hand side represent DNA ladder molecular weight values in kb.

The five microarray experiments generated extensive data on Fkh2's possible functions during both yeast and hyphal growth. This will be covered in two sections: firstly data will be presented and discussed on the role of Fkh2 and its phospho-regulation during invasive hyphal growth. This will be followed by a more detailed analysis, with presentation of the expression data from yeast growth, and further mining of both the yeast and hyphal expression data to try and elucidate other possible biological roles for Fkh2 in *C. albicans*.

### 5.2.1. Overview: regulation of *C. albicans* virulence factor expression during filamentous invasive growth through phosphorylation of Fkh2

Microarrays C and D (Fig. 5.2.2-3) show that genes known to be expressed during hyphal growth and pathogenesis are down-regulated compared with the controls in both the *fkh2Δ/Δ* and *fkh2(6A<sub>CDK</sub>)* strains. These include the known regulatory targets *HYR1* and *ECE1* that were identified in the limited study by Bensen et al. In addition to this, the secreted aspartyl proteases *SAP4-6*, the chitinase *CHT2*, and the hyphal specific kinesin like protein *KIP4* also show reduced expression in both strains.

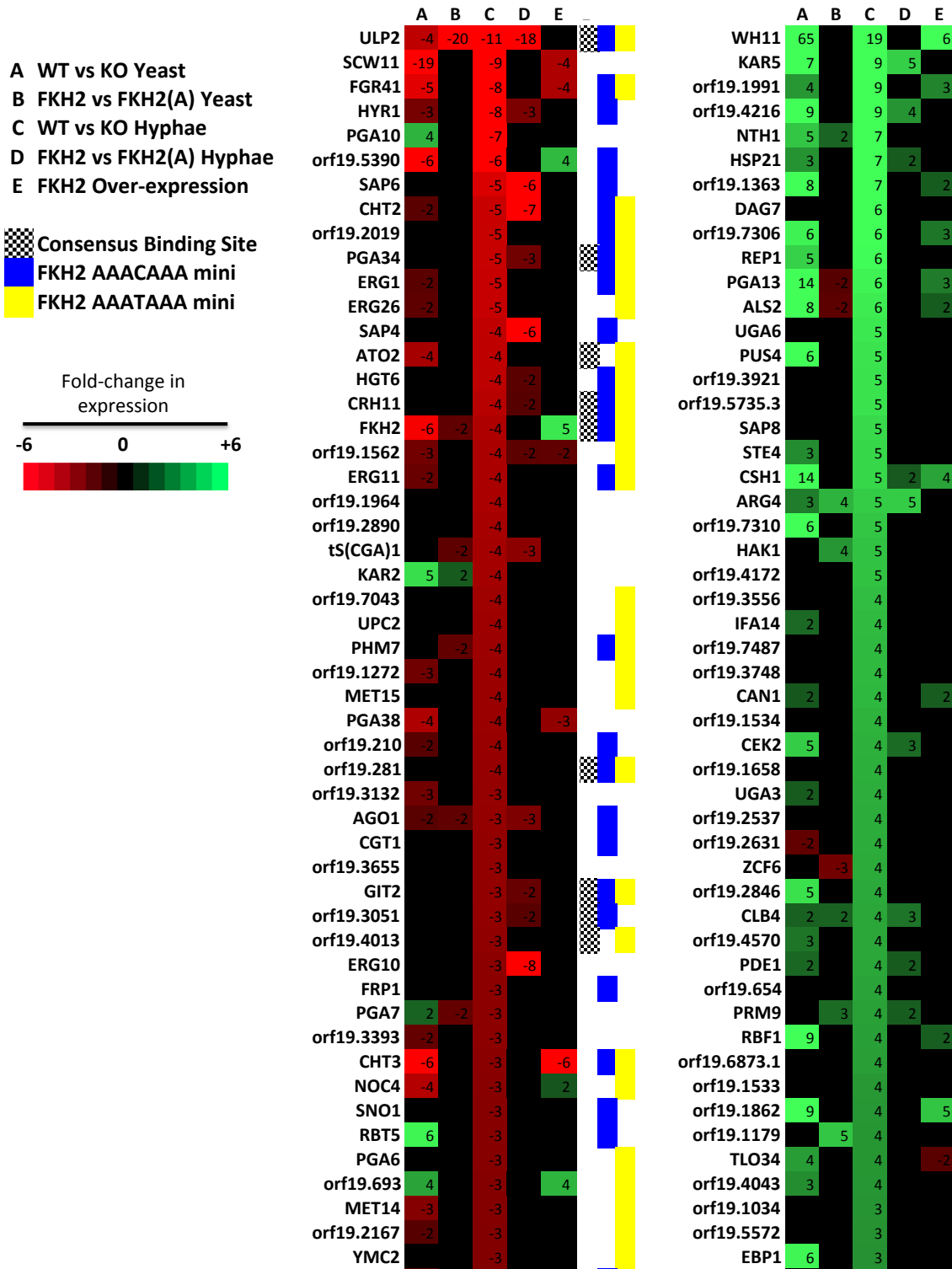


**Fig. 5.2.2. Genes down or up-regulated in the absence of *FKH2* during hyphal growth.** Excel spreadsheet sorted for genes with reduced or increased expression in array C. Displayed are the top 50 genes showing reduced/increased expression, along with the presence/absence of Fkh2 binding sites in the 1kb upstream of the gene.

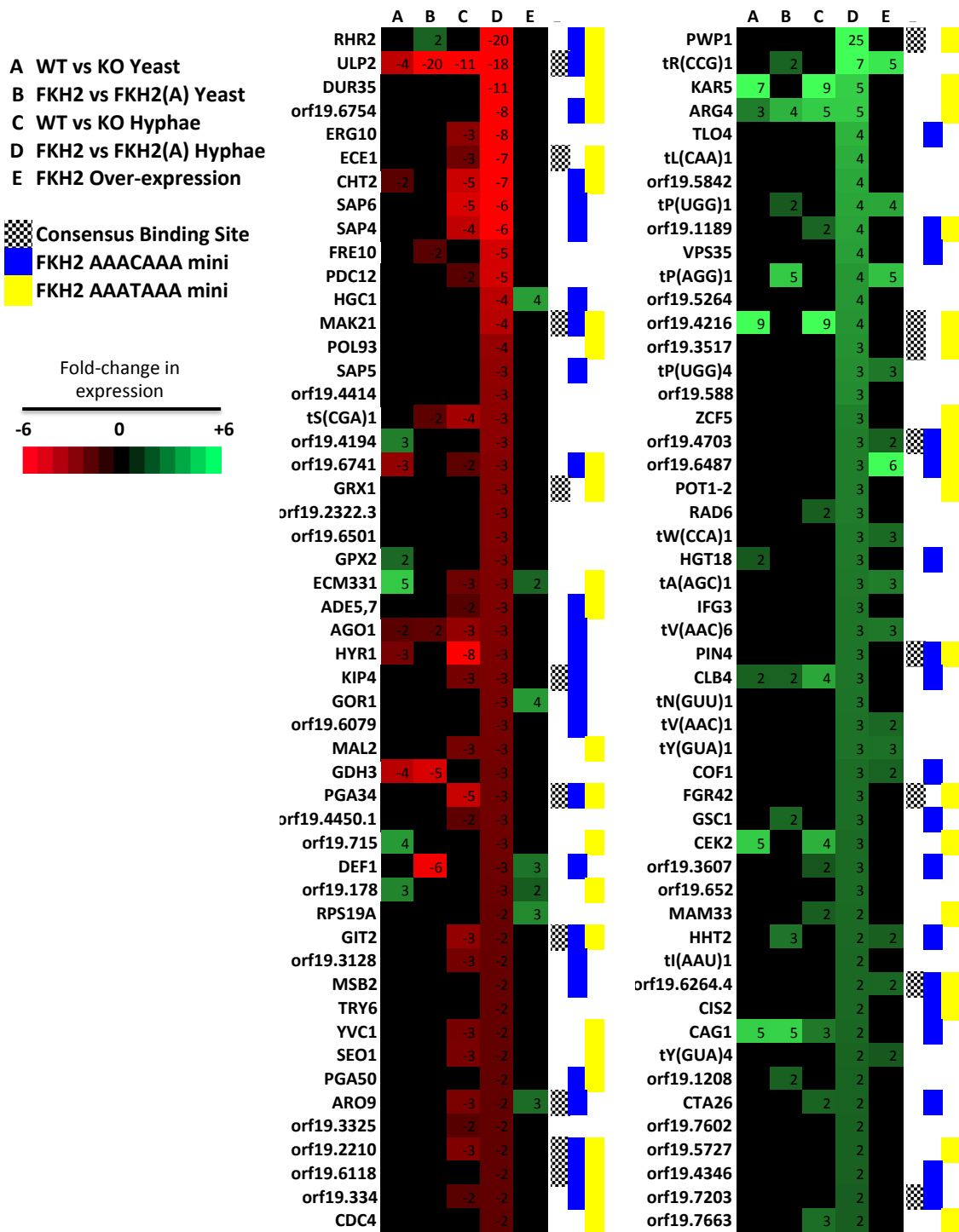


**Fig. 5.2.3. Genes down or up-regulated on blocking Fkh2 phosphorylation during hyphal growth.** Excel spreadsheet sorted for genes with increased or decreased expression in array D. Displayed are the top 50 genes down/up-regulated during hyphal growth in the absence of Fkh2 phosphorylation, with the presence or absence of a Fkh2 DNA binding site in the 1kb upstream of the gene.



**Fig. 5.2.4.** Venn diagrams comparing genes with altered expression during hyphal growth in the *fkh2Δ/Δ* and *fkh2(6A<sub>CDK</sub>)* strains. **A)** Genes down-regulated during hyphal growth **B)** Genes up-regulated during hyphal growth.

The role of Fkh2 in filamentous growth and pathogenesis is further highlighted by the GO analysis of genes with significantly decreased expression during hyphal growth in the *fkh2Δ/Δ* and *fkh2(6A<sub>CDK</sub>)* strains (See supplementary CD). In the *fkh2Δ/Δ* strain the GO slim process terms for filamentous growth (13.6%), pathogenesis (6.8%) and biofilm formation (4.7%) are all represented. GO slim analysis for *fkh2(6A<sub>CDK</sub>)* shows increased representation of the categories:

filamentous growth (14.9%), biofilm formation (12.2%) and pathogenesis (8.1%) compared with the *fkh2Δ/Δ* strain. GO term analysis of the *fkh2Δ/Δ* down regulated gene set shows that in addition to hyphal specific genes, genes involved in a wide range of cell functions are significantly affected. Indeed, in the *fkh2Δ/Δ* gene set the only GO term associated with hyphal growth is “response to a biotic substance” (See GO term spreadsheet) which refers to a response to serum (Inglis et al. 2013). In terms of significance this is ranked 18 out of 21 terms identified. In contrast, the GO term analysis of the *fkh2(6A<sub>CDK</sub>)* data shows that the processes significantly affected are almost exclusively associated with functions such as adhesion, biofilm formation, interaction with the host and immune system response. Also, in the *fkh2(6A<sub>CDK</sub>)* strain the hyphal specific cyclin *HGC1* shows reduced expression during hyphal growth, which is not the case in the *fkh2Δ/Δ* strain (Fig. 5.2.2). The above results indicate that the hyphal phosphorylation of Fkh2 may be specifically required for the expression of pathogenesis genes in *C. albicans*.

To further differentiate between the effect of loss of *FKH2* and blocking Fkh2 phosphorylation, GO term-finder/slim-mapper process analysis was carried out separately for genes down-regulated only in the *fkh2Δ/Δ* (*fkh2Δ/Δ*-only), for genes only down regulated in the *fkh2(6A<sub>CDK</sub>)* (*fkh2(6A<sub>CDK</sub>)*-only) strain, and for genes that are down-regulated in both strains. Interestingly GO slim analysis showed that GO terms for pathogenesis, interspecies interaction and biofilm formation show strong representation in the *fkh2(6A<sub>CDK</sub>)*-only group, and the set of genes down-regulated in both strains, but not in the *fkh2Δ/Δ*-only gene set (Table 5.1.). This is further supported using the GO term-mapper analysis, which only shows significant enrichment of genes involved in host interaction and pathogenesis in the *fkh2(6A<sub>CDK</sub>)*-only (Table 5.2) and down-regulated in both strains gene sets (Table 5.3), but not in the *fkh2Δ/Δ*-only gene set (Table 5.4). Thus, Fkh2 phosphorylation is required to specifically activate a subset of genes that are associated with invasion, biofilm formation, host-pathogen interaction and commensalism. For genes that are down-regulated in both *fkh2Δ/Δ* and *fkh2(6A<sub>CDK</sub>)* strains, further down-regulation is generally observed in the *fkh2(6A<sub>CDK</sub>)* strain compared to the *fkh2Δ/Δ* strain. Thus, lack of Fkh2 phosphorylation specifically changes the properties of Fkh2 rather than simply impairing its function. A hypothesis that would explain why there is greater loss of

gene function with loss of the Fkh2 phosphorylation sites compared to the absence of *FKH2* is that the phosphorylation changes the action of Fkh2 from a repressor to an inducer of gene expression.

Gene Set	GO Slim Process term			
	Filamentous Growth	Biofilm Formation	Pathogenesis	Interspecies interaction between organisms
<i>fkh2Δ/Δ</i> only	13.4%	4%	6%	3%
<i>fkh2(6A<sub>CDK</sub>)</i> only	15.4%	15.4%	5.1%	10.3%
<i>Fkh2 Δ/Δ</i> and <i>fkh2(6A<sub>CDK</sub>)</i>	14.3%	8.6%	11.4%	11.4%

**Table. 5.1. Comparison of GO slim process terms associated with virulence for genes down-regulated during hyphal growth in the *fkh2Δ/Δ*-only, *fkh2(6A<sub>CDK</sub>)*-only and in both strains.**

**5.2)**

GO_term	Cluster frequency	Background frequency	Corrected P-value	False discovery rate	Gene(s) annotated to the term
single-species biofilm formation on inanimate substrate	6 out of 39 genes, 15.4%	119 out of 6525 background genes, 1.8%	0.01332	4.00%	SUN41:GCA1:RHR2:HGC1:TRY6:DEF1
intraspecies interaction between organisms	6 out of 39 genes, 15.4%	119 out of 6525 background genes, 1.8%	0.01332	2.00%	SUN41:GCA1:RHR2:HGC1:TRY6:DEF1
single-species biofilm formation	6 out of 39 genes, 15.4%	132 out of 6525 background genes, 2.0%	0.02375	2.00%	SUN41:GCA1:RHR2:HGC1:TRY6:DEF1
biofilm formation	6 out of 39 genes, 15.4%	137 out of 6525 background genes, 2.1%	0.02917	1.50%	SUN41:GCA1:RHR2:HGC1:TRY6:DEF1

**5.3)**

GO_term	Cluster frequency	Background frequency	Corrected P-value	False discovery rate	Gene(s) annotated to the term
activation of immune response	2 out of 35 genes, 5.7%	2 out of 6525 background genes, 0.0%	0.00408	0.00%	SAP6:SAP4
immune system process	2 out of 35 genes, 5.7%	2 out of 6525 background genes, 0.0%	0.00408	0.00%	SAP6:SAP4
adhesion to host	4 out of 35 genes, 11.4%	49 out of 6525 background genes, 0.8%	0.01808	6.00%	RFX2:HYR1:SAP6:SAP4
adhesion to other organism involved in symbiotic interaction	4 out of 35 genes, 11.4%	49 out of 6525 background genes, 0.8%	0.01808	4.50%	RFX2:HYR1:SAP6:SAP4
positive regulation of immune response	2 out of 35 genes, 5.7%	6 out of 6525 background genes, 0.1%	0.06039	11.60%	SAP6:SAP4
positive regulation of immune system process	2 out of 35 genes, 5.7%	7 out of 6525 background genes, 0.1%	0.08427	12.67%	SAP6:SAP4

## 5.4)

GO_term	Cluster frequency	Background frequency	Corrected P-value	False discovery rate	Gene(s) annotated to the term
phytosteroid metabolic process	4.50%	0.40%	4.84E-05	0.00%	ERG24:ERG6:ARE2:NCP1:ERG26:UPC2:ERG1:ERG2:ERG11
ergosterol metabolic process	4.50%	0.40%	4.84E-05	0.00%	ERG24:ERG6:ARE2:NCP1:ERG26:UPC2:ERG1:ERG2:ERG11
sterol metabolic process	5.00%	0.60%	8.31E-05	0.00%	ERG24:ERG6:orf19.2050:ARE2:NCP1:ERG26:UPC2:ERG1:ERG2:ERG11
steroid metabolic process	5.00%	0.60%	0.0001	0.00%	ERG24:ERG6:orf19.2050:ARE2:NCP1:ERG26:UPC2:ERG1:ERG2:ERG11
cellular alcohol metabolic process	4.50%	0.50%	0.00013	0.00%	ERG24:ERG6:ARE2:NCP1:ERG26:UPC2:ERG1:ERG2:ERG11
phytosteroid biosynthetic process	4.00%	0.40%	0.00038	0.00%	ERG24:ERG6:NCP1:ERG26:UPC2:ERG1:ERG2:ERG11
cellular alcohol biosynthetic process	4.00%	0.40%	0.00038	0.00%	ERG24:ERG6:NCP1:ERG26:UPC2:ERG1:ERG2:ERG11
ergosterol biosynthetic process	4.00%	0.40%	0.00038	0.00%	ERG24:ERG6:NCP1:ERG26:UPC2:ERG1:ERG2:ERG11
sterol biosynthetic process	4.00%	0.40%	0.00103	0.00%	ERG24:ERG6:NCP1:ERG26:UPC2:ERG1:ERG2:ERG11
steroid biosynthetic process	4.00%	0.40%	0.00103	0.00%	ERG24:ERG6:NCP1:ERG26:UPC2:ERG1:ERG2:ERG11
small molecule biosynthetic process	11.90%	4.00%	0.00123	0.00%	ERG24:ERG6:SPT23:MIS11:NCP1:PDC11:CEK1:ERG26:SNO1:LYS2:EHT1:SCS7:UPC2:PSD2:ERG1:ECM17:TRP5:RIM20:orf19.4960:MET15:FAS2:ERG2:ERG11:MET14
cellular cation homeostasis	7.50%	1.70%	0.00143	0.00%	TFP1:VMA5:SPF1:orf19.3132:VCX1:FET34:orf19.4240:CTR2:orf19.55:FRP1:RBT5:PGA10:VAM3:DUR3:VPH1
cellular chemical homeostasis	8.00%	2.00%	0.00176	0.00%	TFP1:RAS1:VMA5:SPF1:orf19.3132:VCX1:FET34:orf19.4240:CTR2:orf19.55:FRP1:RBT5:PGA10:VAM3:DUR3:VPH1
cation homeostasis	7.50%	1.80%	0.00223	0.00%	TFP1:VMA5:SPF1:orf19.3132:VCX1:FET34:orf19.4240:CTR2:orf19.55:FRP1:RBT5:PGA10:VAM3:DUR3:VPH1
cellular ion homeostasis	7.50%	1.90%	0.00341	0.00%	TFP1:VMA5:SPF1:orf19.3132:VCX1:FET34:orf19.4240:CTR2:orf19.55:FRP1:RBT5:PGA10:VAM3:DUR3:VPH1
alcohol metabolic process	6.50%	1.40%	0.00362	0.00%	ERG24:ERG6:orf19.2050:orf19.21:ARE2:NCP1:PDC11:ERG26:UPC2:PSD2:ERG1:ERG2:ERG11
organic hydroxy compound biosynthetic process	5.50%	1.00%	0.00409	0.00%	ERG24:ERG6:NCP1:PDC11:ERG26:SNO1:UPC2:PSD2:ERG1:ERG2:ERG11
chemical homeostasis	8.00%	2.10%	0.00427	0.00%	TFP1:RAS1:VMA5:SPF1:orf19.3132:VCX1:FET34:orf19.4240:CTR2:orf19.55:FRP1:RBT5:PGA10:VAM3:DUR3:VPH1
small molecule metabolic process	19.90%	9.70%	0.00521	0.00%	SEC23:CDS1:orf19.1460:ERG24:ERG6:TFP1:SPT23:RAS1:orf19.2050:orf19.21:ARE2:MIS11:FRS1:NCP1:PDC11:CEK1:ERG26:orf19.2915:SNO1:LYS2:EHT1:SCS7:GCV2:UPC2:orf19.3922:PSD2:ERG1:ECM17:TRP5:RIM20:ADE12:orf19.4960:MET4:MET15:SHM2:FAS2:ERG2:VPH1:ERG11:MET14
alcohol biosynthetic process	5.00%	0.90%	0.00601	0.00%	ERG24:ERG6:NCP1:PDC11:ERG26:UPC2:PSD2:ERG1:ERG2:ERG11
organic hydroxy compound metabolic process	7.00%	1.70%	0.00658	0.00%	ERG24:ERG6:orf19.2050:orf19.21:ARE2:NCP1:PDC11:ERG26:SNO1:UPC2:PSD2:ERG1:ERG2:ERG11
ion homeostasis	7.50%	2.00%	0.00685	0.00%	TFP1:VMA5:SPF1:orf19.3132:VCX1:FET34:orf19.4240:CTR2:orf19.55:FRP1:RBT5:PGA10:VAM3:DUR3:VPH1
response to starvation	12.90%	5.10%	0.00717	0.00%	PLD1:CDS1:orf19.1364:MEP1:RAS1:orf19.2401:CEK1:FCY2:FGR6-4:PSD2:ERG1:DDR48:FET34:orf19.4246:VPS11:FGR41:LIP5:FRP1:SNF4:VAM3:orf19.6064:DHH1:MHP1:DUR3:orf19.7196:SET3

response to external stimulus	13.90%	5.70%	0.00779	0.00%	PLD1:CDS1:orf19.1364:MEP1:RAS1:orf19.2401:CEK1:FCY2:FGR6-4:PSD2:ERG1:DDR48:FET34:orf19.4246:VPS11:FGR41:LIP5:GAL4:FRP1:SNF4:VAM3:orf19.6064:DHH1:MHP1:DUR3:orf19.7196:SET3:BUD2
cellular response to starvation	12.40%	4.90%	0.01192	0.00%	PLD1:CDS1:orf19.1364:MEP1:RAS1:orf19.2401:CEK1:FCY2:FGR6-4:ERG1:DDR48:FET34:orf19.4246:VPS11:FGR41:LIP5:FRP1:SNF4:VAM3:orf19.6064:DHH1:MHP1:DUR3:orf19.7196:SET3
response to nutrient levels	13.40%	5.60%	0.01496	0.08%	PLD1:CDS1:orf19.1364:MEP1:RAS1:orf19.2401:CEK1:FCY2:FGR6-4:PSD2:ERG1:DDR48:FET34:orf19.4246:VPS11:FGR41:LIP5:GAL4:FRP1:SNF4:VAM3:orf19.6064:DHH1:MHP1:DUR3:orf19.7196:SET3
response to extracellular stimulus	13.40%	5.70%	0.0165	0.07%	PLD1:CDS1:orf19.1364:MEP1:RAS1:orf19.2401:CEK1:FCY2:FGR6-4:PSD2:ERG1:DDR48:FET34:orf19.4246:VPS11:FGR41:LIP5:GAL4:FRP1:SNF4:VAM3:orf19.6064:DHH1:MHP1:DUR3:orf19.7196:SET3
cellular homeostasis	8.00%	2.40%	0.02013	0.07%	TFP1:RAS1:VMA5:SPF1:orf19.3132:VCX1:FET34:orf19.4240:CTR2:orf19.55:FRP1:RBT5:PGA10:VAM3:DUR3:VPH1
cellular response to nutrient levels	12.90%	5.40%	0.02233	0.07%	PLD1:CDS1:orf19.1364:MEP1:RAS1:orf19.2401:CEK1:FCY2:FGR6-4:ERG1:DDR48:FET34:orf19.4246:VPS11:FGR41:LIP5:GAL4:FRP1:SNF4:VAM3:orf19.6064:DHH1:MHP1:DUR3:orf19.7196:SET3
cellular response to extracellular stimulus	12.90%	5.50%	0.02585	0.07%	PLD1:CDS1:orf19.1364:MEP1:RAS1:orf19.2401:CEK1:FCY2:FGR6-4:ERG1:DDR48:FET34:orf19.4246:VPS11:FGR41:LIP5:GAL4:FRP1:SNF4:VAM3:orf19.6064:DHH1:MHP1:DUR3:orf19.7196:SET3
cellular response to external stimulus	12.90%	5.50%	0.03283	0.06%	PLD1:CDS1:orf19.1364:MEP1:RAS1:orf19.2401:CEK1:FCY2:FGR6-4:ERG1:DDR48:FET34:orf19.4246:VPS11:FGR41:LIP5:GAL4:FRP1:SNF4:VAM3:orf19.6064:DHH1:MHP1:DUR3:orf19.7196:SET3
lipid biosynthetic process	7.50%	2.30%	0.03891	0.06%	CDS1:ERG24:ERG6:SPT23:NCP1:ERG26:EHT1:SCS7:UPC2:PSD2:ERG1:orf19.4240:FAS2:ERG2:ERG11
cellular metal ion homeostasis	5.50%	1.40%	0.06429	0.12%	VMA5:SPF1:orf19.3132:VCX1:FET34:orf19.4240:CTR2:orf19.55:FRP1:RBT5:PGA10
metal ion homeostasis	5.50%	1.40%	0.09637	0.24%	VMA5:SPF1:orf19.3132:VCX1:FET34:orf19.4240:CTR2:orf19.55:FRP1:RBT5:PGA10

**Tables. 5.2-4. GO term finder analysis for down-regulated gene sets. 5.2)** Genes down regulated in *fkx2(6A<sub>CDK</sub>)*-only set during hyphal growth. **5.3)** Gene that shown down-regulation in both the *fkx2Δ/Δ* and *fkx2(6A<sub>CDK</sub>)* strains during hyphal growth. **5.4)** Genes that are only down-regulated in the *fkx2Δ/Δ* -only set during hyphal growth.

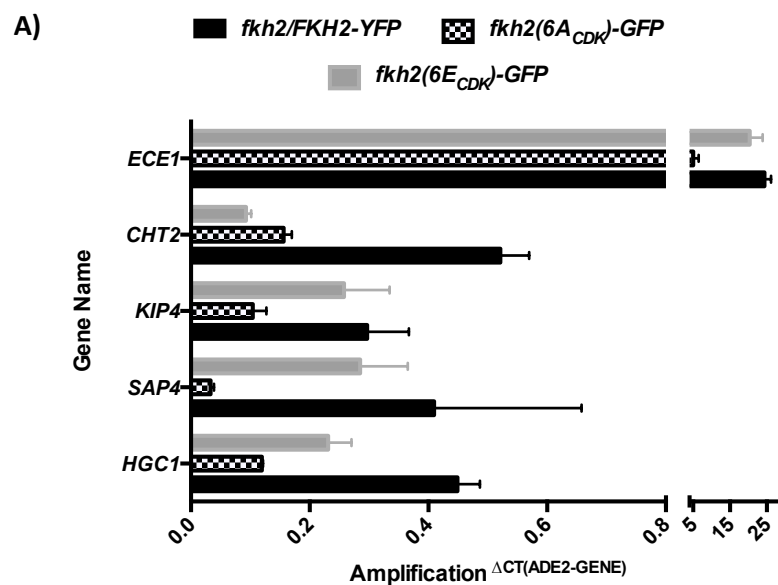
### 5.2.2. Confirming Fkh2's phosphorylation-dependent regulation of genes for filamentous invasive growth.

It was shown that a number of hyphal specific genes are down-regulated in the absence of Fkh2 phosphorylation. However as previously mentioned the *FKH2/FKH2-YFP* control strain used was not the most appropriate, as the results observed may be due to haploinsufficiency of the *fkx2/fkx2(6A<sub>CDK</sub>)* strain. Also, only the *fkx2(6A<sub>CDK</sub>)* phosphorylation mutant strain was used in the microarray, therefore the transcriptional effect of the phosphomimetic *fkx2(6E<sub>CDK</sub>)* mutant

remains unknown. To investigate both of these problems, and to confirm the results observed in the above microarrays, the expression of the hyphal-specific genes *ECE1*, *KIP4*, *HGC1*, *SAP4* and *CHT2* was determined in the *fkh2/FKH2-YFP*, *fkh2(6A<sub>CDK</sub>)* and *fkh2(6E<sub>CDK</sub>)* strains using quantitative PCR (qPCR).

For the experiment, cells were grown in hyphal-inducing conditions as previously described. Total RNA was then isolated from the strains and reverse transcribed to cDNA, from which qPCR was carried out using primer pairs specific to each of the genes in question. Expression levels were normalised against the expression of the housekeeping gene *ADE2*. For each strain two biological replicates were carried out, with three technical replicates of each primer pair. The normalised threshold  $C_T$  values for each gene in the respective strains were combined, being used as the exponent to the experimentally derived amplification value for the primer pair. This gives a value for the amount of the target gene transcript present in the total starting RNA from the different strains. These values are shown for each strain in Figure 5.2.5A, allowing comparison of the amount of each transcript in the mutant and wild-type strains.

The normalised transcript levels in the phosphorylation mutants and wild-type *fkh2/FKH2-YFP* strain were then further compared using the  $\Delta\Delta^{CT}$  method as described in the materials and methods. These results are shown in Figure 5.2.5B.



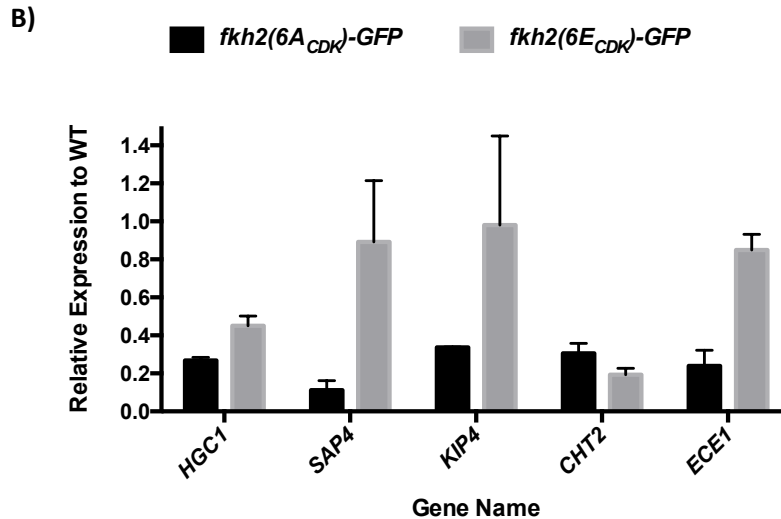


**Fig. 5.2.5. qPCR confirmation of genes that with altered expression in the Fkh2 phosphorylation mutants.** RNA was isolated from *fkh2/FKH2-YFP*, *fkh2(6A<sub>CDK</sub>)* and *fkh2(6E<sub>CDK</sub>)* strains after 3 hours of hyphal growth. A) Graph showing amplification of the target transcripts in the wild-type Fkh2 strain and the phospho-mutants. B)  $\Delta\Delta^{CT}$  analysis of transcript expression in the Fkh2 phosphorylation mutants, showing the relative level of each transcript compared to the wild-type Fkh2 strain. Results are from two biological replicate experiments, each with three technical replicates. Error bars represent 1 standard deviation.

All of the invasive filamentation-specific genes show a reduction in expression in the *fkh2(6A<sub>CDK</sub>)-GFP* strain compared with the *fkh2/FKH2-YFP* strain, with transcripts being present at less than half the wild-type level in the phosphorylation blocked mutant. *ECE1*, *KIP4* and *SAP4* show expression levels that are similar to wild-type in the *fkh2(6E<sub>CDK</sub>)-GFP* strain (Fig. 5.14B.). However *HGC1* and *CHT2* show reduced levels of expression in the phosphomimetic strain compared with the *fkh2/FKH2-YFP* strain. The *CHT2* transcript also appears to be less abundant in the phosphomimetic Fkh2 strain than in the phosphorylation blocked strain (Fig. 5.14B.). This is not the case for the other genes, all of which show a higher transcript abundance in the *fkh2(6E<sub>CDK</sub>)-GFP* strain compared to the *fkh2(6A<sub>CDK</sub>)-GFP* strain. These results confirm the general trends evident in the microarray, and show that the *FKH2/FKH2-YFP* control did not distort the results of the microarray experiments.

### 5.2.3. Detailed analysis of the microarray results: *FKH2* deletion alters gene expression during yeast growth

#### 5.2.3.1 Genes down-regulated during yeast growth upon *FKH2* deletion

GO slim process analysis was carried out for genes that are at least two-fold down-regulated in *fkh2Δ/Δ* yeast. The largest category, as for most of the arrays, is for genes whose biological function is unknown (25.8%). This is due to the limited annotation of the *C. albicans* genome, especially for genes of which no known *S. cerevisiae* homologue exists. Therefore it is likely that the percentage values for each category under-represent the actual number of genes present in the category. The best-represented annotated categories are: regulation of biological processes (23.8%), transport (17.2%), and response to chemical stimulus (15.9%). Genes involved in cell-cycle progression show lower than expected representation at 8.6%; however a number of genes involved in stress response (15.9%) are down-regulated, suggesting some relation to the function of *S. cerevisiae* *FKH1* and *FKH2* in regulating stress response (Postnikoff et al. 2012).

The cell wall proteins *RBE1*, *SCW11*, *FGR41*, *HYR1*, *RHD3* and *PGA53* all show down-regulation in the absence of *FKH2* (Fig. 5.2.6.). However this may be an indirect effect as *EFG1* is also down-regulated, which is known to regulate the expression of cell wall proteins (Sohn et al. 2003). The failure of *fkh2Δ/Δ* yeast cells to separate could be attributed to reduced expression of the cytokinetic protein *HOF1*, and the chitinases *CHT2/3*. *FKH2* has previously been shown to regulate histone genes in *C. albicans* (Bensen et al. 2002), which is confirmed by the observed down-regulation of the histone H2A *HTA2*, and the histone acetyl transferase *TRA1*. Evidence for the role of *FKH2* in cell cycle regulation can be taken from decreased expression of the Cdk1 tyrosine phosphatase *MIH1*, the orthologue of the kinetochore component *ScSPC42*, *ORF19.1484*; and *ULP2*, a SUMO deconjugating enzyme with roles in transcription and DNA replication (Huaping et al. 2007) (Fig. 5.6.2.). *ULP2* is shown to be down-regulated under all conditions tested except *FKH2* over-expression, strongly suggesting positive regulation by Fkh2. This is supported by the presence of a Fkh2 consensus binding site in the 1kb upstream of the *ULP2* coding sequence. Another interesting gene that shows

reduced expression in most of the *Fkh2* mutants is for the putative argonaute protein *AGO1*, which again contains a *Fkh2* minimal binding motif in its promoter.

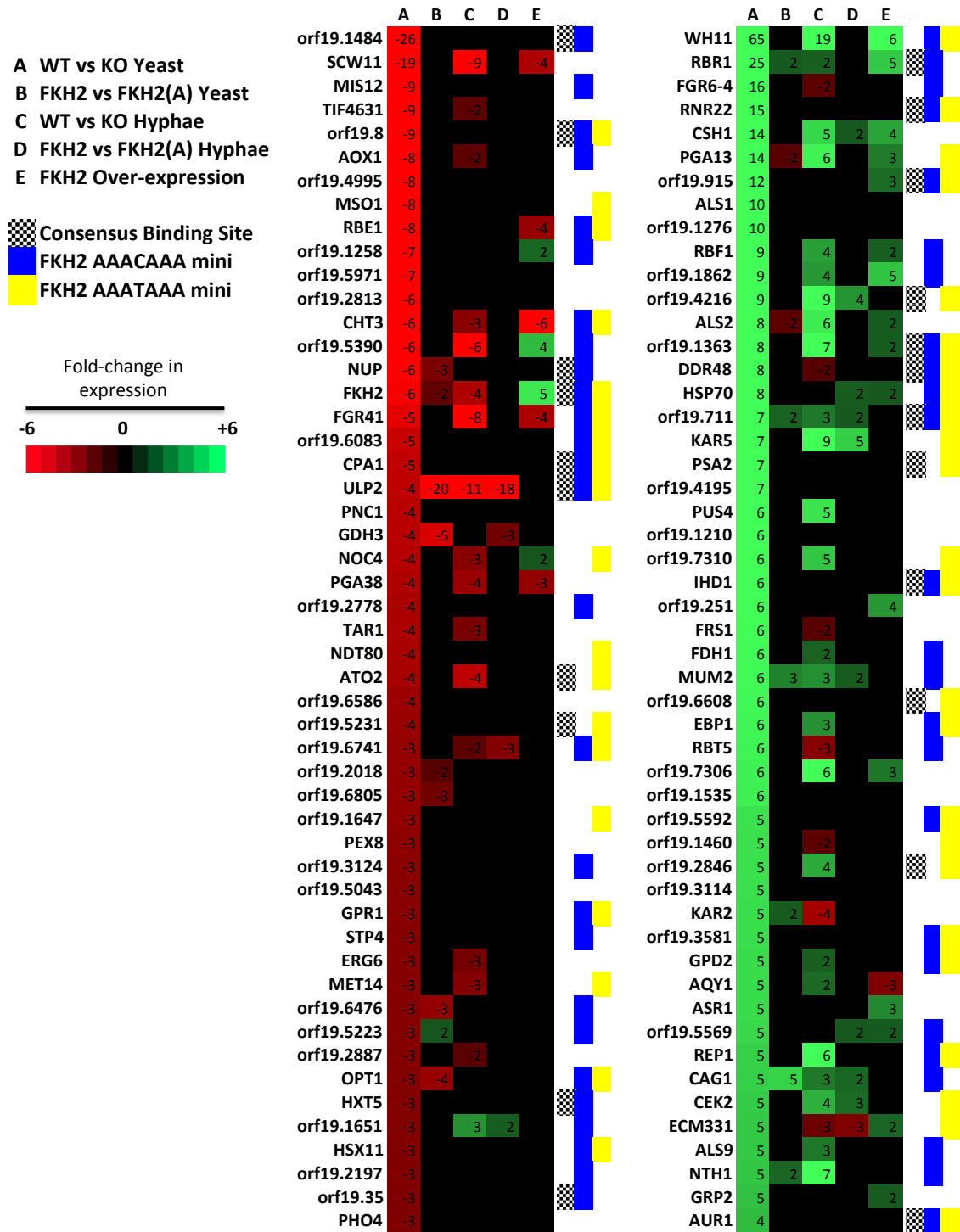


**Fig. 5.2.6. Genes down or up-regulated in the absence of *FKH2* during yeast growth.** Excel spreadsheet sorted for genes showing decreased/increased expression in array A. Displayed are the top 50 genes down-regulated during yeast growth on deletion of *FKH2*, included with the presence or absence of a *Fkh2* binding site in the 1kb upstream of the gene.

### 5.2.3.2. Genes up-regulated during yeast growth upon *FKH2* deletion

For genes with increased expression in the *fkh2Δ/Δ* mutant during yeast growth the GO analysis shows similar representation to that observed for down-regulated genes. This includes strong representation of the GO categories: regulation of biological processes (18.2%), response to stress (15.1%), and response to chemical stimulus (14.7%); showing that Fkh2 can differentially regulate subsets of genes involved in a similar process. The Cdk1 B-type cyclin *CLB4* is up-regulated, confirming the results of Bensen et al, and serving as a positive control to show that the microarray experiments are working correctly.

A number of adhesin genes (*ALS1*, *ALS2* and *ALS9*) are up-regulated during yeast growth (Fig. 5.2.6.), suggesting an explanation for the observed clumping phenotype. There is also up-regulation of a subset of stress response genes; combating problems such as: genotoxic stress (*RAD51* and *DAP1*), heat stress (*HSP21*, *HSP31* and *HSP70*) and reactive oxygen species (*SOD4* and *SOD5*). However this up-regulation may be indirect; being due to the decreased fitness of the *fkh2Δ/Δ* strain, rather than loss of direct repression from Fkh2. *HSP21*, *HSP70*, *RAD51* and *SOD4/5* all contain a minimal Fkh2 binding motif in their 1kb of upstream sequence, suggesting that they may indeed be negatively regulated by Fkh2 *in vivo*. Interestingly - the pheromone response MAPK pathway components *STE4* and *CEK2* are also up-regulated in this mutant. Increased expression of the cAMP phosphodiesterase *PDE1* could explain the difficulty of the *fkh2Δ/Δ* strain to respond to hyphal inducing signals, preventing the level of cAMP reaching that required for activation of the PKA pathway. *PDE1* is also shown to be up-regulated in other Fkh2 mutant arrays during hyphal growth (Fig. 5.2.2.)

### 5.2.4. Blocking Fkh2 phosphorylation affects gene expression during yeast growth

Compared with the *fkh2Δ/Δ* mutant the transcriptional changes observed in the *fkh2(6A<sub>CDK</sub>)* mutant are not as extensive; with only 44 genes being down and 76 genes up-regulated, compared with the 151 down and 292 genes up-regulated during yeast growth in the *fkh2Δ/Δ* mutant. Of the genes that are down-regulated,

only 15 show reduced expression in both the *fkh2Δ/Δ* strain and *fkh2(6A<sub>CDK</sub>)* strain. For up-regulated genes only 18 are shared between the two strains (Fig. 5.2.7.).

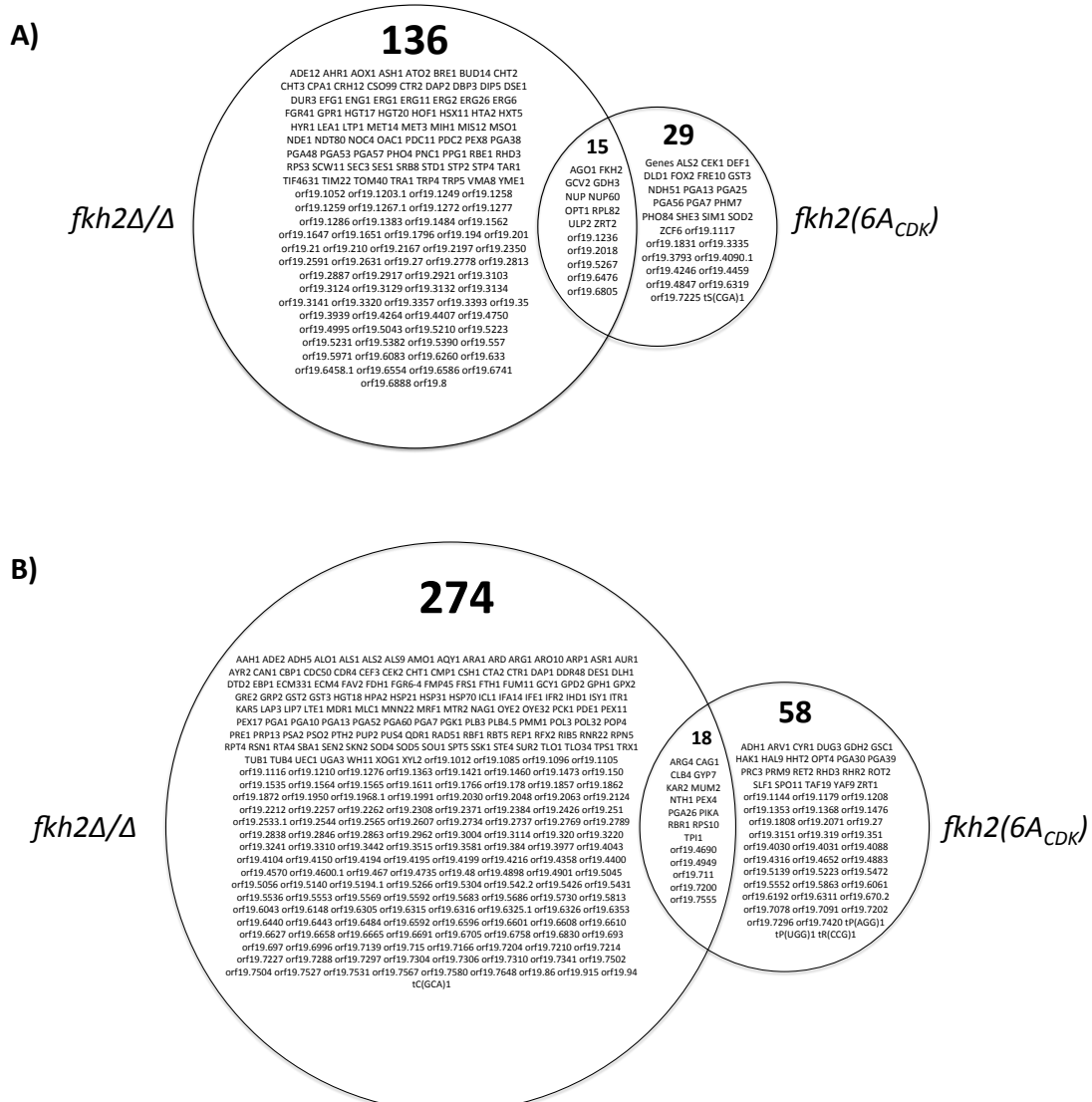


**Figure 5.2.7. Venn diagrams comparing genes with altered expression during yeast growth in the *fkh2Δ/Δ* and *fkh2(6A<sub>CDK</sub>)* strains. A) Genes that are down-regulated. B) Genes that are up-regulated.**

#### **5.2.4.1. Genes down-regulated during yeast growth on blocking Fkh2 phosphorylation**

The majority of down-regulated genes fall into similar GO slim process categories as for the *fkh2Δ/Δ* strain; with most genes being involved in: regulation of biological processes (25%), transport (20.5%), filamentous growth (20.5%), stress response (18.2%), chemical response (11.4%) or cell cycle regulation (9.4%). The *FKH2* transcript itself is down-regulated (Fig. 5.2.8.), supporting the idea that phosphorylation of Fkh2 may positively reinforce its own expression. A number of cell surface protein genes (*PGA7*, *PGA13*, *PGA25* and *PGA56*) and genes involved in mineral acquisition (*ZRT2*, *FRE10*, *ORF19.4459*) are also down-regulated. Other interesting genes with reduced expression are: the mRNA binding protein She3, the MAPK Cek1 and the RNA Polymerase II regulator Def1 (Fig. 5.2.8.).

#### **5.2.4.2. Genes up-regulated during yeast growth on blocking of Fkh2 phosphorylation.**

GO slim mapping process analysis again shows strong representation of the groups: regulation of biological processes (26.3%), transport (15.8%), stress (13.2%) and chemical stimulus response (11.8%). However, there is increased representation for genes involved in carbohydrate metabolism (11.8%) and cell cycle regulation (11.8%). *CLB4* is again shown to be up-regulated, suggesting that Fkh2 phosphorylation may be required to negatively regulate *CLB4* expression during the cell cycle. A number of genes involved in DNA maintenance and regulation are up-regulated; these include: the endonuclease *SPO11*, involved in recombination during the parasexual cycle; the histone H3 *HHT2*, and *ORF19.7420*, which is thought to be involved in the regulation of RNA polymerase II. There is also an increased transcript level of the adenylyl cyclase *CYR1*, implying that there may be higher levels of intracellular cAMP in the *fkh2(6A<sub>CDK</sub>)* strain. Consistent with this hypothesis, *PDE1* does not show up-regulation in *fkh2(6A<sub>CDK</sub>)* during yeast growth, which would be required to negatively regulate cAMP levels (Fig. 5.2.8.).

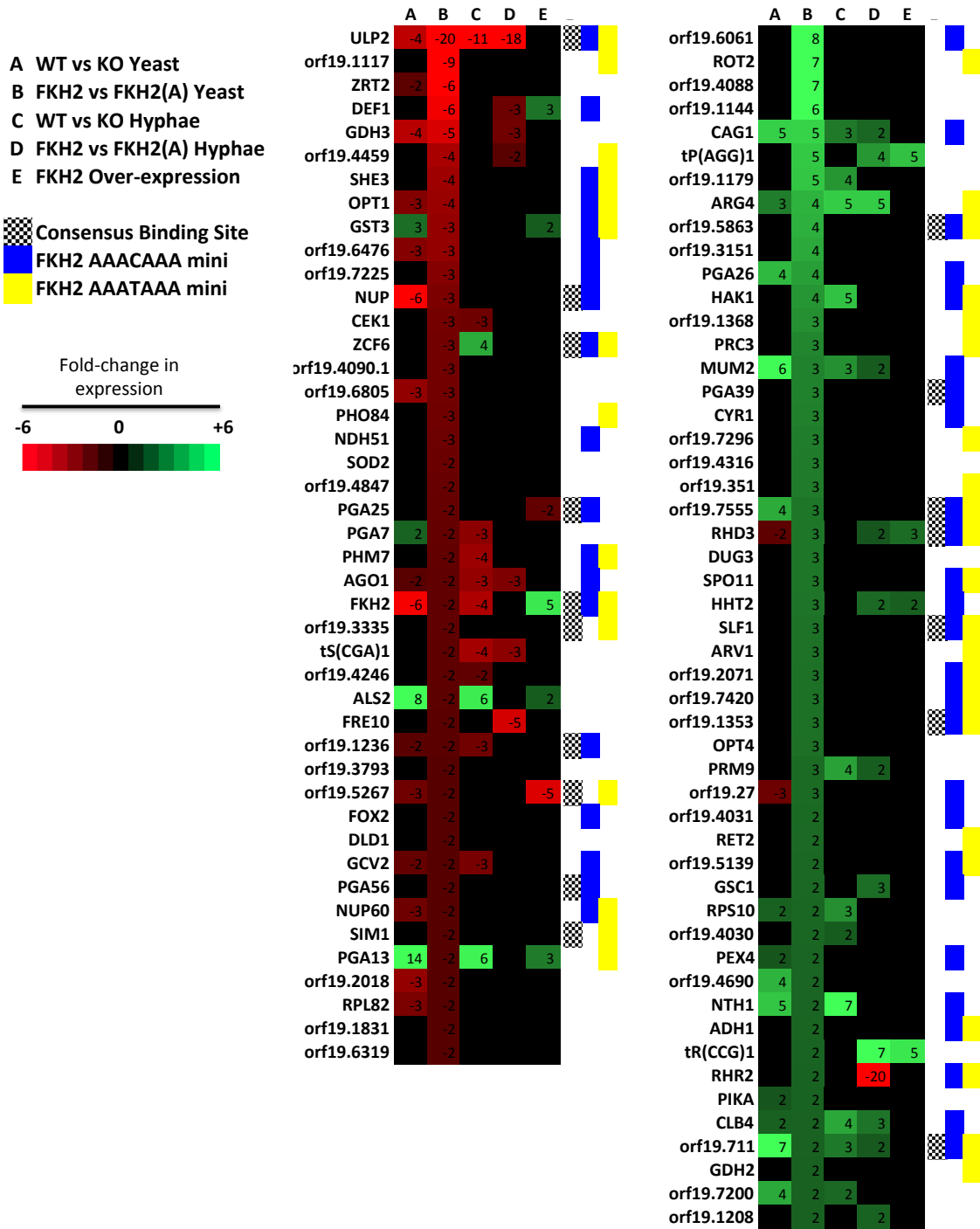


**Fig. 5.2.8. Genes down or up-regulated on blocking Fkh2 phosphorylation during yeast growth.** Excel spreadsheet sorted for genes with reduced expression in array B. Displayed are the 44 down-regulated genes on blocking Fkh2 phosphorylation during yeast growth and the top 50 up-regulated genes, included with the presence or absence of a Fkh2 binding site in the 1kb upstream of the gene.

### 5.2.5. *FKH2* Deletion alters hyphal transcriptional programs.

Deletion on *FKH2* appears to have a much greater negative effect on gene expression during hyphal growth than yeast growth (Fig. 5.2.9.), with 236 genes showing decreased expression during hyphal growth compared with 151 during yeast growth (Fig. 5.2.9A.). The number of genes up-regulated remains relatively consistent: 292 yeast vs. 252 hyphae, as does the number of shared genes: 58 down and 88 up-regulated (Fig. 5.2.9B.).

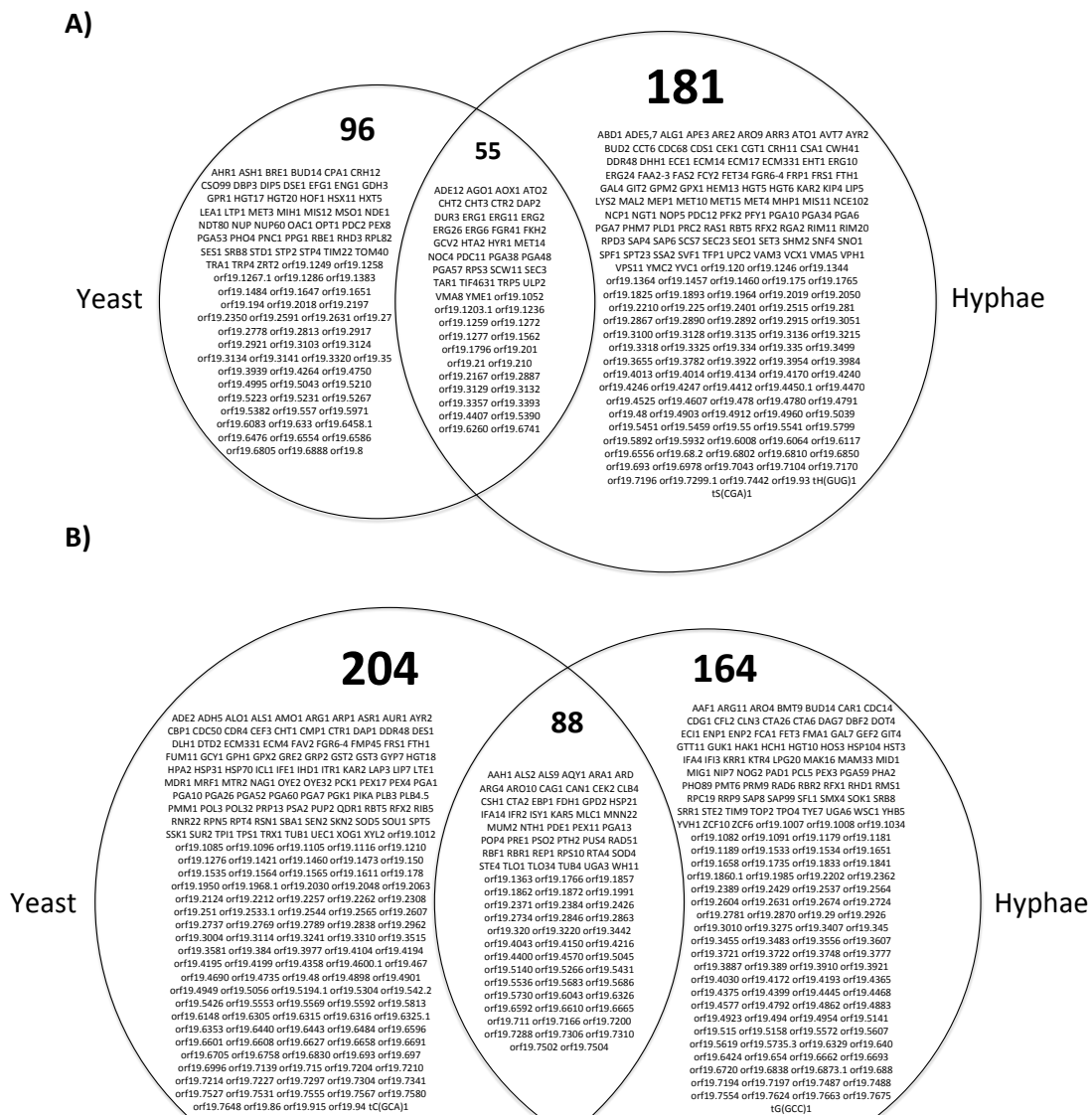


Figure 5.2.9. Venn diagrams comparing genes with altered expression in the *fkh2Δ* strain during yeast and hyphal growth. A) Genes that are down-regulated. B) Genes that are up-regulated.

### 5.2.5.1. Genes down regulated during hyphal growth upon *FKH2* deletion

GO slim process analysis shows that one-quarter (25.4%) of down-regulated genes are of unknown function. Response to stress shows strong representation (20.8%), possibly related to inability to react to the change in temperature and the increased stresses hyphal growth puts on the cell. The other main GO categories represented are: transport (20.3%), regulation of biological processes (18.6%), response to chemical stimulus (15.3%), and organelle organization (14%). The *RAS1* GTPase, that regulates the cAMP-PKA and MAPK pathways, shows reduced expression, as again does the *CEK1* MAPK (Fig. 5.2.2.). This suggests a possible inability to activate the transcription factor Cph1 that is required for filamentation on solid media (Liu et al. 1994). The promoters of *RAS1* and *CEK1* both contain a Fkh2 minimal binding site, suggesting possible direct regulation. As shown for the other arrays there is strong representation of cell wall/GPI anchored proteins, such as: *RBT5*, *HYR1*, *PGA10*, *SCW11*, *FGR41*, *PGA34* and *PGA6* (Fig. 5.2.2.). The polarity regulating proteins *SEC3* and *BUD2* show a reduction in expression, indicating a possible reason for the inability of the *fkh2Δ/Δ* strain to form highly polarised true hyphae. Other groups of genes that are down-regulated are those for iron acquisition/utilization (*FET34*, *FTH1* and *FRP1*), and histone regulation (*SET3*, *RPD3* and *HTA2*).

### 5.2.5.2. Genes up-regulated during hyphal growth upon *FKH2* deletion

GO slim process analysis of genes up-regulated during hyphal growth in the absence of *FKH2* shows a similar pattern as seen for the previous arrays, with regulation of biological processes (23.8%) being the largest group of genes with a known function. Interestingly, the next best-represented group is for genes involved in filamentous growth (15.1%). Response to stress (13.5%), chemical stimulus response (12.3%), transport (11.9%), RNA metabolism (11.1%) and cell cycle (10.7%) groups all show similar levels of representation.

The hyphal repressor *SFL1*, along with the Tup1 co-repressor *MIG1*, is up-regulated (Fig. 5.2.2.); possibly as a cause or consequence of the inability to form true hyphae. The cytokinetic kinase *DBF2*, and phosphatase *CDC14* also show

increased expression during hyphal growth in the absence of *FKH2*. As does *MLC1* (Fig. 5.2.2.), a component of both the actomyosin ring for cytokinesis, and the actomyosin based polarised secretion system in filamentous growth. Again components of the mating response pathway (*CAG1*, *STE2*, *SET4* and *CEK2*) and genes involved in DNA damage response (*RAD51*, *RAD5* and *RFX1*) have increased expression on *FKH2* deletion. The Cdk1 cyclins *CLN3* and *CLB4* both show up-regulation, further supporting a role for Fkh2 in cell cycle regulation. A kinase related protein that shows increased expression in the absence of *FKH2* is *SOK1*, which is known to be involved in biofilm formation and hyphal development (Nobile et al. 2012).

#### **5.2.6. Further transcriptional investigation of blocking Fkh2 phosphorylation during hyphal growth**

As for the *fkh2Δ/Δ* strain, blocking Fkh2 phosphorylation has a greater negative impact on hyphal growth compared to yeast growth. 74 genes show a greater than two-fold reduction in expression in *fkh2(6A<sub>CDK</sub>)* hyphae compared with 44 genes during yeast growth (Fig. 5.2.10A.). The number of genes up-regulated in the *fkh2(6A<sub>CDK</sub>)* strain is more comparable, with 76 genes showing up-regulation during hyphal growth vs. 91 genes during yeast growth (Fig. 5.2.10B.).

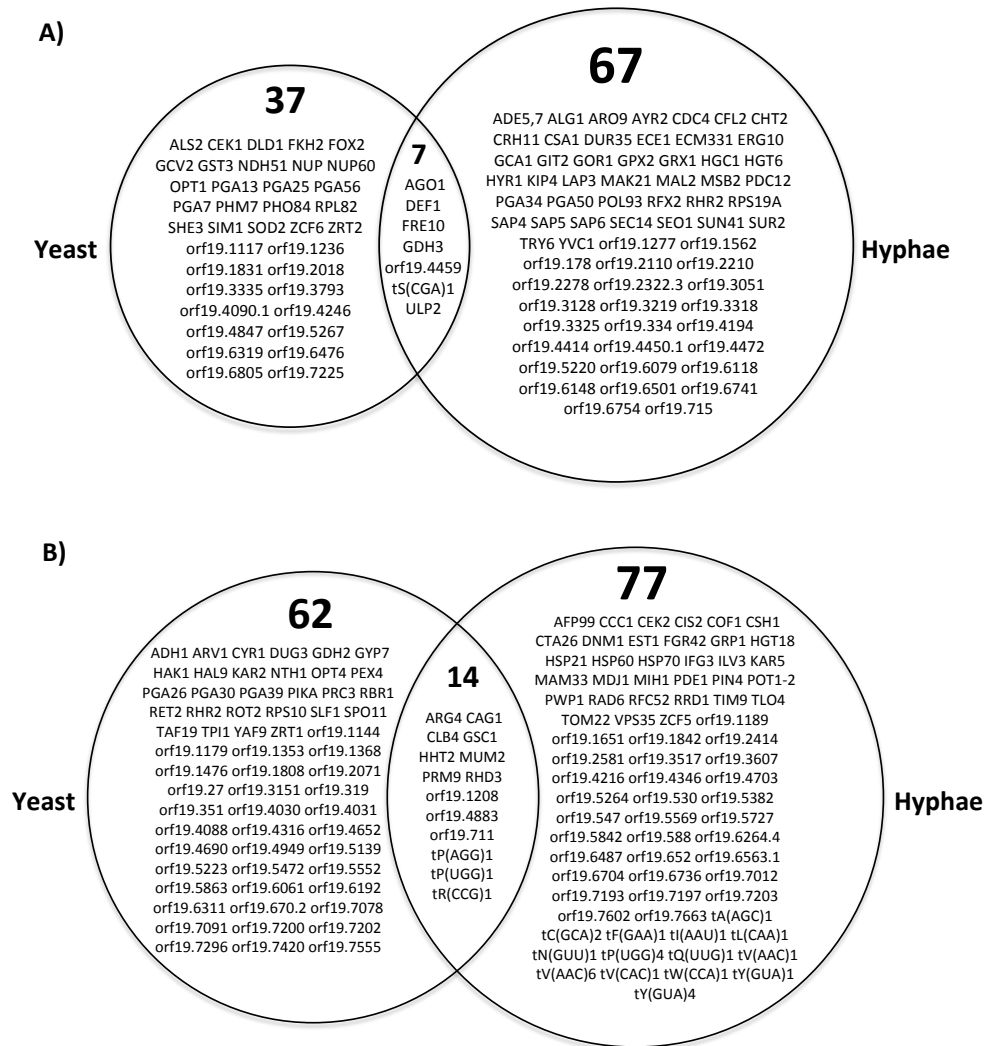


**Figure 5.2.10. Venn diagrams comparing genes with altered expression in the *fkh2(6A<sub>CDK</sub>)* strain during yeast and hyphal growth. A) Genes that are down-regulated in the *fkh2(6A<sub>CDK</sub>)* strain. B) Genes that are up-regulated in the *fkh2(6A<sub>CDK</sub>)* strain.**

### 5.2.6.1. Genes down-regulated during hyphal growth on blocking Fkh2 phosphorylation

Most of the genes of interest that are down-regulated on blocking Fkh2 phosphorylation during hyphal growth have already been discussed above; however a few other interesting genes remain to be noted.

The glycerol-3-phosphatase *RHR2* is the most down-regulated gene in the array (Fig. 5.2.3.), but interestingly shows partial up-regulation on the *fkh2(6A<sub>CDK</sub>)* mutant during yeast growth. It is normally required for osmotic stress tolerance and is up-regulated on hyphal induction or stress response (Smith et al. 2004).

*CDC4*, a component of ubiquitin ligase Skip-Cullin-Fbox (SCF) complex, shows reduced expression in *fkh2(6A<sub>CDK</sub>)* hyphae, but not in the other mutants and conditions tested (Fig. 5.2.3.). The SCF complex has a known role in hyphal morphogenesis (Atir-Lande et al. 2005), so it is of interest that it may be positively regulated by Fkh2.

Another gene that shows reduced expression is for the *MSB2* cell wall sensor that is upstream of the Cek1-MAPK pathway (Román, Cottier, et al. 2009) (Fig. 5.2.3.), further highlighting the role of Fkh2 in the regulation of this pathway.

#### **5.2.6.2. Genes up-regulated during hyphal growth on blocking Fkh2 phosphorylation**

GO slim analysis of genes with increased ( $\geq 2$  fold) expression in *fkh2(6A<sub>CDK</sub>)* hyphae shows different GO term representations compared with other arrays. The largest category is for genes involved in translation (22%), with many genes for transfer RNAs (tRNAs) being up-regulated. Regulation of biological processes (20.9%) and response to stress (15.4%) again show strong representation. Other GO slim terms that the up-regulated genes sort into are for: organelle organization (18.7%), cell cycle regulation (14.3%), biological processes (18.7%), filamentous growth (13.2%) and transport (12.1%). This provides further evidence supporting the cell cycle regulatory role of Fkh2, as well as presenting a possibly different role for Fkh2 in regulating genes for organelle organization.

Of the up-regulated genes, *CLB4* and *PDE1* are known to be negative regulators of filamentation (Bensen et al. 2005; Wilson et al. 2010). The gene with the greatest increase in expression in *fkh2(6A<sub>CDK</sub>)* hyphae is for the putative RNA processing protein *PWP1* (Fig. 5.2.3.). Interestingly *PWP1* does not show any changes in expression in the other mutants and conditions tested. DNA damage response genes *RAD6* and *PIN4* show up-regulation, along with genes for the heat shock proteins: Hsp21, Hsp60 and Hsp70 (Fig. 5.2.3.). The H3 histone *HHT2* shows increased expression, as is also the case in the *fkh2(6A<sub>CDK</sub>)* strain during yeast growth. This suggests that the phosphorylation of Fkh2 may be important for *HHT2* expression. The Cdk1 phosphatase, *MIH1*, is up-regulated in the *fkh2(6A<sub>CDK</sub>)* strain during hyphal growth, but interestingly is down-regulated during yeast

growth in the absence of *FKH2* (Fig. 5.2.3.). The MAPK *CEK2* is again up-regulated, as it is in the absence of *FKH2* in both yeast and hyphae (Fig. 5.2.3.).

### **5.3. Searching for interacting partners of Fkh2**

In order to try and determine the possibly cell cycle-independent functions of Fkh2 early after hyphal induction, the proteins that interact with Fkh2 at this time were sought after.

#### **5.3.1. Mass-Spectromic identification of Fkh2 interacting partners**

Fkh2-6xMyc expressing cells were grown over-night to stationary phase in YEPD, before being re-inoculated into hyphal-inducing media for 40mins. Fkh2-6xMyc was IP'd from the lysate generated from these cells, with the IP being washed four times, and then run on a 12% SDS-PAGE gel before Coomassie staining (Fig. 5.3.1A.). Multiple bands were present as well as the band of the expected size for Fkh2-6xMyc (Fig. 5.3.1B). In order to determine the identity of the co-precipitating proteins in the bands, these were cut out of the gel, de-stained and then dried for shipment. Mass spectrometry used to identify the protein bands was carried out at the proteomics center at the University of Albany in the USA.

This identified only a few proteins with a high number of peptide hits; two of which were not found to be present in  $\alpha$ Myc IPs carried out previously in the lab. These were: Pob3, whose *S. cerevisiae* homologue is involved in chromatin modifications for DNA replication and transcription (Schlesinger & Formosa 2000); and Srp1, whose *S. cerevisiae* homologue functions in the nuclear import of proteins, and possibly in regulation of protein degradation (Tabb et al. 2000). The functionality of both of these proteins does suggest possible roles in conjunction with Fkh2. Interestingly the suspected interacting protein Mcm1 was not found to co-precipitate with Fkh2 in this experiment.

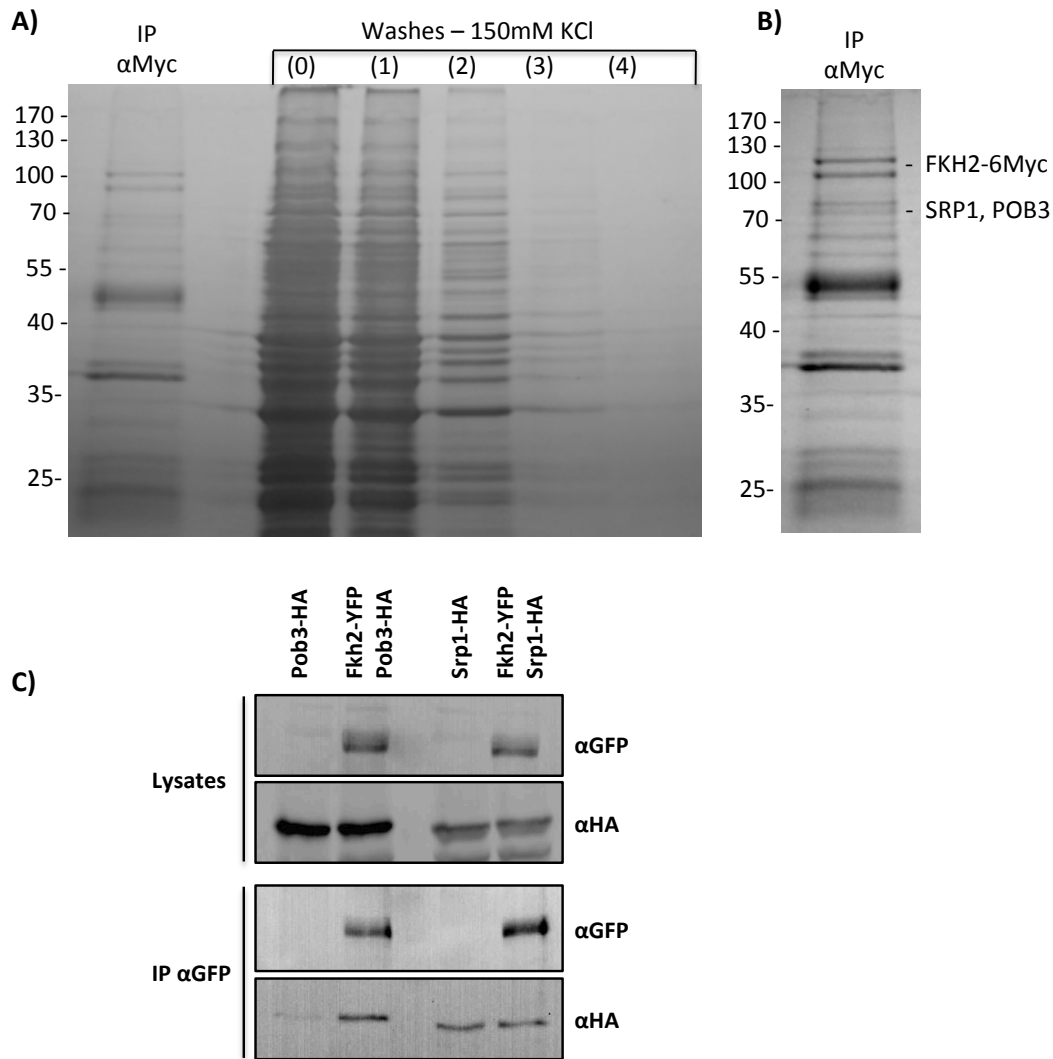


**Fig. 5.3.1. Novel interacting partners of Fkh2 early in hyphal growth.** Samples were grown for 40mins post hyphal induction when Fkh2 is known to be phosphorylated **A)** Coomassie stained gel of Fkh2-6Myc immunoprecipitation (IP αMyc) including total lysate of starting material (0) and elution from washes of the IP (1-4). **B)** Cut-out of the IP lane from the gel showing the proteins that were identified by mass-spectrometry peptide identification. **C)** CoIP confirming Fkh2's interaction with Pob3, but not Srp1..

### 5.3.2. Pob3 physically interacts with Fkh2

In order to confirm that Pob3 and Srp1 interact with Fkh2, both proteins were separately C-terminally epitope tagged with 3xHA in a *FKH2/FKH2-YFP* strain, allowing co-immunoprecipitation (CoIP) experiments to be carried out (Fig. 5.3.1C.). The strains were induced as hyphae for 40mins and then harvested for protein extraction. αGFP and were run on an 8% gel and Western blotted for detection with both αGFP and αHA antibodies. 50µg lysates were run to confirm strain identity and allow the extent of the IP to be viewed. On IP of Fkh2-YFP,

bands could be detected corresponding to both Pob3-HA and Srp1-HA. However only the Pob3 interaction could be seen as specific under the conditions tested, with a band for Srp1 also being present in the negative  $\alpha$ GFP IP from a strain that only has Srp1 tagged with HA.

#### **5.3.4. Fkh2's interaction with Pob3 is dependent on Fkh2's phosphorylation status.**

As it is known in *S. cerevisiae* that phosphorylation of Fkh2 is required to mediate interaction with Ndd1 (Pic-Taylor et al. 2004), an experiment was carried out to determine whether phosphorylation of *CaFkh2* affected its interaction with the chromatin modifier Pob3. Pob3 was C-terminally tagged with HA in the *fkh2/FKH2-YFP*, *fkh2(6A<sub>CDK</sub>)-GFP* and *fkh2(6E<sub>CDK</sub>)-GFP* strains. Fkh2-YFP/GFP was then IP'd from each of these strains grown for 40mins post hyphal induction. The presence of Pob3-HA was detected by running the IP samples on a gel and probing the subsequent Western blot with an  $\alpha$ HA antibody (Fig. 5.3.2.). The blot was then stripped and re-probed with an  $\alpha$ GFP antibody to confirm IP of Fkh2. Pob3-HA could be detected associated with both the wild-type and phosphomimetic forms of Fkh2, but not the phosphorylation blocked form of Fkh2. Thus, the phosphorylation status of Fkh2 appears to affect its interaction with Pob3 on hyphal induction.

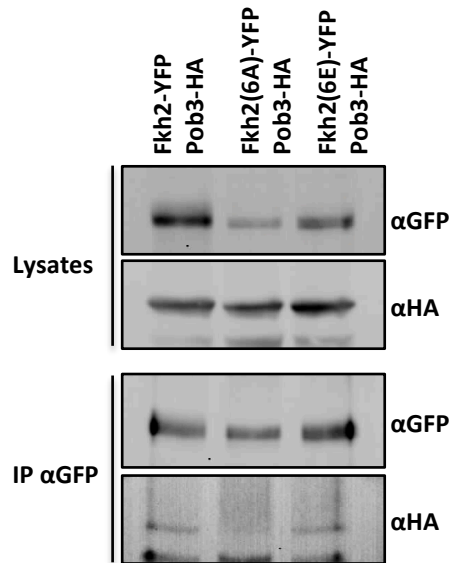


**Fig. 5.3.2. Investigating the effect of Fkh2 phosphorylation on its interaction with Pob3.**  $\alpha$ GFP IP of wild-type Fkh2-YFP and the *fkh2(6A<sub>CDK</sub>)/(6E<sub>CDK</sub>)-GFP* proteins in strains where Pob3 is tagged with HA. The presence of co-precipitating Pob3 was determined by  $\alpha$ HA Western blot.  $\alpha$ GFP Western blot was used as a loading control for the  $\alpha$ GFP IP. Lysates confirm strain identity and quality of immunoprecipitation.

## 5.4. *FKH2* Over-expression

### 5.4.1. Over-expression strategy

Initially over-expression of *FKH2* was sought in order to obtain a sufficient amount of the protein product for phospho-peptide mapping. In order to do this, a *P<sub>GAL1</sub>-FKH2-3HA* vector was constructed.

Firstly a *BamHI* restriction site was introduced between the end of the *FKH2* promoter and beginning of the *FKH2* gene in *pCIP10U P<sub>FKH2</sub>-FKH2-6xMYC*. This allowed the native promoter sequence to be cut out with *AscI/BamHI*, and then replaced with an *AscI-P<sub>GAL1</sub>-BamHI* fragment generated by PCR from BWP17 genomic DNA. Correct insertion of the fragment was checked by *AscI/BamHI* restriction digest, before sequencing of newly amplified promoter region. After this the 6xMYC epitope tag in the vector was swapped for a HA tag through *XhoI/PstI* sub-cloning from another pCIP10 vector. This was again checked through restriction digest.

The pCIP10U *P<sub>GAL1</sub>-FKH2-HA* vector was integrated through digesting with *BglII*, which cuts once within the *P<sub>GAL1</sub>* sequence present, and then transforming to

allow recombination with the  $P_{GAL1}$  genomic locus. Transformant colonies were taken and grown over-night in YEPG to check that Fkh2-HA was being expressed using an anti-HA ( $\alpha$ HA) Western blot. The over-night cultures of the transformants did not grow well in YEPG, and were highly filamentous (Fig. 5.4.1.). Recently the observation that over-expression of Fkh2 leads to filamentation had been published by another group (Chauvel et al. 2012). However how this filamentation occurs remains to be investigated.

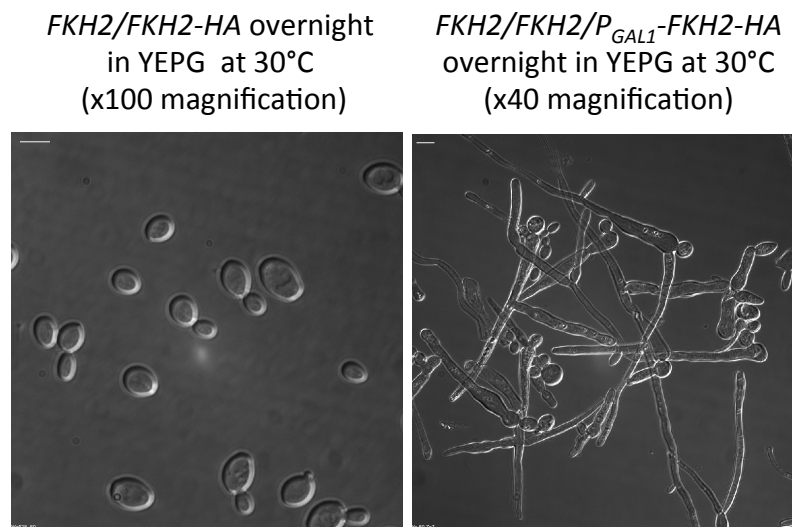


**Fig. 5.4.1. FKH2 overnight over-expression phenotype.** *FKH2/FKH2-HA* and  $P_{GAL1}$ -*FKH2-HA* strains were grown overnight in galactose complete media (YEPG) to induce the *GAL1* promoter. Scale bars represent 5 $\mu$ m.

#### 5.4.2. Comparison of Fkh2 expression levels upon over-expression

Comparison of the  $P_{GAL1}$ -*FKH2-HA* strain with the *FKH2/FKH2-HA* strain was not possible due to the number of copies of HA present in the tag. The wild-type *FKH2-HA* strain had six copies of HA and ran at a higher molecular weight on a western blot than the  $P_{GAL1}$ -*FKH2-HA* strain, which only had one copy of HA. Due to this the tag on the  $P_{GAL1}$ -*FKH2* strain was swapped to GFP, allowing comparison with the *FKH2/FKH2-YFP* strain used in many other experiments.  $P_{GAL1}$ -*FKH2-GFP* and *FKH2/FKH2-YFP* strains were grown for 3 hours in YEPG and YEPD to allow high or reduced expression from the *GAL1* promoter respectively. Over-expression

was confirmed when 50µg aliquots were ran on a 10% gel, and expression levels were visualized with αGFP in a Western blot experiment (Fig. 5.4.2.). Equal loading was confirmed using the αPSTAIRES antibody that recognises the Cdk1 and Pho85 proteins.

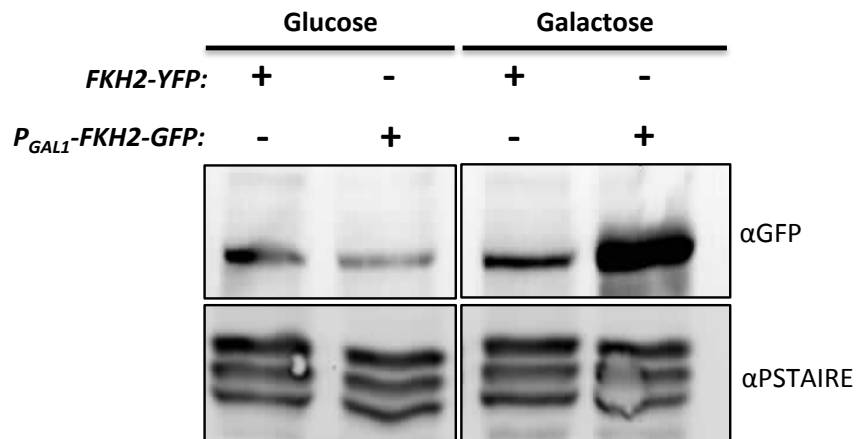


**Fig. 5.4.2. Confirmation of Fkh2 over-expression.** *FKH2/FKH2-YFP* and *P<sub>GAL1</sub>-FKH2-GFP* strains were re-inoculated into YEPD or YEPG at 30°C and grown for 3hours. 50µg of total lysate from the samples was run on a 10% SDS-PAGE gel, which was subsequently Western blotted. The blot was probed with αGFP to detect Fkh2-YFP/GFP and αPSTAIRES as a loading standard.

### 5.4.3. *FKH2* over-expression causes filamentation under yeast growth conditions

*FKH2/FKH2-YFP* and *P<sub>GAL1</sub>-FKH2-GFP* strains were grown up overnight in YEPD and serial diluted onto YEPG plates, which were left to grow at 30°C for 5 days (Fig. 5.4.3.). Over-expression of Fkh2 caused wrinkly colonies to form on the solid media, which when washed away, could be seen to have invaded the agar substratum (Fig. 5.4.3.). Furthermore, dilution of the *P<sub>GAL1</sub>-FKH2-GFP* strain more than 10<sup>-2</sup> resulted in minimal growth on the agar, suggesting that *FKH2* over-expression may be a terminal phenotype. The *FKH2/FKH2-YFP* negative control strain showed partial invasive growth under the conditions tested, but this was not as severe as that of *FKH2* over-expression.

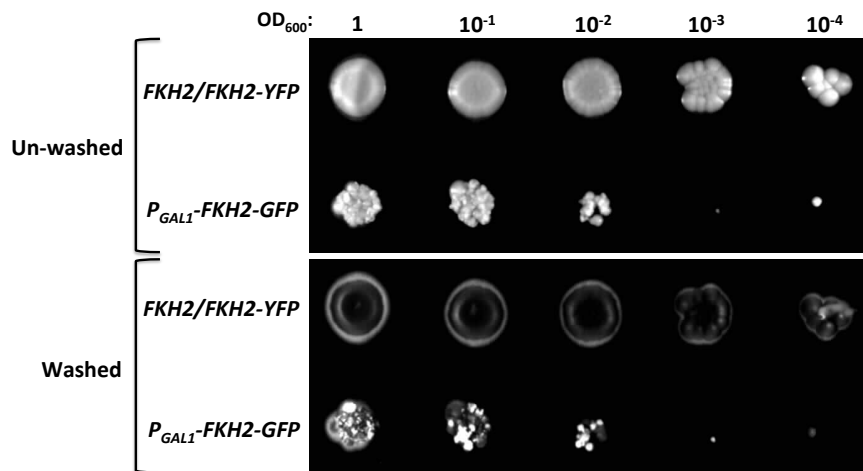


**Fig. 5.4.3. *FKH2* over-expression causes filamentation on solid media under yeast growth conditions.**  $P_{GAL1}$ -*FKH2*-GFP and *FKH2*/*FKH2*-YFP overnight cultures were diluted to an  $OD_{600}$  of 1.0 before 10 fold serial dilutions were carried out. 2 $\mu$ l of each dilution was spotted and dried onto a YEPG agar plate, and then left to grow at 30°C for 5 days. Surface colonies were imaged and then washed away with deionised water.

#### 5.4.4. *FKH2* over-expression causes a cell cycle arrest phenotype

Expression of *FKH2* was carried out in liquid YEPG ( $P_{GAL1}$  ON) and YEPD ( $P_{GAL1}$  OFF) media to gain a better understanding of the morphological consequences of *FKH2* over-expression (Fig. 5.4.4.). On over-expression of *FKH2* cells begin to form a bud, but there is a failure to switch to isotropic growth, with the bud continuing to polarise. The filaments formed are reminiscent of those formed in cells arrested at later times in the cell cycle, which fail to complete mitosis (Bachewich et al. 2005). These cells phenocopy things such as: depletion of the cyclin *CLB2* (Bensen et al. 2005), treatment of the cells with Hydroxyurea (Bachewich et al. 2005), or inhibition of the heat-shock response protein Hsp90 (Senn et al. 2012). DAPI staining shows a mildly aberrant nuclear morphology, with some elongated nuclei showing slow progression through mitosis. In YEPD media Fkh2-GFP is barely visible when expressed from the *GAL1* promoter; but provides a very strong signal in the nucleus when the strain is grown in YEPG media. This further demonstrates the over-expression of *FKH2*, and provides another marker for the nucleus.

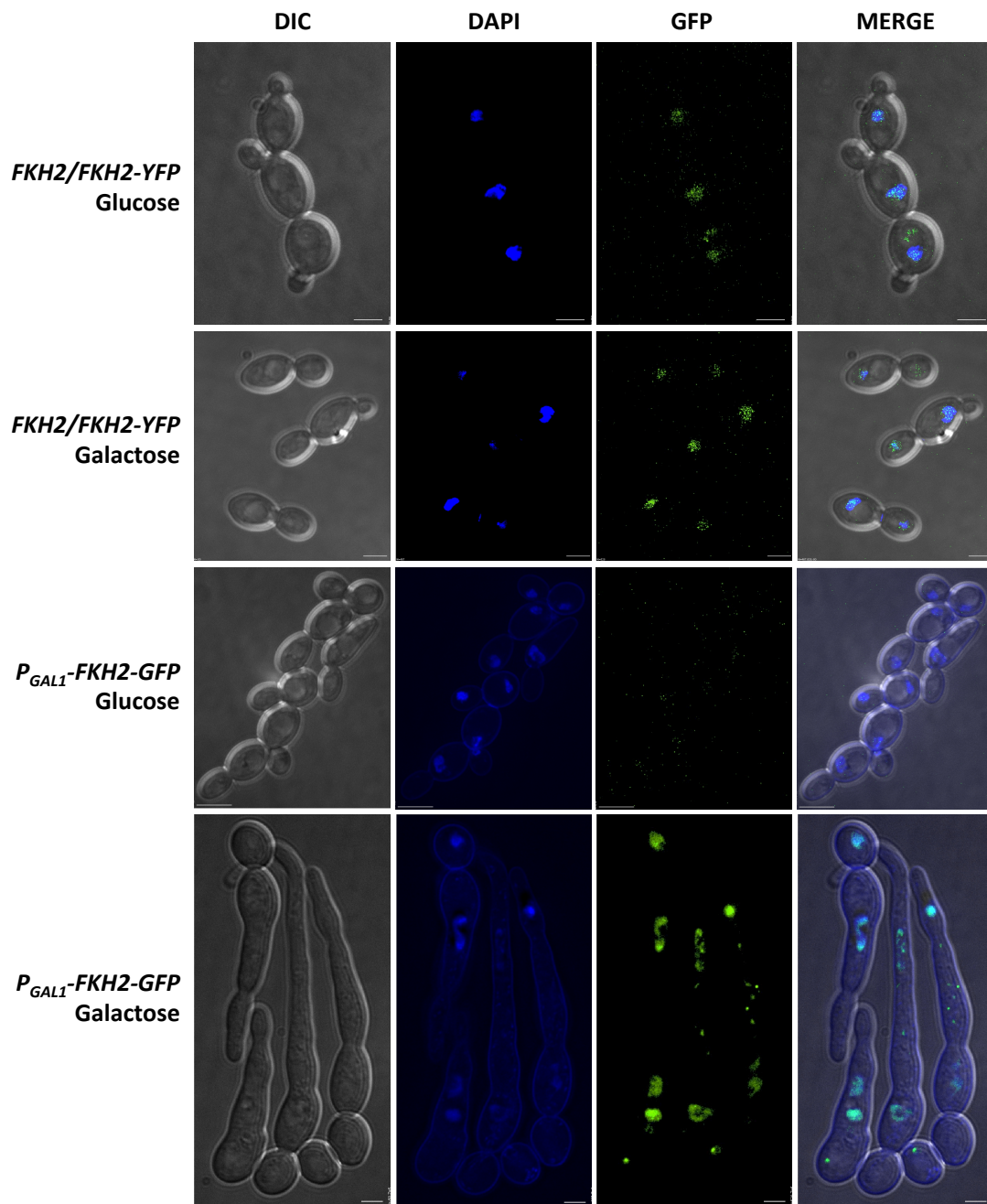


**Fig. 5.4.4. *FKH2* over-expression phenotype after re-inoculation from stationary phase into yeast growth conditions.** *FKH2*/*FKH2*-YFP and  $P_{GAL1}$ -*FKH2*-GFP strains were grown for 5 hours in glucose or galactose to repress or induce the *GAL1* promoter respectively. Microscope images were taken with an Olympus Delta Vision fluorescence microscope (Applied Precision) Scale bars in bottom right hand corners represent 5 $\mu$ m.

### 5.4.5. Microarray analysis of *FKH2* over-expression

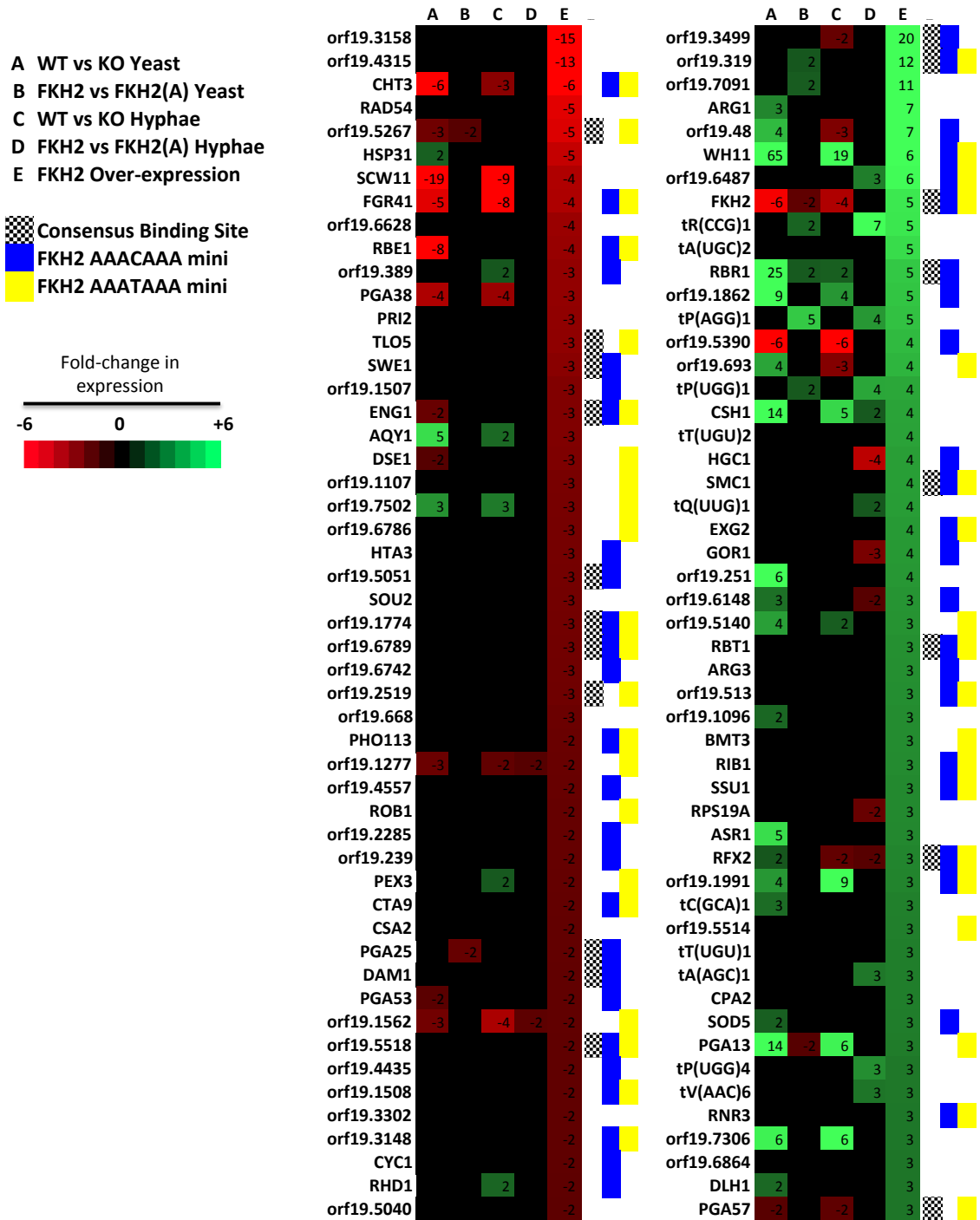


**Fig. 5.4.5. Genes down or up-regulated on over-expression of *FKH2*.** Excel spreadsheet sorted for genes with decreased/increased expression in array E. Displayed are the top 50 down or up-regulated genes on *FKH2* over-expression, with the presence or absence of a *Fkh2* binding site in the 1kb upstream of the gene.

#### 5.4.5.1. Genes down-regulated upon *FKH2* over-expression

The GO slim process terms for genes with  $\geq 2$ -fold down-regulation on *FKH2* over-expression follow a similar pattern as previously observed. The best-represented slim terms are for genes involved in: biological processes (38.7%), regulation of biological processes (25.3%), organelle organization, cell cycle regulation (21.3%), and response to stress (18.7%). This further supports a role for Fkh2 in regulation of these processes. However these may be pleiotropic effects that are due to the severe, terminal phenotype associated with *FKH2* over-expression. A number of genes involved in cytokinesis show reduced expression (Fig. 5.4.5.), providing an explanation for why the cells fail to separate. These include genes for the mitotic exit phosphatase Cdc14 and the septin associated kinase Gin4, along with genes for mother-daughter cell separation such as *ENG1*, *CHT3* and the essential *DSE1* (Fig. 5.4.5.). Deletion of *GIN4* has previously been shown to be associated with constitutive filamentation (Wightman et al. 2004), and therefore reduced expression of *GIN4* may contribute to the observed filamentation phenotype. Genes for two essential subunits of the Dam1 complex, *ASK1* and *DAM1* (Thakur & Sanyal 2011), also show reduced expression (Fig. 5.4.5.). The down-regulation of these genes provides a possible mechanism for the observed cell cycle arrest phenotype on *FKH2* over-expression. In addition to this the morphogenesis checkpoint gene *SWE1* is also down-regulated (Fig. 5.4.5.), suggesting the inability to activate this checkpoint.

#### 5.4.5.2. Genes up-regulated upon *FKH2* over-expression

*FKH2* is, as expected, up-regulated on *FKH2* over-expression, being present at five-fold the basal level (Fig. 5.4.5.). This further confirms that the over-expression strategy is working. GO slim mapping analysis follows a similar theme as observed in the other array experiments; however there is an increased amount of genes up-regulated for which the biological function is unknown (28.9%). As observed for the *fkh2(6A<sub>CDK</sub>)* strain under hyphal inducing conditions, a number of genes involved in translation (16.9%) are up-regulated, with many of these encoding tRNAs. Stress response genes show good GO term representation (12%).

These include the heat-shock genes *ASR1* and *HSP70*, the DNA damage response genes *RFX2*, *SMC1*, and *DLH1*, and the peroxide stress combating superoxide dismutase *SOD5* (Fig. 5.4.5.). This shows that the cells are undergoing a number of different stresses that they need to combat. The hyphal specific cyclin *HGC1* shows up-regulation on *FKH2* over-expression (Fig. 5.4.5.), and could be a positive regulator of the observed filamentation phenotype. Indeed – overexpression of G1 cyclins in *S. cerevisiae* leads to hyperpolarized growth (Loeb, Kerentseva, et al. 1999). Interestingly the telomere-associated genes *TLO1*, *TLO7* and *TLO9* also show increased expression (Fig. 5.4.5.).

## 5.5. Discussion

### 5.5.1. Fkh2 phosphorylation affects yeast and hyphal morphologies

In the previous chapter Fkh2 phosphorylation site mutants were made, showing that Fkh2 is phosphorylated in CDK consensus phosphorylation motifs during yeast and hyphal growth. Phenotypic observation of these mutants showed that phosphorylation of Fkh2 is a requirement for correct yeast and hyphal morphologies. Blocking phosphorylation at CDK consensus sites on Fkh2 gives yeast cells that are enlarged and show slight elongation (Fig. 5.1.1). However during hyphal growth the loss of Fkh2 phosphorylation is more profound, with cells failing to maintain filamentous invasive growth (Fig. 5.1.2-3.). Further mutants generated for CDK consensus and minimal sites, along with truncation of the phosphorylation sites, confirmed the observed filamentation defects (Fig. 5.1.5-7.). Phosphomimetic mutants of Fkh2 grew normally as yeast (Fig. 5.1.1.) and were still able to filament in liquid and on solid media (Fig. 5.1.2-3, Fig. 5.1.5-6.). Previously it was shown that *FKH2* is required for both yeast and true hyphal morphogenesis (Bensen et al. 2002). These results support this observation; although, blocking Fkh2 phosphorylation does not give as severe a phenotype as deletion of *FKH2*, suggesting that Fkh2 has phosphorylation dependent and independent functions. In the aforementioned study it was shown that Fkh2 localises to the nucleus. This distinct localisation has been confirmed (Fig. 3.2.14.), and shown not to be dependent of the phosphorylation status of Fkh2 (Fig. 5.1.4-5,

Fig. 5.1.7). These results above suggest that the early phosphorylation of Fkh2 is a requirement for the long-term maintenance of hyphal growth; however they do not indicate the mechanism by which this is achieved.

### 5.5.2. Fkh2 and transcriptional programs

Fkh2 and its homologues are known transcriptional regulators (Bensen et al. 2002; Zhu et al. 2000), suggesting that the observed mutant phenotypes may be due to transcriptional changes in these strains. Due to the limited coverage of previous *fkh2Δ/Δ* array data (Bensen et al. 2002), this was repeated using probes covering every *C. albicans* ORF (Fig. 5.2.2-3, 5.2.6, 5.2.8.). Ideally a global Chromatin Immunoprecipitation (ChIP) analysis should have been carried out together with the microarrays using the same samples; as this would provide information of whether Fkh2 can directly regulate genes showing altered levels of expression in the Fkh2 mutants. However performing ChIP with Fkh2 has proved difficult; therefore we only have the presence of a predicted Fkh2 binding site upstream of the gene as an indication of whether it is an *in vivo* regulatory target. All the genes of interest mentioned in the results section are combined in Fig. 5.5.1.

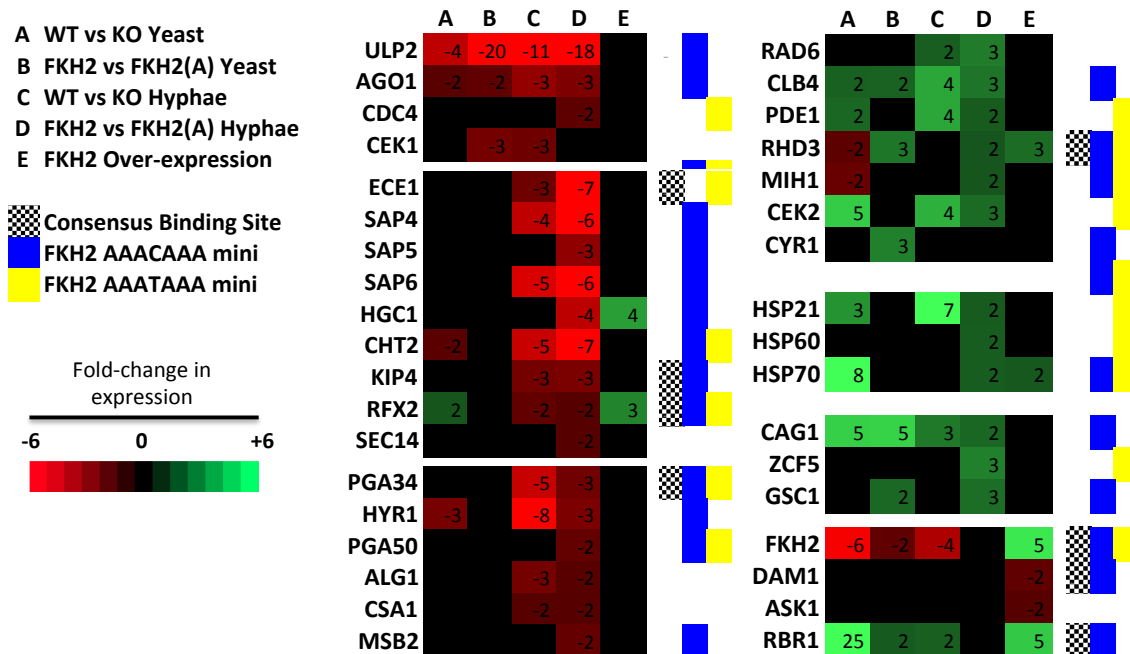


**Fig. 5.5.1. Combined genes of interest across all arrays.** Genes of interest selected from the excel spreadsheet along with their expression data across all five arrays, and information on the presence or absence of a Fkh2 DNA binding site in their 1kb upstream.

### 5.2.2.1. Fkh2 phosphorylation is required to regulate genes for filamentous invasive growth and pathogenesis.

Previously it has been shown that *FKH2* is required for the expression of the hyphal-specific genes *ECE1*, *HYR1* and *HWP1* (Bensen et al. 2002). In the above results it is shown that along with *ECE1* and *HYR1*, *FKH2* is required for the expression of the hyphal expression specific genes *SAP4*, *SAP6*, *KIP4* and *CHT2* (Fig. 5.2.2.). Further to this, these genes are also down-regulated in the absence of Fkh2 phosphorylation (Fig. 5.2.3.), and show further down-regulation than is observed in the *fkh2Δ/Δ* strain (Fig. 5.5.1.). Comparing genes down-regulated between the *fkh2Δ/Δ* and *fkh2(6A<sub>CDK</sub>)* strains shows that: genes down-regulated in *fkh2(6A<sub>CDK</sub>)*-only and in both *fkh2Δ/Δ* and *fkh2(6A<sub>CDK</sub>)* strains are primarily involved in pathogenic processes, such as host interaction and biofilm formation (Tables. 5.1-4). This indicates that loss of Fkh2 phosphorylation has a more dominant effect on the expression of invasive growth and pathogenesis related genes than *FKH2* deletion, highlighting the importance of Fkh2 phosphorylation in the *C. albicans* pathogenesis program. All of the above mentioned hyphal specific genes contain a Fkh2 minimal binding motif in their promoter, suggesting that they may be true regulatory targets of Fkh2.

The hyphal specific Cdk1 cyclin *HGC1* shows reduced expression in the *fkh2(6A<sub>CDK</sub>)* strain, but not in the *fkh2Δ/Δ* strain (Fig. 5.5.1.), suggesting that *HGC1* regulation is dependent on Fkh2 phosphorylation. This observation fits well with the early hyphal timing of Fkh2 phosphorylation (Fig. 4.2.2.), which would cause up-regulation of *HGC1* to orchestrate many processes required for hyphal development (Wang 2009). Hgc1 is known to be required for maintenance of hyphal growth (Sinha et al. 2007), and its reduced expression in *fkh2(6A<sub>CDK</sub>)* hyphae suggests a reason for the strain's inability to maintain filamentation. A problem with this hypothesis is that *HGC1* only shows half the level of wild-type expression in the *fkh2(6E<sub>CDK</sub>)* strain (Fig. 5.14B.). However Fkh2 is only phosphorylated for a short period on hyphal induction and then remains dephosphorylated. It maybe that maintaining Fkh2 in a phosphorylated state causes reduced expression of genes that are up-regulated early in hyphal growth.

It would be of interest to over-express *HGC1* in the *fkh2(6A<sub>CDK</sub>)* strain to see if this restores the ability to maintain filamentous growth.

In the qPCR experiments the results from the microarrays were confirmed (Fig. 5.2.5.), showing that the use of the *fkh2/FKH2* was acceptable for the microarrays. The results showed that *SAP4*, *KIP4* and *ECE1* transcript levels in the *fkh2(6E<sub>CDK</sub>)* strain are virtually that of their wild-type level in hyphal growth (Fig. 5.2.5B.), allowing the assumption that their regulation depends on Fkh2's phosphorylation status. However, this is not the case for *CHT2*, which shows further decreased expression in the *fkh2(6E<sub>CDK</sub>)* strain compared with the *fkh2(6A<sub>CDK</sub>)* strain (Fig. 5.2.5B.). This could be due to the correct phosphorylation of Fkh2 being required for *CHT2* expression, and Fkh2 being locked in either a phosphorylated or dephosphorylated state preventing this.

The known virulence factors *ECE1* and *SAP4-6* show decreased expression on blocking Fkh2 phosphorylation, implying that the *fkh2(6A<sub>CDK</sub>)* strain may show reduced virulence, as is the case for the *fkh2Δ/Δ* strain. Further to this, GO analysis implies that expression of genes required for pathogenesis is a phosphorylation dependent function of Fkh2 (Tables 5.1-4.). The virulence of the Fkh2 phosphorylation mutants is currently under investigation through collaboration with Dr. Julian Naglik's group at Kings College London. As the *fkh2(6A<sub>CDK</sub>)* strain does not show a reduction in adhesin gene expression, it should still be able to bind epithelial cells. Therefore this will allow observation of virulence requirements post host cell adhesion. A role for Fkh2 in pathogenesis can also be implied by the observation that *FKH2* is up-regulated in a reconstituted human oral epithelium model of infection (Zakikhany et al. 2007).

Along with the down-regulated genes in the *fkh2(6A<sub>CDK</sub>)* strain that are required for filamentous growth, there is also increased expression of negative regulators of filamentation (Fig. 5.5.1.): *CLB4*, *RAD6* and *PDE1* (Bensen et al. 2005; Leng et al. 2000; Wilson et al. 2010). This further explains the inability of the *fkh2(6A<sub>CDK</sub>)* strain to maintain filamentous growth. And suggests that one possible role of Fkh2 during hyphal growth is to repress negative regulators of filamentation.

### 5.5.2.2. Other roles of Fkh2 in the regulation of transcriptional programs

Deletion of *FKH2* causes drastic transcriptional changes, with 443 genes in yeast and 488 genes in hyphal growth showing a greater than two-fold change in expression (Fig. 5.2.9.). Such changes can account for the severe phenotype observed in the *fkh2Δ/Δ* strain; however some changes may be pleiotropic in response to the deleterious phenotype of *fkh2Δ/Δ*, such as the common up-regulation of stress response genes (See GO spreadsheets). Deletion of *FKH2* has a greater positive effect on gene transcription during yeast growth, but a more negative effect during hyphal growth (Fig. 5.2.9.). This implies that Fkh2 may act primarily as a repressor during yeast growth, and as a transcriptional activator during hyphal growth. Very few cell cycle regulated transcripts show changes in expression in the arrays A-D; likely due to the experimental design. Zhu et al. found in *S. cerevisiae* that differential regulation of the *CLB2* cluster was only observed in synchronous *fkh1Δ/fkh2Δ* cells, and not in asynchronous cultures (Zhu et al. 2000). Such an experiment was not possible with *C. albicans fkh2Δ/Δ* cells, as the constitutively pseudohyphal phenotype meant that elutriation was not possible, and no means of chemical synchronisation exists for white phase *C. albicans* cells. Such an experiment may however be possible using a heterozygous *FKH2* strain under the control of a regulatable promoter. The experiments were therefore carried out using the same design as for Bensen et al., allowing comparison of the results between the two studies.

Throughout the *fkh2Δ/Δ* and *fkh2(6ACDK)* arrays there are emerging patterns. Stress response genes show altered regulation in absence of *FKH2* and when Fkh2 phosphorylation is blocked. Genes for heat, reactive oxygen and genotoxic stress show a general up-regulation in both yeast and hyphae (See GO spreadsheets). This suggests that Fkh2 may have a role in the negative regulation, or possible fine-tuning of stress responses. This could be tested further by looking at responses of the Fkh2 mutant to: further elevated temperatures above 37°C, exposure to hydrogen peroxide, and exposure to DNA damaging agents such as Methyl methanesulfonate.

Components of the mating response MAPK pathway and the cAMP-PKA pathway show altered regulation in the Fkh2 mutants. *RAS1*, an upstream

component of both the MAPK and PKA pathways, is down-regulated in *fkh2Δ/Δ* hyphae (Fig. 5.5.1.). This provides a good explanation for the inability of *fkh2Δ/Δ* cells to properly respond to hyphal inducing signals. The cAMP phosphodiesterase *PDE1* shows increased expression under all conditions except *fkh2(6A<sub>CDK</sub>)* yeast growth (Fig. 5.5.1.); under which the adenylyl cyclase *CYR1* is up-regulated (Fig. 5.5.1.). This suggests that Fkh2 can regulate cellular cAMP levels, but that in yeast this regulation is independent of Fkh2's phosphorylation status.

The MAPKs Cek1 and Cek2 appeared to be differentially regulated by Fkh2; with *CEK1* being down-regulated in *fkh2Δ/Δ* hyphae and *fkh2(6A<sub>CDK</sub>)* yeast cells, whereas *CEK2* is up-regulated under all conditions except *fkh2(6A<sub>CDK</sub>)* yeast growth and *FKH2* over-expression (Fig. 5.5.1.). It is interesting that these kinases, that are thought to be partially redundant (Chen et al. 2002), may be differentially regulated. The cell wall sensor for the MAPK pathway, *MSB2*, shows decreased expression in *fkh2(6A<sub>CDK</sub>)* hyphae (Fig. 5.5.1.), implying that Fkh2 phosphorylation is required for its expression. This presents an interesting idea for a model in which the Cek1 MAPK could phosphorylate Fkh2, activating it for increased expression of the *MSB2* sensor to allow further activation of the MAPK pathway in a positive feedback loop. Evidence for this comes from the stabilization of Fkh2 and prominent phosphorylation in a *hog1Δ/Δ* strain. Hog1 is thought to negatively regulate Cek1 (Eisman et al. 2006); and therefore loss of Hog1 repression would result in a highly active Cek1 that could phosphorylate and stabilise Fkh2. Also secreted aspartyl proteases, which we have shown to be regulated by Fkh2 (Fig. 5.5.1.), are required for Msb2 cleavage to activate Cek1 MAPK signaling (Puri et al. 2012); thus providing another possible level of positive feedback. Therefore it would be of interest to test whether Cek1 is responsible for Fkh2 phosphorylation *in vivo*.

### 5.5.3. Novel Interacting Partners of Fkh2

Currently no interaction data is available for *CaFkh2*, therefore possible interactors can only be inferred from what is known in *S. cerevisiae*. However, due to the proposed cell cycle independent role of Fkh2 in hyphal growth, it is likely that different interactions would be involved. This was shown to be true, as early

in hyphal growth Fkh2 was found to be complexed with the chromatin modifier Pob3 (Fig. 5.3.1.), which is known to be involved in transcription and DNA replication (Schlesinger & Formosa 2000), and deletion of which is known to affect filamentous growth (Uhl et al. 2003). The observation that Fkh2 interacts with a chromatin modifier early on hyphal induction suggests that transcriptional changes dependent on Fkh2 may occur via an epigenetic mechanism. This correlates well with previous report that proposes an early window of epigenetic changes on hyphal induction, which are required for long term maintenance of hyphal growth (Lu et al. 2011). Due to the early hyphal phosphorylation of Fkh2 occurring within this window, it can be speculated that Fkh2 is phosphorylated in order to interact with Pob3, epigenetically activating genes that are required to maintain filamentation. This is indeed the case, as the interaction only appears to be maintained when Fkh2 is in a phosphorylated state (Fig. 5.3.2.).

#### **5.5.4. *FKH2* over-expression causes cell cycle arrest filamentation**

Expression of *FKH2* under the *GAL1* promoter gives a five-fold increase in *FKH2* levels (Fig. 5.4.5. 5.5.1.), causing cells to filament under yeast growth conditions on solid and in liquid media (Fig. 5.4.1. 5.4.3-4.). These filaments resemble those formed on cell cycle arrest (Bachewich et al. 2005). A number of genes required for cell cycle progression and cytokinesis are down-regulated in this strain (Fig. 5.4.5), possibly as a cause or effect of the observed phenotype. Two essential genes that are down-regulated are for the Dam1 and Ask1 components of the Dam1 complex (Fig. 5.4.5.), required for spindle attachment to kinetochores (Thakur & Sanyal 2011). Failure of this event to happen would likely activate the spindle checkpoint, leading to the observed cell cycle arrest filamentation (Berman 2006). To confirm whether Fkh2 regulates these genes directly ChIP experiments could be carried out. Previous microarray analysis of chemical and *CDC5* depletion cell cycle arrest did not show *DAM1* and *ASK1* to be down-regulated (Bachewich et al. 2005), suggesting that their reduced expression is Fkh2 dependent.

The hyphal specific cyclin *HGC1* is up-regulated on *FKH2* over-expression (Fig. 5.4.5.), but has also previously been shown to be up-regulated on cell cycle arrest. Interestingly - cell cycle arrest causes a 1.2 fold increase in *HGC1* expression

(Bachewich et al. 2005), whereas on *FKH2* over-expression *HGC1* is up-regulated four-fold. This suggest that the increase in *HGC1* is due to a higher level of Fkh2, and not due to the associated cell cycle arrest phenotype; providing support for the idea that *HGC1* is a direct regulatory target of Fkh2.

#### **5.5.5. Conclusion**

Taken together these results show that Fkh2 has a phosphorylation dependent function during hyphal growth, regulating the expression of genes for invasive growth and pathogenesis. Absence of Fkh2 phosphorylation results in decreased invasive growth, suggesting that the phosphorylation will be an important requirement for virulence. This appears to mechanistically through a phosphorylation dependent interaction with the chromatin modifier Pob3. Finally – over-expression of *FKH2* results in constitutively filamentous growth, likely as a result of cell cycle perturbation.

This study initially sought to identify regulatory targets of Cdk1 that are differentially phosphorylated between yeast and hyphal growth. Of the four proteins investigated (Orf19.3469, Orf19.1948, Sfl1 and Fkh2), only the transcription factor Fkh2 showed a different pattern of phosphorylation timing during yeast and hyphal growth. During yeast growth Fkh2 expression and phosphorylation is regulated in concert with cell cycle progression; whereas during hyphal growth, phosphorylation and de-phosphorylation occurs before the beginning of the cell cycle. Fkh2 and its homologues are involved in cell cycle progression, being themselves regulated in a cell cycle dependent manner (Bensen et al. 2002; Zhu et al. 2000; Shimada et al. 2008). The loss of cell cycle dependent regulation of Fkh2 during hyphal growth suggested a specialised function in this morphology. Further analysis of this phosphorylation showed that Fkh2 is phosphorylated at CDK consensus sites on hyphal induction. However, unexpectedly, the phosphorylation is not dependent on the CDKs Cdk1 or Pho85, although there may be redundancy between these two kinases. Other kinase mutants were tested that can phosphorylate CDK consensus motifs (*hog1*, *ssn3*, *tpk1* and *crk1*) and are important for hyphal growth, but again the absence of these kinases did not affect the phosphorylation status of Fkh2.

Although the kinase responsible for phosphorylating Fkh2 remains elusive, the role of Fkh2 phosphorylation was examined using phospho-site mutants. Blocking Fkh2 phosphorylation causes minor morphological defects during yeast and hyphal growth in liquid media, which are not as severe as those previously observed on *FKH2* deletion. However, blocking the phosphorylation of Fkh2 has a strong negative effect on filamentous invasive growth on solid media, as observed by the inability to invade the agar substratum. The reduced invasive capacity of the *fkh2(6<sub>CDK</sub>)* strain implies that phosphorylation of Fkh2 may be important for virulence. This is currently under investigation by our collaborators in London, whose initial results appear to support the above hypothesis.

In order to understand how blocking Fkh2 phosphorylation lead to the observed loss of invasive capacity, global transcriptional analysis was carried out

in the Fkh2 phosphorylation blocked mutant. In addition to this more comprehensive transcriptional data was generated for the *FKH2* deletion strain, along with data on over-expressing *FKH2* to investigate the hyper-filamentous phenotype. The transcriptional analysis showed that blocking Fkh2 phosphorylation causes altered expression of a different set of genes than deletion of *FKH2*. Thus the phosphorylation of Fkh2 serves to alter and not simply impair its function. The most notable transcriptional changes in the microarray experiments were observed during hyphal growth, with deletion of *FKH2* or blocking Fkh2 phosphorylation having a more negative impact on hyphal rather than yeast transcription. A simple explanation for this is that during yeast growth the presence and phosphorylation of Fkh2 may serve a primarily repressive function. However, although fewer than down-regulated, there are many genes that show up-regulation on deletion of Fkh2 or blocking Fkh2 phosphorylation. This would imply that Fkh2 acts as both an activator and repressor of gene expression. As this dual activational-repressive ability is not dependent on phosphorylation it would be of interest to investigate how it is achieved, possibly due to the different sequences in Fkh2 DNA binding sites, the location of the site in the upstream sequence of the gene, or through interactions with other transcription factors.

The key observation from the microarray experiments is that: expression of genes required for host-interaction, biofilm formation and pathogenesis are specifically down-regulated on blocking Fkh2 phosphorylation compared with *FKH2* deletion. For the pathogenesis related genes that are also down-regulated on *FKH2* deletion, the decrease in expression is not as severe as for blocking Fkh2 phosphorylation, suggesting pathogenesis gene regulation is a phosphorylation dependent function of Fkh2. Fkh2 phosphorylation was also shown to repress known negative regulators of filamentous invasive growth. Therefore the early hyphal phosphorylation of Fkh2 is an unexpected but necessary event for the positive regulation of the virulence program in *C. albicans*.

The mechanism by which Fkh2 affects transcription of genes required for pathogenesis appears to be via interaction of Fkh2 with the chromatin modifier Pob3 early on hyphal induction, suggesting epigenetic regulation of the aforementioned genes may be occurring. Epigenetic regulation of invasive growth

and pathogenesis genes on hyphal induction by Fkh2 would complement previous data; which suggests that the promoters of certain 'hyphal-specific' genes occupied by Nrg1 are re-modeled on hyphal induction, and that this is a requirement for the long term maintenance of filamentous growth (Lu et al. 2011). This study by Lu et al. proposes an early 'window of opportunity' on hyphal induction where such epigenetic changes occur. The timing of the window appears to fit well with the observed phosphorylation pattern of Fkh2 during hyphal growth, and would explain why the phosphorylation is observed as a singular event. It was shown that Fkh2's interaction with Pob3 is phosphorylation dependent; suggesting that epigenetic regulation may be occurring due phosphorylation of Fkh2 bringing Pob3 to the required promoters. The presence of Fkh2 and Pob3 on the promoters of the specific genes could be tested by chromatin IP with the Fkh2 phosphorylation mutants, and by looking at the histone occupancy of the pathogenesis related genes regulated by Fkh2.

A key problem during this project has been defining the kinase responsible for phosphorylating Fkh2, with it no longer being possible to make assumptions of the kinase involved. To this end a different approach has been taken to attempt to find the elusive kinase. This involves screening the kinase mutant library produced by Blankenship et al (Blankenship et al. 2010) based on the ability of the kinase mutant to invade the agar substratum on solid media with serum. As blocking Fkh2 phosphorylation results in reduced invasive growth, it can be speculated that the kinase responsible for the phosphorylation would have a similar phenotype. This screen showed that mutants of components of the pheromone response MAPK pathway, the PAK *cla4* and MAPKK *hst7*, have reduced invasive capacity similar to that observed for the *fkh2(6ACDK)* and *fkh2(15ACDK)* strains (See included CD). Another mutant that shows decreased invasion of the agar substratum is *sok1*. Sok1 is not a protein kinase, but over-expression has been shown to rescue PKA pathway defects in *S. cerevisiae* (Ward & Garrett 1994), suggesting a role in regulating this pathway. The final MAPK in the pheromone response pathway, Cek1, provides a good starting point for future attempts to elucidate the kinase responsible for Fkh2 phosphorylation; unfortunately however this strain is not available in above mentioned kinase mutant library. *CEK1* deletion has previously

been shown to reduce filamentous invasive growth on solid media, supporting the above hypothesis. Further to this, anecdotal evidence for the role of Cek1 is also present. Cek1 is regulated by the quorum sensing molecule farnesol (Román, Alonso-Monge, et al. 2009); and it is only when Fkh2-YFP expressing cells are washed in water before re-inoculation that the early hyphal phosphorylation of Fkh2 is clear. Washing away the farnesol from the over-night culture would mean that repression of Cek1 would be relieved quicker, allowing the observed spike of Fkh2 phosphorylation. Other evidence comes from the microarray experiments where, as previously mentioned, the *MSB2* sensor upstream of the MAPK pathway shows reduced expression in *fkh2(6A<sub>CDK</sub>)* strain. This suggests that a positive feedback loop could be present that would enforce the signal through the MAPK pathway. Therefore future experiments to elucidate the kinase should begin by looking at Cek1.

In addition to the kinase responsible for Fkh2 phosphorylation, the de-phosphorylation of Fkh2 remains uninvestigated. The late cell cycle timing of Fkh2 de-phosphorylation during yeast growth suggests that Cdc14 may be responsible; however this would unlikely be the case during hyphal growth, with Fkh2 being dephosphorylated before Cdc14 is known to be expressed (Clemente-Blanco et al. 2006). It would therefore be of interest to further investigate the phosphatase(s) responsible for the de-phosphorylation of Fkh2.

In conclusion, we have shown in this study that Fkh2 switches from cell cycle dependent phospho-regulation during yeast growth, to a specific early phospho-regulatory event during hyphal growth, which is independent of the cell cycle. The early hyphal phosphorylation is a necessary event for the maintenance of filamentous invasive growth, being required for positive regulation of genes involved in invasive growth and pathogenesis. Therefore we can propose a new mechanism, by which *C. albicans* specifically modifies a key component of its cell cycle transcription machinery in the switch from commensalism to pathogenicity.

# Figure List

---

## Chapter 1

1.1. Comparison of mating programs between <i>S. cerevisiae</i> and <i>C. albicans</i> .....	2
1.2. <i>C. albicans</i> morphological forms.....	4
1.3. Differences in growth and cell cycle organisation between the three main morphological forms of <i>C. albicans</i> .....	5
1.4. The MAPK and cAMP-PKA morphogenesis pathways in <i>C. albicans</i> .....	8
1.5. Cell cycle arrest filamentation in <i>C. albicans</i> .....	12
1.6. Roles of Cdc42 in <i>S. cerevisiae</i> morphogenesis.....	14
1.7. Polarised secretion in <i>S. cerevisiae</i> .....	16
1.8. Polarised growth in <i>C. albicans</i> hyphae.....	17
1.9. Regulation of cell separation in yeast and hyphal cells.....	19
1.10. Roles of ubiquitination and sumoylation in <i>C. albicans</i> .....	22

## Chapter 3

3.1.1. Roles of Cdk1 during bud morphogenesis in <i>S. cerevisiae</i> .....	64
3.1.2. Inhibition of Cdk1 during hyphal growth in <i>C. albicans</i> .....	65
3.1.3. Roles of Cdk1-Hgc1/Ccn1 in <i>C. albicans</i> hyphal growth.....	67
3.2.1 Domain structure of Orf19.3469, including potential CDK phosphorylation sites.....	69
3.2.2. Schematic of C-terminal PCR cassette epitope tagging.....	70
3.2.3. C-terminal epitope tagging of Orf19.3469.....	71
3.2.4. Orf19.3469 phosphorylation during yeast and hyphal growth.....	72
3.2.5. Domain structure of Orf19.1948 including potential CDK phosphorylation sites.....	73
3.2.6. Phosphorylation of Orf19.1948 during yeast and hyphal growth.....	74
3.2.7. Orf19.1948-GFP localisation during yeast and hyphal growth.....	75
3.2.8. <i>sfl1Δ/Δ</i> constitutive filamentation phenotype.....	76
3.2.9. Domain structure of <i>C. albicans</i> Sfl1, including potential CDK phosphorylation sites.....	76
3.2.10. Sfl1 phosphorylation during yeast and hyphal growth.....	77
3.2.11. Sfl1-YFP localisation during yeast and hyphal growth.....	78
3.2.12. <i>fkh2Δ/Δ</i> yeast and hyphal phenotypes.....	79
3.2.13. Domain structure of <i>C. albicans</i> Fkh2 including potential CDK phosphorylation sites.....	79
3.2.14. Fkh2 phosphorylation during yeast and hyphal growth.....	80
3.2.15. Fkh2-GFP localisation during yeast and hyphal growth.....	81

## Chapter 4

4.1.1. Fork-head transcription factor deletion phenotypes in <i>S. cerevisiae</i> .....	87
4.1.2. Schematic of Mcm1-Fkh2-Ndd1 complex formation at <i>CLB2</i> cluster promoters.....	88
4.1.3. Schematic comparing <i>CaFkh2</i> homology with <i>ScFkh1</i> and <i>ScFkh2</i> .....	90
4.1.4. Transcriptional effects of knocking out <i>FKH2</i> in <i>C. albicans</i> .....	90
4.2.1. Fkh2 undergoes cell cycle-dependent phosphorylation during synchronous yeast growth.....	92
4.2.2. Fkh2 is phosphorylated early after hyphal induction, independent of cell cycle stage. ....	93
4.2.3. Investigating Fkh2 early hyphal phosphorylation by mass-spectrometry phospho-peptide mapping.....	95
4.2.4. Investigating Fkh2 phosphorylation with phospho-specific antibodies.....	96
4.2.5. Construction of a <i>fkh2Δ/Δ</i> strain.....	98
4.2.6. Construction of a <i>FKH2-GFP</i> vector for phosphorylation site mutagenesis.....	100
4.2.7. Mutational analysis of Fkh2 phosphorylation.....	101
4.2.8. Comparison of Fkh2 phospho-mutants.....	103
4.2.9. Truncation of Fkh2 affects its phosphorylation status.....	104
4.2.10. Purification of GST-Fkh2(CT) from <i>E. coli</i> .....	105
4.2.11. Cdk1 can phosphorylate the C-terminus of Fkh2 <i>in vitro</i> .....	106
4.2.12. Inhibiting Cdk1 does not affect Fkh2 phosphorylation.....	107
4.2.13. Investigating Fkh2 phosphorylation in Cdk1 cyclin knockouts/shutdown strains.....	108
4.2.14. Examining if Fkh2 and Cdk1 physically interact.....	109
4.2.15. Investigating if other kinases phosphorylate Fkh2.....	110
4.2.16. Fkh2 Phosphorylation is not affected by repression/over-expression of <i>PHO85</i> .....	113

## Chapter 5

5.1.1. Phenotypes of Fkh2 phospho-mutants during yeast growth.....	119
5.1.2. Phenotypes of Fkh2 phospho-mutants in liquid hyphal culture.....	120
5.1.3. Invasive ability of Fkh2 phospho-mutants on solid media.....	121
5.1.4. Localisation of Fkh2 CDK consensus site mutants during yeast and hyphal growth.....	122
5.1.5. Phenotypes and localisation of Fkh2 CDK consensus and minimal site mutants during yeast and hyphal growth.....	123
5.1.6. Invasive ability of other Fkh2 phosphorylation mutants on solid media.....	124
5.1.7. Phenotypes and localisation of other Fkh2 phosphorylation mutants during yeast and hyphal growth.....	124

5.2.1. Determination of RNA quality from Fkh2 mutant strains before microarrays.....	128
5.2.2. Genes down or up-regulated in the absence of <i>FKH2</i> during hyphal growth.....	129
5.2.3. Genes down or up-regulated on blocking Fkh2 phosphorylation during hyphal growth.....	130
5.2.4. Venn diagrams comparing genes with altered expression during hyphal growth in the <i>fkh2Δ/Δ</i> and <i>fkh2(6A<sub>CDK</sub>)</i> strains. ....	131
5.2.5. qPCR confirmation of genes with altered expression in the Fkh2 phosphorylation mutants.....	136-137
5.2.6. Genes down or up-regulated in the absence of <i>FKH2</i> during yeast growth.....	139
5.2.7. Venn diagrams comparing genes with altered expression during yeast growth in the <i>fkh2Δ/Δ</i> and <i>fkh2(6A<sub>CDK</sub>)</i> strains.....	141
5.2.8. Genes down or up-regulated on blocking Fkh2 phosphorylation during yeast growth.....	143
5.2.9. Venn diagrams comparing genes with altered expression in the <i>fkh2Δ/Δ</i> strain during yeast and hyphal growth.....	144
5.2.10. Venn Diagrams comparing genes with altered expression in the <i>fkh2(6A<sub>CDK</sub>)</i> strain during yeast and hyphal growth.....	147
5.3.1. Novel interacting partners of Fkh2 early in hyphal growth.....	150
5.3.2. Investigating the effect of Fkh2 phosphorylation on its interaction with Pob3.....	152
5.4.1. <i>FKH2</i> overnight over-expression phenotype.....	153
5.4.2. Confirmation of Fkh2 over-expression.....	154
5.4.3. <i>FKH2</i> over-expression causes filamentation on solid media under yeast growth conditions.....	155
5.4.4. <i>FKH2</i> over-expression phenotype after re-inoculation from stationary phase into yeast growth conditions.....	156
5.4.5. Genes down or up-regulated on over-expression of <i>FKH2</i> .....	157
5.5.1. Combined genes of interest across all arrays.....	160

# Table List

---

## Chapter 2

<i>C. albicans</i> strains used in this study.....	46
<i>E. coli</i> strains used in this study.....	48
Vectors used in this study.....	49
Primers used in this study.....	52
Antibodies used in this study.....	59

## Chapter 5

Comparison of GO slim process terms associated with virulence for genes down-regulated during hyphal growth in the <i>fkh2Δ/Δ</i> -only, <i>fkh2(6A<sub>CDK</sub>)</i> -only and in both strains.....	133
Genes down regulated in <i>fkh2(6A<sub>CDK</sub>)</i> -only set during hyphal growth.....	133
Gene that shown down-regulation in both the <i>fkh2Δ/Δ</i> and <i>fkh2(6A<sub>CDK</sub>)</i> strains during hyphal growth.....	133
Genes that are only down-regulated in the <i>fkh2Δ/Δ</i> -only set during hyphal growth.....	134

## References

---

- Adams, A.E. et al., 1990. CDC42 and CDC43, two additional genes involved in budding and the establishment of cell polarity in the yeast *Saccharomyces cerevisiae*. *The Journal of cell biology*, 111(1), pp.131–42.
- Alani, E., Cao, L. & Kleckner, N., 1987. A Method for Gene Disruption That Allows Repeated Use of. , 1(Miller 1972), pp.0–4.
- Almeida, R.S., Wilson, D. & Hube, B., 2009. *Candida albicans* iron acquisition within the host. *FEMS yeast research*, 9(7), pp.1000–12.
- Amon, a et al., 1993. Mechanisms that help the yeast cell cycle clock tick: G2 cyclins transcriptionally activate G2 cyclins and repress G1 cyclins. *Cell*, 74(6), pp.993–1007.
- Atir-Lande, A., Gildor, T. & Kornitzer, D., 2005. Role for the SCFCDC4 ubiquitin ligase in *Candida albicans* morphogenesis. *Molecular biology of the cell*, 16(6), pp.2772–85.
- Bachewich, C., Nantel, A. & Whiteway, M., 2005. Cell cycle arrest during S or M phase generates polarized growth via distinct signals in *Candida albicans*. *Molecular microbiology*, 57(4), pp.942–59.
- Bahn, Y.-S., Staab, J. & Sundstrom, P., 2003. Increased high-affinity phosphodiesterase PDE2 gene expression in germ tubes counteracts CAP1-dependent synthesis of cyclic AMP, limits hypha production and promotes virulence of *Candida albicans*. *Molecular microbiology*, 50(2), pp.391–409.
- Bai, C. et al., 2002. Spindle assembly checkpoint component CaMad2p is indispensable for *Candida albicans* survival and virulence in mice. *Molecular microbiology*, 45(1), pp.31–44.
- Bartnicki-Garcia, S., Hergert, F. & Gierz, G., 1989. Computer simulation of fungal morphogenesis and the mathematical basis for hyphal (tip) growth. *Protoplasma*, 153(1-2), pp.46–57.
- Barton, R. & Gull, K., 1988. Variation in cytoplasmic microtubule organization and spindle length between the two forms of the dimorphic fungus *Candida albicans*. *Journal of cell science*, 91 ( Pt 2), pp.211–20.
- Barwell, K.J. et al., 2005. Relationship of DFG16 to the Rim101p pH response pathway in *Saccharomyces cerevisiae* and *Candida albicans*. *Eukaryotic cell*, 4(5), pp.890–9.

- Bassilana, M., Blyth, J. & Arkowitz, R.A., 2003. Cdc24, the GDP-GTP exchange factor for Cdc42, is required for invasive hyphal growth of *Candida albicans*. *Eukaryotic cell*, 2(1), pp.9–18.
- Bauer, J. & Wendland, J., 2007. *Candida albicans* Sfl1 suppresses flocculation and filamentation. *Eukaryotic cell*, 6(10), pp.1736–44.
- Bender, a, 1993. Genetic evidence for the roles of the bud-site-selection genes BUD5 and BUD2 in control of the Rsr1p (Bud1p) GTPase in yeast. *Proceedings of the National Academy of Sciences of the United States of America*, 90(21), pp.9926–9.
- Bender, a & Pringle, J.R., 1989. Multicopy suppression of the cdc24 budding defect in yeast by CDC42 and three newly identified genes including the ras-related gene RSR1. *Proceedings of the National Academy of Sciences of the United States of America*, 86(24), pp.9976–80.
- Bensen, E.S. et al., 2005. The Mitotic Cyclins Clb2p and Clb4p Affect Morphogenesis in *Candida albicans*. , 16(July), pp.3387–3400.
- Bensen, E.S., Filler, S.G. & Berman, J., 2002. A forkhead transcription factor is important for true hyphal as well as yeast morphogenesis in *Candida albicans*. *Eukaryotic cell*, 1(5), pp.787–98.
- Berman, J., 2006. Morphogenesis and cell cycle progression in *Candida albicans*. *Current opinion in microbiology*, 9(6), pp.595–601.
- Berman, J. & Sudbery, P.E., 2002. *Candida Albicans*: a molecular revolution built on lessons from budding yeast. *Nature reviews. Genetics*, 3(12), pp.918–30.
- De Bernardis, F. et al., 1998. The pH of the host niche controls gene expression in and virulence of *Candida albicans*. *Infection and immunity*, 66(7), pp.3317–25.
- Bi, E. & Park, H.-O., 2012. Cell polarization and cytokinesis in budding yeast. *Genetics*, 191(2), pp.347–87.
- Bishop, A. et al., 2010. Hyphal growth in *Candida albicans* requires the phosphorylation of Sec2 by the Cdc28-Ccn1/Hgc1 kinase. *The EMBO journal*, 29(17), pp.2930–42.
- Biswas, K. & Morschhäuser, J., 2005. The Mep2p ammonium permease controls nitrogen starvation-induced filamentous growth in *Candida albicans*. *Molecular microbiology*, 56(3), pp.649–69.
- Blankenship, J.R. et al., 2010. An extensive circuitry for cell wall regulation in *Candida albicans*. *PLoS pathogens*, 6(2), p.e1000752.

- Bockmühl, D.P. et al., 2001. Distinct and redundant roles of the two protein kinase A isoforms Tpk1p and Tpk2p in morphogenesis and growth of *Candida albicans*. *Molecular microbiology*, 42(5), pp.1243–57.
- Bockmühl, D.P. & Ernst, J.F., 2001. A potential phosphorylation site for an A-type kinase in the Efg1 regulator protein contributes to hyphal morphogenesis of *Candida albicans*. *Genetics*, 157(4), pp.1523–30.
- Booher, R.N., Deshaies, R.J. & Kirschner, M.W., 1993. Properties of *Saccharomyces cerevisiae* wee1 and its differential regulation of p34CDC28 in response to G1 and G2 cyclins. *The EMBO journal*, 12(9), pp.3417–26.
- Boros, J. et al., 2003. Molecular determinants of the cell-cycle regulated Mcm1p-Fkh2p transcription factor complex. *Nucleic acids research*, 31(9), pp.2279–88.
- Braun, B.R. et al., 2000. Identification and characterization of TUP1-regulated genes in *Candida albicans*. *Genetics*, 156(1), pp.31–44.
- Braun, B.R. & Johnson, A.D., 1997. Control of filament formation in *Candida albicans* by the transcriptional repressor TUP1. *Science (New York, N.Y.)*, 277(5322), pp.105–9.
- Braun, B.R., Kadosh, D. & Johnson, a D., 2001. NRG1, a repressor of filamentous growth in *C.albicans*, is down-regulated during filament induction. *The EMBO journal*, 20(17), pp.4753–61.
- De Bruin, R. a M., Kalashnikova, T.I. & Wittenberg, C., 2008. Stb1 collaborates with other regulators to modulate the G1-specific transcriptional circuit. *Molecular and cellular biology*, 28(22), pp.6919–28.
- Buck, V. et al., 2004. Fkh2p and Sep1p regulate mitotic gene transcription in fission yeast. *Journal of cell science*, 117(Pt 23), pp.5623–32.
- Calderon, J. et al., 2010. PHR1, a pH-regulated gene of *Candida albicans* encoding a glucan-remodelling enzyme, is required for adhesion and invasion. *Microbiology (Reading, England)*, 156(Pt 8), pp.2484–94.
- Cao, F. et al., 2006. The Flo8 transcription factor is essential for hyphal development and virulence in *Candida albicans*. *Molecular biology of the cell*, 17(1), pp.295–307.
- Care, R.S. et al., 1999. The MET3 promoter: a new tool for *Candida albicans* molecular genetics. *Molecular microbiology*, 34(4), pp.792–8.
- Carlisle, P.L. et al., 2009. Expression levels of a filament-specific transcriptional regulator are sufficient to determine *Candida albicans* morphology and virulence. *Proceedings of the National Academy of Sciences of the United States of America*, 106(2), pp.599–604.

- Carlisle, P.L. & Kadosh, D., 2013. A genome-wide transcriptional analysis of morphology determination in *Candida albicans*. *Molecular biology of the cell*, 24(3), pp.246–60.
- Carlisle, P.L. & Kadosh, D., 2010. *Candida albicans* Ume6, a filament-specific transcriptional regulator, directs hyphal growth via a pathway involving Hgc1 cyclin-related protein. *Eukaryotic cell*, 9(9), pp.1320–8.
- Chang, F. & Herskowitz, I., 1990. Identification of a gene necessary for cell cycle arrest by a negative growth factor of yeast: FAR1 is an inhibitor of a G1 cyclin, CLN2. *Cell*, 63(5), pp.999–1011.
- Chapa, B., Bates, S. & Sudbery, P., 2005. The G 1 Cyclin Cln3 Regulates Morphogenesis in *Candida albicans*. , 4(1), pp.90–94.
- Chauvel, M. et al., 2012. A versatile overexpression strategy in the pathogenic yeast *Candida albicans*: identification of regulators of morphogenesis and fitness. *PLoS one*, 7(9), p.e45912.
- Chen, C. & Noble, S.M., 2012. Post-transcriptional regulation of the Sef1 transcription factor controls the virulence of *Candida albicans* in its mammalian host. *PLoS pathogens*, 8(11), p.e1002956.
- Chen, J. et al., 2002. A conserved mitogen-activated protein kinase pathway is required for mating in *Candida albicans*. *Molecular microbiology*, 46(5), pp.1335–44.
- Chen, J. et al., 2000. Crk1, a novel Cdc2-related protein kinase, is required for hyphal development and virulence in *Candida albicans*. *Molecular and cellular biology*, 20(23), pp.8696–708.
- Chi, A. et al., 2007. Analysis of phosphorylation sites on proteins from *Saccharomyces cerevisiae* by electron transfer dissociation ( ETD ) mass spectrometry CHEMISTRY. , 104(7).
- Choudhary, C. et al., 2009. Lysine acetylation targets protein complexes and co-regulates major cellular functions. *Science (New York, N.Y.)*, 325(5942), pp.834–40.
- Cid, V.J. et al., 2001. Cell cycle control of septin ring dynamics in the budding yeast. *Microbiology (Reading, England)*, 147(Pt 6), pp.1437–50.
- Citiulo, F. et al., 2012. *Candida albicans* scavenges host zinc via Pra1 during endothelial invasion. *PLoS pathogens*, 8(6), p.e1002777.
- Clark, K.L. et al., 1993. Co-crystal structure of the HNF-3/fork head DNA-recognition motif resembles histone H5. *Nature*, 364(6436), pp.412–20.

- Cleary, I. a et al., 2010. Pseudohyphal regulation by the transcription factor Rfg1p in *Candida albicans*. *Eukaryotic cell*, 9(9), pp.1363–73.
- Clemente-Blanco, A. et al., 2006. The Cdc14p phosphatase affects late cell-cycle events and morphogenesis in *Candida albicans*. *Journal of cell science*, 119(Pt 6), pp.1130–43.
- Cohen, P., 2000. The regulation of protein function by multisite phosphorylation--a 25 year update. *Trends in biochemical sciences*, 25(12), pp.596–601.
- Cormack, B.P. et al., 1997. Yeast-enhanced green fluorescent protein (yEGFP): a reporter of gene expression in *Candida albicans*. *Microbiology (Reading, England)*, 143 ( Pt 2)(1 997), pp.303–11.
- Costanzo, M., Schub, O. & Andrews, B., 2003. G1 transcription factors are differentially regulated in *Saccharomyces cerevisiae* by the Swi6-binding protein Stb1. *Molecular and cellular biology*, 23(14), pp.5064–77.
- Côte, P., Hogues, H. & Whiteway, M., 2009. Transcriptional analysis of the *Candida albicans* cell cycle. *Molecular biology of the cell*, 20(14), pp.3363–73.
- Court, H. & Sudbery, P., 2007. Regulation of Cdc42 GTPase activity in the formation of hyphae in *Candida albicans*. *Molecular biology of the cell*, 18(1), pp.265–81.
- Crampin, H. et al., 2005. *Candida albicans* hyphae have a Spitzenkörper that is distinct from the polarisome found in yeast and pseudohyphae. *Journal of cell science*, 118(Pt 13), pp.2935–47.
- Cvrcková, F. & Nasmyth, K., 1993. Yeast G1 cyclins CLN1 and CLN2 and a GAP-like protein have a role in bud formation. *The EMBO journal*, 12(13), pp.5277–86.
- Darieva, Z. et al., 2010. A competitive transcription factor binding mechanism determines the timing of late cell cycle-dependent gene expression. *Molecular cell*, 38(1), pp.29–40.
- Darieva, Z. et al., 2003. Cell cycle-regulated transcription through the FHA domain of Fkh2p and the coactivator Ndd1p. *Current biology : CB*, 13(19), pp.1740–5.
- Darieva, Z. et al., 2006. Polo kinase controls cell-cycle-dependent transcription by targeting a coactivator protein. *Nature*, 444(7118), pp.494–8.
- Darieva, Z. et al., 2012. Protein kinase C regulates late cell cycle-dependent gene expression. *Molecular and cellular biology*, 32(22), pp.4651–61.
- Diezmann, S. et al., 2012. Mapping the Hsp90 genetic interaction network in *Candida albicans* reveals environmental contingency and rewired circuitry. *PLoS genetics*, 8(3), p.e1002562.

- Dirick, L., Böhm, T. & Nasmyth, K., 1995. Roles and regulation of Cln-Cdc28 kinases at the start of the cell cycle of *Saccharomyces cerevisiae*. *The EMBO journal*, 14(19), pp.4803–13.
- Donaldson, a D. et al., 1998. CLB5-dependent activation of late replication origins in *S. cerevisiae*. *Molecular cell*, 2(2), pp.173–82.
- Egelhofer, T. a et al., 2008. The septins function in G1 pathways that influence the pattern of cell growth in budding yeast. *PloS one*, 3(4), p.e2022.
- Eisman, B. et al., 2006. The Cek1 and Hog1 mitogen-activated protein kinases play complementary roles in cell wall biogenesis and chlamydospore formation in the fungal pathogen *Candida albicans*. *Eukaryotic cell*, 5(2), pp.347–58.
- Enserink, J.M. & Kolodner, R.D., 2010. An overview of Cdk1-controlled targets and processes. *Cell division*, 5, p.11.
- Evangelista, M. et al., 1997. Bni1p, a yeast formin linking cdc42p and the actin cytoskeleton during polarized morphogenesis. *Science (New York, N.Y.)*, 276(5309), pp.118–22.
- Evans, T. et al., 1983. Cyclin: a protein specified by maternal mRNA in sea urchin eggs that is destroyed at each cleavage division. *Cell*, 33(2), pp.389–96.
- Fang, H.-M. & Wang, Y., 2006. RA domain-mediated interaction of Cdc35 with Ras1 is essential for increasing cellular cAMP level for *Candida albicans* hyphal development. *Molecular microbiology*, 61(2), pp.484–96.
- Fanning, S. & Mitchell, A.P., 2012. Fungal biofilms. *PLoS pathogens*, 8(4), p.e1002585.
- Figurski, D., 2013. *Genetic Manipulation of DNA and Protein - Examples from Current Research*,
- Finley, K.R. & Berman, J., 2005. Microtubules in *Candida albicans* hyphae drive nuclear dynamics and connect cell cycle progression to morphogenesis. *Eukaryotic cell*, 4(10), pp.1697–711.
- Fonzi, W.A., 1999. PHR1 and PHR2 of *Candida albicans* encode putative glycosidases required for proper cross-linking of beta-1,3- and beta-1,6-glucans. *Journal of bacteriology*, 181(22), pp.7070–9.
- Fonzi, W.A. & Irwin, M.Y., 1993. Isogenic strain construction and gene mapping in *Candida albicans*. *Genetics*.
- Fu, Z. et al., 2008. Plk1-dependent phosphorylation of FoxM1 regulates a transcriptional programme required for mitotic progression. *Nature cell biology*, 10(9), pp.1076–82.

- García-Sánchez, S. et al., 2005. Global roles of Ssn6 in Tup1- and Nrg1-dependent gene regulation in the fungal pathogen, *Candida albicans*. *Molecular biology of the cell*, 16(6), pp.2913–25.
- Gill, G., 2004. SUMO and ubiquitin in the nucleus: different functions, similar mechanisms? *Genes & development*, 18(17), pp.2046–59.
- Gladfelter, A.S. et al., 2002. Septin ring assembly involves cycles of GTP loading and hydrolysis by Cdc42p. *The Journal of cell biology*, 156(2), pp.315–26.
- Gomez-Raja, J. & Davis, D. a, 2012. The  $\beta$ -arrestin-like protein Rim8 is hyperphosphorylated and complexes with Rim21 and Rim101 to promote adaptation to neutral-alkaline pH. *Eukaryotic cell*, 11(5), pp.683–93.
- González-Novo, A. et al., 2008. Sep7 is essential to modify septin ring dynamics and inhibit cell separation during *Candida albicans* hyphal growth. *Molecular biology of the cell*, 19(4), pp.1509–18.
- Gordân, R., Pyne, S. & Bulyk, M.L., 2012. Identification of cell cycle-regulated, putative hyphal genes in *Candida albicans*. *Pacific Symposium on Biocomputing. Pacific Symposium on Biocomputing*, pp.299–310.
- Gow, N. a R., Brown, A.J.P. & Odds, F.C., 2002. Fungal morphogenesis and host invasion. *Current opinion in microbiology*, 5(4), pp.366–71.
- Haase, S.B., Winey, M. & Reed, S.I., 2001. Multi-step control of spindle pole body duplication by cyclin-dependent kinase. *Nature cell biology*, 3(1), pp.38–42.
- Harcus, D. et al., 2004. Transcription profiling of cyclic AMP signaling in *Candida albicans*. *Molecular biology of the cell*, 15(10), pp.4490–9.
- Hardie, D.G., 1999. *Protein phosphorylation : a practical approach*,
- Hartwell, L.H. et al., 1974. Genetic control of the cell division cycle in yeast. *Science (New York, N.Y.)*, 183(4120), pp.46–51.
- Hassan, I. et al., 2009. Excess mortality, length of stay and cost attributable to candidaemia. *The Journal of infection*, 59(5), pp.360–5.
- Hausauer, D.L. et al., 2005. Hyphal guidance and invasive growth in *Candida albicans* require the Ras-like GTPase Rsr1p and its GTPase-activating protein Bud2p. *Eukaryotic cell*, 4(7), pp.1273–86.
- Hazan, I. & Liu, H., 2002. Hyphal tip-associated localization of Cdc42 is F-actin dependent in *Candida albicans*. *Eukaryotic cell*, 1(6), pp.856–64.
- Hazan, I., Sepulveda-Becerra, M. & Liu, H., 2002. Hyphal elongation is regulated independently of cell cycle in *Candida albicans*. *Molecular biology of the cell*, 13(1), pp.134–45.

- He, B. & Guo, W., 2009. The exocyst complex in polarized exocytosis. *Current opinion in cell biology*, 21(4), pp.537–42.
- Henchoz, S. et al., 1997. Phosphorylation- and ubiquitin-dependent degradation of the cyclin-dependent kinase inhibitor Far1p in budding yeast. *Genes & development*, 11(22), pp.3046–60.
- Hickman, M. a et al., 2013. The “obligate diploid” *Candida albicans* forms mating-competent haploids. *Nature*, 494(7435), pp.55–9.
- Hicks, J.B., Strathern, J.N. & Herskowitz, I., 1977. Interconversion of Yeast Mating Types III. Action of the Homothallism (HO) Gene in Cells Homozygous for the Mating Type Locus. *Genetics*, 85(3), pp.395–405.
- Ho, Y. et al., 1999. Regulation of transcription at the *Saccharomyces cerevisiae* start transition by Stb1, a Swi6-binding protein. *Molecular and cellular biology*, 19(8), pp.5267–78.
- Hollenhorst, P.C. et al., 2000. Forkhead genes in transcriptional silencing, cell morphology and the cell cycle. Overlapping and distinct functions for FKH1 and FKH2 in *Saccharomyces cerevisiae*. *Genetics*, 154(4), pp.1533–48.
- Hollenhorst, P.C., Pietz, G. & Fox, C. a, 2001. Mechanisms controlling differential promoter-occupancy by the yeast forkhead proteins Fkh1p and Fkh2p: implications for regulating the cell cycle and differentiation. *Genes & development*, 15(18), pp.2445–56.
- Howell, A.S. et al., 2012. Negative feedback enhances robustness in the yeast polarity establishment circuit. *Cell*, 149(2), pp.322–33.
- Howell, A.S. et al., 2009. Singularity in polarization: rewiring yeast cells to make two buds. *Cell*, 139(4), pp.731–43.
- Howell, A.S. & Lew, D.J., 2012. Morphogenesis and the cell cycle. *Genetics*, 190(1), pp.51–77.
- Hoyer, L.L. et al., 1994. A *Candida albicans* cyclic nucleotide phosphodiesterase: cloning and expression in *Saccharomyces cerevisiae* and biochemical characterization of the recombinant enzyme. *Microbiology (Reading, England)*, 140 ( Pt 7(1 994), pp.1533–42.
- Huaping, L. et al., 2007. Cloning and functional expression of ubiquitin-like protein specific proteases genes from *Candida albicans*. *Biological & pharmaceutical bulletin*, 30(10), pp.1851–5.
- Ibrahim, a S. et al., 1995. Evidence implicating phospholipase as a virulence factor of *Candida albicans*. *Infection and immunity*, 63(5), pp.1993–8.

- Inglis, D.O. et al., 2013. Improved gene ontology annotation for biofilm formation, filamentous growth, and phenotypic switching in *Candida albicans*. *Eukaryotic cell*, 12(1), pp.101–8.
- Iwase, M. et al., 2006. Role of a Cdc42p effector pathway in recruitment of the yeast septins to the presumptive bud site. *Molecular biology of the cell*, 17(3), pp.1110–25.
- Jackson, L.P., Reed, S.I. & Haase, S.B., 2006. Distinct mechanisms control the stability of the related S-phase cyclins Clb5 and Clb6. *Molecular and cellular biology*, 26(6), pp.2456–66.
- Johnson, E.S. & Blobel, G., 1999. Cell cycle-regulated attachment of the ubiquitin-related protein SUMO to the yeast septins. *The Journal of cell biology*, 147(5), pp.981–94.
- Jones, L. a & Sudbery, P.E., 2010. Spitzenkorper, exocyst, and polarisome components in *Candida albicans* hyphae show different patterns of localization and have distinct dynamic properties. *Eukaryotic cell*, 9(10), pp.1455–65.
- Kadosh, D. & Johnson, A.D., 2005. Induction of the *Candida albicans* filamentous growth program by relief of transcriptional repression: a genome-wide analysis. *Molecular biology of the cell*, 16(6), pp.2903–12.
- Kadosh, D. & Johnson, A.D., 2001. Rfg1, a protein related to the *Saccharomyces cerevisiae* hypoxic regulator Rox1, controls filamentous growth and virulence in *Candida albicans*. *Molecular and cellular biology*, 21(7), pp.2496–505.
- Kadota, J. et al., 2004. Septin ring assembly requires concerted action of polarisome components, a PAK kinase Cla4p, and the actin cytoskeleton in *Saccharomyces cerevisiae*. *Molecular biology of the cell*, 15(12), pp.5329–45.
- Kaestner, K.H., Knochel, W. & Martinez, D.E., 2000. Unified nomenclature for the winged helix/forkhead transcription factors. *Genes & development*, 14(2), pp.142–6.
- Kaldis, P., Sutton, a & Solomon, M.J., 1996. The Cdk-activating kinase (CAK) from budding yeast. *Cell*, 86(4), pp.553–64.
- Kebaara, B.W. et al., 2008. *Candida albicans* Tup1 is involved in farnesol-mediated inhibition of filamentous-growth induction. *Eukaryotic cell*, 7(6), pp.980–7.
- Keil, B., 1992. *Specificity of Proteolysis*, Berlin, Heidelberg: Springer Berlin Heidelberg.
- Klengel, T. et al., 2005. Fungal adenylyl cyclase integrates CO<sub>2</sub> sensing with cAMP signaling and virulence. *Current biology : CB*, 15(22), pp.2021–6.

- Knapp, D. et al., 1996. The transcription factor Swi5 regulates expression of the cyclin kinase inhibitor p40SIC1. *Molecular and cellular biology*, 16(10), pp.5701–7.
- Knaus, M. et al., 2007. Phosphorylation of Bem2p and Bem3p may contribute to local activation of Cdc42p at bud emergence. *The EMBO journal*, 26(21), pp.4501–13.
- Knott, S.R. V et al., 2012. Forkhead transcription factors establish origin timing and long-range clustering in *S. cerevisiae*. *Cell*, 148(1-2), pp.99–111.
- Komander, D., 2009. The emerging complexity of protein ubiquitination. *Biochemical Society transactions*, 37(Pt 5), pp.937–53.
- Kono, K. et al., 2008. G1/S cyclin-dependent kinase regulates small GTPase Rho1p through phosphorylation of RhoGEF Tus1p in *Saccharomyces cerevisiae*. *Molecular biology of the cell*, 19(4), pp.1763–71.
- Koranda, M. et al., 2000. Forkhead-like transcription factors recruit Ndd1 to the chromatin of G2/M-specific promoters. *Nature*, 406(6791), pp.94–8.
- Korver, W., Roose, J. & Clevers, H., 1997. The winged-helix transcription factor Trident is expressed in cycling cells. *Nucleic acids research*, 25(9), pp.1715–9.
- Kozubowski, L. et al., 2008. Symmetry-breaking polarization driven by a Cdc42p GEF-PAK complex. *Current biology : CB*, 18(22), pp.1719–26.
- Kurat, C.F. et al., 2009. Cdk1/Cdc28-dependent activation of the major triacylglycerol lipase Tgl4 in yeast links lipolysis to cell-cycle progression. *Molecular cell*, 33(1), pp.53–63.
- Laoukili, J. et al., 2008. Activation of FoxM1 during G2 requires cyclin A/Cdk-dependent relief of autorepression by the FoxM1 N-terminal domain. *Molecular and cellular biology*, 28(9), pp.3076–87.
- Laoukili, J. et al., 2005. FoxM1 is required for execution of the mitotic programme and chromosome stability. *Nature cell biology*, 7(2), pp.126–36.
- Leach, M.D., Stead, D. a, Argo, E. & Brown, A.J.P., 2011. Identification of sumoylation targets, combined with inactivation of SMT3, reveals the impact of sumoylation upon growth, morphology, and stress resistance in the pathogen *Candida albicans*. *Molecular biology of the cell*, 22(5), pp.687–702.
- Leach, M.D., Stead, D. a, Argo, E., MacCallum, D.M., et al., 2011. Molecular and proteomic analyses highlight the importance of ubiquitination for the stress resistance, metabolic adaptation, morphogenetic regulation and virulence of *Candida albicans*. *Molecular microbiology*, 79(6), pp.1574–93.

- Leach, M.D. & Brown, A.J.P., 2012. Posttranslational modifications of proteins in the pathobiology of medically relevant fungi. *Eukaryotic cell*, 11(2), pp.98–108.
- Leach, M.D. & Cowen, L.E., 2013. Surviving the heat of the moment: a fungal pathogens perspective. *PLoS pathogens*, 9(3), p.e1003163.
- Leberer, E. et al., 1996. Signal transduction through homologs of the Ste20p and Ste7p protein kinases can trigger hyphal formation in the pathogenic fungus *Candida albicans*. *Proceedings of the National Academy of Sciences of the United States of America*, 93(23), pp.13217–22.
- Lee, J.M. & Greenleaf, A.L., 1991. CTD kinase large subunit is encoded by CTK1, a gene required for normal growth of *Saccharomyces cerevisiae*. *Gene expression*, 1(2), pp.149–67.
- Leng, P., Sudbery, P.E. & Brown, a J., 2000. Rad6p represses yeast-hypha morphogenesis in the human fungal pathogen *Candida albicans*. *Molecular microbiology*, 35(5), pp.1264–75.
- Lesage, G. & Bussey, H., 2006. Cell wall assembly in *Saccharomyces cerevisiae*. *Microbiology and molecular biology reviews : MMBR*, 70(2), pp.317–43.
- Lew, D.J. & Reed, S.I., 1993. Morphogenesis in the yeast cell cycle: regulation by Cdc28 and cyclins. *The Journal of cell biology*, 120(6), pp.1305–20.
- Li, C. et al., 2012. CDK regulates septin organization through cell-cycle-dependent phosphorylation of the Nim1-related kinase Gin4. *Journal of cell science*, 125(Pt 10), pp.2533–43.
- Li, M. et al., 2004. *Candida albicans* Rim13p, a protease required for Rim101p processing at acidic and alkaline pHs. *Eukaryotic cell*, 3(3), pp.741–51.
- Li, Y. et al., 2007. Roles of *Candida albicans* Sfl1 in hyphal development. *Eukaryotic cell*, 6(11), pp.2112–21.
- Lim, F. et al., 2003. Mcm1p-induced DNA bending regulates the formation of ternary transcription factor complexes. *Molecular and cellular biology*, 23(2), pp.450–61.
- Liu, H., Köhler, J. & Fink, G.R., 1994. Suppression of hyphal formation in *Candida albicans* by mutation of a STE12 homolog. *Science (New York, N.Y.)*, 266(5191), pp.1723–6.
- Loeb, J.D., Sepulveda-Becerra, M., et al., 1999. A G1 cyclin is necessary for maintenance of filamentous growth in *Candida albicans*. *Molecular and cellular biology*, 19(6), pp.4019–27.
- Loeb, J.D., Kerentseva, T.A., et al., 1999. *Saccharomyces cerevisiae* G1 cyclins are differentially involved in invasive and pseudohyphal growth independent of

- the filamentation mitogen-activated protein kinase pathway. *Genetics*, 153(4), pp.1535–46.
- Lu, Y. et al., 2011. Hyphal development in *Candida albicans* requires two temporally linked changes in promoter chromatin for initiation and maintenance. *PLoS biology*, 9(7), p.e1001105.
- Luo, G. et al., 2013. Mitotic phosphorylation of Exo84 disrupts exocyst assembly and arrests cell growth. *The Journal of cell biology*, 202(1), pp.97–111.
- Maidan, M.M. et al., 2005. The G protein-coupled receptor Gpr1 and the Galpha protein Gpa2 act through the cAMP-protein kinase A pathway to induce morphogenesis in *Candida albicans*. *Molecular biology of the cell*, 16(4), pp.1971–86.
- Mann, M. et al., 2002. Analysis of protein phosphorylation using mass spectrometry: deciphering the phosphoproteome. *Trends in biotechnology*, 20(6), pp.261–8.
- Martchenko, M. et al., 2004. Superoxide dismutases in *Candida albicans*: transcriptional regulation and functional characterization of the hyphal-induced SOD5 gene. *Molecular biology of the cell*, 15(2), pp.456–67.
- Martin, D.E., Soulard, A. & Hall, M.N., 2004. TOR regulates ribosomal protein gene expression via PKA and the Forkhead transcription factor FHL1. *Cell*, 119(7), pp.969–79.
- Martin, R. et al., 2007. Functional analysis of *Candida albicans* genes whose *Saccharomyces cerevisiae* homologues are involved in endocytosis. *Yeast (Chichester, England)*, 24(6), pp.511–22.
- Martin, R. et al., 2011. Host-pathogen interactions and virulence-associated genes during *Candida albicans* oral infections. *International journal of medical microbiology: IJMM*, 301(5), pp.417–22.
- Mazanka, E. & Weiss, E.L., 2010. Sequential counteracting kinases restrict an asymmetric gene expression program to early G1. *Molecular biology of the cell*, 21(16), pp.2809–20.
- McCusker, D. et al., 2007. Cdk1 coordinates cell-surface growth with the cell cycle. *Nature cell biology*, 9(5), pp.506–15.
- McNemar, M.D. & Fonzi, W.A., 2002. Conserved serine/threonine kinase encoded by CBK1 regulates expression of several hypha-associated transcripts and genes encoding cell wall proteins in *Candida albicans*. *Journal of bacteriology*, 184(7), pp.2058–61.

- Miller, L.G., Hajjeh, R. a & Edwards, J.E., 2001. Estimating the cost of nosocomial candidemia in the united states. *Clinical infectious diseases : an official publication of the Infectious Diseases Society of America*, 32(7), p.1110.
- Miwa, T. et al., 2004. Gpr1, a putative G-protein-coupled receptor, regulates morphogenesis and hypha formation in the pathogenic fungus *Candida albicans*. *Eukaryotic cell*, 3(4), pp.919–31.
- Morschhäuser, J., 2010. Regulation of white-opaque switching in *Candida albicans*. *Medical microbiology and immunology*, 199(3), pp.165–72.
- Murad, a M. et al., 2000. Clp10, an efficient and convenient integrating vector for *Candida albicans*. *Yeast (Chichester, England)*, 16(4), pp.325–7.
- Murad, a M. et al., 2001. NRG1 represses yeast-hypha morphogenesis and hypha-specific gene expression in *Candida albicans*. *The EMBO journal*, 20(17), pp.4742–52.
- Murakami, H. et al., 2010. Regulation of yeast forkhead transcription factors and FoxM1 by cyclin-dependent and polo-like kinases. *Cell cycle (Georgetown, Tex.)*, 9(16), pp.3233–42.
- Nakayama, H. et al., 2000. Tetracycline-regulatable system to tightly control gene expression in the pathogenic fungus *Candida albicans*. *Infection and immunity*, 68(12), pp.6712–9.
- Nicholls, S. et al., 2011. Activation of the heat shock transcription factor Hsf1 is essential for the full virulence of the fungal pathogen *Candida albicans*. *Fungal genetics and biology : FG & B*, 48(3), pp.297–305.
- Nigg, E. a, 1993. Cellular substrates of p34(cdc2) and its companion cyclin-dependent kinases. *Trends in cell biology*, 3(9), pp.296–301.
- Nobile, C.J. et al., 2012. A recently evolved transcriptional network controls biofilm development in *Candida albicans*. *Cell*, 148(1-2), pp.126–38.
- Nobile, C.J. et al., 2003. Genetic control of chlamydospore formation in *Candida albicans*. *Microbiology (Reading, England)*, 149(Pt 12), pp.3629–37.
- Noble, S.M. et al., 2010. Systematic screens of a *Candida albicans* homozygous deletion library decouple morphogenetic switching and pathogenicity. *Nature genetics*, 42(7), pp.590–8.
- Noble, S.M. & Johnson, A.D., 2007. Genetics of *Candida albicans*, a diploid human fungal pathogen. *Annual review of genetics*, 41, pp.193–211.
- Nurse, P. & Thuriaux, P., 1980. Regulatory genes controlling mitosis in the fission yeast *Schizosaccharomyces pombe*. *Genetics*, 96(3), pp.627–37.

- Ofir, A. & Kornitzer, D., 2010. *Candida albicans* cyclin Clb4 carries S-phase cyclin activity. *Eukaryotic cell*, 9(9), pp.1311–9.
- Oh, Y. & Bi, E., 2011. Septin structure and function in yeast and beyond. *Trends in cell biology*, 21(3), pp.141–8.
- Park, H.-O. & Bi, E., 2007. Central roles of small GTPases in the development of cell polarity in yeast and beyond. *Microbiology and molecular biology reviews : MMBR*, 71(1), pp.48–96.
- Park, H.-O., Kang, P.J. & Rachfal, A.W., 2002. Localization of the Rsr1/Bud1 GTPase involved in selection of a proper growth site in yeast. *The Journal of biological chemistry*, 277(30), pp.26721–4.
- Park, H.O., Chant, J. & Herskowitz, I., 1993. BUD2 encodes a GTPase-activating protein for Bud1/Rsr1 necessary for proper bud-site selection in yeast. *Nature*, 365(6443), pp.269–74.
- Peck, S.C., 2006. Analysis of protein phosphorylation: methods and strategies for studying kinases and substrates. *The Plant journal : for cell and molecular biology*, 45(4), pp.512–22.
- Pfaller, M. a & Diekema, D.J., 2010. *Epidemiology of invasive mycoses in North America.*
- Phan, Q.T. et al., 2007. Als3 is a *Candida albicans* invasin that binds to cadherins and induces endocytosis by host cells. *PLoS biology*, 5(3), p.e64.
- Pic, a et al., 2000. The forkhead protein Fkh2 is a component of the yeast cell cycle transcription factor SFF. *The EMBO journal*, 19(14), pp.3750–61.
- Pic-Taylor, A. et al., 2004. Regulation of cell cycle-specific gene expression through cyclin-dependent kinase-mediated phosphorylation of the forkhead transcription factor Fkh2p. *Molecular and cellular biology*, 24(22), pp.10036–46.
- Postnikoff, S.D.L. et al., 2012. The yeast forkhead transcription factors fkh1 and fkh2 regulate lifespan and stress response together with the anaphase-promoting complex. *PLoS genetics*, 8(3), p.e1002583.
- Pramila, T. et al., 2006. The Forkhead transcription factor Hcm1 regulates chromosome segregation genes and fills the S-phase gap in the transcriptional circuitry of the cell cycle. *Genes & development*, 20(16), pp.2266–78.
- Pruyne, D. et al., 2004. Mechanisms of polarized growth and organelle segregation in yeast. *Annual review of cell and developmental biology*, 20, pp.559–91.

- Puri, S. et al., 2012. Secreted aspartic protease cleavage of *Candida albicans* Msb2 activates Cek1 MAPK signaling affecting biofilm formation and oropharyngeal candidiasis. *PloS one*, 7(11), p.e46020.
- Reynolds, D. et al., 2003. Recruitment of Thr 319-phosphorylated Ndd1p to the FHA domain of Fkh2p requires Clb kinase activity: a mechanism for CLB cluster gene activation. *Genes & development*, 17(14), pp.1789–802.
- Richardson, H. et al., 1992. Cyclin-B homologs in *Saccharomyces cerevisiae* function in S phase and in G2. *Genes & development*, 6(11), pp.2021–34.
- Richman, T.J. et al., 2004. Analysis of cell-cycle specific localization of the Rdi1p RhoGDI and the structural determinants required for Cdc42p membrane localization and clustering at sites of polarized growth. *Current genetics*, 45(6), pp.339–49.
- Rocha, C.R. et al., 2001. Signaling through adenylyl cyclase is essential for hyphal growth and virulence in the pathogenic fungus *Candida albicans*. *Molecular biology of the cell*, 12(11), pp.3631–43.
- Rock, J.M. & Amon, A., 2009. The FEAR network. *Current biology : CB*, 19(23), pp.R1063–8.
- Roig, P. et al., 2000. Molecular cloning and characterization of the *Candida albicans* UBI3 gene coding for a ubiquitin-hybrid protein. *Yeast (Chichester, England)*, 16(15), pp.1413–9.
- Román, E., Cottier, F., et al., 2009. Msb2 signaling mucin controls activation of Cek1 mitogen-activated protein kinase in *Candida albicans*. *Eukaryotic cell*, 8(8), pp.1235–49.
- Román, E., Alonso-Monge, R., et al., 2009. The Cek1 MAPK is a short-lived protein regulated by quorum sensing in the fungal pathogen *Candida albicans*. *FEMS yeast research*, 9(6), pp.942–55.
- Román, E., Nombela, C. & Pla, J., 2005. The Sho1 adaptor protein links oxidative stress to morphogenesis and cell wall biosynthesis in the fungal pathogen *Candida albicans*. *Molecular and cellular biology*, 25(23), pp.10611–27.
- Ross, H., Armstrong, C.G. & Cohen, P., 2002. A non-radioactive method for the assay of many serine/threonine-specific protein kinases. *The Biochemical journal*, 366(Pt 3), pp.977–81.
- Ruggieri, R. et al., 1992. RSR1, a ras-like gene homologous to Krev-1 (smg21A/rap1A): role in the development of cell polarity and interactions with the Ras pathway in *Saccharomyces cerevisiae*. *Molecular and cellular biology*, 12(2), pp.758–66.

- Russell, P., Moreno, S. & Reed, S.I., 1989. Conservation of mitotic controls in fission and budding yeasts. *Cell*, 57(2), pp.295–303.
- Sagot, I., Klee, S.K. & Pellman, D., 2002. Yeast formins regulate cell polarity by controlling the assembly of actin cables. *Nature cell biology*, 4(1), pp.42–50.
- Saito, K. et al., 2007. Transbilayer phospholipid flipping regulates Cdc42p signaling during polarized cell growth via Rga GTPase-activating proteins. *Developmental cell*, 13(5), pp.743–51.
- Salminen, a & Novick, P.J., 1987. A ras-like protein is required for a post-Golgi event in yeast secretion. *Cell*, 49(4), pp.527–38.
- Sanglard, D. et al., 1997. A triple deletion of the secreted aspartyl proteinase genes SAP4, SAP5, and SAP6 of *Candida albicans* causes attenuated virulence. *Infection and immunity*, 65(9), pp.3539–46.
- Santamaría, D. et al., 2007. Cdk1 is sufficient to drive the mammalian cell cycle. *Nature*, 448(7155), pp.811–5.
- Santos, M. a & Tuite, M.F., 1995. The CUG codon is decoded in vivo as serine and not leucine in *Candida albicans*. *Nucleic acids research*, 23(9), pp.1481–6.
- Sato, T. et al., 2004. Farnesol, a morphogenetic autoregulatory substance in the dimorphic fungus *Candida albicans*, inhibits hyphae growth through suppression of a mitogen-activated protein kinase cascade. *Biological & pharmaceutical bulletin*, 27(5), pp.751–2.
- Schlesinger, M.B. & Formosa, T., 2000. POB3 is required for both transcription and replication in the yeast *Saccharomyces cerevisiae*. *Genetics*, 155(4), pp.1593–606.
- Schneider, B.L., Yang, Q.H. & Futcher, A.B., 1996. Linkage of replication to start by the Cdk inhibitor Sic1. *Science (New York, N.Y.)*, 272(5261), pp.560–2.
- Schneider, J. & Fanning, E., 1988. Mutations in the phosphorylation sites of simian virus 40 (SV40) T antigen alter its origin DNA-binding specificity for sites I or II and affect SV40 DNA replication activity. *Journal of virology*, 62(5), pp.1598–605.
- Schwob, E. et al., 1994. The B-type cyclin kinase inhibitor p40SIC1 controls the G1 to S transition in *S. cerevisiae*. *Cell*, 79(2), pp.233–44.
- Senn, H., Shapiro, R.S. & Cowen, L.E., 2012. Cdc28 provides a molecular link between Hsp90, morphogenesis, and cell cycle progression in *Candida albicans*. *Molecular biology of the cell*, 23(2), pp.268–83.
- Seufert, W., Futcher, B. & Jentsch, S., 1995. Role of a ubiquitin-conjugating enzyme in degradation of S- and M-phase cyclins. *Nature*, 373(6509), pp.78–81.

- Shapiro, R.S. et al., 2009. Hsp90 orchestrates temperature-dependent *Candida albicans* morphogenesis via Ras1-PKA signaling. *Current biology : CB*, 19(8), pp.621–9.
- Shapiro, R.S., Sellam, A., et al., 2012. Pho85, Pcl1, and Hms1 signaling governs *Candida albicans* morphogenesis induced by high temperature or Hsp90 compromise. *Current biology : CB*, 22(6), pp.461–70.
- Shapiro, R.S., Zaas, A.K., et al., 2012. The Hsp90 co-chaperone Sgt1 governs *Candida albicans* morphogenesis and drug resistance. *PloS one*, 7(9), p.e44734.
- Sherriff, J. a, Kent, N. a & Mellor, J., 2007. The Isw2 chromatin-remodeling ATPase cooperates with the Fkh2 transcription factor to repress transcription of the B-type cyclin gene CLB2. *Molecular and cellular biology*, 27(8), pp.2848–60.
- Shimada, M. et al., 2008. Cdc2p controls the forkhead transcription factor Fkh2p by phosphorylation during sexual differentiation in fission yeast. *The EMBO journal*, 27(1), pp.132–42.
- Shimada, Y. et al., 2004. The nucleotide exchange factor Cdc24p may be regulated by auto-inhibition. *The EMBO journal*, 23(5), pp.1051–62.
- Shimada, Y., Gulli, M.P. & Peter, M., 2000. Nuclear sequestration of the exchange factor Cdc24 by Far1 regulates cell polarity during yeast mating. *Nature cell biology*, 2(2), pp.117–24.
- Sinha, I. et al., 2007. Cyclin-dependent kinases control septin phosphorylation in *Candida albicans* hyphal development. *Developmental cell*, 13(3), pp.421–32.
- Smith, D.A. et al., 2004. A conserved stress-activated protein kinase regulates a core stress response in the human pathogen *Candida albicans*. *Molecular biology of the cell*, 15(9), pp.4179–90.
- Smith, G.R. et al., 2002. GTPase-activating proteins for Cdc42. *Eukaryotic cell*, 1(3), pp.469–80.
- Sohn, K. et al., 2003. EFG1 is a major regulator of cell wall dynamics in *Candida albicans* as revealed by DNA microarrays. *Molecular microbiology*, 47(1), pp.89–102.
- Songyang, Z. et al., 1996. A structural basis for substrate specificities of protein Ser/Thr kinases: primary sequence preference of casein kinases I and II, NIMA, phosphorylase kinase, calmodulin-dependent kinase II, CDK5, and Erk1. *Molecular and cellular biology*, 16(11), pp.6486–93.
- Sopko, R. et al., 2007. Activation of the Cdc42p GTPase by cyclin-dependent protein kinases in budding yeast. *The EMBO journal*, 26(21), pp.4487–500.

- Spiro, R.G., 2002. Protein glycosylation: nature, distribution, enzymatic formation, and disease implications of glycopeptide bonds. *Glycobiology*, 12(4), p.43R–56R.
- Staab, J.F. et al., 1999. Adhesive and mammalian transglutaminase substrate properties of *Candida albicans* Hwp1. *Science (New York, N.Y.)*, 283(5407), pp.1535–8.
- Su, C. et al., 2009. Mss11, a transcriptional activator, is required for hyphal development in *Candida albicans*. *Eukaryotic cell*, 8(11), pp.1780–91.
- Sudbery, P., Gow, N. & Berman, J., 2004. The distinct morphogenic states of *Candida albicans*. *Trends in microbiology*, 12(7), pp.317–24.
- Sudbery, P.E., 2011. Growth of *Candida albicans* hyphae. *Nature reviews. Microbiology*, 9(10), pp.737–48.
- Sudbery, P.E., 2001. The germ tubes of *Candida albicans* hyphae and pseudohyphae show different patterns of septin ring localization. *Molecular microbiology*, 41(1), pp.19–31.
- Szilagyi, Z. et al., 2012. Cyclin-dependent kinase 8 regulates mitotic commitment in fission yeast. *Molecular and cellular biology*, 32(11), pp.2099–109.
- Tabb, M.M. et al., 2000. Evidence for separable functions of Srp1p, the yeast homolog of importin alpha (Karyopherin alpha): role for Srp1p and Sts1p in protein degradation. *Molecular and cellular biology*, 20(16), pp.6062–73.
- Tang, C.S.L. & Reed, S.I., 2002. Phosphorylation of the septin cdc3 in g1 by the cdc28 kinase is essential for efficient septin ring disassembly. *Cell cycle (Georgetown, Tex.)*, 1(1), pp.42–9.
- Teh, E.M., Chai, C.C. & Yeong, F.M., 2009. Retention of Chs2p in the ER requires N-terminal CDK1-phosphorylation sites. *Cell cycle (Georgetown, Tex.)*, 8(18), pp.2964–74.
- Thakur, J. & Sanyal, K., 2011. The essentiality of the fungus-specific Dam1 complex is correlated with a one-kinetochore-one-microtubule interaction present throughout the cell cycle, independent of the nature of a centromere. *Eukaryotic cell*, 10(10), pp.1295–305.
- Tingley, W.G. et al., 1997. Characterization of protein kinase A and protein kinase C phosphorylation of the N-methyl-D-aspartate receptor NR1 subunit using phosphorylation site-specific antibodies. *The Journal of biological chemistry*, 272(8), pp.5157–66.
- Ubersax, J.A. et al., 2003. Targets of the cyclin-dependent kinase Cdk1. *Nature*, 425(6960), pp.859–64.

- Uhl, M.A. et al., 2003. Haploinsufficiency-based large-scale forward genetic analysis of filamentous growth in the diploid human fungal pathogen *C.albicans*. *The EMBO journal*, 22(11), pp.2668–78.
- Ullmann, B.D. et al., 2004. Inducible defense mechanism against nitric oxide in *Candida albicans*. *Eukaryotic cell*, 3(3), pp.715–23.
- Wächtler, B. et al., 2011. From attachment to damage: defined genes of *Candida albicans* mediate adhesion, invasion and damage during interaction with oral epithelial cells. *PloS one*, 6(2), p.e17046.
- Walch-Solimena, C., Collins, R.N. & Novick, P.J., 1997. Sec2p mediates nucleotide exchange on Sec4p and is involved in polarized delivery of post-Golgi vesicles. *The Journal of cell biology*, 137(7), pp.1495–509.
- Wang, A. et al., 2009. Hyphal chain formation in *Candida albicans*: Cdc28-Hgc1 phosphorylation of Efg1 represses cell separation genes. *Molecular and cellular biology*, 29(16), pp.4406–16.
- Wang, I. et al., 2005. Forkhead box M1 regulates the transcriptional network of genes essential for mitotic progression and genes encoding the SCF (Skp2-Cks1) ubiquitin ligase. *Molecular and cellular biology*, 25(24), pp.10875–94.
- Wang, I.-C. et al., 2008. FoxM1 regulates transcription of JNK1 to promote the G1/S transition and tumor cell invasiveness. *The Journal of biological chemistry*, 283(30), pp.20770–8.
- Wang, Y., 2009. CDKs and the yeast-hyphal decision. *Current opinion in microbiology*, 12(6), pp.644–9.
- Ward, M.P. & Garrett, S., 1994. Suppression of a yeast cyclic AMP-dependent protein kinase defect by overexpression of SOK1, a yeast gene exhibiting sequence similarity to a developmentally regulated mouse gene. *Molecular and cellular biology*, 14(9), pp.5619–27.
- Wedlich-Soldner, R. et al., 2003. Spontaneous cell polarization through actomyosin-based delivery of the Cdc42 GTPase. *Science (New York, N.Y.)*, 299(5610), pp.1231–5.
- Wegener, A.D. & Jones, L.R., 1984. Phosphorylation-induced mobility shift in phospholamban in sodium dodecyl sulfate-polyacrylamide gels. Evidence for a protein structure consisting of multiple identical phosphorylatable subunits. *The Journal of biological chemistry*, 259(3), pp.1834–41.
- Weigel, D. et al., 1989. The homeotic gene fork head encodes a nuclear protein and is expressed in the terminal regions of the *Drosophila* embryo. *Cell*, 57(4), pp.645–58.

- Weigel, D. & Jäckle, H., 1990. The fork head domain: a novel DNA binding motif of eukaryotic transcription factors? *Cell*, 63(3), pp.455–6.
- Weiss, E.L., 2012. Mitotic exit and separation of mother and daughter cells. *Genetics*, 192(4), pp.1165–202.
- Whiteway, M., Dignard, D. & Thomas, D.Y., 1992. Dominant negative selection of heterologous genes: isolation of *Candida albicans* genes that interfere with *Saccharomyces cerevisiae* mating factor-induced cell cycle arrest. *Proceedings of the National Academy of Sciences of the United States of America*, 89(20), pp.9410–4.
- Wightman, R. et al., 2004. In *Candida albicans*, the Nim1 kinases Gin4 and Hsl1 negatively regulate pseudohypha formation and Gin4 also controls septin organization. *The Journal of cell biology*, 164(4), pp.581–91.
- Wilson, D. et al., 2010. *Candida albicans* Pde1p and Gpa2p comprise a regulatory module mediating agonist-induced cAMP signalling and environmental adaptation. *Fungal genetics and biology : FG & B*, 47(9), pp.742–52.
- Wilson, R.B., Davis, D. & Mitchell, a P., 1999. Rapid hypothesis testing with *Candida albicans* through gene disruption with short homology regions. *Journal of bacteriology*, 181(6), pp.1868–74.
- Wolf, J.M. & Davis, D. a, 2010. Mutational analysis of *Candida albicans* SNF7 reveals genetically separable Rim101 and ESCRT functions and demonstrates divergence in bro1-domain protein interactions. *Genetics*, 184(3), pp.673–94.
- Wu, H. et al., 2010. The Exo70 subunit of the exocyst is an effector for both Cdc42 and Rho3 function in polarized exocytosis. *Molecular biology of the cell*, 21(3), pp.430–42.
- Wysong, D.R. et al., 1998. Cloning and sequencing of a *Candida albicans* catalase gene and effects of disruption of this gene. *Infection and immunity*, 66(5), pp.1953–61.
- Xu, W. & Mitchell, A.P., 2001. Yeast PalA/AIP1/Alix homolog Rim20p associates with a PEST-like region and is required for its proteolytic cleavage. *Journal of bacteriology*, 183(23), pp.6917–23.
- Xu, X.-L. et al., 2008. Bacterial peptidoglycan triggers *Candida albicans* hyphal growth by directly activating the adenylyl cyclase Cyr1p. *Cell host & microbe*, 4(1), pp.28–39.
- Yoshida, S., Asakawa, K. & Toh-e, A., 2002. Mitotic exit network controls the localization of Cdc14 to the spindle pole body in *Saccharomyces cerevisiae*. *Current biology : CB*, 12(11), pp.944–50.

- Zakikhany, K. et al., 2007. In vivo transcript profiling of *Candida albicans* identifies a gene essential for interepithelial dissemination. *Cellular microbiology*, 9(12), pp.2938–54.
- Zhang, J. et al., 1999. Phosphatidylinositol polyphosphate binding to the mammalian septin H5 is modulated by GTP. *Current biology : CB*, 9(24), pp.1458–67.
- Zhang, T. et al., 2008. CaSfl1 plays a dual role in transcriptional regulation in *Candida albicans*. *Chinese Science Bulletin*, 53(17), pp.2624–2631.
- Zhang, X. et al., 2001. Cdc42 interacts with the exocyst and regulates polarized secretion. *The Journal of biological chemistry*, 276(50), pp.46745–50.
- Zhao, X. et al., 2004. ALS3 and ALS8 represent a single locus that encodes a *Candida albicans* adhesin; functional comparisons between Als3p and Als1p. *Microbiology (Reading, England)*, 150(Pt 7), pp.2415–28.
- Zheng, X., Wang, Y. & Wang, Y., 2004. Hgc1, a novel hypha-specific G1 cyclin-related protein regulates *Candida albicans* hyphal morphogenesis. *The EMBO journal*, 23(8), pp.1845–56.
- Zheng, X.-D. et al., 2007. Phosphorylation of Rga2, a Cdc42 GAP, by CDK/Hgc1 is crucial for *Candida albicans* hyphal growth. *The EMBO journal*, 26(16), pp.3760–9.
- Zheng, Y., Cerione, R. & Bender, A., 1994. Control of the yeast bud-site assembly GTPase Cdc42. Catalysis of guanine nucleotide exchange by Cdc24 and stimulation of GTPase activity by Bem3. *The Journal of biological chemistry*, 269(4), pp.2369–72.
- Zhu, G. et al., 2000. Two yeast forkhead genes regulate the cell cycle and pseudohyphal growth. *Nature*, 406(6791), pp.90–4.
- Ziman, M. et al., 1993. Subcellular localization of Cdc42p, a *Saccharomyces cerevisiae* GTP-binding protein involved in the control of cell polarity. *Molecular biology of the cell*, 4(12), pp.1307–16.
- Znaidi, S. et al., 2013. A Comprehensive Functional Portrait of Two Heat Shock Factor-Type Transcriptional Regulators Involved in *Candida albicans* Morphogenesis and Virulence. *PLoS pathogens*, 9(8), p.e1003519.
- Zou, H. et al., 2010. *Candida albicans* Cyr1, Cap1 and G-actin form a sensor/effector apparatus for activating cAMP synthesis in hyphal growth. *Molecular microbiology*, 75(3), pp.579–91.